UNIVERSITY OF WOLVERHAMPTON

The modification of Laponite® with silver or copper and investigation of their antibacterial activity

A thesis presented for the award of
Doctor of Philosophy

Festus Ibhamiokhon Ituah

June 2012

The modification of Laponite® with silver or copper and investigation of their antibacterial activity

Festus Ibhamiokhon Ituah **B.Sc., M.Sc.**

A thesis submitted in partial fulfilment of the requirements of the University of Wolverhampton for the degree of Doctor of Philosophy

June **2012**

Signature:

Date:

Abstract

Silver and copper modified Laponite® RD were synthesised either by ion exchange or isomorphous substitution into Laponite® RD sheet. Six different concentrations of silver-exchanged Laponite® RD (AGLAP1-6) or copper exchanged Laponite® RD (CULAP1-6) were produced in this work via ion exchange and three different concentrations of silver incorporated Laponite® RD (AL1-3) and a concentration of copper incorporated Laponite® RD (CL1) were synthesized via isomorphous substitution.

The silver or copper modified Laponite® RD were characterised with X-ray diffraction (XRD), Fourier transformed infrared spectroscopy (FTIR), energy dispersive X-ray spectroscopy (EDX), thermogravimetric analysis (TGA), magic angle spinning nuclear magnetic resonance (MAS NMR), scanning electron microscopy (SEM) and transmission electron microscopy (TEM). The XRD showed changes in the phase purity of pure and modified Laponite® RD. The amount of silver or copper exchanged or incorporated into Laponite® RD interlayer or sheet were determined by EDX. The TEM image analysis indicated that the Ag^{+} and Cu^{2+} ions were in the nanometer range with a modal size of 13±1 and 15±1nm for silver and copper-exchanged Laponite® RD, 10 and 18nm for silver and copper incorporated Laponite® RD respectively.

The antibacterial activity was investigated by exposing *Escherichia coli* K12W-T, *Staphylococcus aureus* NCIM B6571 and *Pseudomonas aeruginosa* NCIMB8295 in tryptone soya broth to the different silver-Laponite® RD and copper-Laponite® RD nanocomposites for a period of 72 hours. All concentrations of silver-Laponite® RD and copper-Laponite® RD reduced the growth of all the bacterial spcies. There was no growth of *P. aeruginosa* after 6 hours, *E. coli* after 8 hours and *S. aureus* after 24 hours with silver-exchanged Laponite® RD containing 2.35 wt. % Ag (AGLAP6); *P. aeruginosa* after 8 hours, *E. coli*

after 24 hours and *S. aureus* after 24 hours with silver-exchnaged Laponite® RD containing 1.76 wt. % Ag (AGLAP4). Similarly total inhibition was obtained in the medium supplemented with silver incorporated Laponite® RD containing 1.10 wt. % Ag (AL3) for *P. aeruginosa* at 6 hours, both *E. coli* and *S. aureus* at 8 hours; with silver incorporated Laponite® RD 0.58 wt. % Ag (AL2) for *P. aeruginosa* at 8 hours, both *E. coli* and *S. aureus* at 24 hours.

To access the persistency and slow release of the antibacterial agents the release profile was compared with $AgNO_3$ and $CuSO_4$. While all the silver-Laponite® RD and copper-Laponite® RD showed slow and consistent release over the whole investigation period, $AgNO_3$ and $CuSO_4$ were abrupt, signifying that Laponite® RD is an efficient slow release material.

In addition, silver ions eluted more quickly from the silver incorporated Laponite® RD than the silver-exchanged Laponite® RD. Unmodified Laponite® RD showed no antibacterial property to any of the bacteria tested, but was responsible for the consistent and controlled slow release of the metal nanoparticles into the tryptone soya broth, a phenomenon potentially utilizable in bandages where release for long duration is crucial.

Acknowledgement

I give thanks to God the Father, the Son and the Holy Spirit for the love peace, quietness, guardians, provision and protection I enjoyed throughout the duration of my studies. I appreciate my director of studies, *Prof Craig Williams*, my supervisor, *Dr Izabela Radecka* for their constructive discussion throughout the research period.

I am grateful to *Prof John Darling*, Dean School of Applied Sciences for his support. I value the support I received from the technical team; *Dianne Spencer, Barbara Hodson, Dave Townrow, Keith Jones, Andrew Brook, Ann Dawson, Balbir Bains,* friends and colleagues; *Dr Inman Malcom, Tang James, Adams Watt, Dr Ezekiel Chinyio* and *Dr David Oloke*. I also thank my colleagues and fellow researchers in Room MA 028 namely, *Adetiya Bhat, Paul Obara, Shawna Bolton* and *Adetoro Ogunleye*

I specially appreciate the management and staff of Rockwood Additives Ltd; *Dr David Shaw, Tex Timperley, Jane Doyle* and *Webb Maurice* who provided training and support for this piece of work. Also *Paul Stanley* at the University of Birmingham, *Dr Paul Hodgkinson*, University of Durham and *Mark Smith* at the Coventry University for use of their facilities for some of the analysis.

Finally, my heartfelt gratitude go to my beloved wife *Deborah Ituah* and my dearest daughter *Favour Ituah,* my brothers and sisters; *Jolly, Innocent, Josephine, Stella, Kate, Georgina and Constance* for their outstanding love, bravery, support, encouragement and being with me all the way throughout the duration of my studies.

Dedication

This work is dedicated to my Lord, God and saviour *Christ Jesus*

to my wife,

Deborah Ituah

and my daughter,

Favour Ituah

List of Figures **Page**

List of Tables **Page**

Appendices

Content **Page**

List of Abbreviations

Ag^{+}	Silver ions
AGLAP	Silver exchanged laponite® RD
AgNPs	Silver nanoparticles
AL	Silver incorporated Laponite® RD
CL	Copper incorporated Laponite® RD
Cu^{2+}	Copper ions
CULAP	Copper exchanged Laponite® RD
EDX	Energy dispersive X-ray spectroscopy
FTIR	Fourier transformed infra red spectroscopy
ICDD	International centre for diffraction data
ICP-AES	Inductively coupled plasma atomic emission spectroscopy
IR	Infra red spectrum
JCPDS	Joint committee for powder diffraction standards
PC	Personal computer
PPM	Parts per million
PPB	Parts per billion
RD	Rapid dispersion

SEM	Scanning electron microscopy
TEM	Transmmission electron microscopy
TGA	Thermogavimetric analysis
XRD	X-ray diffraction
JSA	Japanese standards association
DNA	Deoxyribonucleic acid
RNA	Ribonucleic acid
MIC	Minimum inhibitory concentration
MBC	Minimum bacteriocidal concentration
FCC	Fluid catalytic cracking
BET	Brunauer Emmett Teller

Chapter 1

Introduction and Literature review

This chapter reviews Laponite and the bacteria used in this study, a review on the literature on Laponite and its antibacterial activities. The hypothesis on which this work is based along with the aims and objectives have also been included.

1.1 Introduction

Clays have traditionally been used for production of ceramics. They show great adaptability in terms of manipulation of their reactions and subsequent diverse utility in different fields (Carretero and Lagaly, 2007). Smectites belong to the hydrous clay mineral group. These expand in the presence of water and other solvents. Smectites are divided into two parts: di- and tri-octahehrals. Dioctahadrals are made up of aluminium smectites and the iron-rich ferruginous smectites and nontronites (Ding and Frost, 2002 and Dekov *et al.,* 2007), while hectorite, saponite, stevensite, sauconite, swinefordite and Laponite® belong to the trioctahedrals (Fig. 1.1).

1.2 Structure and property of Laponite®

Laponite® is a cationic model of a synthetic smectites mineral, a negatively charged colloid (Rosta *et al.,* 1991) bearing a resemblance to natural hectorite (Aceman *et al.,* 1997). Aqueous dispersions of Laponite® in low ionic concentration undergo ageing or structural evolution with time (Kumar *et al.,* 2008). A study of the physical properties and aqueous dispersion characteristics of Laponite® XLG (gel-forming grade with no additives) showed thin plate-like crystals with a mean diameter of 20nm. The dissolution of Laponite® occurred at pH < 9 in a solution containing Mg (10^{-3} mol dm^{-3}).

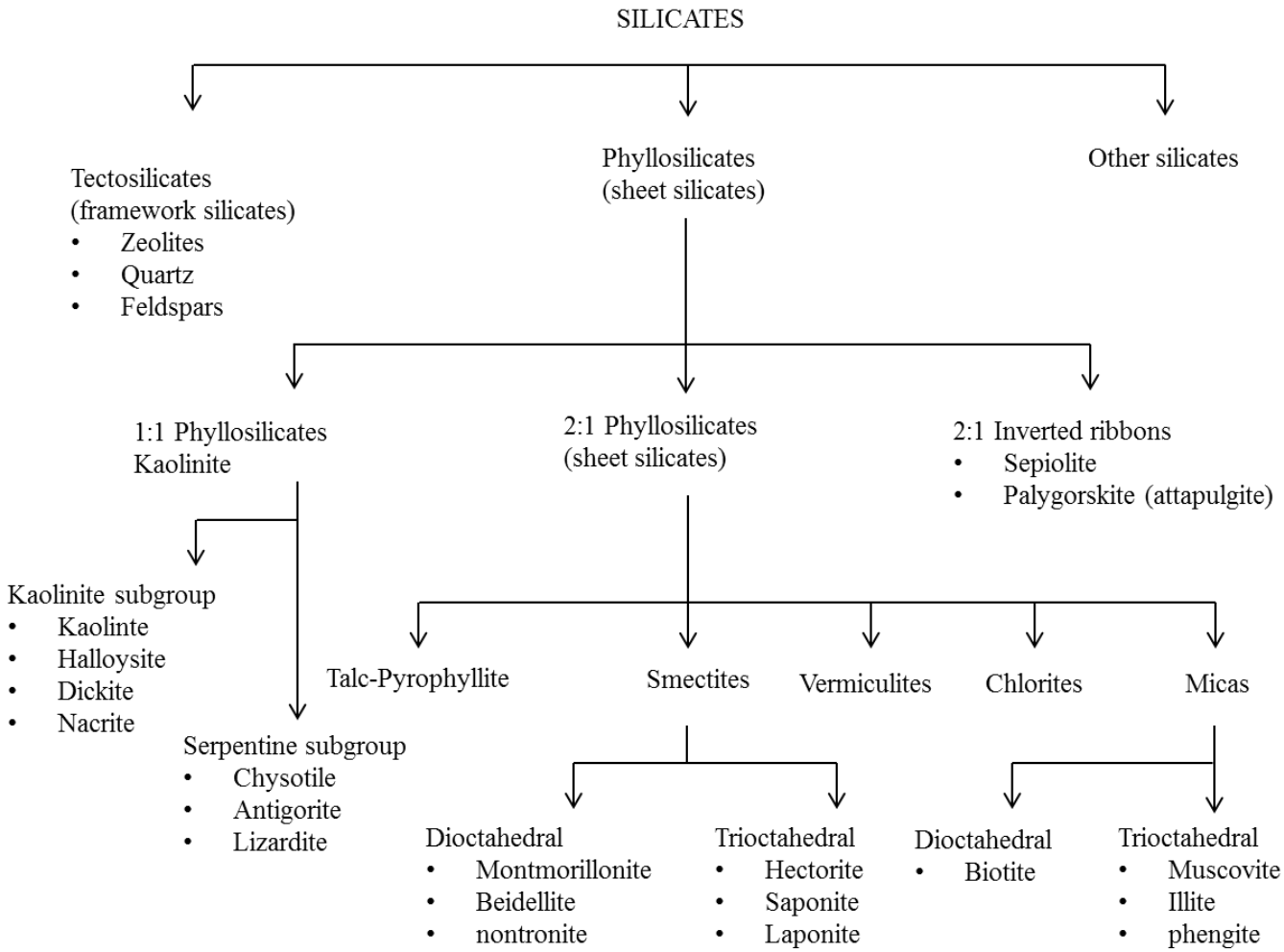

Fig. 1.1: Classification of silicates (adapted from Adamis *et al*., 2005; Bailey, 1980 and Rieder *et al*., 1998)

The cation exchange capacity obtained in base (pH 8–10) range indicated no significant pH–dependent surface charge of Laponite® particles in aqueous electrolyte (NaCl) solution, suggesting that Laponite® XLG may be a model material for studies on the behaviors of natural smectites clay minerals, though this requires careful attention to dispersion preparation methods and control of the pH (Thompson *et al.*, 1992).

Laponite® being synthetic possesses a known and consistent composition. It is composed of magnesium and silicon in a layer-lattice similar to those of the natural, trioctahedral smectites clay minerals such as hectorite and saponite. The terms 'clay' and 'clay mineral' are often used interchangeably, but, technically, 'clay' refers to the parent material, while 'clay minerals' refers to the content of the material. The Joint Nomenclature Committee (JNC) defined clay(s) as "naturally occurring material composed primarily of fine grained minerals, which is generally plastic at appropriate water contents and which harden when dried or fired", but also defined "clay minerals" separately as a class of hydrated phyllosilicates making up the fine-grained fraction of clays, thereby stressing further that these phyllosilicates minerals impart plasticity to clay and harden upon drying or firing (Guggenheim and Martin, 1995 and Bergaya *et al*., 2006).

Clay minerals are made of layered silicates mostly based on 2-dimentional structures. They have oxides or hydroxides of silicon present, as $Si(O, OH)_4$, and oxides or hydroxides of metal ions, $M(O, OH)_6$ as their basic building blocks. The metal ions may be Al^{3+}, Mg^{2+} or Fe^{3+}. The $Si(O, OH)_4$ is located tetrahedrally while the $M(O, OH)_6$ groups occupy the octahedral sheet giving the structure a layer thickness of ~0.7nm in clays such as kaolinites or serpentinites with 1:1 mineral type clays. However, Laponite® belongs to the 2:1 type clays (Table 1.1) of 0.92nm thick, and two silicates-tetrahedral sheets.

Table 1.1: Classification of 2.1 clay minerals (adapted from Schoonheydt, 1991 and Vaccari, 1998).

Layer charge per unit cell (the sum of all individual charge in a unit cell make up the layer charge**)**	**Group**	**Subgroup**	**Name**
0.0	Pyrophyllite	Dioctahedral	Pyrophyllite
	Talc	Trioctahedral	Talc
0.5 - 1.2	Smectite	Dioctahedral	Montmorillinite
			Beidelite
		Trioctahedral	Saponite
			Hectorite
			Laponite
1.2 - 1.8	Vermiculite	Dioctahedral	Vermiculite
		Trioctahedral	Vermiculite
~2.0	Mica	Dioctahedral	Muscovite
			Paragonite
		Trioctahedral	Biotite
			Phlogopite
~4.0	Brittle mica	Dioctahedral	Margarite
		Trioctahedral	Clintonite
Variable	Chlorite	Dioctahedral	Donbassite
		Trioctahedral	Clinochlore

The crystal lattice consists of two-dimensional layers where a central octahedral sheet of magnesium is fused to two external silica tetrahedrals by the apex bonding the oxygen ions of the octahedral sheet to the tetrahedral sheets (Clausen *et al*., 2011). An octahedral layer of Mg or Li(O, OH) is sandwiched between the tetrahedral sheets (Fig.1.2). Each unit cell of Laponite® consists of six octahedral Mg^{2+} ions located in the interlayer of four tetrahedral Si

atoms. The charge difference in the structure is balanced by twenty atoms of oxygen and four atoms of hydroxyl groups respectively (Huang and Yang, 2008). Thus, Laponite® has three sites per unit cell occupied by Mg and Li. These are potential sites for isomorphous substitutions of other organic, inorganic or metal cations, each or any of which may alter the properties of the Laponite® structure. This may be in the pore size, thermal conductivity, or perhaps alteration in the rheological properties of the clay itself and subsequently affect the suitability of the clay mineral as a useful candidate for antimicrobial applications.

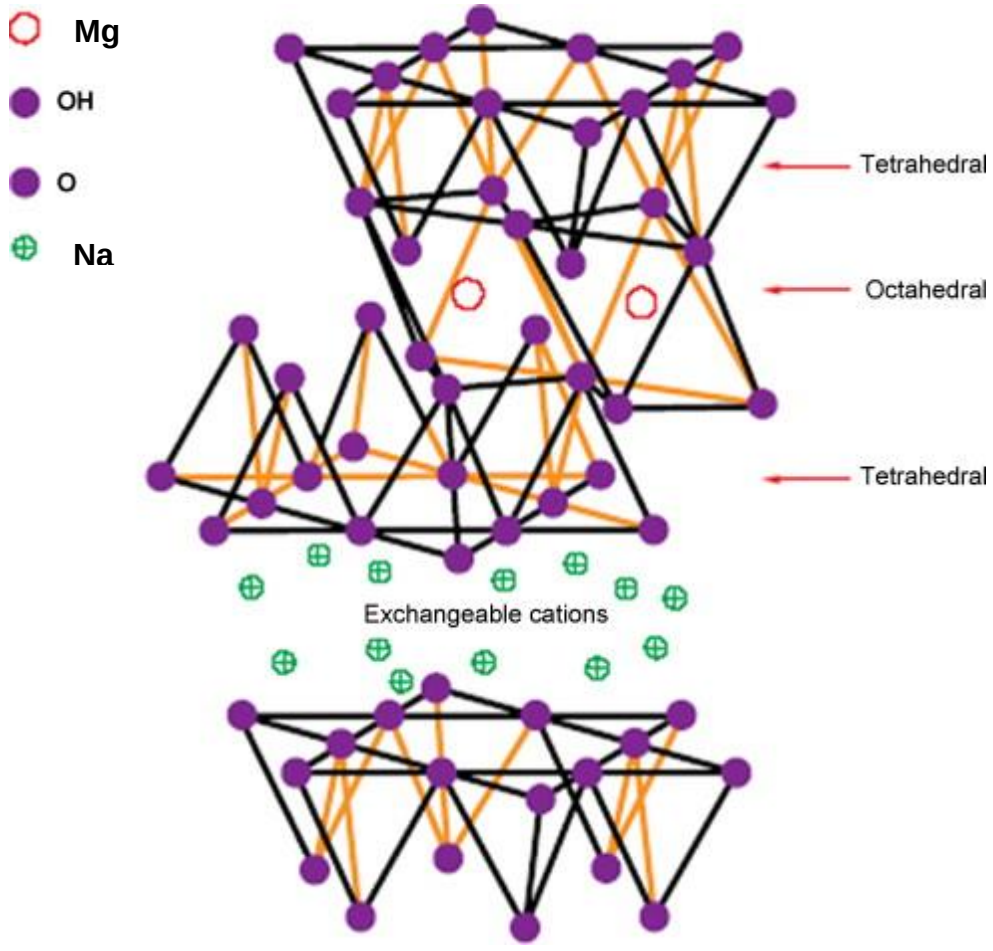

Fig. 1. 2: Structure of Laponite® (adapted from Pavlidou and Papaspyrides, 2008).

Furthermore, during isomorphous substitution, incoming cations with lower valence electrons than those outgoing cations renders the lattice negatively charged. Charge neutrality only returns to the structure by the exchangeable cations (Vaccari, 1998), specifically, trioctahedral clays, such as Laponite® which possess the general formula:

$$(Si_{8-x}M_x)^T\ (Mg_{6-y}\ M'_y)^o\ (OH)_x\ O_{20}\ M''^{n+}_{x+y/n}\ mH_2O \qquad (1)$$

Where *T* and *O* are the tetra- and octahedral sheets, M and M´ have one unit of charge less than the substituted cation and M´´ is the exchangeable cation with *n* number of valence. While *x* and *y* refers to the degree of isomorphous substitution in the tetrahedral and octahedral sheets respectively. Other trioctahedral smectites, layered silicates chemical formula most commonly used in nanocomposite materials are as shown in Table 1. 2.

Table 1. 2: Chemical Structure of 2.1 Smectites (Adapted from Alexandre and Dubois, 2000).

2.1 Phyllosilicates	**General formula**
Montmorillonite	$M_x(Al_{4-x}Mg_x)Si_8O_{20}(OH)_4$
Hectorite	$M_x(Mg_{6-x}Li_x)Si_8O_{20}(OH)_4$
Saponite	$M_xMg_6(Si_{8-x}Al_x)O_{20}(OH)_4$
Laponite	$M_x(Mg_{6-x}Li_x)Si_8O_{20}(OH)_4$ (not always full replacement of cations therefore, develop net negative charge e.g. -0.7)

M-monovalent cation, *x* – degree of isomorphous substitution (between 0.5 and 1.3).

However, although isomorphous substitution predominates in the octahedral layer (Vaccari, 1998), it may also occur in the tetrahedral sheet. For most smectites (such as montmorillonite), being dioctahedral, the isomorphous substitution occurs in the octahedral sheet, where the Al^{3+} is partially replaced by Mg^{2+} in the montmorillonite structure, whereas Li^+ displace Mg^{2+} in hectorite. However, the situation is different for the dioctahedral beidellite and the trioctahedral saponite where in both cases the isomorphous substitutions

occur solely on the tetrahedral sheets. Here the net negative charge structure emerges due to the substitution of Al^{3+} for Si^{4+} ions (Vaccari, 1998). Nontronites also belong to the smectites group, but contain Fe^{3+} instead of Al^{3+} in the octahedral sheets (Vaccari, 1998). For more on nontronites the reader should refer to Murnane and Clague, 1983; Alt, 1988; Wang and Huang, 1989; Mackenzie *et al.,* 1993; Zen *et al.,* 1996; Heidbrink *et al.,* 1996; Yan and Stucki, 2000; Frost and Kloprogge, 2000; Ding and Frost, 2002; Jaisi *et al.,* 2005; Johnson *et al.,* 2005; Gupta *et al.,* 2006; Tang and Valix, 2006; O'Reilly *et al.,* 2006; Dekov *et al.,* 2007; Furukawa and O'Reilly, 2007; Jaisi *et al.,* 2007 and Jaisi *et al.,* 2008.

Chemical analysis has revealed that Laponite® RD (rapid dispersion grade; other grades and their applications are shown in Table 1.3) is composed of SiO_2, MgO, Na_2O and LiO_2 in the respective mean chemical composition; 65.82%, 30.15%, 3.20% and 0.83% (Levitz *et al.*, 2000; Cummins, 2007).

Table 1.3: Laponite® RD grades and applications (http://www.scprod.com).

Gel forming grades	**Temporary sol forming grades**	**Permanent sol forming grades**	**Applications**
RD, B	RDS	S482 SL25	For rheology control in surface coatings, household products and general and industrial applications
XLG	XLS		High purity, low heavy metal, controlled microbiological content for rheology control in personal care/ cosmetic applications
D,DF	DS		Rapid dispersion in sorbitol solution for rheology control in toothpaste applications.
	S, JS	S482 SL25	High sol stability grades for electrically conductive, antistatic and barrier films.

There are several different grades of Laponite® available for different commercial applications (Table 1.3 with Laponite® RD the most frequently studied grade, being used in many household and industrial products. Laponite® XLG is a high-purity grade of Laponite® RD devoid of heavy metal impurities such as lead and arsenic (Cummins, 2007). Single Laponite® RD crystals are disc-shape, almost uniform in dimension, with a density of 2.53gm cm^{-3} and measure approximately 25nm in diameter and 0.92nm thick (Fig. 1.3), being smaller than hectorite at 2μm diameter.

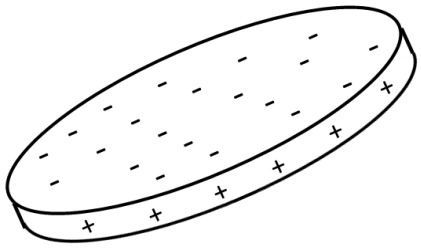

Fig. 1. 3: Single Laponite® RD crystal, disc 25nm x 0.92nm thick (Adapted from http://www.scprod.com).

Each Laponite® RD crystal is composed of octahedrally coordinated magnesium oxides sandwiched between two layers of tetrahedral silicon oxide. This renders the crystal face negatively charged while the edges are positively charged. The whole structure has a net negative charge (the sum of all individual charge in a unit cell make up the net layer charge for that unit cell thus, Laponite; $Na^{+}_{0.7}[(Si_8\ Mg_{5.5}\ Li_{0.3})\ O_{20}\ (OH)_4\ ]^{-0.7}$ = 0.7(+1) + [8(+4) + 5.5(+2) + 0.3(+1) + 20(-2) + 4(-1) + (-0.7) = +44 – 44.7 = -0.7 charge/unit cell=\), stabilised by electrostatic interaction between the negatively charged faces and positively charged edges of the disc-shaped colloidal particles. The charge is balanced by a cation such as

sodium. This gives rise to the formation of double layers when dispersed in water (Cummins, 2007).

Both Laponite® RD and hectorite possess similar structures but differ in layer diameter, which is ~0.03µm (as determined by Cool and Vansant, 1996, but 25nm reported in http://www.scprod.com. 0.03µm = 30nm) in Laponite® RD, whereas hectorite and most natural smectites measure 2µm. However, due to the nature of the Laponite® RD layer; tactoids (random stacking of particles) do occur in edge-to-face and edge-to-edge fashion, giving rise to a high surface area, $350 m^2 g^{-1}$ and a micropore volume of $0.243 cm^3 g^{-1}$ (Cool and Vansant, 1996).

Laponite® RD adsorbs water molecules and swells, forming distinct sheets or platelets having dimensions of 25nm x 0.92nm. On dispersion in water it forms a colourless, transparent liquid and the particles become stable when electrostatic repulsive forces are greater than the van der Waals attractive forces (Labanda and Llorens, 2008). Laponite® RD does not actually dissolve in water: rather the insoluble crystals hydrate visibly causing the layer stack to swell as the inter-lamellae cations adsorb water molecules (Huang and Yang, 2008) causing formation of a uniform dispersion. The crystal edges are positively charged while the disk surface is negatively charged and this charge difference results in edge-surface electrostatic attraction which ultimately culminates in the unique thixotropy (Huang and Yang, 2008). Laponite® RD has a negative face charge, but a pH-dependent rim charge that may be positive or negative (Mongondry *et al.*, 2005).

Laponite® XLG exhibited a complex non-linear behaviour (Pozzo and Walker, 2004) and on vigorous shaking forms a "shake-gel", a shear-induced non-Newtonian fluid motion on mixing with a polymer, e.g. polyethylene oxide (Zebrowski *et al.*, 2003). The whole process of shake-gel (i.e. a semi-solid, able to support its own weight due to its self-sufficient

elasticity) formation is reversible. However, it easily relaxes back to a fluid state with a relaxation time highly dependent on the concentration of the polyethylene oxide (Zebrowski *et al.,* 2003). Polyethylene oxide become a common denominator in this reaction because of characteristics such as being a good host electrolyte with a versatile chain structure, and for its ionic transport properties as well as being solvent for metal salts (Stefanescu *et al.,* 2008). Furthermore, polyethylene oxide is comparable with Laponite® RD, as well as the natural montmorillonite, in that the trio exhibit hydrophilicity. This property of polyethylene oxide during nanocomposition with Laponite® RD enhances its interpenetration of the clay platelets and subsequent adsorption to the clay surface. However, the amount of the adsorbed polyethylene oxide is balanced by the layer charge on the clay surface (Stefanescu *et al.,* 2008 and Bujdak *et al.,* 2000). This occurs on both the Laponite® RD gel phase and in the aqueous form and ultimately results in a clear transparent suspension, whereas under similar conditions montmorillonite becomes opaque. In the presence of polyethylene oxide the hygroscopic property of Laponite® RD is increased causing it to adsorb large amount of water on exposure to air (Stefanescu *et al.,* 2008). Laponite® RD forms three-dimensional gel-like structures on dispersion in aqueous media. This property enhances its usefulness as a thickening, plasticizing, or emulsifying agent in finished industrial products such as paints, plasters, and cosmetics, toothpaste and fillers (Willenbacher, 1996). Two mechanisms have been proposed for the elation of Laponite® RD dispersions. The first is the electrostatic repulsion between interacting double-layers with the formation of an equilibrium structure, proposed by Norrish in 1954, and was in agreement with the findings of Callaghan and Ottewill (1974).

The second mechanism is the compression of the double layers on the platelet faces and the electrostatic attraction between oppositely charged faces and edges, coupled with the attractive van der Waals forces between particles, resulting in edge-to-face and also edge-to-

edge organisation, thus forming a linked, three-dimensional network commonly referred to as a "house-of-cards", shown in Fig. 1.4 (Cummins, 2007 and Willenbacher, 1996). While the first mechanism takes place in low ionic concentration, the second occurs at high ionic strength (Olphen, 1977).

Fig. 1.4: House of card structure (http://www.scprod.com)

Sze Nga Sum *et al.* (2004) synthesised pillared with clay-based Fe nanocomposites. The iron- Laponite® RD nanocomposite complex (Fe-Lap-RD) completely mineralised the model pollutant, azo-dye Acid Black 1. It was shown that Fe-Lap-RD had a catalytic activity and showed promise as a heterogeneous catalyst for the photo-Fenton mineralisation of organic compounds. Laponite® RD modified with hydrophobic groups allowed intercalation of bulky hydrophobic molecules. The introduction of the hydrophobic groups accelerated the intercalating process of heavier hydrophobic species into the Laponite® RD structure (Park *et al.*, 2004). Eu^{3+} or Er^{3+} doped Laponite® RD xerogels and films prepared from colloidal dispersion displayed the potential for optical applications. Tronto *et al.* (2009) observed that the addition of rare earth ions to the Laponite® RD did not alter its thermal stability or phase transition.

Leon-Morales *et al*. (2004) discovered that Laponite® RD was completely retained under low ionic concentration of $7x10^{-2}$ M NaCl while *P. aeruginosa* SG81 was generally less

influenced by ionic strength indicated by its low mobility in 1M NaCl. However, under separate, more suitable, conditions ($7x10^{-2}$ M NaCl for Laponite® RD retention and biofilm stability), Laponite® RD suspension remobilised part of the attached biomass and elicited alteration in the Laponite® RD elution in the presence of biofilm under low ionic conditions. This suggests that reduced ionic strength has an influence on the mobilisation of both biological and inorganic colloids. Colloid-biofilm interaction may have implications for colloid-bound contaminant transport and the remobilisation of pathogens, since most of these events occur in subsurface environments (Leon-Morales *et al.*, 2004).

Much of the research and development in clay mineral science has been in physics and the chemical sciences, and concentrated on mechanical, physical and optical properties. Applications have been used in the automotive industry, electrical and electronics industry, development of batteries, agrochemical flowables, ceramic glazes, enamel frits, paper and polymer films, as well as personal and household products; toothpaste, cosmetics, gelled skin cleaner, nail lacquer, shampoo, oven cleaner, degreaser, gelled bleach cleaner, air freshener, dishwashing detergent, including exchange membrane cells (Yuan *et al*., 2008). The field is now gradually widening into Biology and Medicine where the focus is on its utilization into cosmetics, creams and ointments, and as antimicrobial nanocomposites agent.

1.3 Production process of Laponite® RD

Specifically, Laponite® RD is manufactured by former Laporte Industries Ltd, now Rockwood Additive Ltd, Cheshire, UK. It is synthesised by combining sodium, magnesium and lithium salts with sodium silicate at specific reaction conditions (such as temperature and pH) resulting in an amorphous precipitate which undergoes complete crystallization at high

temperature. The product derived from the production process is first filtered, then washed, and finally dried and milled to fine white powder (Fig. 1.5).

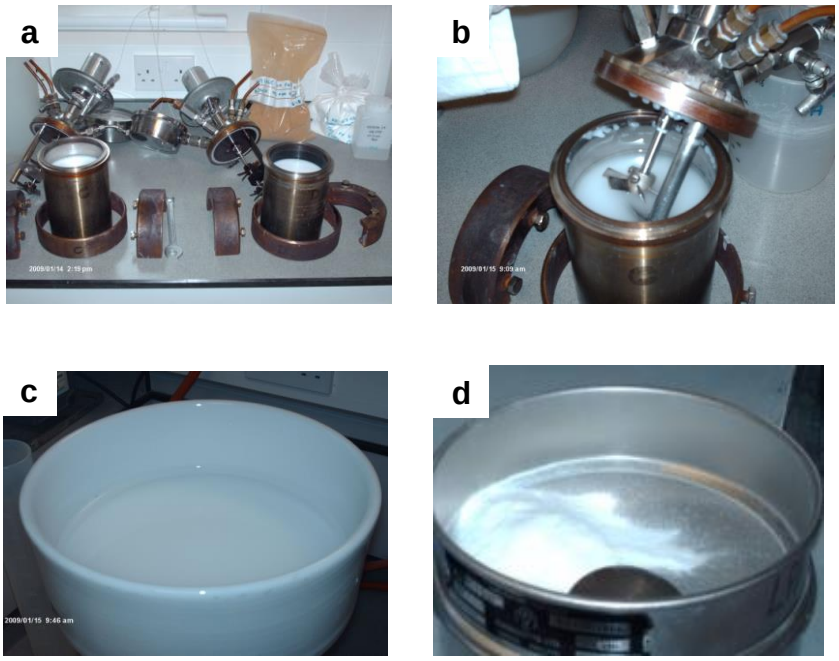

Fig.1.5: Synthesis of Laponite® RD before (a) and after autoclave (b) filtering and drying (c) milling to white powder (d)

Cationic clays are mostly obtained from natural materials which may be contaminated with quartz, calcite, feldspars and other impurities. The mined mixture is centrifuged and the suspension contains clay particles of < 2µm while the precipitate harbours the impurities. Some amorphous oxide of iron and aluminium may remain bound or adsorbed to the clay particles. These are later removed via chemical treatment with dithionate, a difficult process (Stul, 1982, Vaccari, 1998).

1.4 Modification in Laponite® RD

Several methods are used in the synthesis of mineral clays and some of the methods act to modify or improve their properties. Clay minerals allow for tailoring to suit special purposes

in specific applications. The two primary modification methods are ion exchange (Fig. 1.6A) using metal or inorganic cations or cationic complexes (Bergaya and Lagaly, 2001) after synthesis, and isomorphous substitution which is performed *in situ* (Fig. 1.6B). Other techniques may incorporate or modify these methods with specific post synthetic processes including pillaring by poly- or hydroxo-metal cations of cationic clays, delamination and regeneration in smectites, reaction with acids such as acid-treated bentonite (Fernandez-Perez *et al.*, 1999; Fernandez-Perez *et al.*, 2000), silane coupling, intraparticle and interparticle polymerisation, dehydroxylation and calcinations (Liu and Zhang, 2007), and lyophilisation, ultrasound and plasma (de Paiva *et al.*, 2008; Bergaya and Lagaly, 2001).

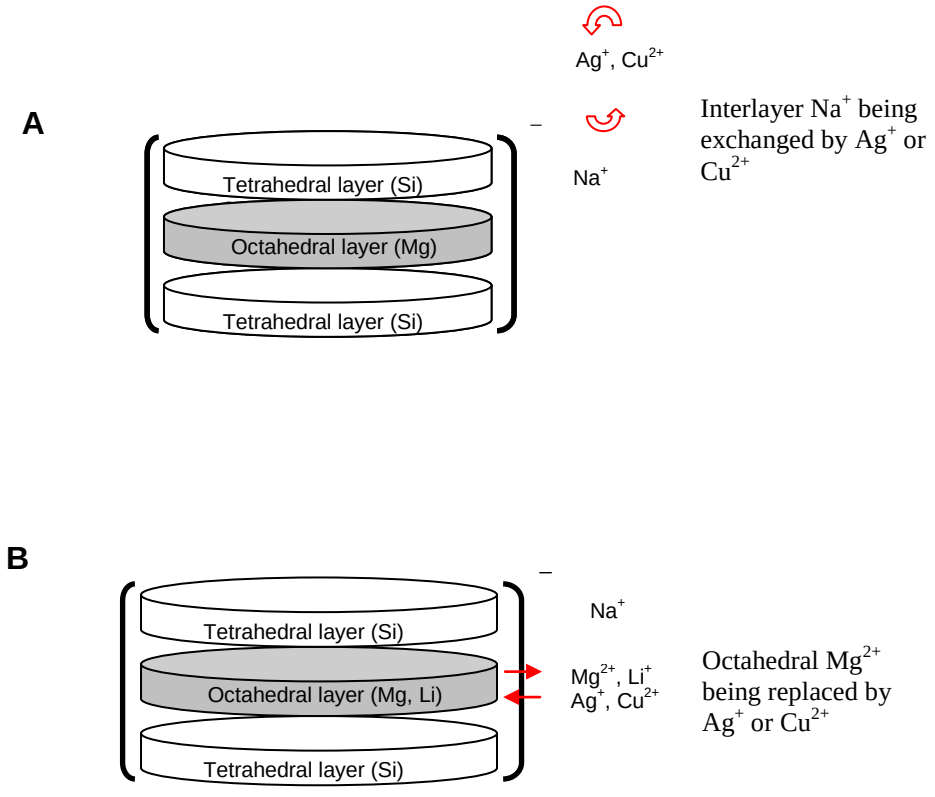

Fig. 1.6: Modification of Laponite® RD; interlayer metal ion exchange (A) and octahedral metal isomorphous substitution (B)

Clays or clay minerals can also be fine-tuned with biological molecules (such as proteins, enzymes, amino acids and peptides) that are utilizable in other applications (de Paiva *et al.*, 2008). Example include clay-protein complexes used in filtration process, purification of high-value protein (de Piava *et al.*, 2008) cleansing of pesticide contaminated groundwater, (Yu *et al.*, 2000) and immobilization of enzymes in packed or fluidised bed reactors used in food and biotechnology (Sanjay and Sugunan, 2005).

1.4.1 Pillaring Process

A key method to improve the property of clay material is the pillaring process. This involves the synthesis of materials having 3-D network structures like those of zeolites (Vaccari, 1999). The main goal of the pillaring process is to produce new and inexpensive materials with unique properties, complementary to those of zeolites, in terms of pore size, pore shape, acidity and redox properties (Vaccari, 1999). With optimum control of the pillaring process materials (solids) with improved properties can be obtained which may exhibit some or all the following characteristics: (i) high surface area up to 600 m^2g^{-1}, (ii) broad spectrum of properties (structural, chemical or catalyst), (iii) controlled internal structures, with reactive sites and/or species chosen to match specific applications or provide host structures for chemical or physical processes. Various agents are used in the pillaring process such as organic compounds, metal tri-schelates (e.g. $M(2,2'\text{-bipyridine})_3^{n+}$ or $M(\text{o-phenanthroline})_3^{n+}$ where M, transition metal ion and *n*, number of electrons (Bekkum, 2001)) organo-metallic complexes, metal cluster cations, metal oxide sols and polyoxocations. The latter are the most widely used pillaring agents and include polyoxocations of Al, Ni, Zr, Fe, Cr, Mg, Si, Bi, Be, B, Nb, Ta, Mo, Ti, and more recently, Cu and Ga (Vaccari, 1999). However, clays with multi-element pillars have also been prepared (Carrado *et al.*, 1986; Occelli, 1986 and Burch,

1987). Only the chemical structure, composition and charge of Al-polyoxocations with the Keggin ion:

$$[Al_{13}O_4\,(OH)_{24}\,(H_2O)_{12}]^{7+} \qquad (2)$$

have been well characterised (Vaccari, 1999). In the reaction with clay, the polyoxocation attaches to the surface of the clay via ion exchange (Plee *et al*., 1985), thereby catalytically impacting the clay surface with active Bronsted and Lewis acid sites (Occelli *et al*., 1985), usually under high temperature and dehydration conditions, then bonds to silicate surface.

Pillared layered clays (PILCs; also called cross-linked clays) are nanocomposite materials with open and rigid structures, obtained by linking robust, 3-dimentional species to a layered host. The properties of PILCs are determined by the pillaring agent, clay type, particle size, pillaring procedure, and thermal treatment used in the manufacturing process. These offer a very powerful and flexible means of designing specific tailored catalysts (Vaccari, 1999). Pillared clays, are smectites saturated with metal-polyhydroxy cations within their interlayer space. For the nature of their structure, i.e. having large distances between their layered structures, they are suitable for and exhibit potential use as molecular sieves. They may also be used as adsorbents for molecules, cracking catalysts, or demonstrate properties of slow releasing agents, when not stuffed with pillars i.e. having large distances between their pillars (Aceman *et al*., 1997).

Occelli *et al.* (1986) treated natural hectorite with Al, ZrAl and Zr polyoxycations that produced pillared hectorite which, after heating in air at 400 ^{o}C, attained a thermal stability of 600–700^{o}C. Meanwhile, spectroscopic studies of sorbed pyridine showed that pillared hectorite, like pillared bentonite, possess both Lewis and Bronsted acid sites distributed as in the parent (acid-washed) hectorite. But, pillared hectorite was not as active compared to pillared bentonite, especially in cracking the 260–426^{o}C boiling range gas oil. However, the

hectorite exhibited greater gasoline selectivity and minimized light gas ($C_2 – C_4$) generation. Cracking activity depends on the surface area generated by pillaring.

Pillaring of Laponite® RD has almost always been associated with catalysis, especially in oil cracking. For instance, Bergaya *et al*. (1991) prepared pillared layer Laponite® RD using mixed Al–Fe pillars, and upon analysis with X-ray diffraction (XRD), nuclear magnetic resonance (NMR) and hydrogen temperature programmed reduction (H_2TPR) the Fe cation replaced some aluminium in the octahedral layer of Laponite® RD in the presence of the aluminium pillars. Further, the thus-formed mixed Al–Fe pillars showed catalytic properties with shape selective characteristics that were different from other Fe catalysts.

Schoonheydt (1991) gave an overview of the properties of smectites, including pillared forms, and some MAS-NMR data as well as redox properties of smectite surface. On EXAFS (extended X-ray absorption fine structure) studies of pillared clay catalysts, Corker *et al.,* (1991) found the oxidized sites of the pillaring agent (Cr(VI) sites/Cr(III) nitrate) with smectites clays to be in the order Laponite® RD > bentonite > beidellite. Stacey (1988) explored the synthesis of alumina-pillared montmorillonite and Laponite® RD to determine their adsorptive properties. The results were characterized by XRD and adsorption of nitrogen, water, n-butane, methanol and neo-pentane with implications to the microstructures.

Matsuda *et al.* (1988) compared the physical and catalytic properties of montmorillonite, saponite and Laponite® RD pillared by alumina. According to XRD and N_2 adsorption studies, montmorillonite possessed well-ordered face-to-face lamellar structure, while Laponite® RD and Saponite aggregates possessed well-ordered face-to-edge or edge-to-edge manner. Saponite had strong Bronsted acidity compared with other pillared clays, perhaps because of the S-O-Al linkage present in the tetrahedral layer.

Occelli, *et al.* (1988), pillared Laponite® RD with organic cations, tetrapropyl and benzyltriethyl ammonium (BTEA) ions. On analysis with XRD and TEM the platelets of Laponite® RD were found to expand by 5.5Å and a surface area of 300 -350 m^2g^{-1} and was stable to 200^{o}C. Cool and Vansant (1996) investigated Zr-pillared Laponite® RD and hectorite and found that the clays exhibited differences in crystallinity, surface area and micropore volume in both the pure and pillared form, based mainly on particle size. However, Zr- Laponite® RD displayed greater adsorption capacities for N_2 and O_2 but low N_2/O_2 selectivity at 0^{o}C. Zr-pillared Laponite® RD showed increased surface area and micropore volume. Interestingly, the micro- and supermicroporosity of the Zr- Laponite® RD pillared hybrid made it useful as gas adsorbent.

1.4.2 Acid treatment

Acid treatment of mineral clay is normally carried out by one of two methods: (a) simple washing with mineral acid whereby the interlamellar cations is exchanged with protons (Laszlo, 1986) or (b), by heating in mineral acid. Acid treatment usually results in clays with loss of exchangeable cations to protons. Acid-activated clays are unstable and easily revert to their stable exchangeable cationic state by abstracting ions from the lattice (Ovcharenlco, 1982). Acid treatment conditions vary with one acid to another and are highly dependent upon the clays chemical composition, level of hydration and nature of the exchangeable cations possessed by the clay material (Vaccari, 1998). Acid-treated clays have been utilised as support for inorganic salt catalyst such as $ZnCl_2$, $FeNO_3$ and $CuNO_3$.

Acid treatment is not a new science. It has been in use for 50 years as in the catalytic cracking of oil in the Houdry process (Vaccari, 1998). However, improvement and development led to its replacement with zeolite in 1964 because of better activity and selectivity (Cornelis and

Laszlo, 1985). Acid-treated montmorillonites have been used to catalyse industrial processes including isomerisation, liquid refining and Friedel-Craft alkylation (Vaccari, 1998). In using these clay modification processes, the ultimate objective has been to fine-tune the characteristics of clay to achieve desirable properties.

1.4.3 Silane coupling

This is a process whereby a silane agent is used to modify the surfaces of silica and layered silicates (Prado *et al.,* 2005; Walcarius *et al.,* 2004; He *et al.,* 2005 and Celis *et al.,* 2000). For example, in the modification with organosilane, a covalent bond is established between the silicate layers, hydroxyl group and the silane molecules in a graft, such that a fictionalised inorganic layered material is formed with either restricted reaction to the external surface (which results in unchanged basal space) or an interlayer surface, whereby expansion at the interlayer exists (de Mello *et al.,* 2009). Literature has shown that such functionalised or hybrid materials synthesised become useful or suitable in adsorption of organic and inorganic pollutants (Okutomo *et al.,* 1999; Churchman *et al.,* 2006; Sayilkan *et al.,* 2004; Fonseca and Airoldi, 2000; Mercier and Pinnavaia, 1998). In addition they may exhibit specific chemical activities with functional groups - amino, thiol, vinyl and long carbon chains, which consequently impact their usage in adsorption, catalyst support (Kuzniarsska-Biernacka *et al.,* 2005), sensor and biosensors, electrode manufacturing (Tonle *et al.,* 2004), polymer or layered silicate nanocomposite (Herrera *et al.,* 2006), drug and enzyme support (Park and Kwon, 2004).

Chemical modification of natural mineral clays, particularly the smectites at their interlayer surfaces, has been well studied. For example, silane modified bentonite is used in the treatment of hard water and also the removal of heavy metals from soils as it exhibits a high

cationic exchange capacity. In addition, according to de Mello *et al.* (2009) bentonite is found in nature as natural deposits (although with impurities) which makes it cheap, and it is characterised by having a high specific surface area in relation to its particle size (Bergaya *et al.,* 2006; Abolino *et al.,* 2003; Brigatti *et al.,* 2004). In another study, bentonite was treated with acid and immobilised with ligands (containing thiol (-SH) groups) by covalent grafting with surface and interlayer silanol groups. The hydrophilic nature of the clay was found to change hydrophobically. Interestingly, the thiol-functionalised bentonite exhibited binding capacity of silver ions up to 10 times more compared to the non-grafted species. Thus, the adsorptive capacity of bentonite improved by surface modification with organo-functional silane coupling agents, showing that the resultant hybrid organo-inorganic material may become a vital tool in separation and pre-concentration of heavy metal ions (de Mello *et al.,* 2009).

1.5 Application of Laponite® RD

Clay minerals have found numerous applications and the variety of uses has continued to diversify due to the versatility and ease of adaptation of the minerals to different applications including adsorption, catalysis, drug support and antimicrobial agents. In addition, they have been utilized to control water, soil and air pollution (Bergaya and Lagaly, 2001) including rheological control, gel formation, paint thinning and thickening, and electrodes (de Paiva *et al*., 2008).

1.5a Colloidal gel and glass: Laponite dispersed in aqueous medium form numerous phases such as colloidal gel, glass, viscous fluid or phase separated flocs (Zebrowski *et al*., 2003; Ruzicka *et al*., 2011). Ruzicka *et al.* (2011) in his experiment demonstrated the topology of the phase diagram of Laponite in water and its slow ageing behaviour and found Laponite to be well in agreement with the behaviour predicted for platelets that interact with directional and anisotropic forces – ie patchy interactions.

Laponite possess anisotropy face-rim charge interaction, the combination of the disk shape and anisotropy of the face-rim charge interaction, produces a disordered phase (gel and glass) and an ordered (nematic) phase, on varying colloidal volume, at fixed ionic strength (Ruzicka *et al.*, 2011). However, at low concentrations (approximately 1wt.%) the system ages (or solidifies) very slowly up to a final non-ergodic state (Kegel and Lekkerkerker, 2011). The description of Laponite colloidal gel, its phases and relationship with glass was provided by Tanaka *et al*. (2004) as shown in Fig. 1.7, Laponite possess two types of isotropic disordered non-ergodic states in colloidal suspension which are gels and glasses. While the non-ergodicity or otherwise, elasticity of gel stems from the existence of a percolated network, that of glasses emanates from caging effects (Tanaka *et al* 2004). Despite this simple definition and/ or differentiation however, it is difficult to distinguish between the two phases experimentally (Tanaka *et al*., 2004). Laponite suspension have been used to demonstrate phase diagram for charge colloidal systems, and confirm that a transition from glass to gel state can be induced by changing the interparticle interactions from predominantly repulsive to attractive interactions (Tanaka *et al.*, 2004). These interactions are due to the competition that exist between electrostatic Coulom repulsion and van der Waals attraction. When repulsion becomes dominant glass (Wiger glass) are formed but when attraction predominates gel formation occurs, leaving out a midway region where both repulsive and

attractive interaction merge to form what is best described as an attractive glass (Tanaka *et al* ., 2004).

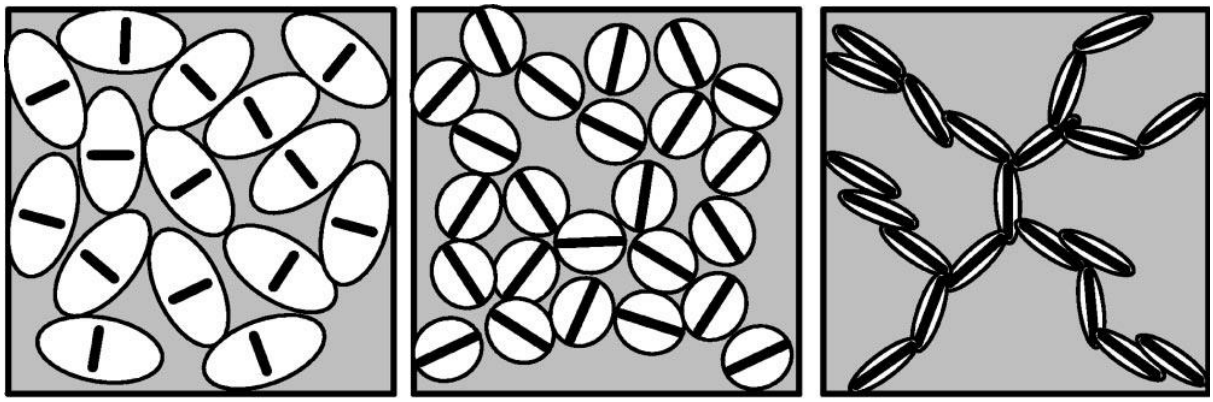

a b c

Fig: 1.7 Schematic representation of Laponite colloidal suspension. (a) repulsive "Wiger" colloidal glass, (b) attractive glass, (c) gel. Each thick line represents a Laponite disk, while a white ellipsoid represents the range of electrostatic repulsions. In (a), long-range electrostatic repulsions dominates, in (b), repulsive interactions still dominate in the slow dynamics of the system though, affected by the spatial distribution or structural factor. In (c), attractive interactions play a dominant role; a percolated network forms, which gives the system its elasticity (Tanaka *et al*., 2004).

However, the behaviour of Laponite colloidal suspension is different if mixed with a polymer. For example, the mixture of Laponite colloid with a long-chained, linear polymer such as polyethylene oxide with vigorous shaking resulted in an elastic gel. The gel was rigid enough to support its own weight and did not fall out from the jar (on which the gel was formed) when inverted (Zebrowski *et al*., 2003). Recently, a so-called "equilibrium gel", a predicted new state of soft matter was confirmed by Ruzicka *et al*. (2011). The new state opens interesting perspective for developing new material like creams or gels that may be both soft and extremely stable over long time (Ruzicka *et al*., 2011).

1.5b Ion exchange: Research has shown that ion exchange with cations such as alkylammonium ions could modify the hydration and swelling properties of Laponite. In a typical ion exchange of Laponite with Alkylammonium cation – resulted in the increase in free energy or adsorption strength, and a single layer of alkylammonium ions adsorbed between the Laponite sheets due to the van der Waals forces and the variation in the hydration state of Laponite (Vansant and Peeters, 1978).

Laponite intercalated Itraconazole via ion exchange reaction subsequently facilitated the slow release of Itracanozole. However, ion exchange reaction are often limited by Laponite hydrophilic surface that greatly inhibits the access to hydrophobic molecules into its reactive sites, mostly at the interlayer space. The situation is worse when the guest molecules are highly hydrophobic and bulky – this will further reduce the possibility to access the reactive site. In this case the conventional ion exchange becomes insufficient in the intercalation of guest molecule as was in the case of Laponite intercalated Itracanezole (Jung et al., 2008). However, prio modification of the surface with organic group renders Laponite accessible to hydrophobic groups and made its intercalation on the surface possible. This confirm that surface modification of Laponite with hydrophobic group could greatly enhance the intercalation rate of hydrophobic molecules via ion exchange without any effect to the crystal structure or uptake capacity (Park *et al*., 2004).

Jung *et al*. (2008) showed that the intercalation of Itracanezole in to Laponite via ion exchange agent did not only enhance the solubilty of Itracanezole but also assisted in the release rate from Laponite-itracanezole hybrid. The work also showed that Laponite (produced via ion exchange) could be used as a solubility controller and can substantially affect the release rate depending on the size of the ion exchange agent (Jung *et al*., 2008).

1.5c Isomorphous substitution: Isomorphous substitution has been used in the pillaring of Laponite by the Keggin cation (Bergaya *et al*., 1993). The isomorphous substitution in Laponite resulted in the negative surface charge – some magnesium ions are substituted by lithium ions forming a unit cell of -0.7e charge. These charges are uniformly distributed over the Laponite surface depending on the pH of the solution (Bergaya *et al*., 1993).

By definition Isomorphous substitution is the replacement of one atom by another of similar size in a crystal lattice during growth without changing the crystal structure (Clay Minerals, 1991). Isomorphous substitutions occur in both the tetrahedral and octahedral layer. For example in the tetrahedral layer Si^{4+} is substituted with Al^{3+} and in the octahedral layer Al^{3+} was substituted with Zn^{2+}. This leads to charge imbalance in Laponite which account for the permanent charge on Laponite particles. The imbalance is responsible for the ability of Laponite to attract ions to its surface (Clay Minerals, 1991). The main source of charge in Laponite is isomorphous substitution and pH-dependent charges. These sorts of charge developed during isomorphous substitution are permanent and does not depend on pH (Clay Minerals, 1991).

1.5.1 Catalysis

Laponite RD is an attractive material for the preparation of supported catalysts. For example, Fe modified Laponite RD catalyst have been used for the photo-Fenton degradation of Orange II and Acid Black I azo-dyes (Sum *et al*., 2005). Apart from its degradative function in the photo-Fenton degradation, Fe modified Laponite RD catalyst have been utilised in disinfection of water. Fe modified Laponite have often been used for the treatment of

commercial waste water beacause of the slowness of biological reactions during biological treatment (Buonocore *et al.,* 2010).

The generation of reactive oxygen species (ROS) have been shown to contribute to AgNPs mediated cytotoxicity in bacteria (Su *et al*., 2009; Kim *et al.,* 2007; Choi and Hu, 2008). The toxicity of ROS is due to its reaction with the components of DNA molecules, damaging both the purine and pyrimidine bases and also the deoxyribose backbone (Buonocore *et al.,* 2010). ROS induced DNA damage involves single or double stranded breaks, purine, pyrimidine or deoxyribose modifications, and DNA cross-links. DNA damage can also result to arrest or induction of transcription, induction of signal pathways, replication errors and genomic instability, all of which are associated with bacterial mutagenesis (Buonocore *et al*., 2010; Marnett, 2000).

In a comparative study with zeolite catalysts Occelli *et al.* (1984) used delaminated Laponite® RD, zeolite-promoted fluid catalytic cracking (FCC) and amorphous aluminosilicate catalysts. The amount of $C_5 - C_{12}$ gasoline obtained with Laponite® was close to that obtained using a zeolite catalyst but far less than that obtained from the amorphous aluminosilicate catalyst. Further in the study the Laponite® yielded higher light-cycle gas oil and lower yields of slurry oil than the zeolite counterpart.

Occelli *et al.* (1987) produced delaminated clay cracking catalyst by reacting sodium Laponite® RD and aluminium chlorohydrate solution and examined its thermal stability and pore size distribution together with other catalytically relevant properties. They concluded that the previously-proposed 'house-of-cards' structure, in which edge-face layer aggregation competes constructively with face-face aggregation, is compatible with the observed physicochemical properties. Thermal analysis and N_2 adsorption measurements indicated that the delaminated structure is retained up to 600^oC, and that heating above this temperature

resulted in nearly total collapse at 730^{o}C. The N_2 and n-pentane adsorption isotherms (type II) are according to BET equation as expected for a macroporous structure. Further, N_2 adsorption data, and Hg intrusion-derived pore sizes of the delaminated clay composed mainly of macroporosity, possessed a qualitatively close resemblance to amorphous aluminosilicate catalysts containing 22 wt.% Al_2O_3. However, this result contrasts with regular microporosity typical of alumina pillared clays which have a well-ordered face-face lamellar structure. Analysis with temperature-dependent IR studies of chemisorbed pyridine on delaminated Laponite® RD indicated that surface acidity is entirely of the Lewis type.

Tsoufis *et al.,* (2008) loaded different transition metals; Cr, Mn, Fe, Co, Ni, Cu and Zn on to smectites; Laponite® RD and montmorillonite as catalyst for the synthesis of carbon nanotubes. Fe, Co, Ni, and Mn -exchanged Laponite® RD were shown to be effective catalysts in the synthesis of carbon nanostructures, while Cu-exchanged Laponite® RD decomposition with acetylene formed carbon spheres. The Ni- exchanged Laponite® RD species gave better crystalline carbon deposits and yielded twice the corresponding carbon amount when compared with the Ni-montmorillonite.

1.5.2 Adsorption

Clays are natural environment-friendly materials that belong to a class of low-cost alternative adsorbents for removal of dyes from contaminated water or wastewater, being placed below alumina, (Adak *et al*., 2005; Adak *et al*., 2006; Huang *et al.,* 2007) silica gel, (McKay *et al.,* 1999) zeolite (Wang and Ariyanto, 2007; Al-Degs *et al.,* 2001; DiGiano and Natter, 1977; Pelekani and Snoyink, 2000; Walker and Weatherley, 1999) because they occur naturally, and may be obtained from waste, or as by-products of industrial processes which make them cheap and readily available alternatives (Gupta and Suhas, 2009).

Cationic surfactant (dodecyltrimethyl ammonium bromide and ethane dibromide)-adsorbed Laponite® RD was used for the adsorption of 2-naphthol and copper ions (Esumi *et al.,* 1999) and showed the simultaneous removal of non-ionic and ionic substances. Previously, David *et al*., (1994) used surfactants to remove toxic material from the soil. This was possible because clay minerals possess ion exchange capacities hence possible to remove toxic non-ionic organic substances and metal ions from soil by surfactants-adsorbed clays (Esumi *et al.,* 1999).

1.5.3 Drug delivery system

1.5.3.1 Laponite® RD - drug interaction

The pharmaceutical industry has witnessed the resurgence of 2-dimensional structured minerals in drug delivery systems. These include smectites, palygorskite, kaolinite and talc (Lee and Fu, 2003; Choy *et al.,* 2004a and Park *et al.,* 2004) having adaptive features such as large specific surface area, increased adsorption capacity, improved rheological property, chemical inertness, with little or no toxicity (Lee and Fu, 2003), Laponite have become well suited to pharmaceutical formulations (Jung *et al* ., 2008b).

However, among the 2-dimentional structured minerals, smectites have showed exceptional potential in their drug delivery capacity, e.g. intercalation of the cytotoxic anticolorectal cancer drug, 5-fluorouracil in montmorillonite (Lin *et al.,* 2002). The intercalation of large molecules into their interlayer space, followed by release via ion exchange (Park *et al.,* 2004) enhanced their efficiency in drug delivery. The interlayer space is large and thus bound neutral drug molecules by ion-dipole interaction but in contrast hybridizes cation or bio-functional groups through ion exchange (Jung *et al.,* 2008b). For instance, the poorly-dissolving water-soluble drug, Itraconazole was hybridized into Laponite® RD to examine its drug release pattern. The drug release rate was low in the aqueous medium and overall

showed low bioactivity (Jung *et al.,* 2008b; Jung *et al.,* 2008c). Although, studies in drug release are limited and clay-drug nanohybrid mechanisms not clearly understood (Jung *et al.,* 2008b). However, the observed slow release rate demonstrated potentiality. In an earlier study Jung *et al.,* (2008a) showed that the Laponite® RD -Intraconzole hybrid indicated no significant change in chemical structure of Itraconzole or in the Laponite® RD. The hybrid demonstrated enhanced solubility and controlled release of itraconzole, up to 75%, which was largely dependent on the cation present in the media (Jung *et al.,* 2008b; Jung *et al.,* 2008c).

Different systems have been designed to incorporate biological materials into inorganic agents (Choy *et al.,* 2004; Choy *et al.,* 2000; Choy *et al.,* 1999). The advantage with these delivery systems is that they provide a controlled, as well as efficient, delivery of therapeutic agents to target tissues or organs (Jung *et al.,* 2008a). Furthermore, following the intercalation of these molecules into the interlayer spaces and consequent stabilisation via electrostatic forces, these molecules are thus protected chemically and biologically from the host's body defences. In addition, the water solubility of the drug is greatly enhanced, being distributed in its ionic form, a point crucial to controlled release of drug such as Intraconazole with a low solubility (Jung *et al.,* 2008a).

Park *et al.* (2008) successfully intercalated the Alzheimer's disease drug, donepezil into smectites clays (Laponite® XLG, saponite and montmorillonite). The donepezil molecules were stabilised within the interlayer spaces of the clays through mono or double layer stacking, while the molecular structure and adsorption quantities depended upon the nature of the cation exchange capacity of the clay. However, the set-up showed improved release rate in the presence of the bulky cationic polymer Eudragit® E-100 because of its effective replacement by intercalated donepezil molecules.

1.5.3.2 Mechanism of interaction

Clay minerals are widely used in pharmaceuticals either as excipients or active agents. Observation and study of clay-drug interactions have shown that specific clay properties such as high retention capacities, swelling and colloid formation, are useful in modulating drug release or delivery (Aguzzi *et al.,* 2007). Interestingly, clays are not the only excipient or inert ingredients in clay-drug formulations. Clay provides targets for a biopharmaceutical product by decreasing or increasing dissolution rate, or targeting drug release (Chien and Lin, 2002). Furthermore, they may be of pharmacological nature (preventing or reducing side effects), technological (by masking taste) or chemical when they increase stability of a drug (Aguzzi *et al.,* 2007).

Various approaches have been proposed to achieve controlled drug release in pharmaceutical formulations. However, the method that has gained the attention of researchers is the ion exchange process (Vikas *et al.*, 2001) whereby the substrate (i.e. the ion exchanger) is mixed with the ionic drug in solution. In systems such as biological fluids, counterions displace the drug from the substrate or exchanger and eventually release it into the host's body. The exchanger then degrades and is subsequently eliminated from the host. Fig. 1.7 shows the *in vivo* mechanism of clay-drug interaction

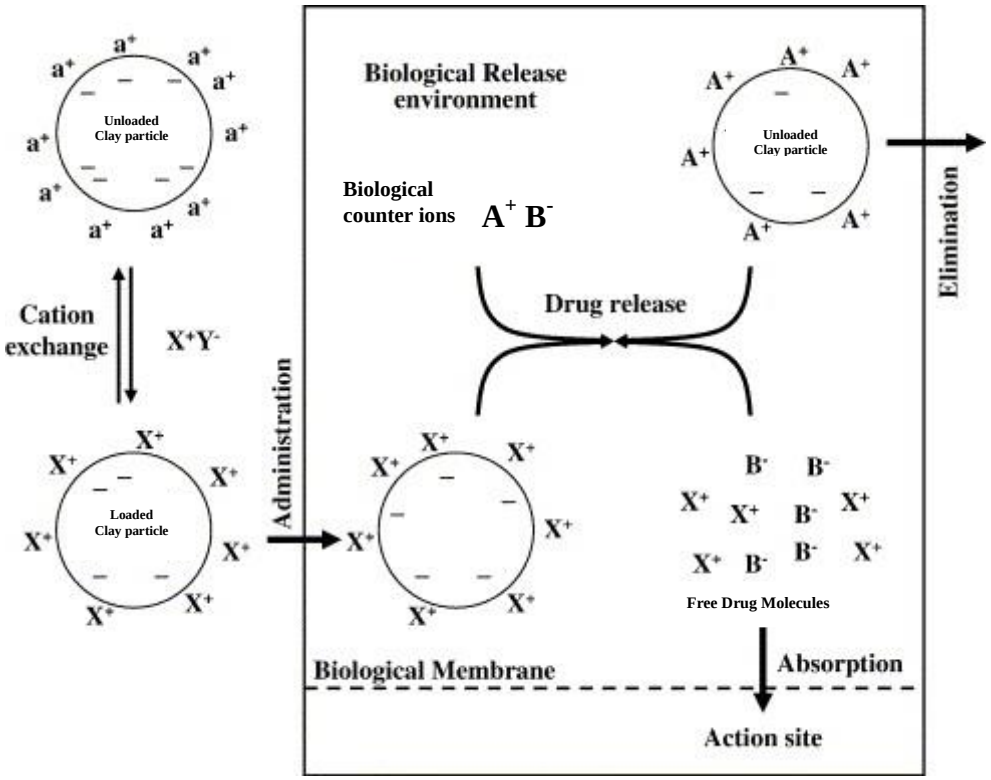

Fig.1. 8: Idealised *in vivo* mechanism of clay-drug interaction (Aguzzi *et al.*, 2007).

Montmorillonite and saponite are the most widely studied inorganic cationic exchanger clays of the smectites, perhaps for their relatively higher cation exchange capacity when compared to other pharmaceutical silicates such as talc, kaolin or fibrous clays (Aguzzi *et al.*, 2007). Several mechanisms are involved in the interaction of clay and drug in monohybrid formulations. The mode of action or mechanism of release is largely dependent upon the clay mineral involved (Browne *et al.*,1980), functional groups of the molecules (Lagaly, 2001), and physical and chemical properties of participating species (Tolls, 2001). Table 1.4. Summarise the interaction of some clay minerals and organic molecules.

Table 1. 4: Interaction between clay minerals and organic compounds (Aguzzi *et al.*, 2007)

Mechanism	Mineral examples	Organic functional groups involved
Hydrophilic interactions (van der Waals)	Any clay with neutral sites (e.g., kaolinite, smectites)	Uncharged, non-polar (e.g., aromatic, alkyl C)
Hydrogen bonding	Any clay with oxygen surfaces (e.g., kaolinite)	Amines, carbonyl, carboxyl, phenylhydroxyl, heterocycle N
Protonation	Aluminosilicate edge sites, Fe and Al oxides, allophane, imogolite	Amines, heterocycle N, carbonyl, carboxylate,
Ligand exchange	Aluminosilicate edge sites, Fe and Al oxides, allophane, imogolite	Carboxylate, Phenolate
Cation exchange (permanent charge sites)	Smectite, vermiculite, illite	Amines, ring NH, heterocyclic N
pH-dependent charge sites (anion exchange usually, cation exchange rarely)	Aluminosilicate edge sites, Fe and Al oxides, allophane, imogolite	Carboxylate for anion exchange, amines, ring NH, heterocyclic N for cation exchange
Cation bridging	Smectite, vermiculite, illite	Carboxylate, amines, carbonyl, alcoholic OH

As reported in Aguzzi *et al.* (2007), previous studies have already elucidated the function of key parameters, such as drug concentration, pH, temperature, dielectric constant, electrolyte concentration and valence in clay-drug adsorption as well as desorption processes, for example in smectites (McGinity and Hill, 1975; Aguzzi *et al.*, 2003; Figueroa *et al.*, 2004), kaolin (Armstrong and Clarke, 1973; Figueroa *et al.*, 2004), halloysite (Viseras *et al.*, 2004; Viseras *et al.*, 2005) and fibrous clays (McGinity and Hill, 1975; Al-Gohary *et al.*, 1987; Al-Gohary *et al.*,1988). These interactions coupled with the unique swelling properties of clay minerals have made them vital and efficient in delayed- or extended-release systems and target- or site-specific releasing systems (Aguzzi *et al.*, 2007). Recently researchers have focused more on drug release patterns and improved drug stability. Table 1.5 illustrates recent strategies involving increasing drug stability while simultaneously enhancing drug delivery patterns in clay delivery systems.

Table 1.5: Drug delivery systems based on clay minerals (Aguzzi *et al.*, 2007).

Issue	Target parameter	Delivery system	Mechanism	Excipients	Original clay
Release Pattern	Dissolution rates	Extended Release Systems	Clay mineral-drug interaction	Natural clay minerals with high cation capacity values.	Smectites, Fibrous clay minerals.
				Synthetic clay minerals.	LDH, hydrotalcites.
				Modified clay minerals and Acid/thermal activated	Bentonite or kaolinite.
				Pillared layered structures.	Montmorillonite and others smectites
				"Swelling clays"	Smectites
			Clay swelling	Montmorillonite	
		Improved Drug Solubility Systems	Adsorption		
		Site-specific systems		Montmorillonite and LDH(oral release)	
	Site of release		Enteric coated	Smectite and halloysite (Local release)	
			Bioadhesion		
Drug Stability and Targeting	Hydrophilic ambient (sensible molecules) and Distribution Profiles	Microparticles.	Encapsulation	Halloysite	
		Nanoparticles	Surface precipitation, inclusion, others	Porous-hollow nanoparticles	Porous silica from clay minerals, halloysite
			Clay-polymer interaction	Clay-polymer nanocomposites	Montmorillonite

1.5.4 Antimicrobial Activity

Antimicrobial application of synthetic Laponite® RD is an emerging area in scientific research. The search continues for more applicable, repeatable, convenient and safe methods to incorporate silver or copper nanoparticles in Laponite® RD structure. Work has suggested that there are two possibilities of modifying the Laponite® RD structure: replacement of the

replaceable sodium ion or the substitution of Li ions within the framework structure (Grandjean and Laszlo, 1991). In either of these reactions the major concerns are the rheological properties that may be altered. Greaves *et al., (*1995) showed that the sodium ions were completely exchanged with potassium ions, and the result was a highly conductive Laponite® RD particle but without the gelling characteristics. McWhinnie *et al.* (1992) obtained a similar result when phenyltin was intercalated onto Laponite® RD. However, of all the monovalent ions exchanged with commercial Laponite® RD only the sol-gel species with higher sodium content exhibited gel formation with water (Greaves *et al.,* 1995).

Silver nanoparticles prepared by photo reduction of $AgNO_3$ in layered Laponite® RD were found to be stable but possessed potent antimicrobial property only for a few months (Huang and Yang, 2008). In another preparation of silver nanoparticles in a Laponite® RD sol, Liu *et al.* (2009) used sodium borohydrate ($NaBH_4$) as the reducing agent. The results suggested that stability and high concentration of the Ag nanoparticle is a crucial requirement in antibacterial agents.

1.6 Use of silver and its compounds

The growing concerns of antimicrobial resistance to antibiotics and spread of infectious diseases caused by pathogenic bacteria have lead scientists to search for novel antibacterial agents to combact disease.

Due to growing microbial resistance against antibiotics and organic antimicrobial agents such as triclosan, hexachlorophene and quaternary ammonium compounds (McDonnell and Russell, 1999), many inorganic metals have been described as antibacterial agents, such as copper, zinc, titanium (Retchkiman-Schabes *et al.,* 2006) gold, magnesium (Gu *et al.,* 2003)

and silver (Table 1.6). Among these silver, especially in a nanoparticle form, has proved to be more effective against a wide spectrum of microorganisms including bacteria, fungi and viruses (Rai *et al.,* 2008 and Gong *et al.,* 2007).

Table 1.6: Properties of silver (Adapted from Silver, 2003 and Everett, 2011)

Characteristics	**Description**
Atomic number	47
Atomic weight	107.868 g mol-1
Electronic configuration	[Kr] 4d105s1
Covalent radius	1.34 Å
Valency	+1 or +2
Atomic radius	1.75 Å
Ionic radius	1 Å
Covalent radius	1.34 Å
Atomic volume	10.3 cm3 mol-1
Crystal structure	Cubic: face centred
Melting point	961.3 ^{o}C
Boiling point	2212 ^{o}C
Density at 20 ^{o}C	10.5 g cm-3

1.6.1 Silver applications

1.6.1.1 Medical application

The use of silver dates back to 1938 and has proved effective against a broad spectrum of microbial activities (Atiyeh *el al.,* 2007, Clement and Jarrett, 1994). In the 19th century, it was the treatment of choice for tetanus. Before the discovery of antibiotics in the 20th century, silver had already found use for common cold and gonorrhoea disease management.

1.6.1.2 Textile application

Silver in the textile industry was utilised for its potent odour removal and antimicrobial action on fibres and fabrics (Anonymous, 2006). The product 'SmartSilver' was developed as part of a new 'nanotechnology', and it has an impressive performance in that while it maintains anti-odour characteristics, fabric construction, durability and elasticity remain uncompromised (Anonymous, 2006).

1.6.2 Silver compounds

1.6.2.1 Colloidal silver

This is one of the various silver products available and was the most common delivery system prior to 1960. Colloidal silver solution is composed of pure silver charged particles of between 3 and 5 mg/L, held together tightly in a suspension by an electric current (Atiyeh *et al.,* 2007). Colloidal silver is less stable than silver salt but unique in that it remained in solution when applied topically to a wound (Atiyeh *et al.,* 2007). Colloidal silver has been proven to be relatively safe for humans, plants and all multi-celled living matter according to Dallas *et al*. (2011).

1.6.2.2 Silver salt

Silver salts were preceded by delivery products based upon silver-complexed proteins which were stable in solution. However, because of their low antibacterial properties, especially when compared with pure ionic silver, they were rapidly phased-out by silver salts in the 1960s (Atiyeh *et al.,* 2007). Silver salt gains its additional stability from the positively charged silver ion being complexed with negatively charged ions as observed in AgCl, $AgNO_3$ or $AgSO_4$ (Atiyeh *et al.*,2007).

Various concentrations of $AgNO_3$ have been tested and a 0.5% solution was found to be the lowest concentration that remained active against bacteria, both *in vitro* on solid agar or broth medium and *in vivo* on burns, and 0.5 % $AgNO_3$ is regarded as the standard and most popular silver salt solution used for topical burn wound treatment (Klasen, 2000). For maximum effectiveness of $AgNO_3$ in wound dressing, the wound is first cleared from fat ointment and dead tissue. To enhance debridement, the patient involved was bathed in Locke's solution for 2 to 6 hours, up to three times a week (Klasen, 2000).

Silver nitrate has been found to be active against a wide range of bacteria including *Staphylococcus aureus*, haemolytic streptococci, *Pseudomonas aeruginosa* and *Escherichia coli*. However, research shows that *Aerobacter* species and other human skin flora remain insensitive to $AgNO_3$ (Klasen, 2000; Moyer *et al.,* 1965). Klasen (2000) reported no insensitivity or resistance following $AgNO_3$ administration. However, a major complication was a drop in serum sodium and chlorine which was attributed to ion exchange between, Ag^+ ions and Cl^-, HCO_3^-, CO_3^{2-} and protein anions leading to the formation of a slight soluble or insoluble salt solutions, an indication that the bacteria was unaffected (Klasen 2000). In addition, $AgNO_3$ treatment led to a black deposit on objects that came in contact with it on exposure to light, but these were easily washed off with hot soapy water or Westcodyne (Klasen, 2000). Contrary to earlier assumptions, Bader (1966) reported significant levels of silver in kidneys, spleen, liver and muscles when *post-mortem* examination was made on two patients. Bacterial resistance to $AgNO_3$ has also been described by Atiyeh *et al.,* (2007).

1.6.2.3 Silver sulphadiazine

Silver sulphadiazine has been widely studied for its antimicrobial efficacy on microorganisms and has been used intensively for burns and wound treatment during the 1970s (Atiyeh *et al.,*

2007) and it was termed the ‘ultimate’ antibacterial agent for topical treatment of burns and wounds. Yet silver sulphadiazine does not offer enough protection to prevent or decelerate the growth of gram-negative bacteria, especially in patients with burns covering more than 50% of the body surface (Klasen, 2000). Subsequently it became common practice to supplement silver sulphadiazine with cerium nitrate for co-operative effectiveness (Fox and Modak, 1974). By composition, silver sulphadiazine is a combined formulation of silver nitrate and sodium sulphadiazine as a result of substituting the metal atom for hydrogen in the sulphadiazine molecule (Klasen, 2000). Interestingly, the effectiveness of silver sulphadiazine appeared to depend upon the slow but continuous release of silver ions into the surrounding wound area and its intense reaction with wound body fluids such as serum and sodium chloride-containing fluids (Fox and Modak, 1974).

The field gradually gaining acceptance with innovation and rapid development is that of nanotechnology. This emerging science holds great potential for researchers (and pharmaceutical companies) looking at antimicrobial resistance because of the unique chemical and physical properties, and high surface area to volume ratio (Morones *et al.*, 2005; Kim *et al.*, 2007).

Nanomaterials are an emerging area in nano-science and nano-technology. This field has attracted huge interest in recent years and may provide solutions to technological and environmental difficulties such as solar energy conversion, catalysis, in medicine and water treatment. (Sharma *et al.*, 2008). Smith *et al.*, (2006); Kearns *et al.*, (2007) cited in Sharma *et al.*, (2008) reported silver, copper and gold use in synthesis of stable dispersions of nanoparticles utilised in photography, catalysis, photonics, optoelectronics, biological labelling and surface-enhanced Raman scattering (SERS) analysis. Nanocrystalline silver, more recently referred to as silver nanoparticles, differ considerably in their biological,

physical and chemical properties from the micro- and macro-scaled materials (Li *et al.,* 2008a).

In wound care, the use of nanocrystalline products, e.g. Anticoat^{TM}, have reduced the problem of rapid inactivation and frequent application experienced when using silver nitrate or silver sulphadiazine (Atiyeh *et al.,* 2007). On examination of nanocrystalline silver in wound care Dunn and Jones (2004) affirmed the active ingredient as Ag^0 which is less rapidly deactivated by organic matter or chloride than the ionic form, Ag^+, stating further as the silver released in to the wound is consumed by the protein target cells in the wound fluid more silver is released from the dressing. Consequently, a sustained and steady supply of silver to the wound is maintained that ultimately affect wound healing. It has also been shown that silver nanoparticles release silver ions that enhance bactericidal activity (Klasen, 2000; Huh and Kwon, 2011).

1.6.2.4 Nanocrystalline silver

Nanocrystalline silver provides a steady and sustained silver releasing system. This has been termed by Atiyeh *et al.,* (2007) as the latest and "greatest innovation" in wound care products and perhaps the most sought after of the silver forms (Dallas *et al*., 2011). It was termed greatest because the silver itself is incorporated within the dressing matrix as opposed to direct topical application found in other silver delivery products. However, this delivery system is not without challenges, including choosing the carrier dressing and the eventual delivery of silver to the wound by the dressing matrix (Atiyeh *et al.,* 2007). Examples of this type of silver delivery system products include Acticoat, Actisorbsilver, Aquacell, Silverlon, SilvaSorb and Arglaes (Atiyeh *et al.,* 2007).

1.6.3 Mechanism of toxicity of silver to microorganisms

Although, the exact mechanism of action of silver on microorganisms is still unclear, possible mechanism of action has been suggested based on morphological as well as structural changes in bacterial cells (Rai *et al.*, 2009). Klasen, 2000 reported silver interaction with the thiol group in respiratory enzymes of bacterial cells. Silver acted by inhibiting the uptake of phosphate and releasing phosphate, mannitol, succinate, proline and glutamine from *E. coli* cells (Rosenkranz, and Carr 1972; Bragg and Rainnie, 1974 and Yamanaka *et al*., 2005). Silver ions interact with DNA turning it into a condensed form (bacteria in condensed form are inactve) and thus loss of it replication ability (Feng *et al.*, 2000).

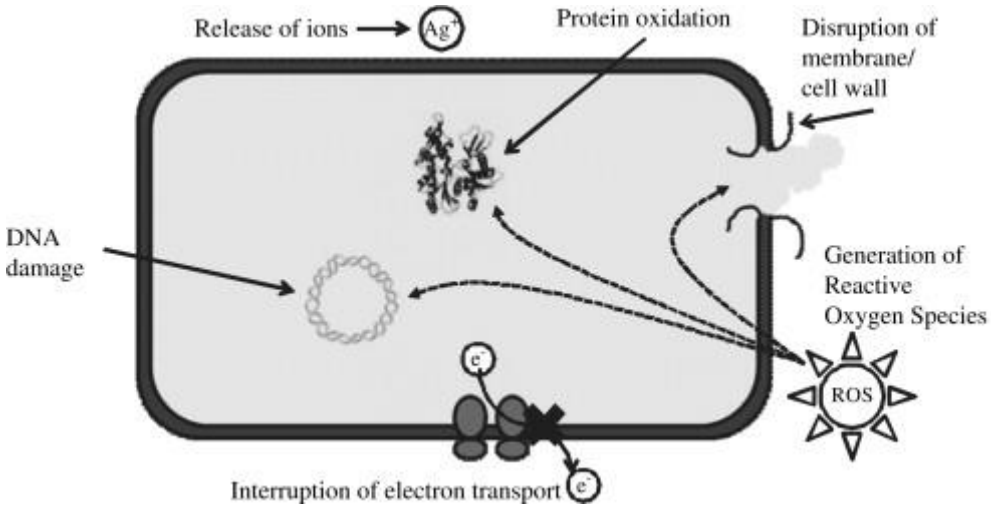

Fig.1.9: Various mechanisms of antimicrobial activity exerted by silver (Li *et al*., 2008b)

Silver nanoparticle interacts with microbial cells through a variety of mechanisms (Fig. 1.8). Silver nanoparticles have been reported to act directly with the microbial cells by interrupting transmembrane electron transfer, disrupting and penetrating the cell envelope, oxidizing cell

components or producing secondary products such as reactive oxygen species or dissolved silver ions resulting in damage to the cell (Li *et al*., 2009a, Li *et al*., 2009b). Upon entry of silver nanoparticles into the bacterial cell it forms a low molecular weight region in the centre of the cell to which the cell accumulate, in effect, protecting the DNA from the silver ion released. The silver nanoparticles preferentially attack the respiratory chain, cell division which ultimately results in cell death (Rai *et al*., 2009a). The silver nanoparticles release silver ions in the bacterial cells which enhance it bactericidal activity (Feng *et al*., 2000; Song *et al* 2005; Morones *et al*., 2005; Sondi and Salopek-Sondi, 2007). Silver nanoparticles affect many different functions of microbial cells, making it non selective and so exhibit antimicrobial property against a broad spectrum of microorganisms including bacteria, fungi and yeasts (Feng *et al*., 2000; Silver *et al*., 2003).

1.7 The uses of copper

Copper was first discovered as a sanitizer by the ancient Greeks in the 4th century BC. It was used to purify drinking water and was prescribed for pulmonary disease (Borkow and Gabbay, 2005). Hindus store water in copper vessels for its anti-fouling and bacteriostatic properties. Phoenician sailors nailed copper strips to their ships' hulls to prevent fouling in order to maintain cleaner vessels for faster and easier manoeuvring (Borkow and Gabbay, 2005). Copper in the 18th century emerged as an effective combatant in the western world for use in clinics, and was used for the treatment of mental disorders and lung ailments.

The use of copper as an antimicrobial agent came into the limelight as a result of pervasive antimicrobial resistance especially in the medical sector. The search for an alternative method to reduce the bioburden in healthcare institutions and their facilities aroused curiosity in discovering unconventional ways of disease prevention. Copper has been identified to exhibit

antibacterial and antifungal properties (see Table 1.7). It has been utilised in water purification, paint, building materials and in the textile industry (Mehtar *et al.*, 2007).

Table 1.7: Properties of copper (Adapted from Everett, 2011)

Characteristics	**Description**
Atomic number	29
Atomic weight	63.546 g mol-1
Electronic configuration	[Ar] 4s-1 3d10
Covalent radius	1.17 Å
Valency	+2 or +1
Atomic radius	1.57 Å
Ionic radius	1 Å
Covalent radius	1.17 Å
Atomic volume	7.1 cm3 mol-1
Crystal structure	Cubic: face centred
Melting point	1084.62 ^{o}C
Boiling point	2562 ^{o}C
Density	8.96 g cm-3

Noyce *et al.,* (2006) and Faundez *et al.,* (2004) reported copper activity against methicillin resistant *Staphylococcus aureus* (MRSA) and *Escherichia coli* O157, *Campylobacter jejuni* and species of *Salmonella.* Singh *et al.,* (2006) reported the biocidal effect of copper on the multidrug-resistant and extremely drug resistant species of *Mycobacterium tuberculosis* in a hospital in South Africa. Inhibition of enteropathogen (*Salmonella enteric*, and *Campylobacter jejuni*) by metallic copper surfaces was investigated by Faundez *et al.,* (2004).

Copper has been used in conjunction with other metals as well as its salts. American navigators placed copper and silver coins in wooden water casks to provide safe drinking

water for their long journey (Borkow and Gabbay, 2005). NASA, for their Apollo flights, used an ionized copper-silver water sterilizing system. Copper sulphate has a proven usefulness in treatment of sores and skin disease, especially in Africa and Asia (Borkow and Gabbay, 2005). Zhao *et al.,* (1998) investigated surfaces coated with different inorganic materials such as copper, zinc, cobalt and cobalt containing alloys of nickel, zinc and chromium, and found a significant inhibition of growth in the pathogenic bacteria examined. However, the challenge in the use of copper is decolourisation, which it presents on exposure to air or oxygen (Mehtar *et al.,* 2007).

1.7.1 Application of copper and its compounds

1.7.1.1 Copper as a fungicide

Copper has become increasingly significant in agriculture. The first recorded use of copper as compound for agricultural purposes was in 1761 for the control of seed-borne fungi (Borkow and Gabbay, 2005). As copper sulphate, it soon became a popular and widespread measure in the control of fungi-infected seeds. The greatest achievement of copper as antifungal agent was reported in 1880 by the French scientist Millardet, who made a mixture of copper sulphate, lime and water and sprayed it on grapes and vines. The infested plants became free from downy mildew. This formulation, forever known as "Bordeaux" mixture, became the fungicide of choice in the United States. Another formulation was "Burgundy" mixture, again of French origin, and was made up of copper sulphate and sodium carbonate. This mixture soon became the established treatment for various fungal diseases of plants. Thus, copper became renowned and gained worldwide popularity as an effective fungicide (Borkow and Gabbay, 2005).

1.7.1.2 Copper as an algaecide

Copper inhibits the growth of algae and it has been used to prevent algal growth in portable water reservoirs, control of green slime and algal scums in farm ponds, rice fields, irrigation, drainage canals, rivers, lakes and swimming pools. However, the major drawback in copper sulphate is its toxicity to aquatic life. Sulphate ions in aqueous medium readily combine with hydrogen to form sulphuric acid which is corrosive (Borkow and Gabbay, 2005). In view of this challenge and the quest for a safe and habitable environment, copper chelate were formed. Chelated copper is non-reactive and does not interact with other chemical substances in water (Borkow and Gabbay, 2005). However, copper sulphate is still very popular for algal control probably because of its ease of application and low cost (Plum, 1991).

1.7.1.3 Copper as a molluscide

Appropriate measures in snail control may bring an end to some human diseases like bilharzia. Bilharziasis is caused by the trematode parasite, *Schistosoma mansoni* using snails and humans as hosts. The International Copper Research Association screened 23 copper compounds including cupric chloride-bis-n-dodecylamine, copper nitrate and copper sulphate for their molluscidal activity in low and high alkalinity, with and without high levels of suspended solids (Borkow and Gabbay 2005). The molluscidal activity was found to be in the order: cupric chloride-bis-n-dodecylamine, > copper nitrate > copper sulphate (www.copperinfo.co.uk).

1.7.1.4 Copper as a virucide

The antiviral activity of copper was first observed by Yamamoto in 1964. He noticed the inactivation of some bacteriophages after copper was applied. Jordan and Nassar, (1971) showed that copper was effective against the virus of the bronchus. Research continued until 1974, when Totsuka and Ohtaki, (1974) reported copper sulphates effect on poliovirus RNA in proportion to its concentration and that most amino acids, with the exception of cysteine, form a protective covering against metal ions such as copper, iron and aluminium (Borkow and Gabbay, 2005). Cupric and ferric ions inactivated different enveloped- or non-enveloped, single- or double-stranded DNA or RNA viruses; phi X174, T7, phi 6, junin and HSV, as investigated by Sagripanti, (1992) and Sagripanti *et al.*,(1993).

The study by Sagripanti *et al* (1993) showed that metals were more effective than glutaraldehyde in the viral inactivation process. Further, on addition of peroxide, the inhibitory effect of Cu^{2+} was greatly enhanced and the viruses were less resistant to copper-peroxide than iron-peroxide, based upon their metal concentrations. Cupric and ferric ions were shown to inactivate the human immunodeficiency virus Type 1 (HIV-1) when it was free in solution, *in vitro*, and after 3 hours of cell infection *in vivo* (Sagripanti and Lightfoote 1996). The investigation further revealed the achievement of 50% inactivation of cell-free Type 1 Human Immunodeficiency Virus (HIV-1) with Cu^{2+} (concentration 0.16-1.6 mM) or Fe^{3+} (concentration 1.8-18 mM), being higher than the equivalent amount required to inactivate the same HIV-1 by glutaraldehyde (0.1mM), sodium hypochlorate (0.3mM) and sodium hydroxide (11.5mM), but significantly lower than those for ethanol requiring 360mM for HIV-1 total inactivation. (Sagripanti and Lightfoote, 1996).

1.7.2 Mechanism of toxicity of copper to microorganisms

Copper, like other metals, is toxic to microorganisms especially at high concentrations. This is possible either through displacement of essential metals from their natural binding sites or through ligand interactions (Fig. 1.9). Another way toxicity may occur is from changes in structural conformation of nucleic acid proteins, interference with oxidative phosphorylation and, rarely, osmotic balance.

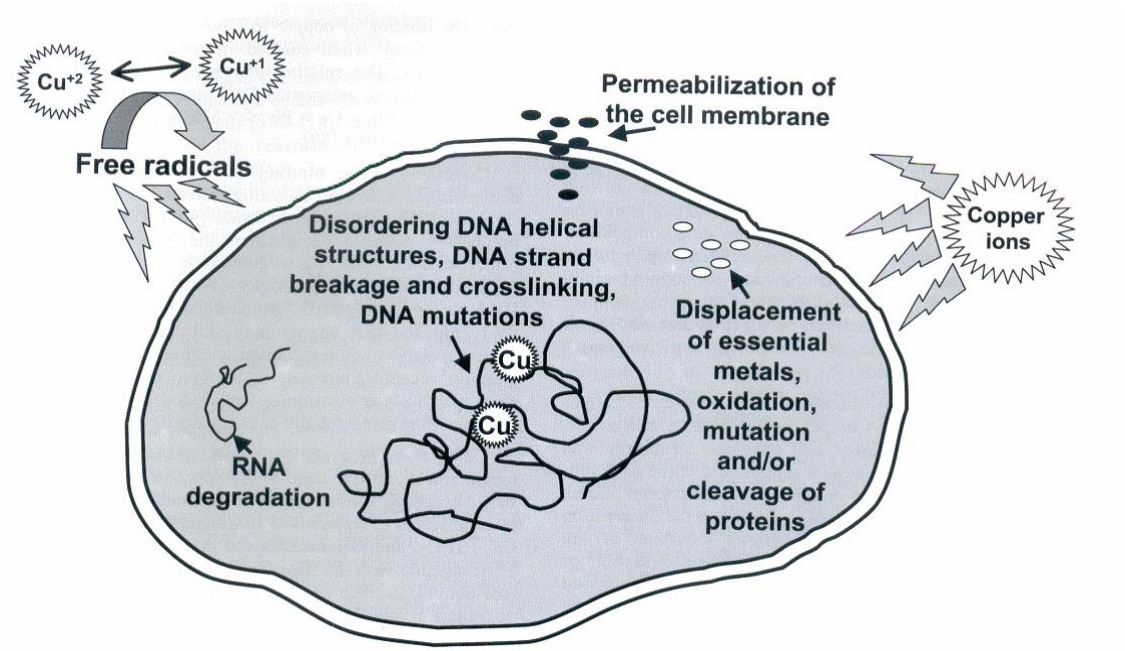

Fig.1.10: Mechanisms of toxicity of copper to microorganisms (Borkow and Gabbay, 2005).

Generally, non-essential metals tend to readily bind to thiol-containing groups and oxygen sites. Copper is a vital element in biological systems because of its redox properties on account of its inherent toxicity. For instance, as illustrated in Fig. 1.8 the redox-cycling inter-conversion of Cu^{2+} to Cu^{1+}, and *vice versa*, may give rise to the catalytic production of highly

reactive hydroxyl radicals. This resultant hydroxyl radical damages biomolecules including lipids, protein and DNA (Borkow and Gabbay, 2005).

1.7.2.1 Copper mediated cell membrane damage

The initial site of action of copper on microorganisms is in the cell membrane. Cervantes and Gutierrez-Corona (1994) exposed fungi and yeast to varying concentrations of copper and noticed a rapid decline in membrane integrity. The initial evidence is a leakage of mobile cellular solutes, such as potassium ions and eventually cell death (Ohsumi *et al.*, 1988). Prolonged metal-induced disruption of membrane integrity promotes loss of cell viability. In many cases, an alteration in the physical properties of biological membranes usually results in marked changes in activities of various essential membrane-dependent functions such as transport protein activity, phagocytosis and ion permeability (Hazel and Williams, (1990); Avery *et al.*, 1995). Generally, the physical properties of a membrane are largely dependent on the lipid composition, which in turn relies upon the degree of unsaturated fatty acid. The fatty acid composition of microbial membranes is highly variable and easily influenced by environmental as well as their inherent factors. Low temperatures increase the unsaturated fatty acid content in microorganisms (Hazel and Williams, 1990, Murata, 1989). As has been suggested, in the relationship between plasma membrane, fatty acid composition and copper toxicity, there was a significant increase in copper-induced plasma membrane permeability and whole-cell toxicity of *Saccharomyces cerevisiae* when it was enriched with polyunsaturated fatty acids (Avery *et al.*, 1996).

1.7.2.2 Copper interaction with nucleic acid

Copper has a specific affinity for DNA, it can bind and disorient helical structures by cross-linking within and between strands (Borkow and Gabbay, 2005). In ddition, Cu^{2+} reversibly denatures DNA in low ionic strength solution by competing with hydrogen bonding present within the DNA molecule (Hostynek *et al.,* 2003). Sagripanti, (1991) showed a DNA double helix containing two kinds of binding site for copper in a kinetic study. One site with high affinity for copper was present on every four nucleotides. The other was an intercalating site for copper present in every base pair. In a copper-DNA binding study, Sagripanti, (1991) revealed that copper exhibited an extremely high specificity to DNA in the presence of other metallic ions. The propensity of different divalent cations to displace Cu^{2+} binding was in the order: Ni = Cd = Mg >>> Zn = Hg > Ca > Pb >>> Mn, adding that Cr^{6+} aided Cu^{2+} binding to DNA.

DNA soaked in cupric chloride showed guanine specific binding of Cu^{2+} in a double stranded DNA (Geierstanger *et al.,* 1991). The covalent bonding occurred at the N-7 position, and this occurrence of preferential Cu^{2+} binding to guanine bases in DNA may throw more light in the already suggested report of specifically Cu^{2+}-induced oxidative DNA damage occurring at the guanine residue (Sagripant and Kraemer, 1989; Yamamoto and Kawanishi, 1989). Further, Morris and Hay, (2001) as cited in Borkow and Gabbay, (2005) suggested copper stabilizes the helix structure through formation of a charge transfer complex by acting as an electron acceptor, in which case it intercalates between two adjacent guanine – cytosine (G-C) base pair in an electron donor fashion. Thus, copper has been confirmed to preferentially bind to G-C pairs (Morris and Hay, 2001).

The cleavage of DNA depends upon physical properties such as temperature, incubation time and contraction. The breakage of DNA strands is proportional to temperature, incubation

time, Cu^{2+} and H_2O_2 concentration (Sagripant and Kraemer 1989). However, metal chelators, catalase, and high levels of free radical scavengers inhibit the breaking of the DNA strand, suggesting that Cu^{2+}, Cu^{1+}, H_2O_2 and OH radicals are involved in the reaction (Borkow and Gabbay, 2005). This fact, coupled with the earlier mentioned specificity of copper–DNA binding at the G-C site, inferred that nucleic acid degradation mediated by copper involves site-specific Fention reactions (Wittberger *et al.,* 2000; Dowjat *et al.,* 1996; Moraes *et al.,* 1989).

The after-effect of the specific binding of copper to nucleic acid is a repeated, cyclic, redox reaction which in turn generates various OH-radicals close to the binding site thereby causing multiple damages to the nucleic acids (Stohs and Bagchi, 1995). Imlay and Linn (1988), with an *E. coli* culture treated with H_2O_2 showed that DNA damage is the main cause of cell death and usually through iron-mediated Fenton reactions (Imlay and Linn, 1988; Imlay *et al.,* 1988). However, under certain conditions, such as those of low availability of iron, copper ions were found to take part in the genotoxicity of H_2O_2 in *E. coli* (Almeida *et al.,* 2000). However, the condition just described is only possible at high concentrations of H_2O_2 (20mM), which means that copper ions only become available in the intracellular environment in the absence of iron and in stringent oxidative stress (Almeida *et al.,* 2000).

Fundamentally, all the copper mediated toxic mechanisms explained in this review are true for bacteria as well as fungi and algae (Borkow and Gabbay, 2005).

1.7.3 Microbial resistance to silver and copper

Many microorganisms show resistance to metals whether in water, soil or on industrial waste. Most bacteria have developed metal resistance systems probably shortly after their prokaryotic ancestry because their ancestral form lacked metal resistance systems (Borkow and Gabbay, 2005). Some microorganisms show high metal resistance while others indicate low or no resistance at all. Ug and Ceylan, (2003) reported some clinical isolates of different *Staphylococcus* species (*S. xylosus,* methicillin resistant *S. aureus, S. capitis*, *S. lentus, S. epidermidis, S. sciuri* and *S. chromogenes*) showed reduced susceptibility to lead and potassium but became highly sensitive to silver and copper. The resistance of a microorganism to metal is dependent on *(a)* the amount and type of mechanisms for metal uptake by the microorganism, *(b)* the role played by each metal in normal metabolism in the cell and *(c)* the presence of genes or plasmids, chromosomes or transposons that may control metal resistance (Rosen, 2002; Andersen, 2003; Nies, 2003; Silver, 2003; Nascimento and Chartone-Souza, 2003; Nies, 1999).

Natural resistance posed by microorganism may be mutation in cellular components that avoid interaction with metals or alteration in cell membrane composition (Borkow and Gabbay, 2005). Microorganisms have evolved other mechanisms to tolerate or eliminate metals (Fig. 1.10). These include:

- Exclusion of metal by permeability barriers such as the cell wall, cell membrane or envelope to protect the internal delicate cellular components (Ug and Ceylan, 2003; Scott and Palmer, 1990; Hoyle and Beveridge 1984; Hoyle and Beveridge 1983).

- Active transport of the metal away from the microorganism by a membrane efflux pump (Frank *et al.,* 2003 and Rensing and Grass, 2003).

- Intra- and extra- cellular sequestration by cell envelope or protein binding.
- Enzymatic detoxification of metal to a less toxic form.
- Alteration in the sensitivity of cellular targets to the metal by way of mutation (Borkow and Gabbay, 2005).

In most cases, the genes responsible for these processes may either be encoded in the chromosomes or by the plasmids.

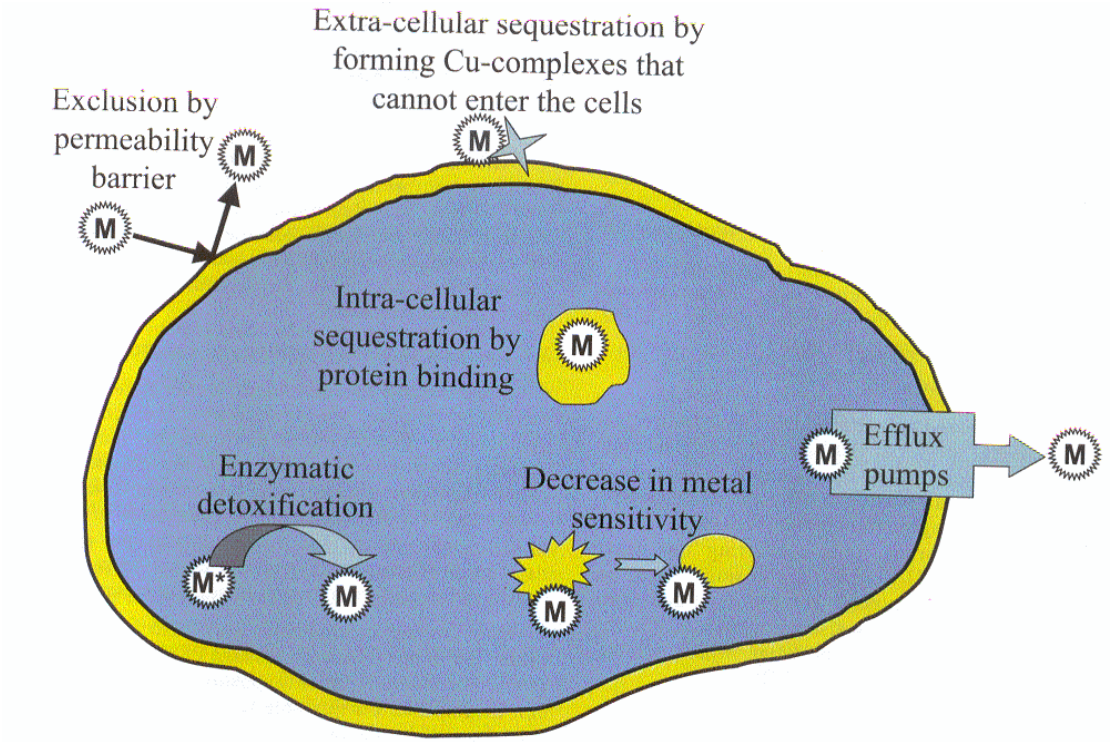

Fig.1.11: Mechanisms of microbial resistance to heavy metals (Borkow and Gabbay, 2005)

Furthermore, resistance may be developed as a consequence of random chromosomal mutations that may projects changes in the gene product, making the new generation more

resistant (Roberts *et al*., 1998). The mutated chromosome may be acquired by the progeny during cell division or from others surrounding cells of same or related species through transformation or transduction (McDonnell and Russell, 1999). However, most bacteria acquire resistance by evolving new genes that code for novel proteins. Hou *et al*, (2001) showed that a small metal binding protein, cysteine rich, metallothionein showed resistance to metals such as silver, copper, mercury, cadmium and zinc in an experimental mouse.

It was also indicated that, the mode of action of metallothionein resistance by bacteria was by the sequestering process but not conversion or exclusion. Bacterial silver resistance was discovered in *Salmonella* strain containing plasmid pMG101 (Gupta *et al*., 1998). Belonging to the group of incompatibility plasmids (IncH12), pMG101 exhibits various antibiotics resistance. Clone and sequenced analysis of specific region of pMG101 that shows increased resistance to silver have been well characterised; *SilP, ORF105, SilAB, ORF96, SilC, SilSR*, and *SilE*. Six of these genes were found similarly expressed in two strains of *E. coli*; *E. coli* K12 and *E. coli* O157:H7. The SilE gene encodes a periplasmic silver binding protein, SilE and showed up to 47% identity to PcoE of the *E. coli* usually associated with copper resistance (Silver, 2003).

There is a marked difference in the cell transport and efflux system of bacteria during their resistance in processes involving essential and non-essential micronutrients. Examples of essential micronutrients are copper, cobalt, zinc and nickel while examples of non-essential nutrients are silver and cadmium. In the latter, most bacteria alter their transport systems only to expel toxic ions, whereas the former adjust their uptake and efflux systems to maintain sufficient intracellular levels of the metals (Borkow and Gabbay, 2005).

Copper is cheaper than silver, easily mixed with polymers and relatively stable in terms of both chemical and physical properties (Ren *et al*., 2009). The silver ion is probably the most powerful antimicrobial agent and shows strong toxicity to broad spectrum of microorganisms but remarkably low toxicity to human cells, plant cells and, in fact, to all multicellular living matter.

1.8 Antimicrobial nanoparticles

Nanocomposites or nanomaterials are emerging as a new class of composites with at least one dimension of the dispersed particles in the nanometer range. Three classes of nanomaterial/nanocomposite can be differentiated based upon the number of dimensions:

i) Isodimentional nanoparticles have all three dimensions in the nanometer range e.g. spherical silica nanoparticles (Mark, 1996; Reynaud *et al.*, 2001) and semiconductor nanoclusters (Herron and Thorn, 1998).

ii) Nanotubes or whiskers when two dimensions are on the nano scale and the third dimension on a larger scale which usually results in an elongated structure, as in the case of carbon nanotubes and cellulose whiskers. Nanotubes and whiskers have been extensively studied as reinforcement nanofillers due to the exceptional properties which they impact on material (Favier *et al*., 1997 and Chazeau *et al*., 1999).

iii) Layered crystals or clays (Pavlidou and Papaspyrides, 2008) which are characterised by only one dimension in the nanometer range. This presents the fillers in the form of sheets from one to a few nanometers wide to a height of

hundreds to thousands of nanometers (Alexandre and Dubois, 2000; Pavlidou and Papaspyrides, 2008).

The general idea in nanocomposite synthesis is to create a large interface between nanosized building blocks and a matrix, which may be based upon a polymer. However, the homogeneous distribution of the nanosized particle may be problematic such that it becomes difficult to create an interface. Whichever way, homogeneous dispersion of nanoparticles for preparation purposes is vital as per acceptable properties (Hari and Pukanszky, 2011). This is because the properties of nanocomposite materials are usually below expectations and hence over estimated. This may be partly due to partial homogeneity, insufficient orientation or entirely too poor adhesion. Examples are found in additives in flame-retardant packages, conductive fillers, and gas permeation and membrane technology, biomedicine and electronics (Hari and Pukanszky, 2011).

Unlike many conventional antimicrobial agents, such as antibiotics, currently being used in medicine, antimicrobial nanoparticles may not pose direct or acute adverse effects, although potential toxicity upon long-term exposure is questionable. Nevertheless, antimicrobial nanoparticles can attack multiple biological pathways present in many microbes (Fig. 1.11) and the microbes would need to develop many simultaneous mutations in order for antimicrobial resistance to occur (Huh and Kwon, 2011). The mechanisms of action of antimicrobial nanoparticles have been noted to be; the photocatalytic production of reactive oxygen species that damage cellular and viral components, perturbation of bacterial cell wall/ membrane, interruption of energy transduction and inhibition of enzyme activity/ DNA synthesis (Li *et al.*, 2008b).

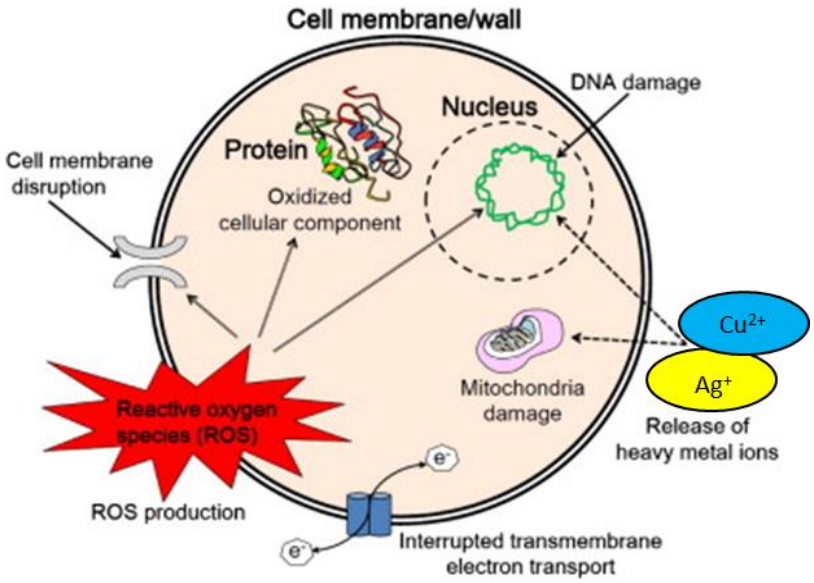

Fig. 1.12: Various antimicrobial mechanisms of nanomaterials (adapted from Huh and Kwon, 2011).

Antimicrobial nanoparticles possess a protracted shelf-life, and can withstand high temperature sterilization (Weir *et al*., 2008 and Huh and Kwon, 2011). The use of nanocomposites in the delivery of silver or copper would therefore offer the combined advantage of uniform distribution, sustained and controlled release into the target tissues, including improved stability, which will assist in patient care by minimising side effects.

1.9 Microorganisms of this study

The microorganisms used in this study were *Staphylococcus aureus*, *Escherichia coli* and *Pseudomonas aeruginosa*.

1.9.1 *Staphylococcus aureus*: Gram positive bacteria. *S. aureus* is the most common species of staphylococcus species causing infection in human (Modric, 2011). *S. aureus* has

been implicated in skin, soft tissue, foreign-body and bloodstream infections, pneumonia, septic arthritis, endocarditis, osteomyelitis including sepsis. Since the isolation of the first methicillin-resistant *S. aureus* strain in 1961 (Mediavilla *et al*., 2012; IWG-SCC, 2009) numerous distinct lineages of MRSA continues to emerge; community-associated MRSA (CA-MRSA) (Mediavilla *et al.*, 2012; Chambers and Deleo 2009), healthcare-associated MRSA (HA-MRSA) (Chambers and Deleo, 2009) displaying increased antimicrobial resistance, hence widening the invasive disease spectrum (Chua *et al.*, 2011; Tenover, and Goering 2009).

HA-MRSA isolate is characterised by a mobile genetic element, the staphylococcal chromosome cassette *mec* (SCC*mec*), belonging to type I, II, or III, which confer resistance to many classes of non-β-lactam antibiotics (Yu *et al*., 2012). While, CA-MRSA is associated with smaller SCC*mec* elements including SCC*mec* type IV or V and are susceptible to many non- β-lactam antibiotics (Boyle-Vavra and Daum, 2007 and David and Daum, 2010). *S. aureus* elicit disease in various ways e.g. by possessing surface protein which promote colonization of host tissues; invasins that promote bacterial spread in tissues (leukocidin, kinases and hyaluronidase); surface factors that inhibit phagocytic engulfment (capsule and protein A); biochemical properties that enhance their survival in phagocytes (carotenoid and catalase production); immunological disguises (protein A and coagulase); membrane-damaging toxins that lyse eukaryotic cell membranes (hemolysins, leukotoxin and leukocidins); exotoxins that damage host tissues or otherwise provoke symptoms of disease (exfoliatin toxin and toxin shock syndrome) (Todar, 2012).

1.9.2 ***Escherichia coli*:** Gram negative rod, forms part of the normal intestinal microflora in humans and worm blooded animals. Some strains possess specific virulent factors which cause diseases such as food poisoning, urinary tract infection and bacteraemia (HPA, 2012).

E. coli causes the most common bacterial infection called urinary tract infection (UTI) in clinical medicine (Olson *et al*., 2009) also, UTI is the most common hospital –acquired infection (Hoban *et al*., 2012). *E. coli* remains the single most common pathogen isolated in hospital acquired UTI (Hoban *et al*., 2012; Jacobsen *et al.*, 2008; Nicolle *et al*., 1996). *E. coli* has shown increased worldwide antimicrobial resistance to once potent agents such as trimethoprim/sulfamethoxazole, amoxicillin, and ciprofloxacin among outpatient UTI (Karlowsky *et al*., 2006; Mazzulli, 2002). This has necessitated the reassessment of antimicrobial susceptibility to maintain antimicrobial efficacy. Pathogenic strains of *E. coli* elicit disease by expression of virulent determinants such as adhesins, invasins, toxins and ability to withstand host defences (Todar, 2012).

1.9.3 ***Pseudomonas aeruginosa*:** is a Gram negative, non-spore forming rod. *P. aeruginosa* is wide spread in nature, inhabiting soil, water, plant and animals including humans. *P. aeruginosa* is an important opportunistic, nosocomial pathogen that causes infection in hospitalised subjects, and has been known to be specially prevalent in hospital-acquired pneumonia in immunecompromised patients, urinary tract infection and bacteraemia (D'Arezzo *et al*., 2012).

P. aeruginosa exhibit a multidrug resistant and pandrug-resistant phenotype, necessitating its reputation as a 'superbug' due to its clinical significance and prevalence in the intensive care unit (Xiao *et al*., 2011).

Recent update based on clinical data, pharmacokinetic/pharmacodynamic properties and minimum inhibitory concentration have shown increased resistance of *P. aeruginosa* to antimicrobial agents (Xiao *et al*., 2012, Wayne, 2011; Wayne, 2012), leading to formulation of a new breakpoint by the clinical and laboratory standards institute (Wayne, 2012 and Xiao *et al.,* 2012).

However, all the bacteria strains used in this study were laboratory strains without any known pathogenicity. As model microorganisms they were used to demonstrate the antibacterial properties of metal modified Laponite RD.

1.10 Conclusion

This review presents recent research findings in Laponite®. In using the modified processes of pillaring, acid treatment, silane coupling and grafting, the aim is to fine-tune clay characteristics to achieve improvements in such purposes as catalyst making, adsorbents for toxic or hazardous substances and as firm support for pharmaceutical formulations. Research is still underway to elucidate the antimicrobial potential of silver as well as copper in Laponite® RD support for antimicrobial applications. Laponite® RD has not been used as an antimicrobial agent, not because of its effectiveness or inefficiency but because of late and slow-paced research work and therefore limited exploration of the potential that lies in this synthetic clay mineral.

Despite the acclaimed activity of silver and its overwhelming reception as the most active antimicrobial metal known, copper has been more institutionalised with a high level of publicity and usage, ranging from hospital to household surface coatings. The antimicrobial copper interest group comprising designers, healthcare professionals, facilities mangers,

product manufacturers and material suppliers (whose membership is well established in Japan, elsewhere in Europe and abroad), aim to provide up-to-date information on copper subjects (www.copperinfo.co.uk). However, copper or any other metal antimicrobial agent is neither a substitute for clinical routine maintenance nor a panacea for household hygiene negligence. It is a supplement and its application should be in conjunction with other maintenance measures.

1.11 Hypothesis

Conventional silver-based antibacterial agents easily leach out their silver content producing material with short active lifetime. This quick leaching effect, coupled with antibacterial resistance, toxicity of antibacterial materials and the broadening use of Laponite® RD in novel application, prompted renewed interest in the use of Laponite® RD as a support material for silver and copper as effective antibacterial agent.

Silver or silver-based antibacterial agents have been in use since ancient times. Silver has been exploited in preservation of water by space workers. This and other uses of silver or silver based-composites have long been abandoned. However, the emergence of bacterial resistance to antibiotics and antibacterial agents informed the resurgence of silver based antibacterial composites. Silver or silver ions are relatively less toxic in human (Russell and Hugo, 1994), but act as biocides to microorganisms, especially at low concentrations (Inoue *et al*., 2002) due to their broad spectrum of antimicrobial activity (Feng *et al*., 2000; Silver *et al*., 2003; Sondi and Salopek-Sondi, 2004 and Kwakye-Awuah *et al*., 2008). Silver ions inhibit bacterial cell wall synthesis (Feng *et al*., 2000), inactivate respiratory enzymes through generation of reactive oxygen species (Matsumura *et al*., 2003), interact with ribosomes ensuing inhibition of the enzymes and proteins essential for ATP production (Yamanaka *et al*., 2005), and bind to microbial DNA leading to replication failure (Thomas *et al*., 2007). Although, copper is an essential nutrient in many microorganisms, including

bacteria, and enzyme-associated copper is a requirement for aerobic metabolism, excess amounts of free copper, or its alloys, often lead to cell toxicity. This toxicity is induced when copper undergoes redox reactions alternating between Cu^{+1} and Cu^{2+} in the Fenton and Haber-Weiss reaction, leading to the generation of hydroxyl radicals and reactive oxygen intermediates (Quaranta *et al*., 2011). These hydroxyl radicals readily attack and damage cellular biomolecules (Santo *et al*., 2010), and the highly reactive oxygen intermediates cause lipid peroxidation and oxidation of protein leading to nucleic acid damage (Halliwell *et al*., 1990). Copper also causes protein inactivation via disruption of Fe-S clusters in proteins such as cytoplasmic hydratases (Macomber and Imlay, 2009).

Laponite® RD has been in use for various applications in textile, agriculture, drilling mud, household and cosmetics. Laponite® RD has a CEC of 62 meq/100 g at pH 7 (Bergaya and Vayer 1997; Thompson and Butteworth 1992) with high tenability and adaptability. Laponite® RD possesses layered structures which accommodate inorganic antibacterial cations within their interlayer space, edges or sheets through ion-exchange or isomorphous substitution process. The unique rheological properties, such as easy swelling and dispersion in aqueous systems, formation of translucent gels and films, enhanced its suitability as reservoir or support material for metal inorganic nanoparticles.

1.12 Aims and objectives

The key aims of this study are:

- To synthesize Laponite® RD and establish its purity.
- To synthesize silver-exchanged Laponite® RD and copper-exchanged Laponite® RD using conventional ion exchange technologies.

- To synthesize silver incorporated Laponite® RD and copper incorporated Laponite® RD with silver or copper held at the Laponite® RD sheet via novel isomorphous substitution techniques.
- To establish the purity of the silver-Laponite® RD and copper-Laponite® RD using variety of analytical tools: X-ray diffraction (XRD), Fourier transformed infrared spectroscopy (FTIR), energy dispersive X-ray spectroscopy (EDX), thermogravimetric analysis (TGA), magic angle spinning nuclear magnetic resonance (MAS NMR), scanning electron microscopy (SEM) and transmission electron microscopy (TEM).
- To assess the antibacterial efficacy of the synthesized silver-Laponite® RD and copper-Laponite® RD by comparing with other antibacterial agents.
- To assess the silver or copper release profile of silver-Laponite® RD or copper-Laponite® RD in aqueous systems in comparison with other antibacterial agents.

To achieve these aims, silver-exchanged Laponite® RD (AGLAP1-6) and copper-exchanged Laponite® RD (CULAP1-6) were synthesised via ion exchange. Silver incorporated Laponite® RD (AL1-3) and copper incorporated Laponite® RD (CL1) were synthesised via isomorphous substitution of silver or copper into the Laponite® RD sheets.

1.13 Analytical techniques used in this study

Laponite® RD being versatile and extremely sensitive to method of preparation, its varying properties and those of its metal-modified forms were monitored using various analytical tools for the qualitative as well as their quantitative identification. XRD was used to confirm the crystalinity and phase purity of the metal-Laponite® RD, FTIR to identify association between new and existing bonds in the Laponite® RD structure. EDX was used to quantify the silver and copper in Laponite® RD matrix while the morphology was determined by SEM

and TEM. TGA displayed the thermal properties of the pure as well as the metal-modified Laponite® RD. Particle analyser was used to determine the particle size of Laponite® RD and its modified forms.

Chapter 2

Experimental Design and Methodology

This chapter is divided into two parts: The general methods involved in the synthesis, modification and characterisation techniques of Laponite® RD will be described in Part I. Experimental protocols for investigation of antimicrobial activity of the metal modified Laponite® RD produced in this work will be discussed in Part II.

PART I

Synthesis and characterization of metal modified Laponite® RD

The schematics plan of experimental work for Laponite® RD synthesis, modification with silver and antimicrobial activity is shown in Figure 2.1.

2.1 Synthesis of Laponite® RD

Laponite® RD, the standard grade of Laponite (Li *et al*., 2009a) used in this study was synthesised according to the protocol delivered by the product company, Rockwood Additives Ltd, Cheshire, UK (Patent # GB1213122 and GB1432770). The precise method used was that used for the commercial manufacture of Laponite® RD and is commercially confidential. However, the general schematics of Laponite® RD synthesis is shown in Figure 2.1

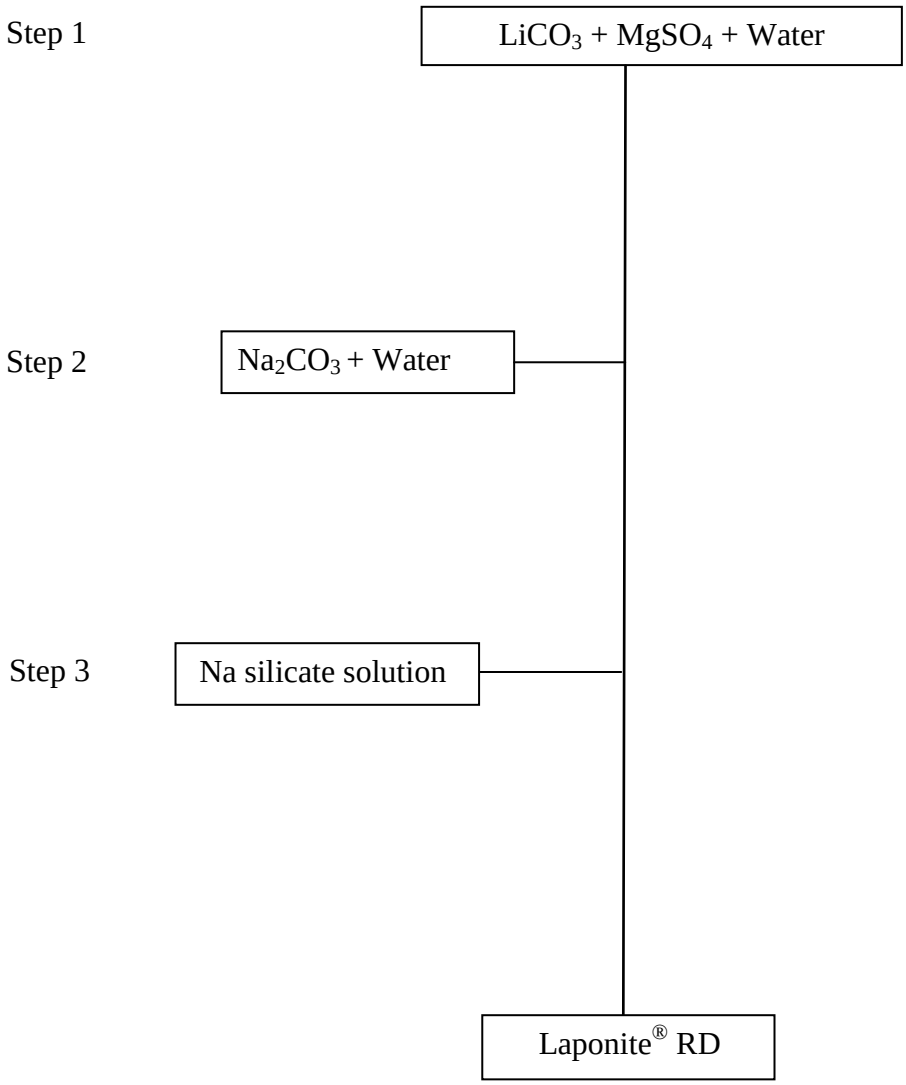

Fig. 2.1: General schematic of Laponite® RD synthesis. Laponite® RD is synthesised by combining sodium, magnesium and lithium salts with sodium silicate at specific reaction conditions with the formation of an amorphous precipitate which undergo complete crystallization at high temperature.

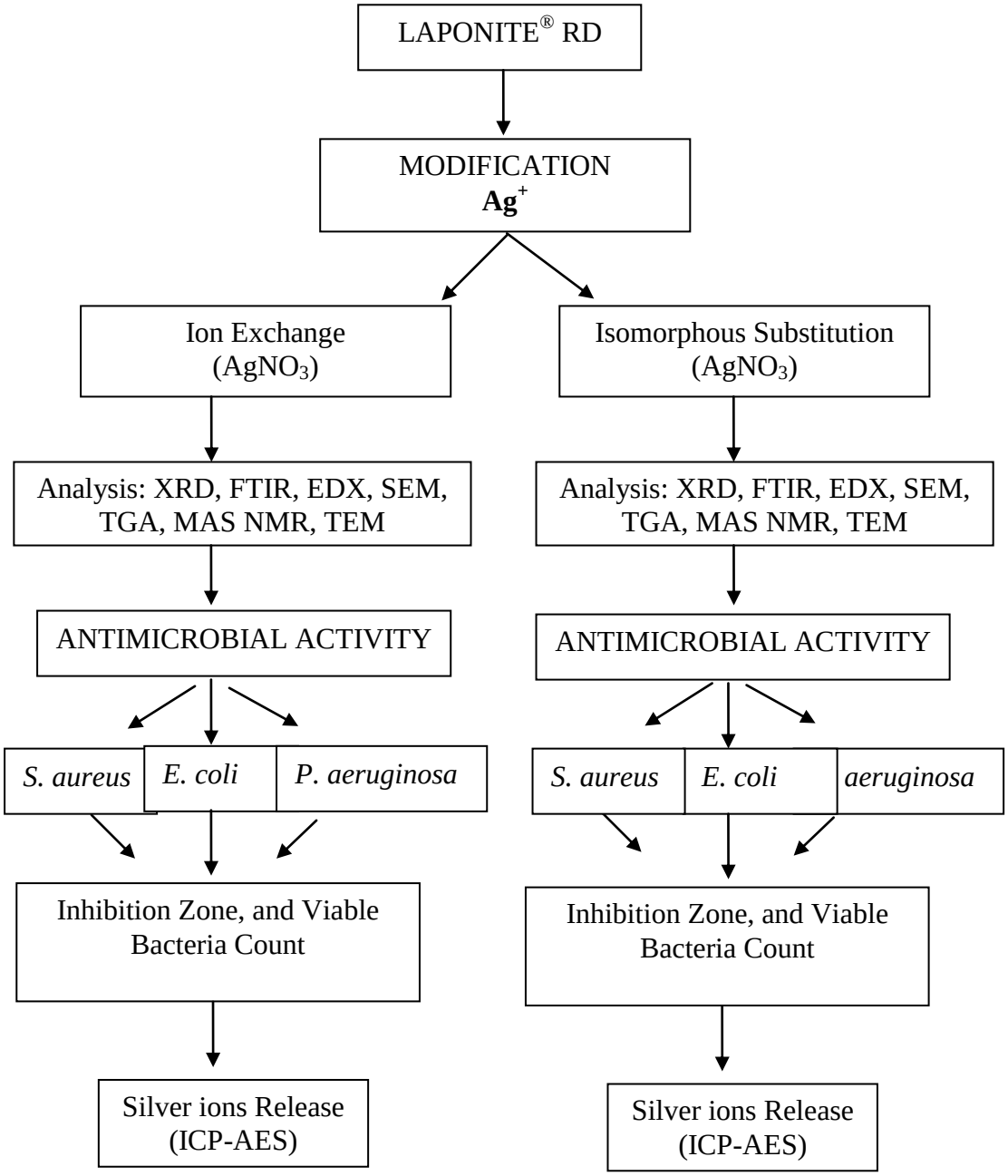

Fig. 2.2: Schematics plan of experimental work: Laponite® RD was synthesised and modified via two methods: Ion exchange and isomorphous substitution using $AgNO_3$. The samples were characterised with XRD, FTIR, EDX, SEM, TGA, MAS NMR and TEM. The antibacterial activity was investigated by exposing *E. coli*, *S. aureus* and *P. aeruginosa* to silver-Laponite® RD in TSB. The efficacy of the silver-Laponite® RD was assessed by obtaining the inhibition zone and viable count. The released silver ion from the silver-Laponite® RD nanocomposite was determined by ICP AES.

2.2 Modification of Laponite® RD with metal

Two approaches were utilised in the modification process with silver or copper (schematics

plan of experimental work for Laponite® RD synthesis, modification with copper and antimicrobial activity is shown in Figure 2.2).

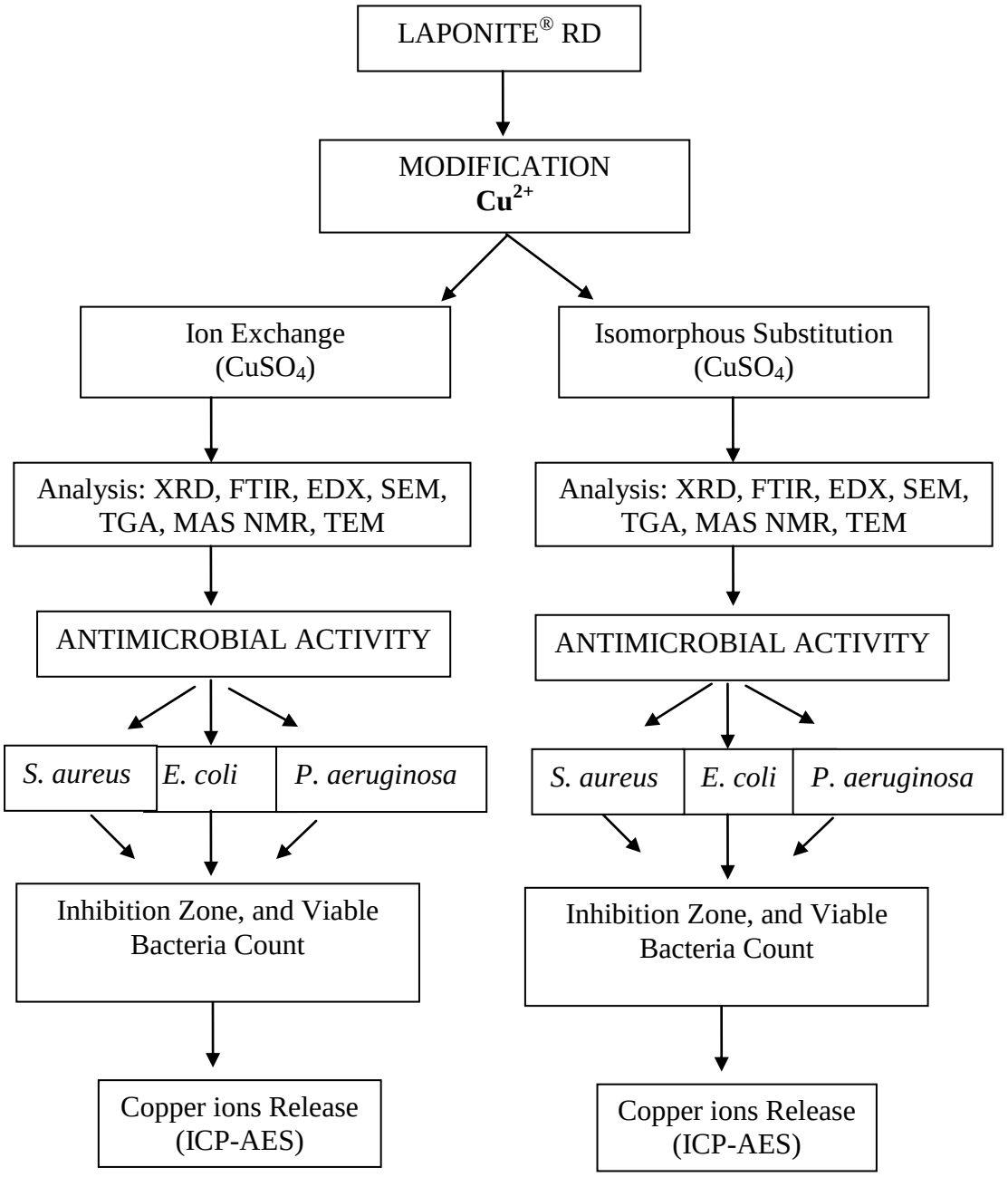

Fig. 2.3: Schematics plan of experimental work: Laponite® RD was synthesised and modified via two methods: Ion exchange and isomorphous substitution using $CuSO_4$. The samples were characterised with XRD, FTIR, EDX, SEM, TGA, MAS NMR and TEM. The antibacterial activity was investigated by exposing *E. coli*, *S. aureus* and *P. aeruginosa* to copper-Laponite® RD in TSB. The efficacy of the copper-Laponite® RD was assessed by obtaining the inhibition zone and viable count. The released copper ion from the copper-Laponite® RD nanocomposite was determined by ICP AES.

The first approach was by ion exchange, which involved the displacement of the interlayer sodium ion (Na^+) by silver or copper ions. The second approach was by isomorphous substitution involving the incorporation of silver or copper within Laponite® RD layers.

2.2.1 The displacement of interlayer sodium by ion exchange

Vansant and Pesters (1978) exchanged alkyl ammonium cations on the Laponite® RD to establish exchange isotherms using a dialysis technique. The exchange between Na^+ and Ag^+ cations on the Laponite® RD was performed in this research using ion exchange technique in order to establish the displacement of the interlayer sodium.

2.2.1.1 Ion exchange with $AgNO_3$

The ion exchange was performed using a method described by Utracki *et al*., (2007) and Lezhnina *et al*., (2011) with some modifications. A 0.8g of $AgNO_3$ (Sigma-Aldrich, UK) was dissolved in 79.2 ml deionised water using a magnetic stirrer. 6.4g of Laponite® RD was gently added to the solution and allowed to disperse (AGLAP1, for AGLAP2, AGLAP3, AGLAP4, AGLAP5 and AGLAP6 see Table 2.1), in a solution to solid ratio of 12.5 : 1. The mixture was then stirred for 3 hrs for total exchange. This was performed in the dark due to the photosensitivity of $AgNO_3$. The colour changed from clear colourless, white, cloudy white, yellow, to golden yellow. After the 3 hrs of exchange, the mixture was then filtered and washed eight times with 25ml, methanol (Sigma-Aldrich, UK) for total removal of the excess exchange solution. The filtered cake was transferred into a Petri dish in a fume cupboard for 1 hour to allow the methanol to evaporate. The sample was then transferred to oven (40^oC) to dry overnight. It was then milled into powder, sieved with a 100 micron mesh and stored in brown sealed capped containers. The amount of Ag exchanged or Na displaced was determined by energy dispersive X-ray (EDX) spectroscopy.

Table 2.1: Preparation of silver modified Laponite® RD by ion exchange

Sample	$AgNO_3$ (g)	H_2O (ml)	Laponite® RD (g)
AGLAP1	0.8	79.2	6.4
AGLAP2	1.6	78.4	6.4
AGLAP3	2.4	77.6	6.4
AGLAP4	3.2	76.8	6.4
AGLAP5	4.0	76.0	6.4
AGLAP6	4.8	75.2	6.4

2.2.1.2 Ion exchange with $CuSO_4$

The ion exchange was performed using a method described by Utracki *et al*., 2007 with some modifications. 0.8g of $CuSO_4 \cdot 5H_2O$ (Sigma-Aldrich, UK) was dissolved in 79.2ml deionised water using a magnetic stirrer. 6.4g of Laponite® RD was gently added to the solution and allowed to dissolve (CULAP1, for CULAP2, CULAP3, CULAP4, CULAP5 and CULAP6 see Table 2.2), in a solution to solid ratio of 12.5 : 1. The mixture was then placed in plastic bottles on a rotation drum to facilitate ion exchange. The slurry was washed eight times with 25ml aliquots of methanol (Sigma-Aldrich, UK) for total removal of the excess exchange solution. The filtered cake was transferred into a Petri dish in fumed cupboard for 1 hour to allow the methanol to evaporate. The sample was then transferred to oven for overnight drying at 40^oC and made into powder and stored in sealed capped containers.

Table 2.2: Preparation of copper modified Laponite® RD by ion exchange

Sample	$CuSO_4$ (g)	H_2O (ml)	Laponite® RD (g)
CULAP1	0.8	79.2	6.4
CULAP2	1.6	78.4	6.4
CULAP3	2.4	77.6	6.4
CULAP4	3.2	76.8	6.4
CULAP5	4.0	76.0	6.4
CULAP6	4.8	75.2	6.4

2.2.2 Incorporation of metal in Laponite® RD layer by isomorphous substitution

The isomorphous substitutions of Laponite® RD with silver and copper were performed to establish their incorporation at the Laponite® RD sheet.

2.2.2.1 Isomorphous substitution using $AgNO_3$

The isomorphous substitution with silver follows the synthesis of Laponite® RD, exception for the addition of $AgNO_3$ prior to crystallization. The synthesis was not successful when $AgNO_3$ was added to Li_2CO_3 at the first instance. 0.42g of Li_2CO_3 was dispersed in 56.6ml deionised water and 12.87g of $MgSO_4$ for AL1 (11.91g $MgSO_4$ for AL2 and 10.35g $MgSO_4$ for AL3) was added and allowed to dissolve for 1 hour. The mixture was heated to 60^oC. 10.35g of Na_2CO_3 was dissolved in 41.4g of deionised water and added drop-by-drop to the

$Li_2CO_3/MgSO_4$ mixture. Sodium silicate (70.5g) was then added drop wise maintaining the temperature at 60°C. The temperature was increased to 98°C for 2 hours. The resultant slurry was transferred to autoclave vessel for complete crystallization at 202°C for 6 hours. The 0.5g $AgNO_3$ was added prior to crystallisation to the reaction vessel for AL1 (2g $AgNO_3$ for AL2 and 4.1g $AgNO_3$ for AL3) and proceeded in the dark for 6 hours. The reaction vessel and its content were allowed to cool to ambient temperature. The slurry was washed with deionised water, filtered, dried and milled.

2.2.2.2 Isomorphous substitution using $CuSO_4$

The isomorphous substitution with copper was slightly different to that of silver substitution and was performed as follows; 0.42g of Li_2CO_3 was dispersed in 56.60g deionised water and 11.38g of $MgSO_4$ was added and allowed to dissolve for 1 hour. 0.24g of $CuSO_4 \cdot 5H_2O$ was added to the mixture and was heated to 60°C. 10.35g Na_2CO_3 was dissolved in 41.40ml of deionised water and added drop-by-drop to the $LiCO_3/MgSO_4$ mixture. Sodium silicate (70.50g) was then added drop wise maintaining the temperature at 60°C. The temperature was then increased to 98°C for 2 hours. The resultant slurry was transferred to an autoclave vessel for complete crystallization at 202°C. The reaction vessel and its content were allowed to cool to ambient temperature. The slurry was washed with deionised water and filtered, dried and milled.

2.3 Characterization of metal modified Laponite® RD

Laponite® RD and silver exchanged Laponite® RD as well as the copper exchanged Laponite® RD were characterised using spectroscopic and microscopic methods.

Spectroscopy techniques used include X-ray Diffraction (XRD), Fourier Transformed Infrared (FTIR) and Energy Dispersive X-ray (EDX). Microscopy methods used were Scanning Electron Microscopy (SEM) and Transmission Electron Microscopy (TEM). Thermogravimetric Analysis (TGA) was used for the thermal characterisation.

2.3.1 X-ray diffraction (XRD)

(a) Introduction

X-ray diffraction is a rapid analytical technique that reveals the crystallographic structure, chemical composition as well as physical properties of natural or synthetic materials. X-ray powder diffraction is the most common technique used for the characterisation of crystalline structures and the determination of mineralogy of fine particles such as Laponite® RD. It identifies the phase of crystalline material and provides information on its unit cell dimensions.

(b) Principle of XRD

Based on Bragg's law: $n\lambda = 2d \sin \theta$

Where:

n – is an integer for "order" of reflection

λ – wavelength of the incident X-rays

d – inter-planar spacing of the crystal

θ – angle of incidence

(c) Experimental method

Samples of Laponite® RD with or without metal were finely grounded and homogenised before analysis. X-ray diffraction patterns of the samples were obtained with a Philips model PW1710 X-ray diffractometer equipped with graphite monochromated CuKα radiation with X-ray tube settings at 40kV and 40mA. The scanning speed was 1 degree 2-theta per minute in 5^o to 50^o range. Data processing was carried out using Philips APD software with a search/match facility and an ICDD (International Centre for Diffraction Data) database on a DEC Microvax 31000 minicomputer interfaced to the diffractometer. The computer correlated the obtained sample pattern with ICDD 9-31 (the PDF powder diffraction file number published by the International Centre for Diffraction Data, formerly the Joint Committee for Powder Diffraction Standards (JCPDS)) reference standard. The X-ray powder diffraction patterns of Laponite® RD, silver-Laponite® RD and copper-Laponite® RD were collected on a conventional source using a flat auto plate. Portions of the samples were placed on the flat auto plate and pressed to fill the entire perimeter using a glass plate. After obtaining a smooth and level surface of the powder, the plates were stacked on an automatic sample chamber one at a time.

2.3.2 Fourier transformed infrared spectroscopy (FTIR)

(a) Introduction

FTIR is an analytical technique based on vibration of atoms in a molecule and provides the most informative single technique for assessing the mineriological and crystal-chemistry of clay minerals. Laponite® RD with or without metal were analysed with a Mattson Genesis II FTIR spectrometer (Mattson Instruments, UK) equipped with a ZnSe crystal plate fitted with a mercury cadmium telluride A (MCTA) detector and a KBr beam splitter.

(b) Principle of FTIR

Clay minerals to be tested adsorb infrared (IR) radiation from the photospectrometer. The extent of adsorption is determined by the atomic mass, length, strength and force constant of interatomic bonds in the structure of the minerals. The symmetry of the unit cell and the local site symmetry of each atom within the unit cell also have contributory influences on the absorption. The detector monitors the wave number range and transmits the signal to a PC. The PC translates the signal into an absorption spectrum.

(c) Experimental method

Laponite® RD (with or without metal) samples were made into powder and a little quantity just enough to cover the disc hole is placed on the disc. The disc is pressed unto the solid holder and the scan of the sample is operated on the PC which further generates the IR spectrum. The range of wave number used in this study was 400 – 4000cm^{-1}.

2.3.3 EDX

(a) Introduction

Energy dispersive X-ray (EDX) spectroscopy was employed in the scanning electron microscope (SEM) for the elemental identification of the Laponite® RD samples, using Zeiss EVO 50 scanning electron microscope fitted with an Oxford EDX, Zeiss, UK.

(a) Principle of EDX

The EDX equipment was fitted in conjunction with a scanning electron microscope. The incident electron beam induces X-ray fluorescence in the sample which is energy-analyzed using a cooled semiconductor detector. The EDX measures the energy of X-rays generated by the atoms of the Laponite® RD samples during interactions with the electron beam. The X-ray spectra formed are characteristic of the atoms that formed them, allowing the chemical composition of the sample to be determined. EDX cannot detect Li or OH due to their low

atomic number and low percentage, total percentage composition being less than 5wt% (Song *et al*., 2009 and Pichonat *et al*., 2010). However, the Li and OH contents were quantified with ICP-AES and TGA respectively. During the analysis the "normalised" function was engaged to measure the concentration of the elements as a proportion totalled to 100%. In addition, the element map was also recorded.

2.3.4 Particle size analyser

(a) Introduction

The particle size distribution per unit volume Laponite® RD without silver or copper and silver or copper modified Laponite® RD were analysed with a Laser Granulometer Hydro 2000MU (Malvern Instrument Ltd, UK), courtesy Coventry University.

(a) Principle of laser granulometer

The particle size analyser is based on the principle that particles scatter and diffract light at certain angles based on their size, shape, and optical properties.

(a) Experimental method

The Laponite® RD without silver or copper and the silver or copper modified Laponite® RD were analysed using 0.1 mg of each sample. Each sample is dispersed in deionised water and loaded into the sample handling chamber which uses mechanical action for stirring to avoid flocculation. The particle measurements and distribution were read from a computer connected to the instrument.

2.3.5 Scanning electron microscopy (SEM)

(a) Introduction

Scanning electron microscopy reveals information about the external morphology, chemical composition and crystalline structure making up the sample. The Zeiss EVO 50 scanning electron microscope was fitted with an Oxford EDX, Zeiss, UK.

(a) Principle of SEM

A scanning electron microscope uses a focused beam of high energy electrons to generate a variety of signals at the surface of solid specimens (Fig. 2.3).

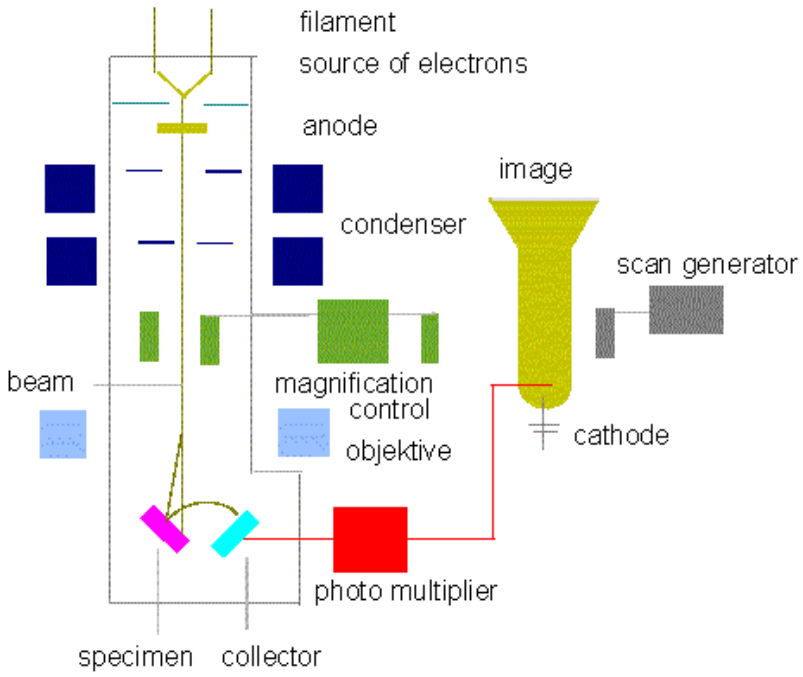

Fig. 2.4: Diagram of scanning electron microscope (Martinez, 2011)

The accelerated electrons dissipate their energy as a variety of signals produced by electron-sample interactions when the incident electrons are decelerated in the solid sample. These signals including the secondary electrons produce SEM images.

(a) Experimental Method

The samples were made into a fine powder and were sprinkled on prepared aluminium stubs with carbon adhesive coating. Some of the samples, where necessary were gold-coated with an Emscope SC500 sputter coater to reduce static charging. The electron micrographs were obtained at various magnifications.

2.3.6 Transmission electron microscopy (TEM)

(a) Introduction

The TEM technique makes it possible to determination the morphology, size and structure of mineral clays. The TEM (Fig. 2.4) analysis was done with Joel 1200EX transmission electron microscope (courtesy EM unit, University of Birmingham) with operating voltage of 80KeV, fitted with a LaB 6 filament using 300 mesh Formvar coated nickel grid, to examine the morphology and size of the silver and copper modified Laponite® RD samples.

(c) Experimental method

Sample preparation is critical for the examination of Laponite® RD, silver-Laponite® RD and copper-Laponite® RD samples by transmission electron microscopy. In this study, the samples were prepared according to the protocol described by Ruparelia *et al* (2008) with some modifications. 0.1mg of Laponite® RD, silver or copper modified Laponite® RD was dispersed in 10ml of methanol and sonicated for 15 minutes. A drop was placed onto a nickel grid and allowed to dry before mounting on the TEM for observation. The nanoparticle size was determined by measuring the nanoparticle size from the TEM micrograph using Image

Pro Plus software, version 4.5.0.19 for Windows 98/NT/2000. The nanoparticle size distribution was plotted and the graph obtained from Microsoft Excel version 2010.

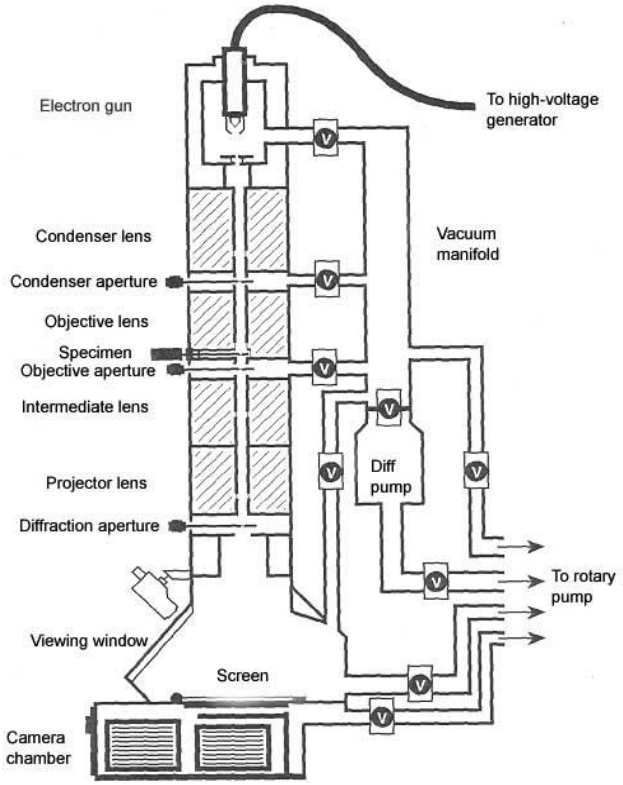

Fig. 2.5: Diagram of transmission electron microscope (Cormia, 2011)

2.3.7 Si^{29} magic angle spinning nuclear magnetic resonance (Si^{29} MAS NMR) spectroscopy

(a) Introduction

Nuclear magnetic resonance (NMR) spectroscopy is an analytical technique that supplies information on the structure and dynamic aspects of clay minerals as well as other solids. The

Varian Unity Inova spectrometer (courtesy Durham University) was used operating at 59.56MHz for ^{29}Si. The samples were referenced to neat, external tetramethylsilane.

(b) Principle

The principle of NMR spectroscopy has to do with the interaction of the nuclear magnetic moment ($\mu n = (h/2\pi)$ Yn I) with an external magnetic field, B_o that induces the splitting of the $2I + 1$ energy level of the nuclear spin I (Sanz, 2006). When a clay sample is irradiated with a radio frequency, absorption of the resonant energy between adjacent energy levels occurs. The precise frequencies at which the spin-active clay resonates is picked up and displayed by the nuclear magnetic resonance spectrometer.

2.3.8 Inductively coupled plasma atomic emission spectroscopy (ICP-AES)

(a) Introduction

The elemental composition of Laponite® RD, silver-Laponite® RD and copper-Laponite® RD were accessed by ICP-AES with SPECTRO CIROS^{CCD}.

(b) Principle

ICP AES uses inductively coupled argon plasma to produce excited atoms and ions that emit electromagnetic radiation of varying wavelengths. Each element possesses a corresponding wavelength which is detected by the charged couple device. The schematic of ICP-AES is shown in Fig. 2.5. The intensity of the emitted radiation is proportional to the concentration of the element in the sample. The radiation detected is then transformed directly into a percentage or measured concentration.

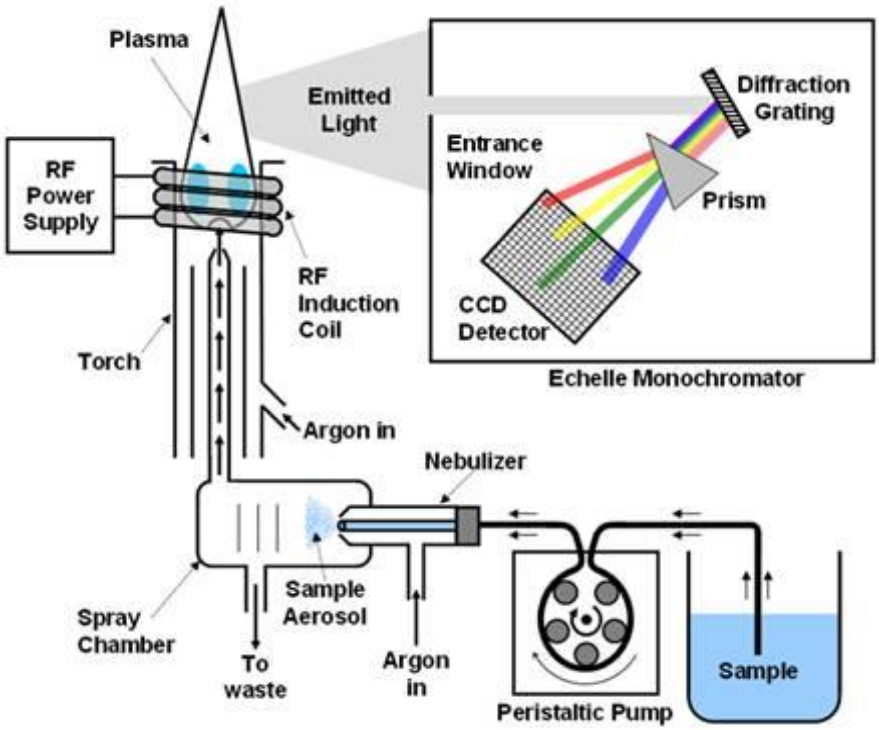

Fig.2.6: Schematics of ICP AES (Concordia analytical instrument laboratory, 2012)

(c) Experimental method

A 2g of the samples were digested in 4ml of 65% HNO_3 and 1ml of 96% H_2SO_4 on MLS-MEGA Microwave and subsequently analysed on ICP-AES. Triplicates readings were obtained and the average was recorded.

2.3.9 Thermogravimetric analysis (TGA)

(a) Introduction

Thermogravimetric analysis (TGA) measures the weight in a material as a function of temperature (or time) under controlled atmospheric conditions. The thermal stability and

composition of Laponite® RD without silver or copper and silver or copper modified Laponite® RD were performed with a Perkin Elmer TGA7 thermogravimetric analyser.

(b) Experimental method

5 – 10mg each of Laponite® RD (without silver or copper) and silver- or copper-Laponite® RD were heated from room temperature to 900 ^{o}C under nitrogen gas flow (20ml/min) at a rate of 5 ^{o}C/min. Sample mass changes due to the applied controlled increasing temperature were automatically recorded using an electrobalance. The data were transformed into weight versus temperature graph by a computer monitor from which the deformation temperature and corresponding weight loss were obtained.

2.3.10 Rheology of Laponite® RD

The rheology of the Laponite® RD, silver and copper modified Laponite® RD was assessed using the pebble and jar test (method supplied by Rockwood Additives Ltd, UK). 1g of Laponite® RD, silver or copper modified Laponite® RD powder were measured into a jar containing a pebble and 9 ml of deionised water was added. The jar and its content were mixed until fully dispersed. The mixture was left on the work bench and was observed for gellation for the duration of the study. The procedure was repeated for the silver as well as the copper modified Laponite® RD.

PART II

Antimicrobial Analysis

2.4 Media preparation

2.4.1 Preparation of tryptone soya broth (TSB)

TSB was obtained from Lab M, UK. The manufacturer's protocol was followed in the preparation procedure. A 6g of TSB were dissolved in 200 ml of de-ionised water in 500 ml conical flasks (0.6g TSB in 20 ml de-ionised water, in a 50 ml conical flask for the starter culture). The conical flasks were capped with foams and covered with aluminium foils. The flasks and its contents were then autoclaved at 121 ^{o}C for 15 minutes and cooled to ambient temperature.

2.4.2 Preparation of tryptone soya agar (TSA)

TSA was obtained from Lab M, UK and was prepared according the manufacturer protocol. 14.8 g TSA was added to 400 ml de-ionised water in 500 ml medical flasks in order to obtain 37 g l^{-1} of TSA. The flasks and its contents were loosely capped and autoclaved at 121^{o}C for 15 minutes and cooled to 50 ^{o}C. The molten agar was poured onto sterile Petri dishes and allowed to solidify at room ambient temperature.

2.4.3 Preparation of Ringer's solution

The Ringer (one-quarter strength) was supplied by Lab M, UK. The Ringer's solution was prepared by dissolving 1 tablet in 500 ml of de-ionised water in a 1 litre flask. The flask was then placed on a magnetic stirrer to dissolve the tablet. 4.5 ml portions were pipetted into test tubes labelled 10^{-1} to 10^{-8} (Fig. 2.6). The test tubes were capped, test tube and contents were autoclaved for 15 minutes at 121^{o}C. The test tubes were allowed to attain room temperature before use.

2.5 Antibacterial activity of silver modified Laponite® RD

2.5.1 Introduction

The antibacterial activity of silver modified Laponite® RD (silver-Laponite® RD) was investigated by exposing three different bacterial strains: *Escherichia coli* K12W-T (Gram negative), *StaphylococcuS. aureus* NCIMB6571 (Gram positive) and *Pseudomonas aeruginosa* NCIMB8295 (Gram negative) to silver-Laponite® RD via ion exchange and isomorphous substitution methods. All three strains were obtained from the University of Wolverhampton culture collection centre. The stock cultures were freeze-dried and kept at -20 ^{o}C. Prior to the investigation, cultures were resuscitated and grown on TSA overnight at 37 ^{o}C. During the investigation all three bacterial strains were separately exposed to silver exchanged Laponite® RD (ion exchange method) and silver incorporated Laponite® RD (isomorphous substitution method) in TSB for a period of 72 hours.

2.5.2 Disk diffusion test

Bacterial sensitivity to antibacterial agents is usually tested using a disk diffusion test, employing antibiotic impregnated disks (Ruparelia *et al*., 2008). A modified test according to those described by Ruparelia *et al.,* (2008) and Yuan and Cranston (2008) were used in this study. A 5 mg ml^{-1} silver modified Laponite® RD was sonicated, then transferred to 8 mm diameter filter paper. To ensure uniform thickness, the filter paper of 8mm diameter was dried in an oven regulated at 40^{o}C for 1 hour. Then small disks of 8mm diameter containing approximately 140 ±20 µg silver nanoparticles were punched out and stored in a desiccator at ambient temperature. The bacterial suspension of 10^5 - 10^6 CFU ml^{-1} was diluted to give a semi-confluent growth of 10^3 -10^4 CFU ml^{-1} and applied on nutrient agar plate surface and spread with a spreader. The disks were aseptically placed on the agar. The plates including the disks were incubated for 24 hours at 37 ^{o}C. The average diameter of the inhibition zone surrounding the disk was measured with a ruler with 1 mm scale, three replicates were performed for each concentration of silver-Laponite® RD for the different bacterial strains and the mean and standard error were recorded. The copper-Laponite® RD disk diffusion test was performed in a similar manner.

2.5.3 Influence of concentration of silver-Laponite® RD and $AgNO_3$ with time on bacterial growth

The inhibitory effect of the silver-Laponite® RD as function of concentration and time was investigated by the experimental method described by Bellantone *et al*., (2002). A single colony from each bacteria was used to inoculate a 20 ml starter culture, which was grown aerobically overnight at 37 ^{o}C in a rotary shaker at 150 rpm (Fig. 2.6). 0.1 ml of each culture

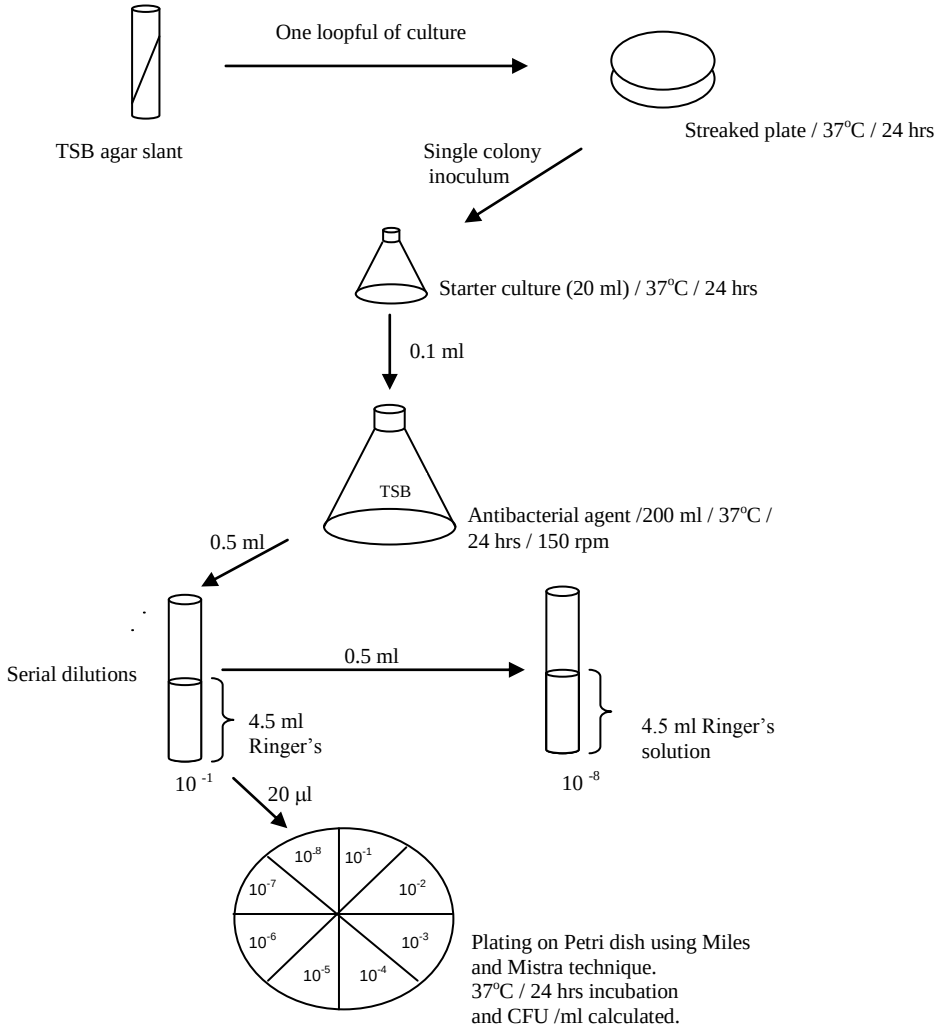

Fig. 2.7: Schematic representation of antibacterial protocol. Determination of viable cell count, CFU ml^{-1}. Fresh slant is inoculated with bacterial stock culture. After overnight incubation, a loopful is transferred to make a streak plate. A single colony inoculum was aseptically transferred to a TSB medium and grown for 24 hrs at 37 ^{o}C. With sterile pipette 0.1 ml was aseptically transferred into flasks containing TSB and the antibacterial agents. Serial dilution was performed and plating on TSA to estimate the colony forming units (CFU ml^{-1}).

(approx. 1x 10^9 CFU ml^{-1}) were then inoculated into 200 ml sterile TSB in 500ml conical flasks to give a final concentration of 1.55 x 10^5 ± 6.33 x 10^4 CFU ml^{-1} (total viable count obtained on the agar plate) for *E. coli*, 1.56 x 10^5 ± 1.45 x 10^4 CFU ml^{-1} for *S. aureus* and 1.65 x10^5 ± 1.18 x 10^4 CFU ml^{-1} for *P. aeruginosa* at time 0. Flasks containing Laponite®

RD (without silver) or silver-Laponite® RD were prepared according to the protocol shown in Tables 2.3 and 2.4. Flasks 1 to 3 contained *E. coli*, *S. aureus* and *P. aeruginosa* in TSB and were used as negative controls; flasks 4 - 6 containing silver modified Laponite® RD and TSB, devoid of inoculum, were used as positive controls. Laponite® RD (without silver) was prepared as follows; 2 gl^{-1} (0.4g per 200 ml) was added to flasks 7, 8 and 9 containing 200ml TSB. The concentration of silver-Laponite® RD used was 2 gl^{-1} (0.4g per 200ml). Flasks 10 to 18 contained the different concentrations of silver-Laponite® RD while flasks 19 – 21 contained 2 gl^{-1} $AgNO_3$ each. 0.5 ml from each sample was serially diluted in ten-fold steps to 10^{-8} and 20 µl of liquid culture

Table 2.3: Summary of experimental procedure used in the antibacterial testing of silver modified Laponite® RD via ion exchange and $AgNO_3$.

Flask No	TSB; ml	Bacteria; ml	*AGLAP6; g	Lap; g	AGLAP1; g	AGLAP4; g	AGLAP6; g	$AgNO_3$; g
1	200	0.1	-	-	-	-	-	-
2	200	0.1	-	-	-	-	-	-
3	200	0.1	-	-	-	-	-	-
4	200	-	0.4	-	-	-	-	-
5	200	-	0.4	-	-	-	-	-
6	200	-	0.4	-	-	-	-	-
7	200	0.1	-	0.4	-	-	-	-
8	200	0.1	-	0.4	-	-	-	-
9	200	0.1	-	0.4	-	-	-	-
10	200	0.1	-	-	0.4	-	-	-
11	200	0.1	-	-	0.4	-	-	-
12	200	0.1	-	-	0.4	-	-	-
13	200	0.1	-	-	-	0.4	-	-
14	200	0.1	-	-	-	0.4	-	-
15	200	0.1	-	-	-	0.4	-	-
16	200	0.1	-	-	-	-	0.4	-
17	200	0.1	-	-	-	-	0.4	-
18	200	0.1	-	-	-	-	0.4	-
19	200	0.1	-	-	-	-	-	0.4
20	200	0.1	-	-	-	-	-	0.4
21	200	0.1	-	-	-	-	-	0.4

*AGLAP was AGLAP6 without bacteria used as positive control

were aseptically transferred on to three TSA plates from each dilution and incubated overnight at 37 ^{o}C for 24 hours. The colony counts (which was the visible bacteria growth judged by the naked eye) were obtained from the averages of the three plates for each dilution (Xu *et al*., 2006 and Gottschaldt *et al*., 2006). The experiment was repeated three times and results expressed as CFU ml^{-1}.

Table 2.4: Summary of experimental procedure used in the antibacterial testing of silver modified Laponite® RD via isomorphous substitution and $AgNO_3$.

Flask No	TSB; ml	Bacteria; ml	*AL3; g	Lap; g	AL1; g	AL2; g	AL3; g	$AgNO_3$; g
1	200	0.1	-	-	-	-	-	-
2	200	0.1	-	-	-	-	-	-
3	200	0.1	-	-	-	-	-	-
4	200	-	0.4	-	-	-	-	-
5	200	-	0.4	-	-	-	-	-
6	200	-	0.4	-	-	-	-	-
7	200	0.1	-	0.4	-	-	-	-
8	200	0.1	-	0.4	-	-	-	-
9	200	0.1	-	0.4	-	-	-	-
10	200	0.1	-	-	0.4	-	-	-
11	200	0.1	-	-	0.4	-	-	-
12	200	0.1	-	-	0.4	-	-	-
13	200	0.1	-	-	-	0.4	-	-
14	200	0.1	-	-	-	0.4	-	-
15	200	0.1	-	-	-	0.4	-	-
16	200	0.1	-	-	-	-	0.4	-
17	200	0.1	-	-	-	-	0.4	-
18	200	0.1	-	-	-	-	0.4	-
19	200	0.1	-	-	-	-	-	0.4
20	200	0.1	-	-	-	-	-	0.4
21	200	0.1	-	-	-	-	-	0.4

*AL was AL3 without bacteria used as positive control

At each time interval triplicate pH measurements were performed and the mean value was calculated. The graph of CFU ml^{-1} was plotted against time using Microsoft Excel (Microsoft corporation, 2010). The protocol was repeated for the AGLAP4 and AGLAP6 in 200ml TSB. The release of Ag^{+} ions from the silver-Laponite® RD into TSB was studied by withdrawing 5 ml of each culture with a sterile pipppete at 2 hours intervals for 8 hours and then at 24, 48 and 72 hours.

2.6 Antibacterial activity of copper modified Laponite® RD

2.6.1 Introduction

The antibacterial activity of copper modified Laponite® RD (copper-Laponite® RD) was investigated by exposing three different bacterial strains: *E. coli* K12W-T (Gram negative), *S. aureus* NCIMB6571 (Gram positive) and *P. aeruginosa* NCIMB8295 (Gram negative) to copper modified Laponite® RD via ion exchange and isomorphous substitution. All three bacteria were obtained from the University of Wolverhampton culture collection centre. The stock cultures were freeze-dried and kept at -20 ^{o}C. Prior to the investigation, cultures were resuscitated and grown on TSA overnight at 37 ^{o}C. During the investigation all three bacterial strains were exposed to copper-exchanged Laponite® RD and copper incorporated Laponite® RD in TSB for a period of 72 hours.

2.6.2 Influence of concentration of copper-Laponite® RD and $CuSO_4$ with time on bacterial growth

The inhibitory effect of the copper-Laponite® RD as a function of concentration and time was investigated by the experimental method as shown in Tables 2.5 and 2.6. A single colony from each bacteria was used to inoculate a 100 ml starter culture, which was grown aerobically overnight at 37 ^{o}C in a rotary shaker at 150 rpm (Fig. 2.6). 0.1 ml of each culture

(approx. 1x 10^9 CFU ml^{-1}) were then inoculated into 200 ml sterile TSB in 500ml conical flasks to give a final concentration of 1.73 x 10^5 ± 6.0 x 10^4 for *E. coli,* 1.70 x 10^5 ± 1.2 x 10^4 CFU ml^{-1} (standard error calculated from the three plates for each dilution performed) for *S. aureus* and 1.60 x 10^5 ± 1.33 x 10^4 CFU ml^{-1} for *P. aeruginosa* at time 0. Flasks containing Laponite® RD (without copper) or copper-Laponite® RD were prepared according to the protocol (Table 2.5 and 2.6), flasks 1 to 3 containing *E. coli*, *S. aureus* and *P. aeruginosa* in TSB were used as negative controls.

Table 2.5: Summary of experimental procedure used in the antibacterial testing of copper modified Laponite® RD via ion exchange and $CuSO_4$.

Flask No	TSB; ml	Bacteria; ml	*CULAP6; g	Lap; g	CULAP1; g	CULAP4; g	CULAP6; g	$CuSO_4$; g
1	200	0.1	-	-	-	-	-	-
2	200	0.1	-	-	-	-	-	-
3	200	0.1	-	-	-	-	-	-
4	200	-	0.4	-	-	-	-	-
5	200	-	0.4	-	-	-	-	-
6	200	-	0.4	-	-	-	-	-
7	200	0.1	-	0.4	-	-	-	-
8	200	0.1	-	0.4	-	-	-	-
9	200	0.1	-	0.4	-	-	-	-
10	200	0.1	-	-	0.4	-	-	-
11	200	0.1	-	-	0.4	-	-	-
12	200	0.1	-	-	0.4	-	-	-
13	200	0.1	-	-	-	0.4	-	-
14	200	0.1	-	-	-	0.4	-	-
15	200	0.1	-	-	-	0.4	-	-
16	200	0.1	-	-	-	-	0.4	-
17	200	0.1	-	-	-	-	0.4	-
18	200	0.1	-	-	-	-	0.4	-
19	200	0.1	-	-	-	-	-	0.4
20	200	0.1	-	-	-	-	-	0.4
21	200	0.1	-	-	-	-	-	0.4

*CULAP was CULAP6 without bacteria used as positive control

A second set of controls (positive) was prepared as follows: 2 g l^{-1} (0.4g per 200 ml) of Laponite® RD (without copper) was added to flasks 4, 5 and 6 without any bacteria. The concentration of copper exchanged Laponite® RD and $CuSO_4$ used was 2 g l^{-1} each in flasks 7 – 18 and 19 – 21 respectively. 0.5 ml from each sample flask was serially diluted in ten-fold steps to 10^{-8} and 20 µl of each dilution was transferred aseptically and spread on TSA plates in triplicate, and incubated overnight at 37 ^{o}C using the Miles and Mistra technique (Hedges, 2002; Weenk, *et al*., 2003) see Fig. 2.6. The investigation was performed under the same experimental conditions although temperature, pH, water activity and available nutrient were not determined experimentally. The colony counts were obtained from the mean of the three plates for each dilution.

Table 2.6: Summary of experimental procedure used in the antibacterial testing of copper modified Laponite® RD via isomorphous substitution and $CuSO_4$.

Flask No	TSB; ml	Bacteria; ml	*CL; g	Lap; g	CL1; g	$CuSO_4$; g
1	200	0.1	-	-	-	-
2	200	0.1	-	-	-	-
3	200	0.1	-	-	-	-
4	200	-	0.4	-	-	-
5	200	-	0.4	-	-	-
6	200	-	0.4	-	-	-
7	200	0.1	-	0.4	-	-
8	200	0.1	-	0.4	-	-
9	200	0.1	-	0.4	-	-
10	200	0.1	-	-	0.4	-
11	200	0.1	-	-	0.4	-
12	200	0.1	-	-	0.4	-
13	200	0.1	-	-	-	0.4
14	200	0.1	-	-	-	0.4
15	200	0.1	-	-	-	0.4

*CL was CL1 without bacteria used as positive control

The whole experiment was performed three times and the results expressed as Log colony forming unit per millilitre (Log CFU ml^{-1}). From each sample flask, 5 ml was withdrawn at two hourly intervals for 8 hours and then at 24, 48 and 72 hours for further analysis with ICP-AES.

2.7 Inductively coupled plasma atomic emission spectroscopy (ICP-AES) analysis

The concentration of silver ions and copper ions released from silver-Laponite® RD and copper-Laponite® RD into TSB at each time interval was determined by ICP-AES. To determine the concentration of silver ions released from the Laponite® RD matrix into the TSB solution, 5 ml portions of the samples were used for Inductively Coupled Plasma Atomic Emission Spectroscopy (ICP-AES) with SPECTRO CIROS^{CCD}. The determination of silver ions or copper ions released from the metal-Laponite® RD sheet into solution gives a better understanding of how much silver or copper was available in the media containing the bacteria, as well as the amount retained in the metal-Laponite® RD matrix.

The release of Ag^+ ions from the silver modified Laponite® RD and Cu^{2+} from the copper modified Laponite® RD into nutrient agar was studied by suspending equal amounts in agar. The suspensions were maintained under the same conditions as for the bacterial test, with a rotary shaker set at 150 rpm. The samples were centrifuged with a Sigma Laboratory Centrifuge 6K15, spin at 5600g, 15,000 rpm for 15 minutes. The concentration of Ag^+ or Cu^{2+} in the supernatant was determined by ICP-AES, initially at starting time zero (0) and after every two hours at 2, 4, 6, 8, 24, 48 and 72 hours.

2.8 Statistical analysis

Antibacterial activity assays were performed in triplicates on different days. Data were expressed as the mean and standard error of the mean. The differences observed between samples were considered to be significant at $P < 0.05$ and extremely significant at $P < 0.001$ (Motulsky, 1999). Statistical procedures were performed with Graphpad Prism 5 using two-way ANOVA with Bonferroni test, some of the results are presented in Appendix 1 and 2.

Chapter 3

Result and Discussion

Synthesis and characterisation of silver modified Laponite® RD

In this chapter the results based on the synthesis of Laponite RD, ion exchange with silver and the characterisation of silver modified Laponite® RD before and after the ion exchange are presented. The production of silver incorporated Laponite® RD via isomorphous substitution and their characterisation are also included.

3.1 Synthesis, ion exchange and characterisation of silver modified ® Laponite RD

3.1.1 Synthesis of Laponite ® RD

Laponite® RD was synthesised according to the protocol already described in Section 2.1 with 2.16 SiO_2/MgO input ratio.

3.1.2 Characterisation of Laponite ® RD

The XRD pattern in Fig. 3.1 shows the crystalinity and phase purity of the synthesised Laponite® RD and is clearly similar to the commercial product. The peaks obtained is typical of Laponite® RD in the 0 – 50 °2Theta range.

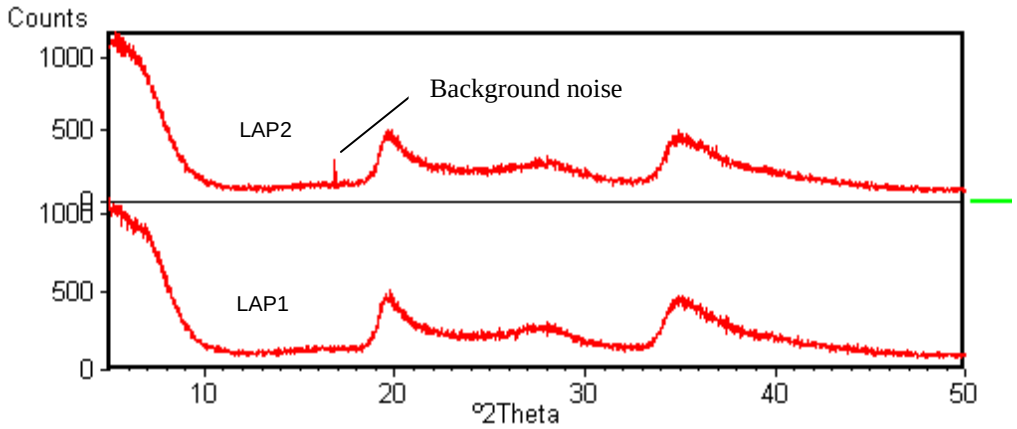

Fig. 3.1: XRD pattern of commercial product, LAP1 and synthesised sample, LAP2.

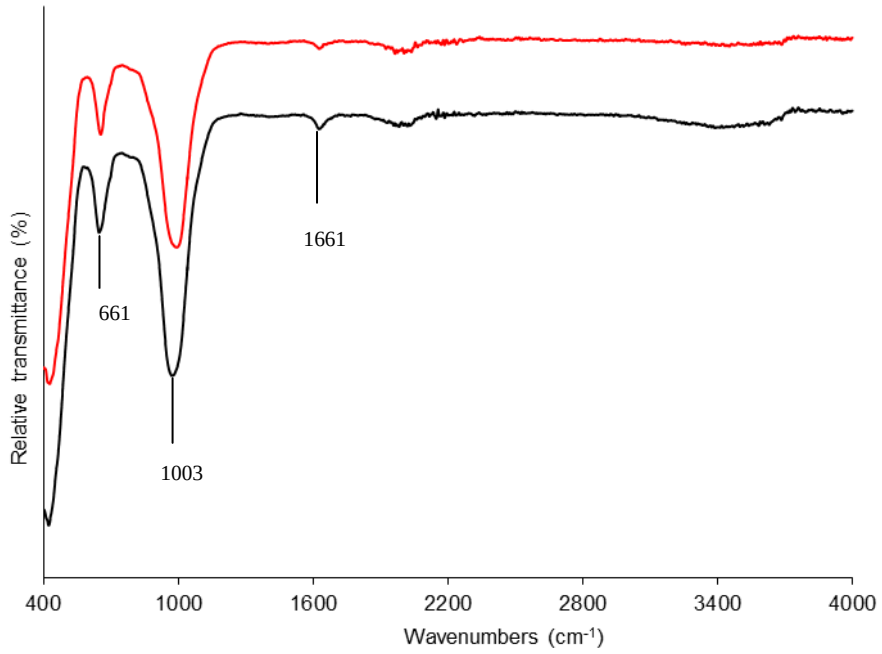

Fig. 3.2: FTIR of commercial product, LAP1 (black) and synthesised sample, LAP2 (red).

The FTIR (Fig. 3.2) also show close matching peaks on the synthesised Laponite® RD and the commercial Laponite® RD which further confirm their similarities as also seen on the SEM micrographs (Fig. 3.3)

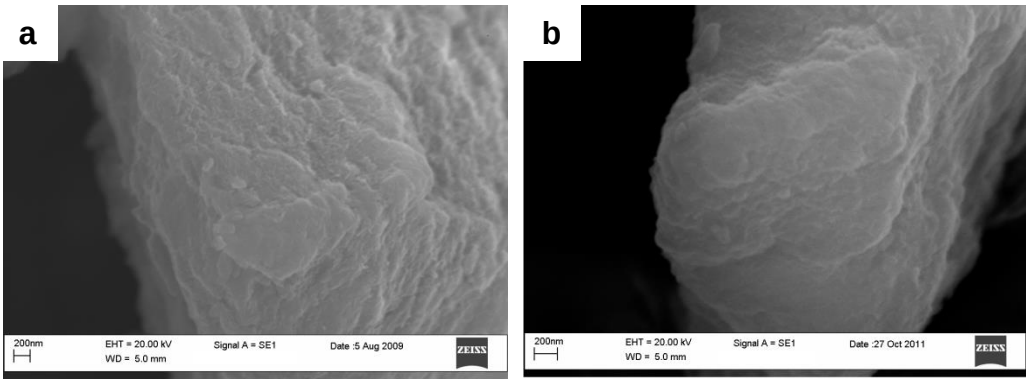

Fig. 3.3: SEM micrographs of commercial product, LAP1 (a) and synthesised sample, LAP2 (b).

3.2. Synthesis of silver-exchanged Laponite® RD (AGLAP1-6) by ion exchange

Ion exchange was carried out on as-synthesised Laponite® RD as described in Section 2.2.1.1. Upon completion of the ion exchange samples were characterised with FTIR, XRD, EDX, SEM, ^{29}Si MAS NMR, TGA and TEM

3.2.1 Characterisation

The evidence of the displacement with silver on the Laponite® RD surface through ion-

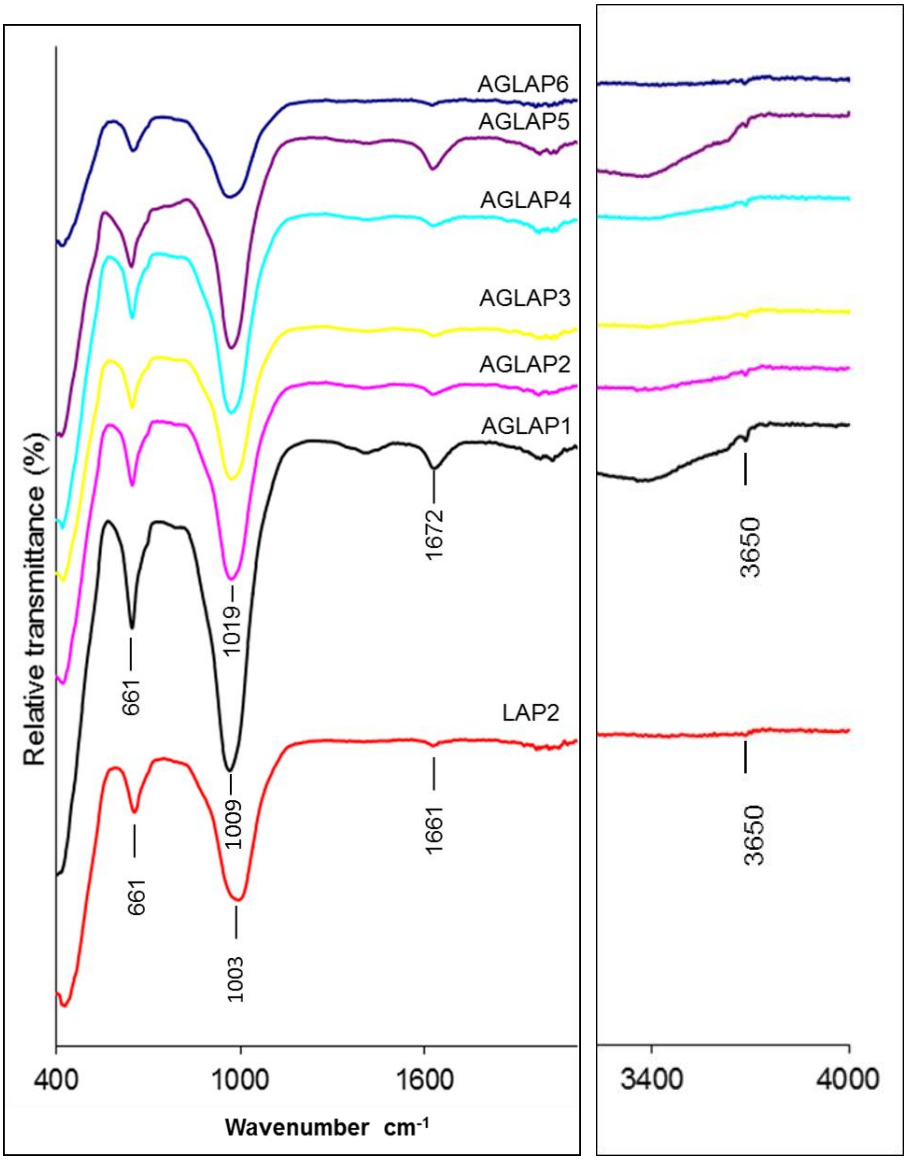

Fig. 3.4: FTIR spectra of Laponite® RD without silver, LAP2 (synthesised sample) and silver-exchanged Laponite® RD (AGLAP1-6).

exchange was provided by FTIR, which gives the qualitative or how well the Na^+ of the Laponite® RD is exchanged by the Ag^+ at the interlayer (Negrete-Harrera *et al.*, 2007). At the same scan time, the transmittance remains relatively unchanged for both the pure Laponite® RD and the silver exchanged species (Fig. 3.4). However, the band corresponding to Si-O-Si stretching vibration at $1003cm^{-1}$ was shifted towards higher wave numbers at 1009 and $1019cm^{-1}$ in the silver-exchanged Laponite® RD species. Similarly, the band at $1661cm^{-1}$ corresponding to OH stretching vibration in the silicate layers was shifted towards the higher wavenumber, $1672cm^{-1}$ (Wang *et al.*, 2010). The presence of the residual Mg-OH groups at $3650cm^{-1}$ after the ion exchange, as expected, indicate that their location were not accessible (Herrera *et al.*, 2005).

The XRD pattern (Fig.3.5) was performed to examine the crystalline structure of silver-

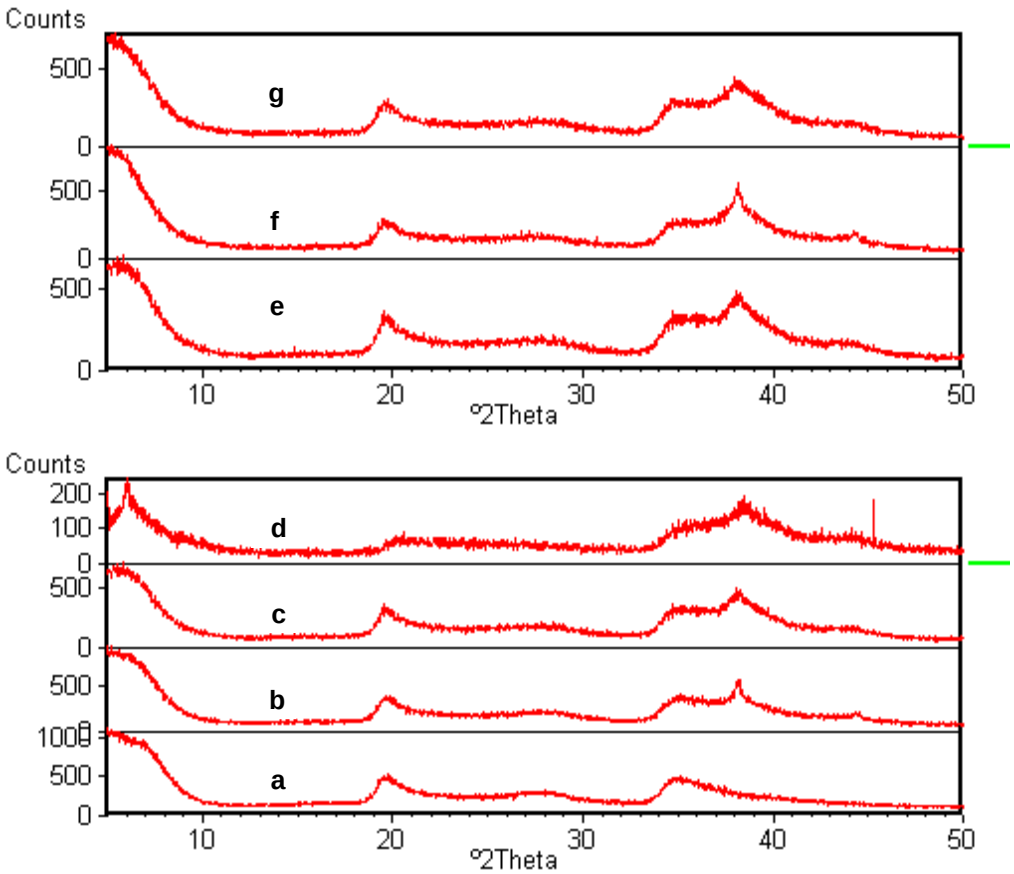

Fig. 3.5: XRD pattern of Laponite® RD, LAP2 (a) and silver-exchanged Laponite® RD; AGLAP1 - 6 (b - g)

exchanged Laponite® RD. The X-ray diffraction peaks at $2\theta^{o}$ of 44.5^{o} was not distinct. The peak around 38^{o} appeared in all the spectra of the silver-exchanged Laponite® RD analysed, with increasing intensity from AGLAP1 – 6, corresponding to crystal facet (111) attributed to silver nanoparticles (Ruparelia *et al*., 2008). The AGLAP5 and AGLAP6 particularly, were 1broader with high intensity corresponding to the crystallographic planes of face-centred cubic silver crystals in agreement with earlier observation by Huang and Yang, (2008). As silver was added the clay became delaminated. The broadening of the peaks is indicative of the Ag crystal size. Thus the broad peak width suggests that Ag possessed a small particle size. Changes in the basal spacing obtained directly from the XRD data showed, 1.28 nm for pure Laponite® RD, 1.48nm for AGLAP1 and 1.49, 1.52, 1.59, 1.63, 1.67nm in the AGLAP2 - 6 respectively, indicated the exchange of silver within the interlayer of Laponite® RD which is in agreement with Carrado, (2000). These characteristics show that Ag^{+} ions had been adsorbed into the Laponite® RD layers but in insufficient quantity to disrupt the formation of gel with deionised water in the AGLAP1- 4. However, further interaction with silver at higher concentrations resulted in the reorganisation of the Laponite® RD structure. Hence, gelation was absent in the AGLAP5 and AGLAP6 silver-exchanged Laponite® RD samples on testing with the pebble and jar test (Section 2.3.10). The surface morphology of Laponite® RD with and without silver is shown in the SEM micrographs Fig 3.6.

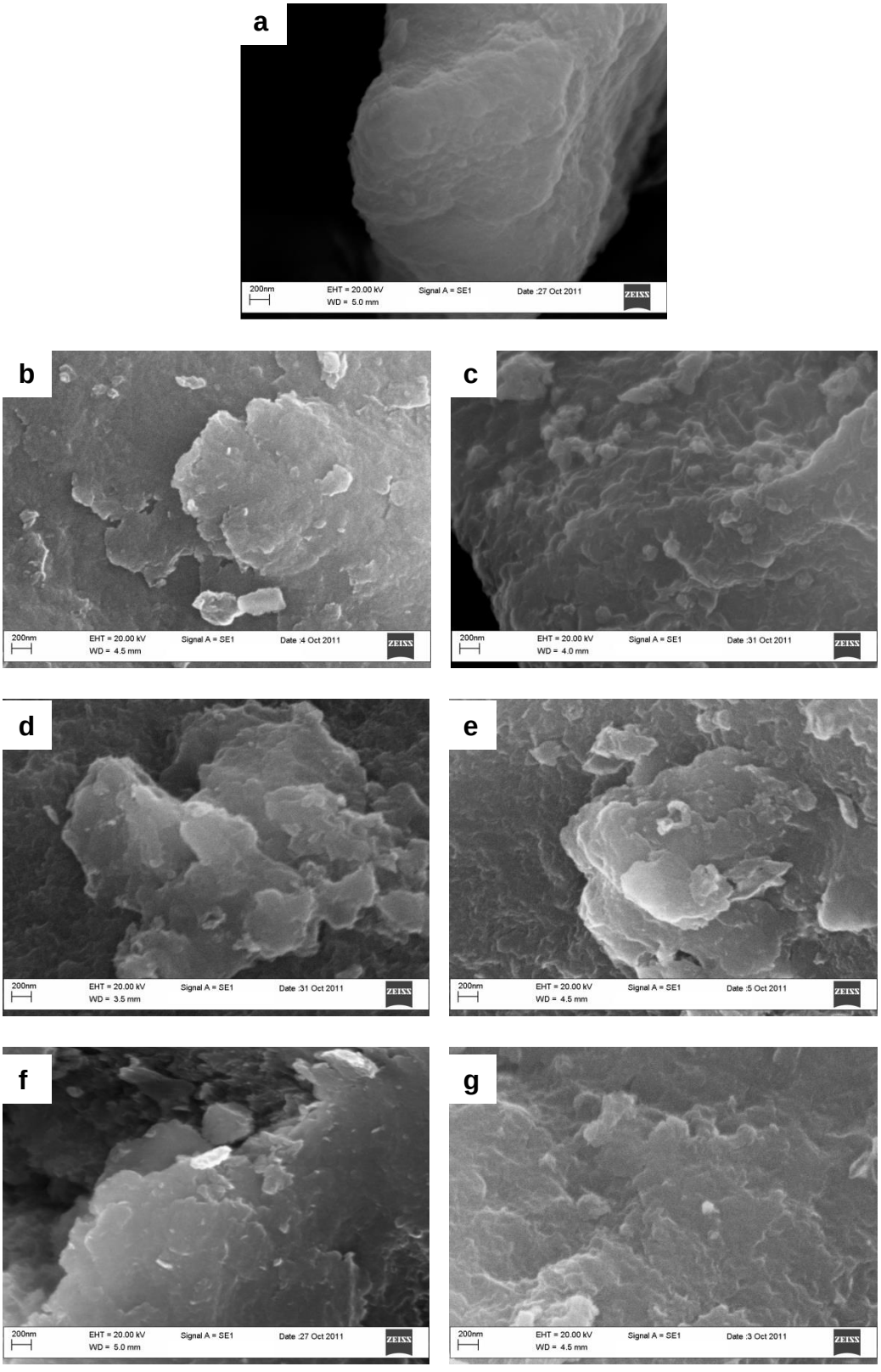

Fig. 3.6: SEM micrographs of Laponite® RD without silver, LAP2 (a) and silver-exchanged Laponite® RD; AGLAP1 (b), AGLAP2 (c), AGLAP3 (d), AGLAP4 (e), AGLAP5 (f) and AGLAP6 (g). The SEM was used to its limits according to the technician. See other characterisation techniques e.g. TEM in Fig. 3.12 and 3.13.

Spot analysis of the silver-exchanged Laponite® RD was performed at eight different positions selected randomly on the surface of the clay (Table. 3.1). EDX cannot detect Li or its compounds in the silver-exchanged Laponite® RD particle due to the low atomic number of these elements and also, total percentage composition being less than 5wt% (Song *et al*., 2009 and Pichonat *et al*., 2010). Therefore, Li and OH were quantified using ICP-AES (Section 2.3.8) and TGA (Section 2.3.9). An excited lithium atom emit electromagnetic radiation of approximately 427nm wavelength which is detected by the charged couple device and subsequently tramsformed directly into percentage weight (wt %). These wt % of Li were then recorded against the respective samples. The dehydroxilation which occurred at ≥700^{o}C was automatically detected on the electrobalance and was then transformed into weight versus temperature graph by a computer from which the OH weight was obtained.

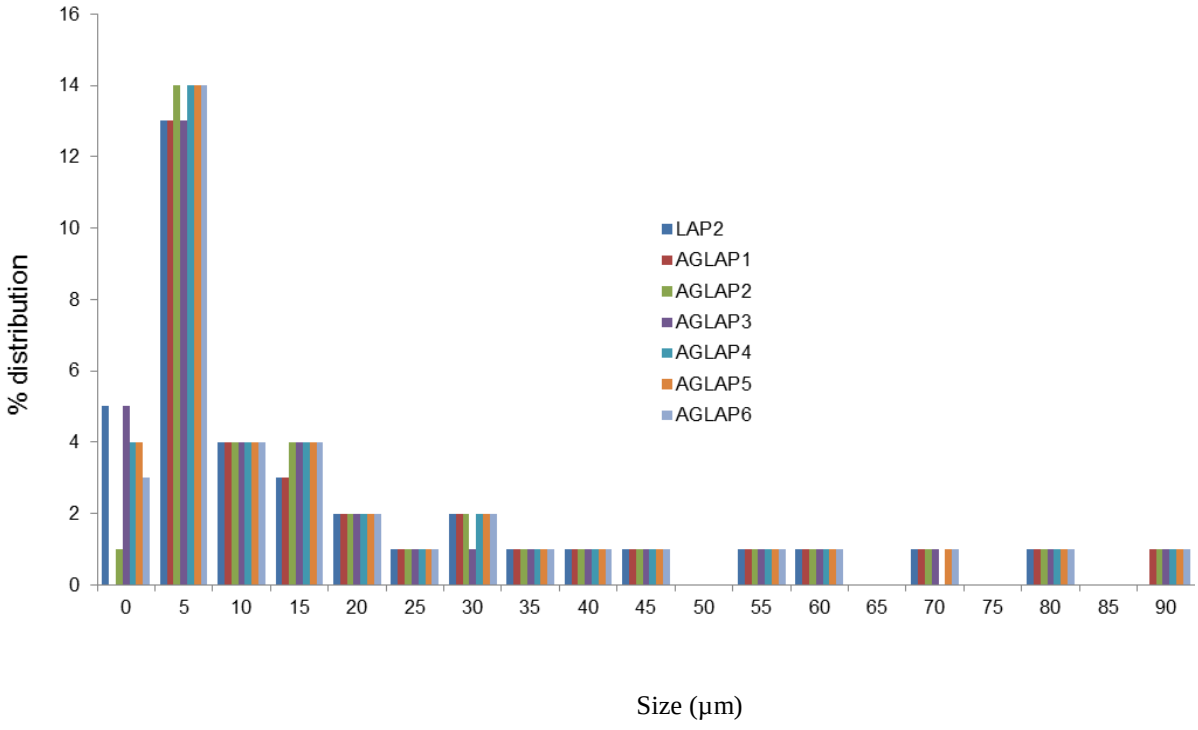

Fig. 3.7: Particle size distribution of Laponite® RD and silver-exchanged Laponite® RD.

In the displacement with the AGLAP1 a total of 20% Na^+ was replaced with Ag^+ ions at pH 6.7 while, 71% and 93% of Na^+ were replaced in the AGLAP4 (pH 6.5) and AGLAP6 (pH 6.3) respectively. The particle size distribution of both the pure Laponite RD and the silver-exchanged Laponite RD according to the Laser Granulometer Hydro 2000MU were similar with a modal distribution of 5µm (Fig. 3.7). The evidence of silver exchange was further supported by the EDX spectra (Fig. 3.8) and the microimages of the elements; Na, Si, Mg and Ag as shown in Fig. 3.9. These indicated the presence of Ag and its distribution across the surface of the Laponite® RD.

Table 3.1: EDX elemental analysis of Laponite® RD without silver and silver-exchanged Laponite® RD.

	Concentration of silver-exchanged Laponite® RD (wt. %)						
Elements	**LAP2**	**AGLAP1**	**AGLAP2**	**AGLAP3**	**AGLAP4**	**AGLAP5**	**AGLAP6**
Na	1.59±0.06	1.27±0.14	0.74±0.14	0.66±0.10	0.45±0.11	0.16±0.04	0.11±0.03
Mg	13.97±0.12	13.41±0.70	13.98±0.13	13.62±0.10	13.91±0.15	13.83±0.16	13.26±0.23
Si	22.23±0.16	22.92±0.68	22.11±0.08	22.18±0.10	22.50±0.85	22.01±0.08	21.70±0.21
Ag	0.00±0.00	0.70±0.15	1.25±0.21	1.61±0.47	1.76±0.26	1.85±0.10	2.35±0.15
O	59.48±0.22	59.35±0.19	59.51±0.04	59.30±0.20	59.17±1.18	59.64±0.12	59.81±0.81
Li	0.03±0.00	0.02±0.00	0.03±0.00	0.03±0.00	0.03±0.00	0.03±0.00	0.02±0.00
OH	2.66±0.03	2.69±0.08	2.53±0.24	2.53±0.24	2.59±0.18	2.50±0.27	2.50±0.27

From Table 3.1 the unit cell formula for each of the samples was calculated thus; the wt. % was converted to gram to determine the number of moles. The number of moles was then divided by the lowest factor to get the ratio of the unit cell in each case.

LAP2 $Na_{16.1}(Si_{58.0}\ Mg_{133.6.5}\ Li)\ O_{864.5}\ (OH)_{36.4}$

AGLAP1 $Na_{19.1}\ Ag_{2.2}(Si_{281.4}\ Mg_{190.2}\ Li)\ O_{1279.1}\ (OH)_{54.5}$

AGLAP2 $Na_{7.5}\ Ag_{2.7}(Si_{183.1}\ Mg_{133.7}\ Li)\ O_{865.0}\ (OH)_{34.6}$

AGLAP3 $Na_{6.7}\ Ag_{0.4}(Si_{183.5}\ Mg_{130.3}\ Li)\ O_{862.0}\ (OH)_{34.6}$

AGLAP4 $Na_{4.6}\ Ag_{3.8}(Si_{186.3}\ Mg_{133.1}\ Li)\ O_{860.0}\ (OH)_{35.4}$

AGLAP5 $Na_{1.6}\ Ag_{4.0}(Si_{182.2}\ Mg_{132.3}\ Li)\ O_{866.9}\ (OH)_{34.2}$

AGLAP6 $Na_{1.7}\ Ag_{7.5}(Si_{266.4}\ Mg_{188.1}\ Li)\ O_{1289.0}\ (OH)_{50.7}$

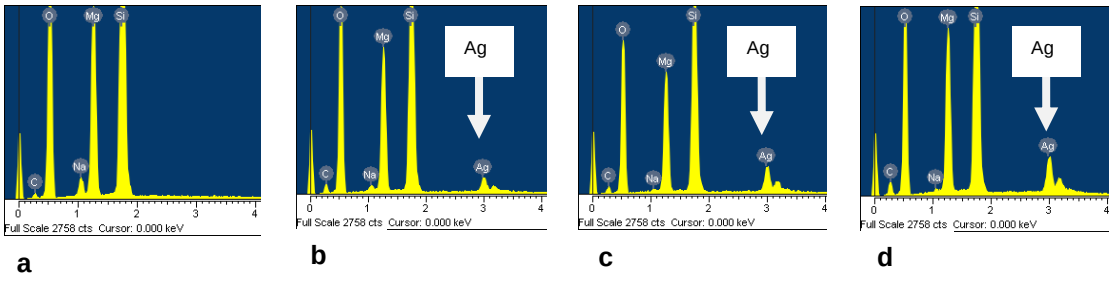

Fig. 3.8: EDX spectra of Laponite® RD without silver, LAP2 and silver-exchanged Laponite® RD; AGLAP1 (b), AGLAP4 (c) and AGLAP6 (d)

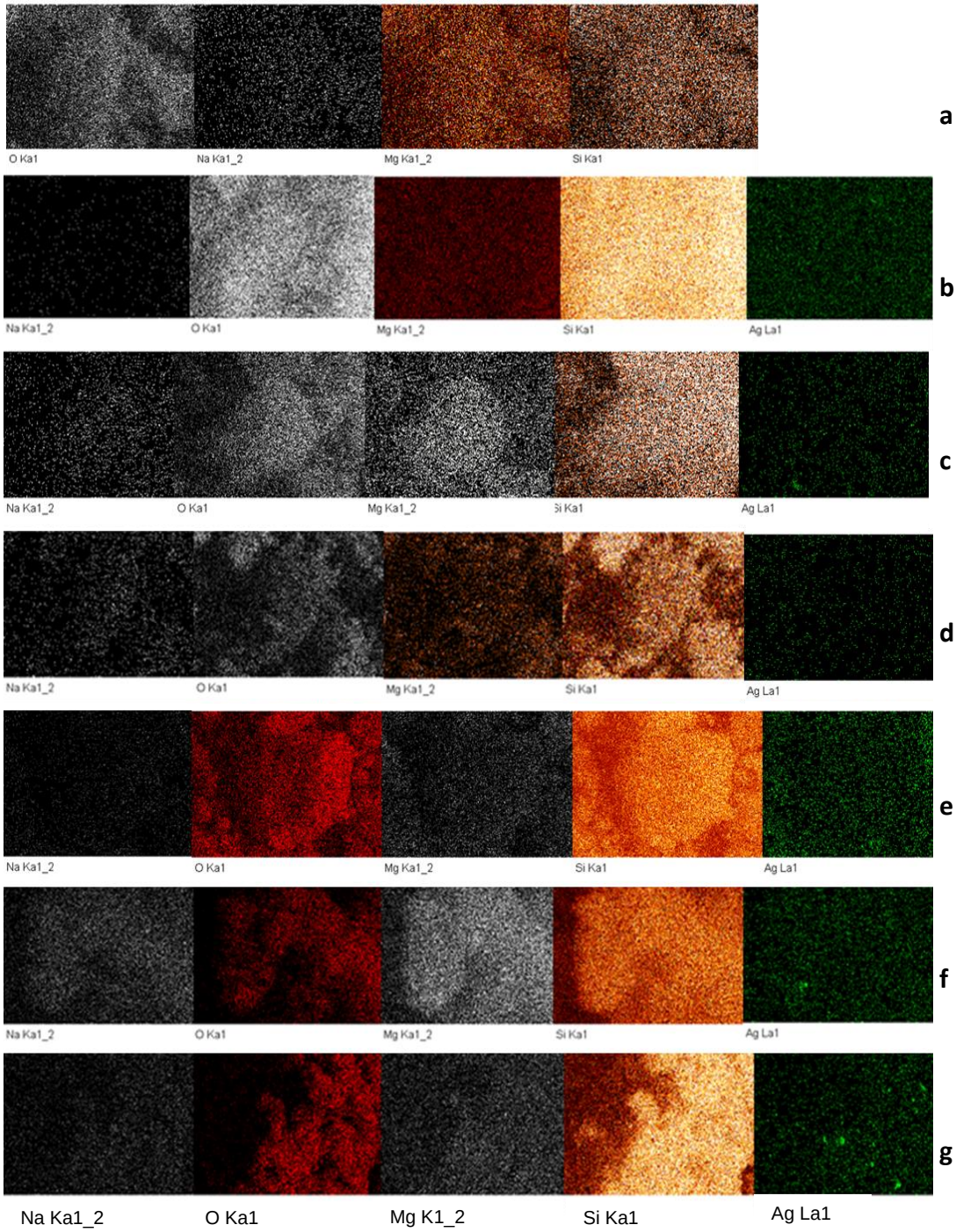

Fig. 3.9: Microimages of elements i1 Laponite® RD without silver, LAP2 (a) and silver-exchanged Laponite® RD; AGLAP1 (b), AGLAP2 (c), AGLAP3 (d), AGLAP4 (e), AGLAP5 (f) and AGLAP6 (g).

Fig. 3.10 show the thermograms of Laponite® RD (without silver), and Laponite® RD (with silver) to gain insight into the evolution of the composite structure. The endothermic character occurred at the temperature range 30 – 200^{o}C with a gradual loss of physisorbed interlayer water which occurred at 100^{o}C corresponding to a mass loss of 17%, followed by the subsequent release of water from the hydration sphere of exchangeable sodium cations (Palkova *et al*., 2010). The loss of structural water occurred at 252^{o}C with a mass loss of 6%, the complete dehydroxylation and eventual collapse of Laponite® RD structure was marked at 752 ^{o}C with a further mass loss of 7% as was similarly observed by Palkova *et al*., 2010. The physisorbed water loss at 100^{o}C for both AGLAP1 and AGLAP2 (Fig. 3.10b,c), 124 ^{o}C for AGLAP3 (Fig3.10c) was accompanied with mass losses of 14% (AGLAP1, AGLAP2) and 13% (AGLAP3). The structural water loss was not apparent in the AGLAP1, AGLAP2 and AGLAP3 but, visible in AGLAP4, AGLAP5 and AGLAP6 at 285, 280 and 256 ^{o}C with corresponding mass loss of 1% (AGLAP4, AGLAP5) and 1.5% for AGLAP6 (Fig. 3.10e,f,g). The dehydroxylation temperature of LAP2 occurred at 752^{o}C and those of the silver-exchanged Laponite RD at 750, 750, 750, 740, 725 and 718^{o}C for AGLAP1 - 6 respectively. This indicated that the pure Laponite® RD was thermally more stable than the silver-exchanged Laponite® RD and tends to decrease as the silver concentration increased.

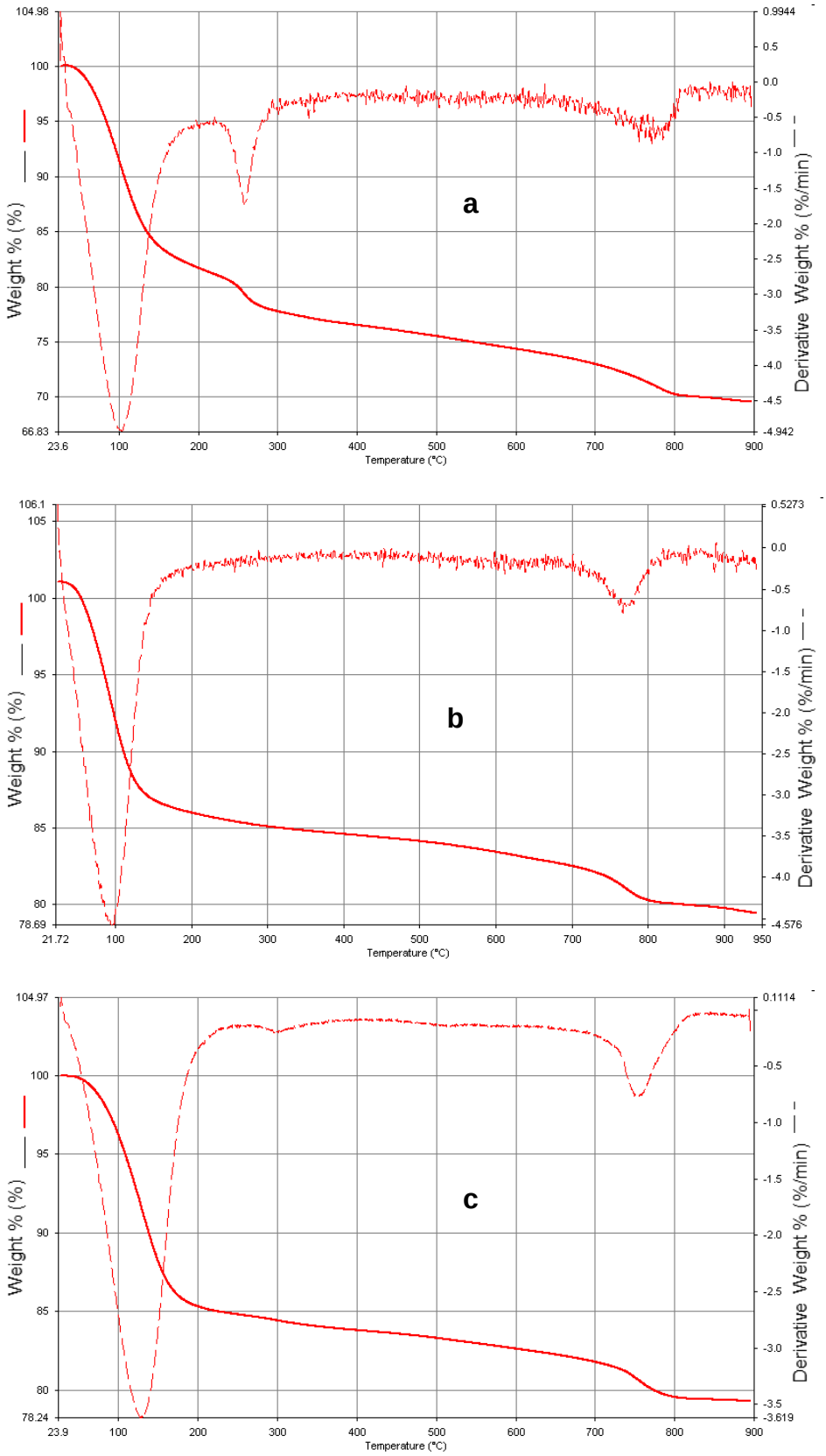

Fig. 3.10: TGA of Laponite® RD without silver, LAP2 (a) and Laponite® RD with silver; AGLAP1 (b), AGLAP2 (c), AGLAP3 (d), AGLAP4 (e), AGLAP5 (f) and AGLAP6 (g). Thermographs of sample (——), sample thermographs first derivatives (-----).

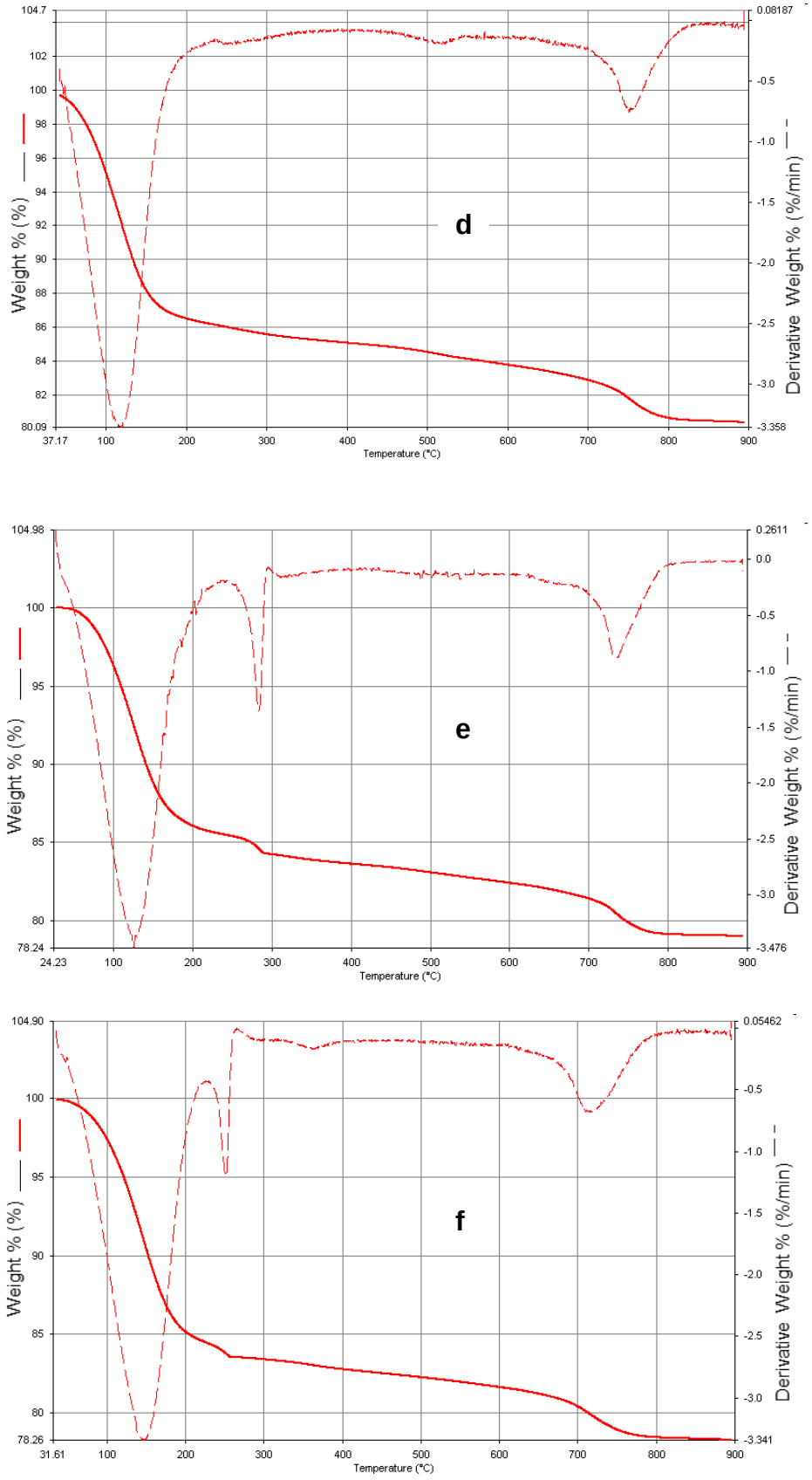

Fig. 3.10: (continued).

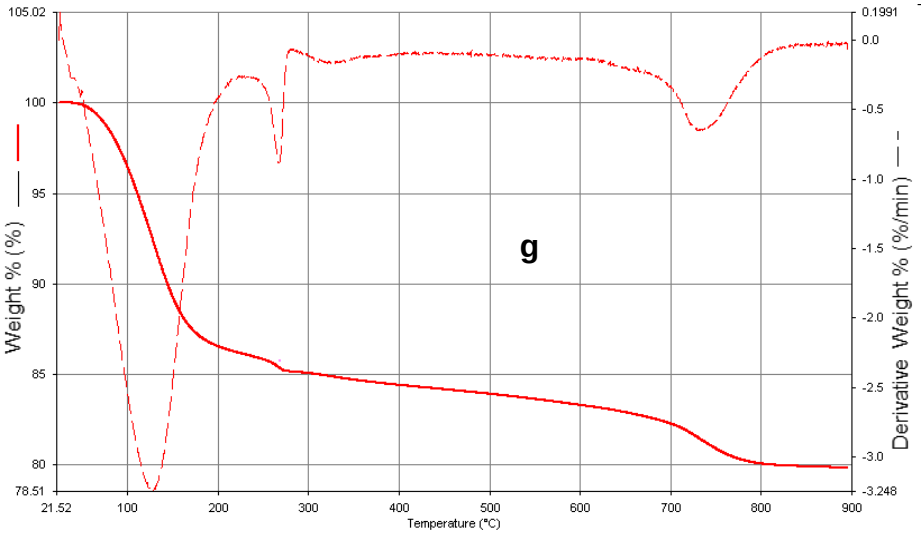

Fig. 3.10: (continued).

The knowledge of the crystal chemistry of Laponite® RD is largely based on ^{29}Si magic angle spinning nuclear magnetic resonance (^{29}Si MAS NMR). Fig. 3.11 shows that the spectra are similar; an indication that the silver had a subtle impact on the Laponite® RD sheet. In ^{29}Si MAS NMR spectroscopy, peaks are assigned the letters, Q_n, T_n, D_n, M_n, based on the number of oxygen atoms bonded to the Si atom, 4, 3, 2 and 1 respectively (Daniel *et al*., 2008) where *n* is the number of oxygen atoms bonded to a further Si atom. In Fig 3.11 Laponite® RD (without silver) is dominated by an intense resonance at -94.287ppm and a small peak around -85.066ppm attributed to Q_3 and Q_2 respectively. The Q_3 peak is the site of the $Si(OMg)(OSi)_3$ located in the Laponite® RD framework (Palkova *et al*., 2009) whereas the small signal, with chemical shift at –85.066ppm, is assigned to Q_2 tetrahedral silicon nuclei connected via oxygen bridges to two other Si centres which may have stem from $Si(OMg)(OSi)_2$ OH silanol groups existing on the Laponite® RD edges (Palkova *et al*., 2009).

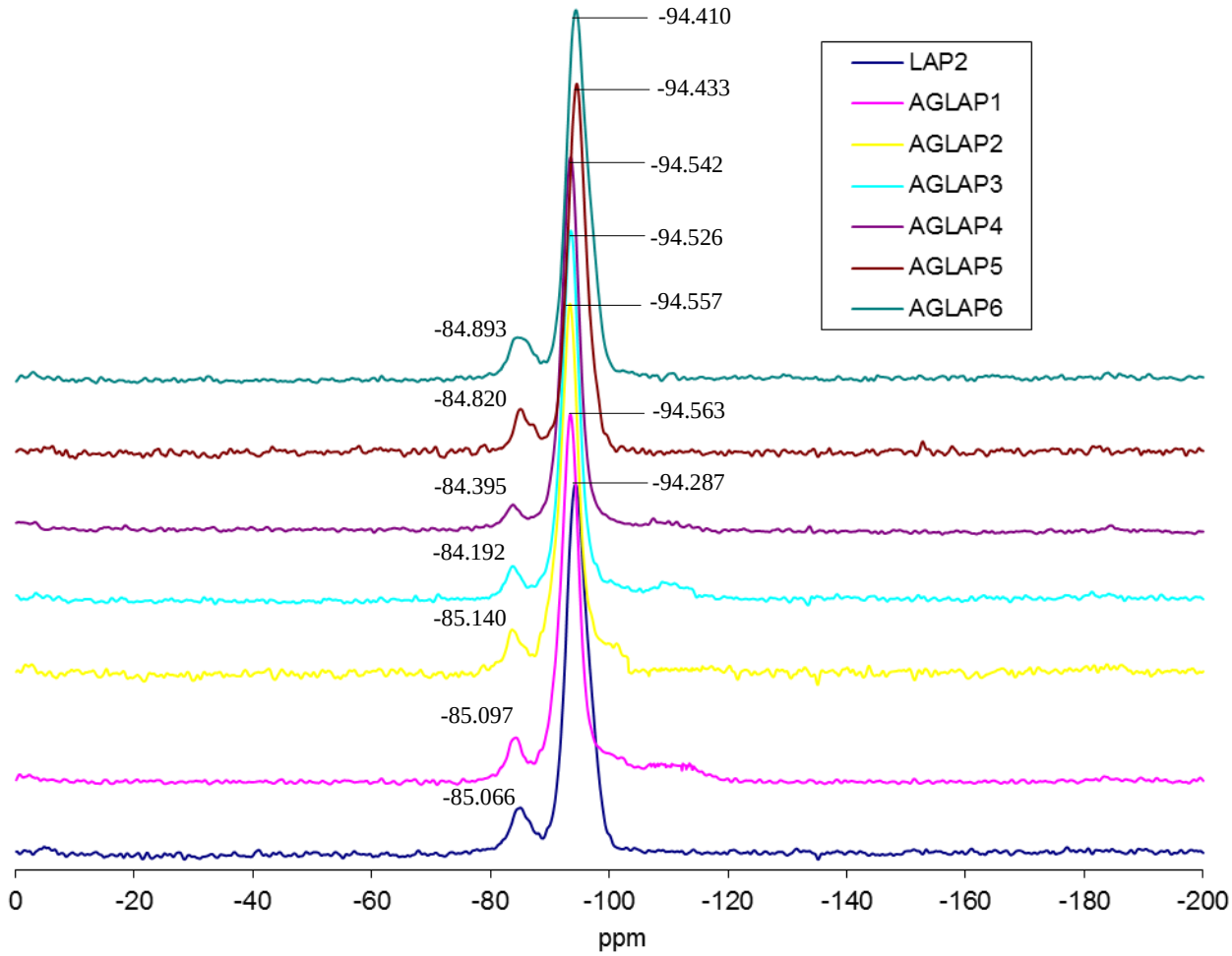

Fig 3.11: ^{29}Si MAS NMR of Laponite® RD without silver and silver-exchanged Laponite® RD.

The silver modified species showed increase in the intensity of the Q_2 peaks and a chemical shift from -85.066 to -85.097, -85.140, -84.192, -84.395, -84.820 and -84.893ppm, in AGLAP1, AGLAP2, AGLAP3, AGLAP4, AGLAP5 and AGLAP6 respectively. This was likely due to the formation of the Ag-O-Si bond consequent to the loss of $Si(OMg)(OSi)_3$ sites located on the Laponite® RD faces. The shift in the peaks is believed to be due to the interaction of silver with Laponite® RD at different silver concentrations. The TEM technique revealed direct morphology or interior structure of Laponite® RD particle. As

shown in Fig. 3.12 the Ag nanoparticle was spherical in shape with particle size distribution of 4 – 20nm (Fig. 3.13) and modal size of 12nm (AGLAP1) and 14nm (AGLAP4 and AGLAP6). The small silver nanoparticles exchanged with Laponite® RD agglomerated into larger particles due to high concentration of the solution, comparable to similar observation by Liu *et al*., 2007, which suggest that stability of small particles is dependent upon concentration of the solution as well as quantity of Laponite® RD. However, the agglomerations of the small nanoparticles were prevented by vigorous stirring. The stirring reduced the local concentration of the silver nanoparticles to a minimal level.

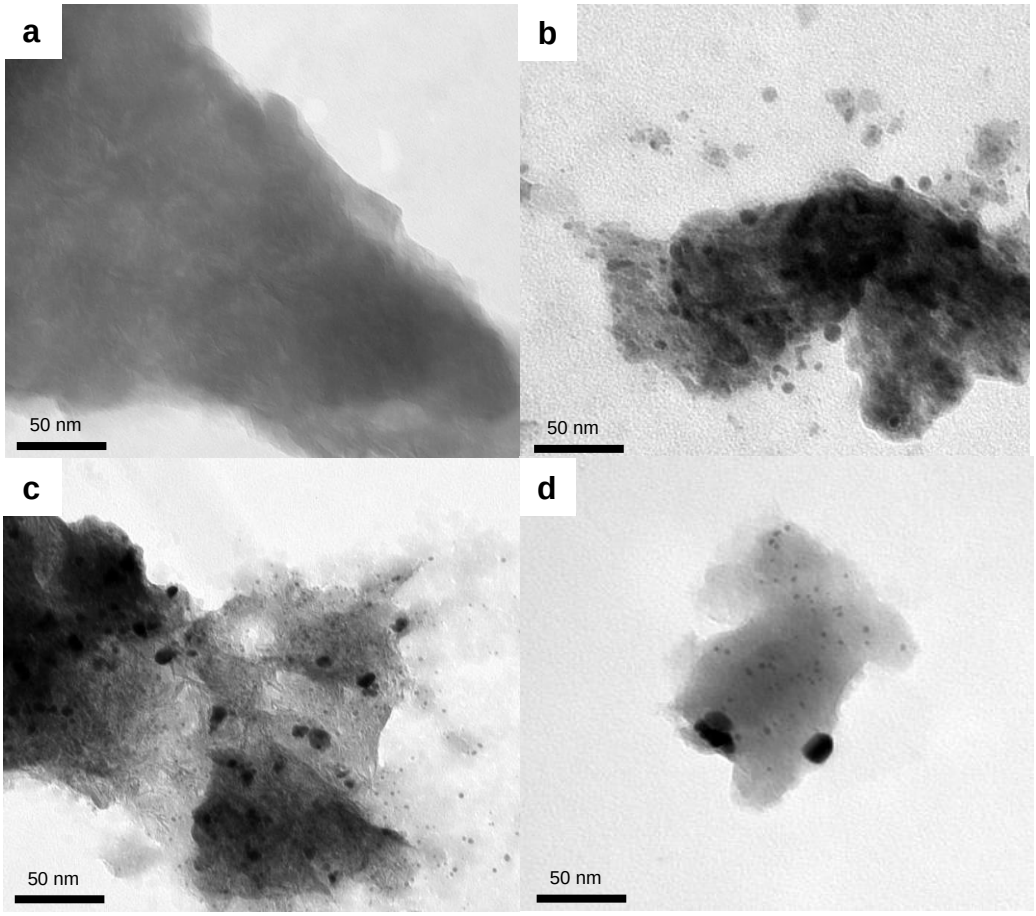

Fig. 3.12: TEM micrographs of Laponite® RD without silver, LAP2 (a) and Laponite® RD with silver; AGLAP1, (b), AGLAP4 (c) and AGLAP6 (d)

This is evident in the fairly uniform sized nanoparticles in Fig. 3.12 and Fig. 3.13. In addition, above certain concentrations of Ag such as AGLAP6 (2.35 – 2.50 wt. %) the aggregation of Ag tend to occur. Thus AGLAP1, AGLAP4 or AGLAP6 showed variable sizes and aggregation of different form leading to formation of large Ag nanoparticles.

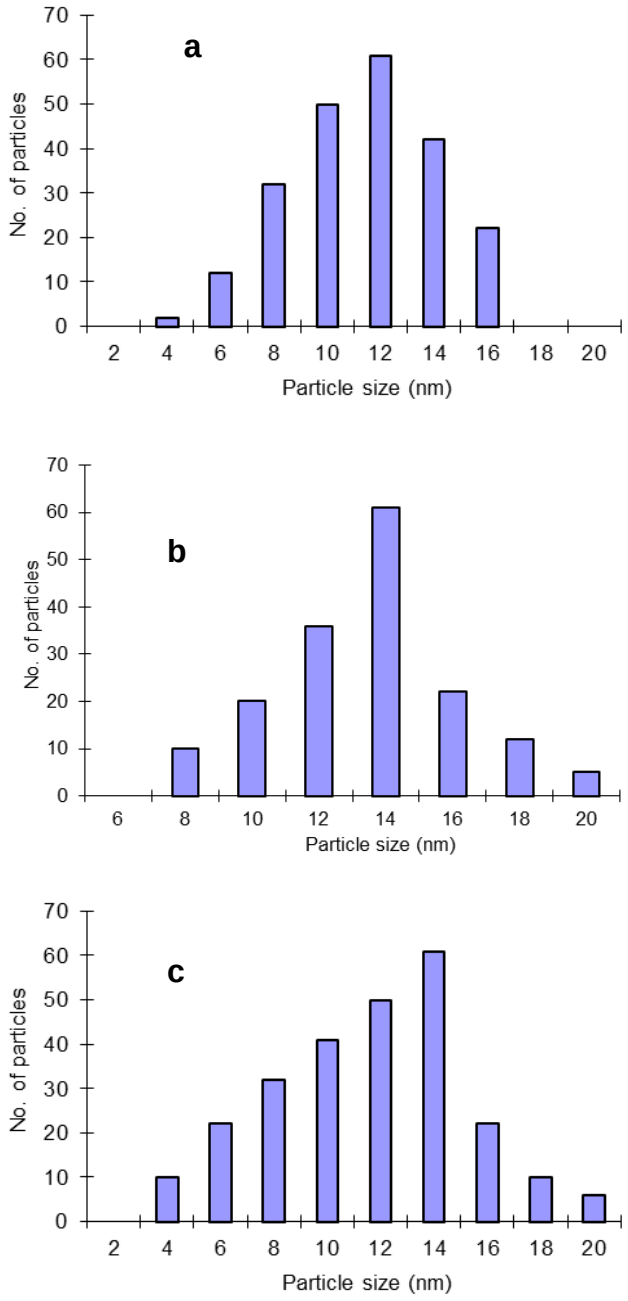

Fig. 3.13: TEM image of silver nanoparticles and particle size distribution obtained by image analysis for AGLAP1 (a), AGLAP4 (b) and AGLAP6 (c).

3.3 Synthesis, isomorphous substitution and characterisation of silver incorporated Laponite® RD

3.3.1 Synthesis of Laponite® RD

Laponite® RD was synthesised as described in Section 2.1

3.3.2 Synthesis of silver incorporated Laponite® RD (AL1-3) by isomorphous substitution

The isomorphous substitution was carried out as described in the synthesis protocol already described (Section 2.2.2.1). Upon completion of the substitution process, the samples were re-characterized by XRD, FTIR, EDX, TGA, SEM, ^{29}Si MAS NMR and TEM.

3.3.3 Characterization

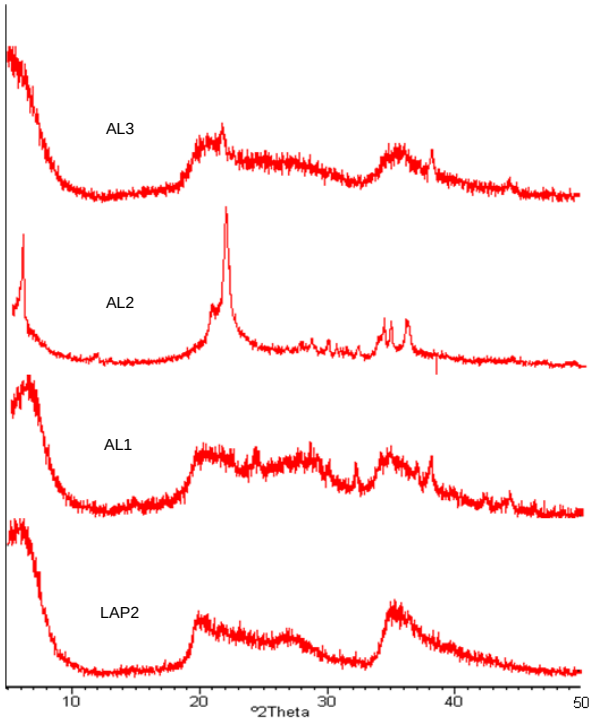

Fig. 3.14: XRD pattern of Laponite® RD and silver modified Laponite® RD

Fig. 3.14 Shows the XRD pattern of Laponite® RD and the silver exchanged form by isomorphous substitution. The pure Laponite® RD exhibited a broad XRD pattern due to its low crystallinity and small particle size (Park *et al*., 2004). The X-ray diffraction peak at 2 theta of 38^{o} was apparent in all the silver incorporated Laponite® RD and can be well assigned to the (111) crystallographic planes of face-centred cubic silver crystals (Huang and Yang, 2008). The line broadenings of the peaks were due to the small particle size which was also confirmed by the SEM and TEM.

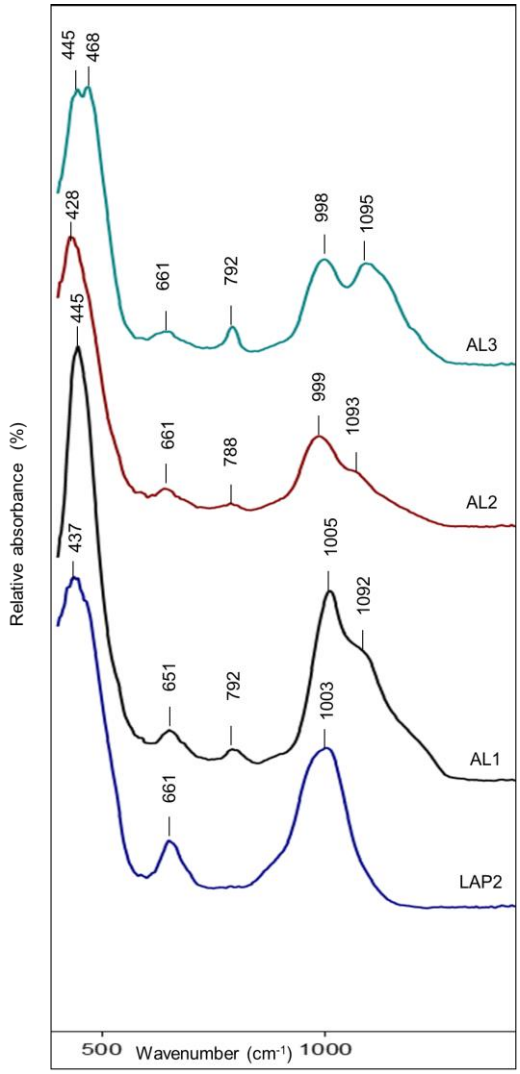

Fig. 3.15: FTIR spectra of Laponite® RD and silver modified Laponite® RD

The FTIR spectra of Laponite® RD (without silver) and Laponite® RD (with silver) in the low

energy range 400 – 2000cm^{-1} are as shown in Fig. 3.15. The broad and intensive band in the low energy region at 1003 cm^{-1} is attributed to Si-O stretching vibrations (Pereira *et al.*, 2007) of the tetrahedral sheet. The narrow bands at 1092, 654, and 466cm^{-1} are related to the metal-oxygen of the silicate layers (Wang *et al.*, 2010).

The absorption band at 661 cm^{-1} is attributed to the Mg-OH bending vibrations of the octahedral sheet. The characteristic overlap of the Si-O-Mg and Si-O-Si bending bands give rise to a complex band with two peaks; 468 and 445 cm^{-1}. Thus, disappearance of the Mg_3–OH band and the appearance of three new bands in the spectrum indicate the presence of silver in Laponite® RD and confirm the incorporation of silver within the sheet. Figure 3.16 shows the EDX spectra of Laponite® RD and the silver exchanged Laponite® RD obtained by isomorphous substitution.

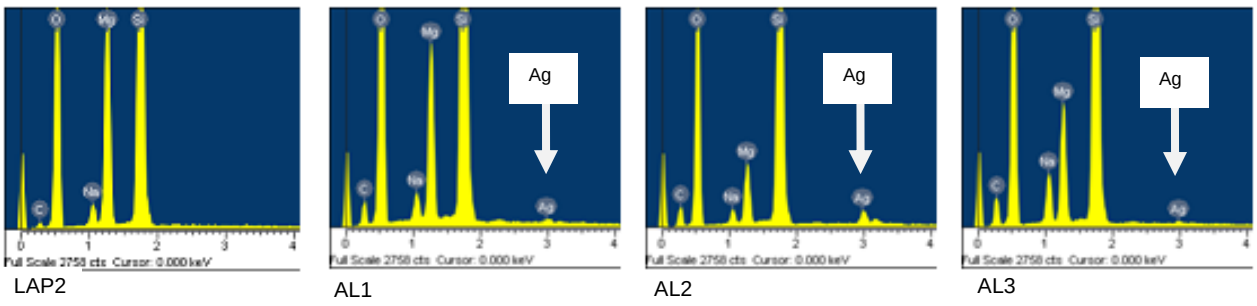

Fig.3.16: EDX spectra of Laponite® RD and the silver exchanged Laponite® RD by isomorphous substitution.

The Ag peaks are distinct (indicated by the arrows) and further confirm the presence of Ag in the Laponite® RD matrix. The EDX maps for the respective elements exhibit the nature of dispersed particles in the clay-metal hybrid. The different colours in Fig. 3.17 showed the dispersion of the different elements. The EDX elemental analysis further confirms the presences of silver in the Laponite® RD layers. There was a steady increase in the amount of Ag exchanged accompanied by a corresponding decrease in the Mg content as shown in

Table 3.2. Fig. 3.18 shows the thermograms of Laponite® RD (without silver) and silver-exchanged Laponite® RD. Interpretation of the thermal analysis data obtained for the silver incorporated Laponite® RD show the loss of the weakly bonded water at 97^{o}C (AL1) and 100^{o}C (AL2, AL3) corresponding to weight losses of 12, 11 and 17% in AL1, AL2 and AL3 respectively (Fig. 3.18b,c,d). There was no apparent chemisorbed water loss but the temperature range 200-700 ^{o}C was accompanied with weight losses of 4% (AL1, AL2) and 10% (AL3). This revealed the stronger interaction between Ag and the water molecules (Mosser *et al*., 1997). The dehydroxylation temperature for the pure Laponite® RD and the silver incorporated Laponite® RD were 752 and 800^{o}C with a designated mass loss of 2% (LAP2), 1% (AL1) and 0.5% (AL2, AL3). The high temperature range >800^{o}C of silver incorporated Laponite® RD over pure Laponite® RD indicated changes in the composition of the octahedral sheet (Mosser *et al*., 1997).

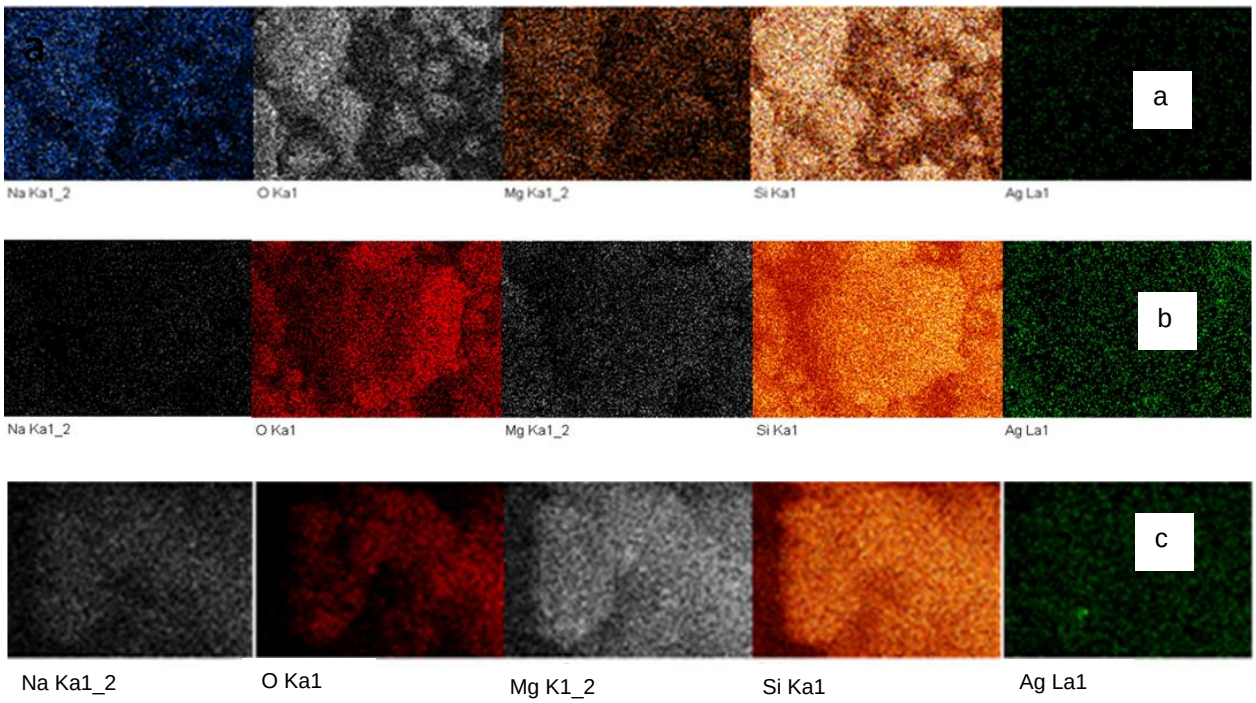

Fig. 3.17: Shows the EDX elemental map of Laponite® RD with silver; AL1 (a), AL2 (b) and AL3 (c).

Table 3.2: EDX elemental analysis of Laponite® RD without silver and silver incorporated Laponite® RD.

		Concentration of silver incorporated Laponite® RD (wt. %)		
Elements	LAP2	AL1	AL2	AL3
Na	1.59±0.06	1.77±0.17	1.57±0.20	1.58±1.20
Mg	13.97±0.12	11.86±1.89	10.06±2.64	9.47±1.14
Si	22.23±0.16	23.63±1.32	22.7±0.70	22.60±1.41
Ag	0.00±0.00	0.09±0.07	0.58±0.16	1.10±0.20
O	59.48±0.22	60.12±1.64	61.91±1.08	60.85±0.54
Li	0.03±0.00	0.02±0.00	0.03±0.00	0.04±0.00
OH	2.66±0.03	1.53±0.69	2.46±1.12	2.34±1.13

From Table 3.2 the unit cell formula for each of the silver incorporated Laponte® RD was calculated thus; the wt. % was converted to gram to determine the number of moles. The number of moles was then divided by the lowest factor to get the ratio of the unit cell in each case.

AL1 $Na_{95.9}$ ($Si_{1051.5}$ $Mg_{188.1}$ Ag $Li_{3.6}$) $O_{4696.9}$ $(OH)_{112.4}$

AL2 $Na_{15.9}$ ($Si_{181.5}$ $Mg_{96.2}$ $Ag_{1.2}$ Li) $O_{899.9}$ $(OH)_{33.6}$

AL3 $Na_{11.9}$ ($Si_{136.7}$ $Mg_{67.2}$ $Ag_{1.8}$ Li) $O_{655.7}$ $(OH)_{23.7}$

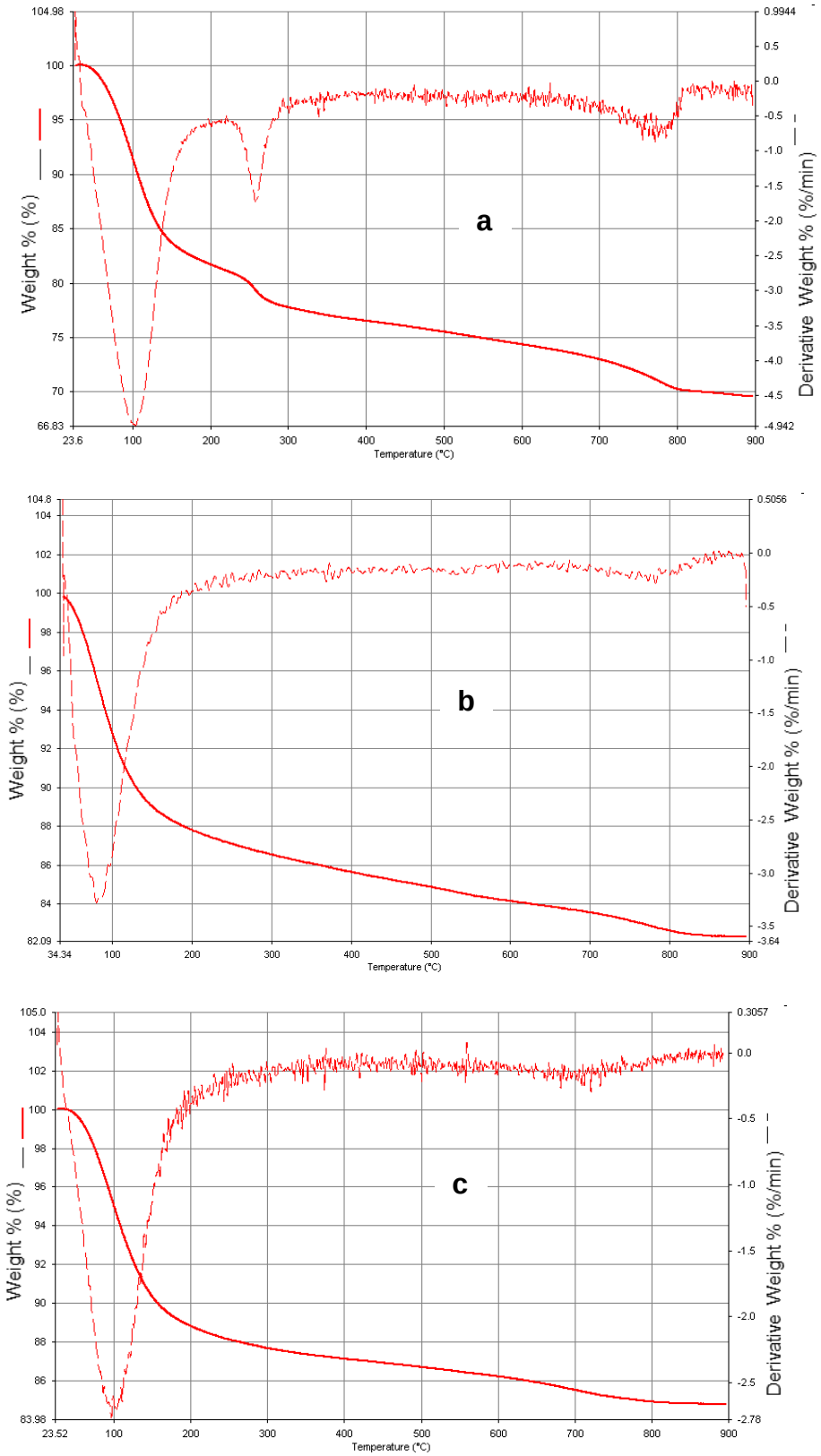

Fig. 3.18: TGA of Laponite® RD without silver, LAP2 (a), Laponite® RD with silver; AL1 (b), AL2 (c) and AL3 (d). Thermographs of sample (——), sample thermographs first derivatives (-----).

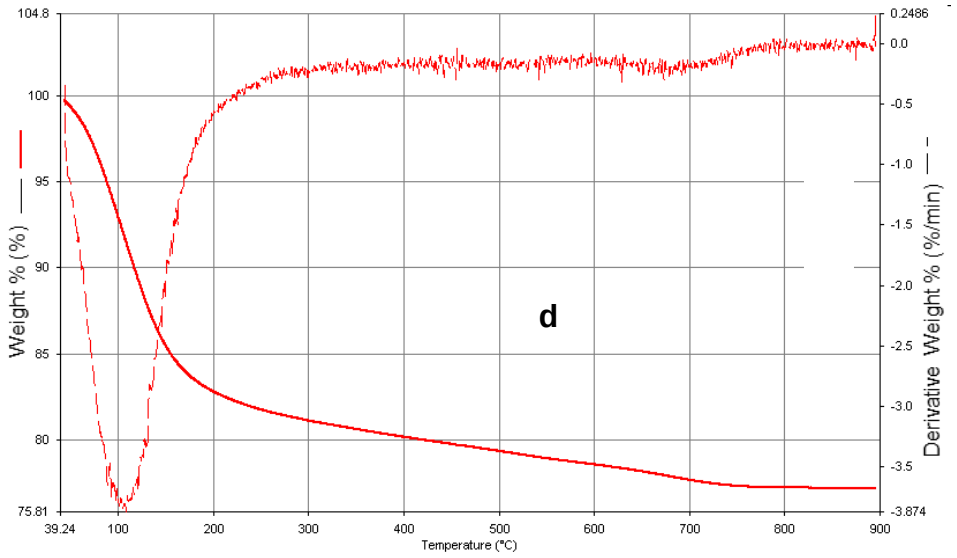

Fig. 3.18: (continued)

Fig. 3.19 shows the SEM images of pure Laponite® RD and Ag-Laponite® RD hybrid. The pure Laponite® RD (Fig.3.19a) showed uniform morphology while silver incorporated Laponite® RD (Fig. 3.19b,c,d) is characterised by lump or seed-like morphology with aggregates.

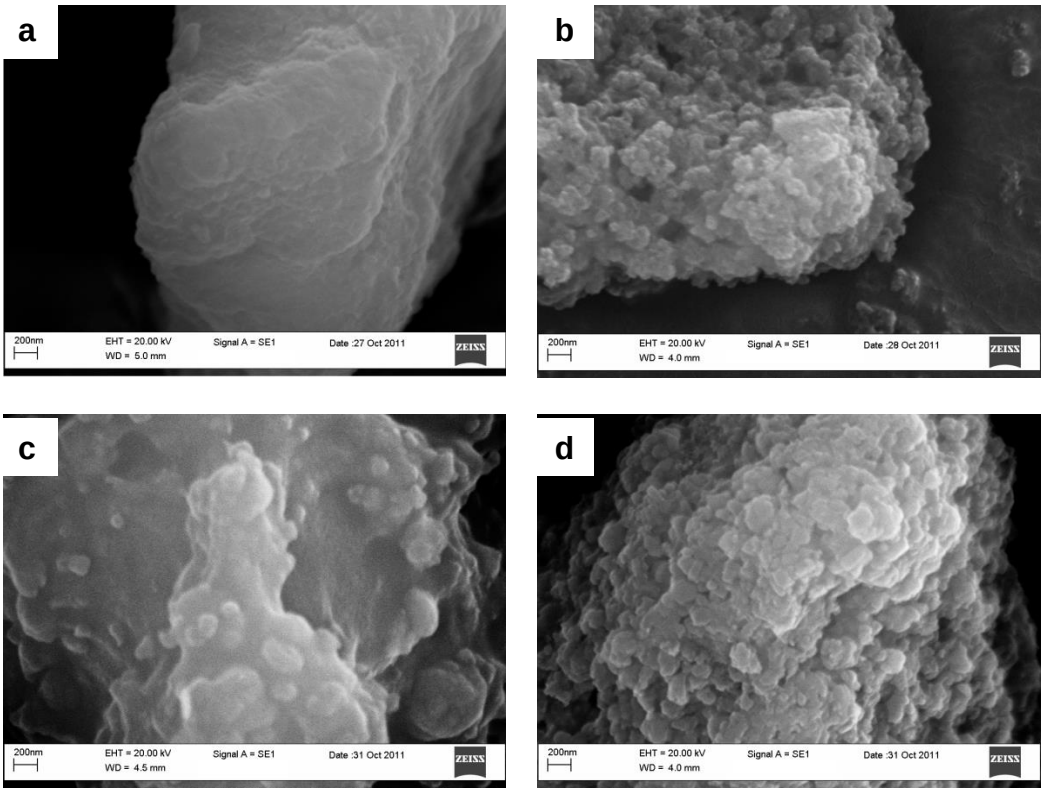

Fig. 3.19: SEM of Laponite® RD without silver; LAP2 (a) and Laponite® RD incorporated with silver; AL1 (b), AL2 (c) and AL3 (d).

Fig. 3.20 show the TEM micrographs of silver incorporated Laponite® RD. The micrographs revealed that the Ag particles are in the nanometer range and spherical in shape with particle size distribution of 4 – 20 nm (Fig. 3.21) and modal size of 10 nm for all the silver incorporated samples analysed (AL1-3).

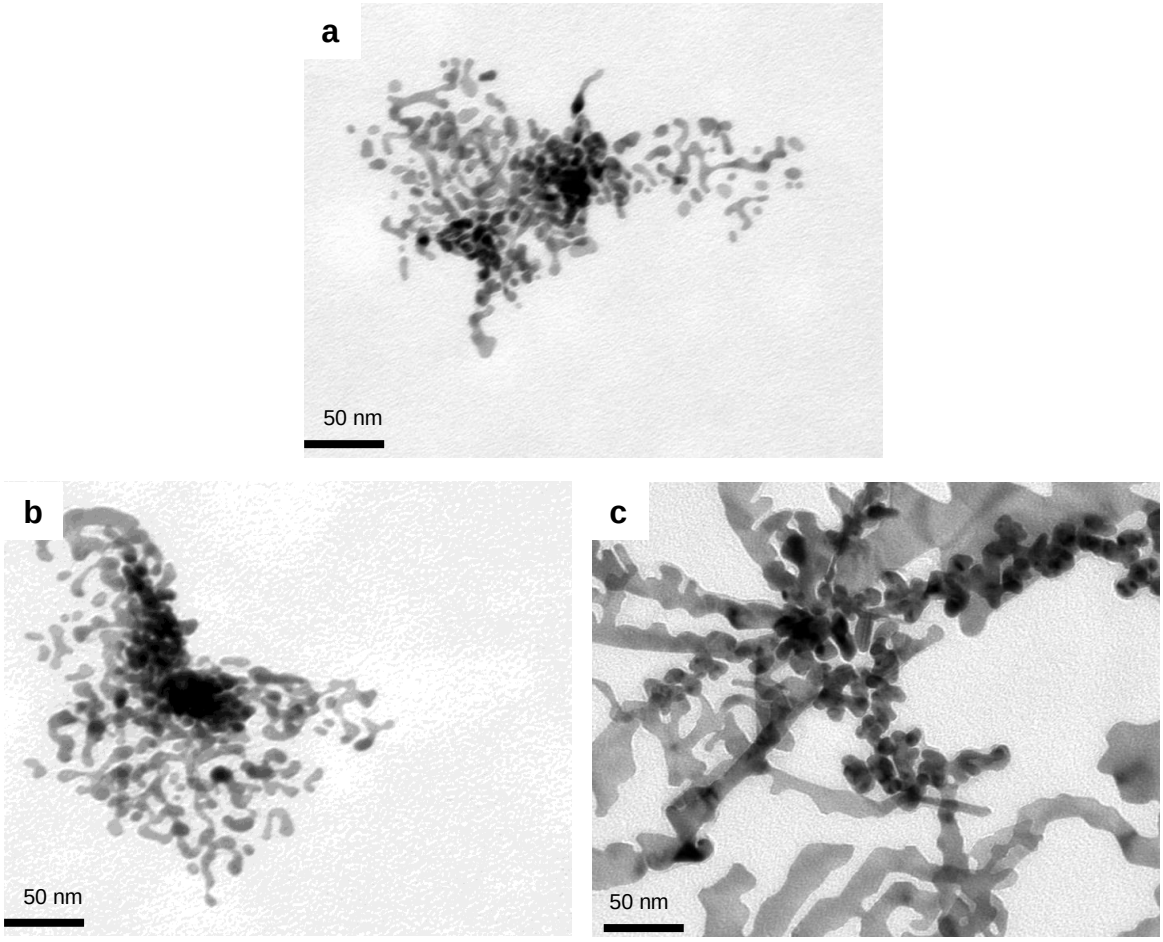

Fig. 3.20: TEM image of silver nanoparticles for AL1 (a), AL2 (b) and AL3 (c).

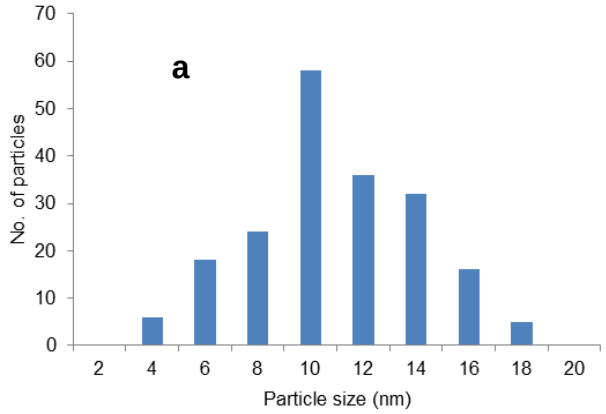

Fig. 3.21: Particle size distribution obtained by image analysis for AL1 (a), AL2 (b) and AL3 (c).

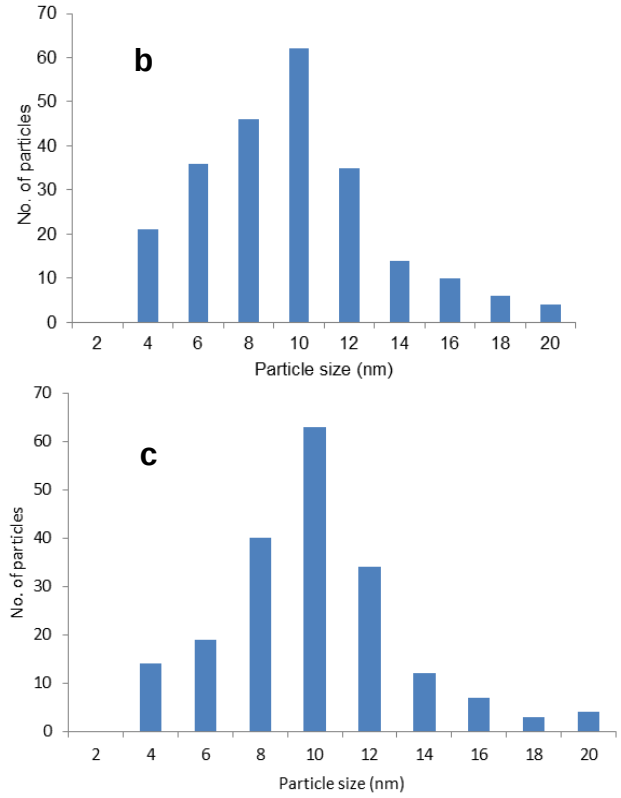

Fig. 3.21: (continued).

The knowledge of the crystal chemistry of Laponite® RD is largely based on the results of magic angle spinning nuclear magnetic resonance (MAS NMR). The ^{29}Si resonances are determined by the chemical incorporation of the octahedral layer via the isomorphous substitution of Mg or Li by Ag in Laponite® RD as shown in Fig. 3.22. The isomorphous substitution of Ag for Mg or Li at the octahedral layer resulted in chemical shift. The chemical shift is based on the Loewenstern's rule and on the maximum dispersion of charge (Catlow *et al.*, 1996 and Bekkam *et al*., 1991).

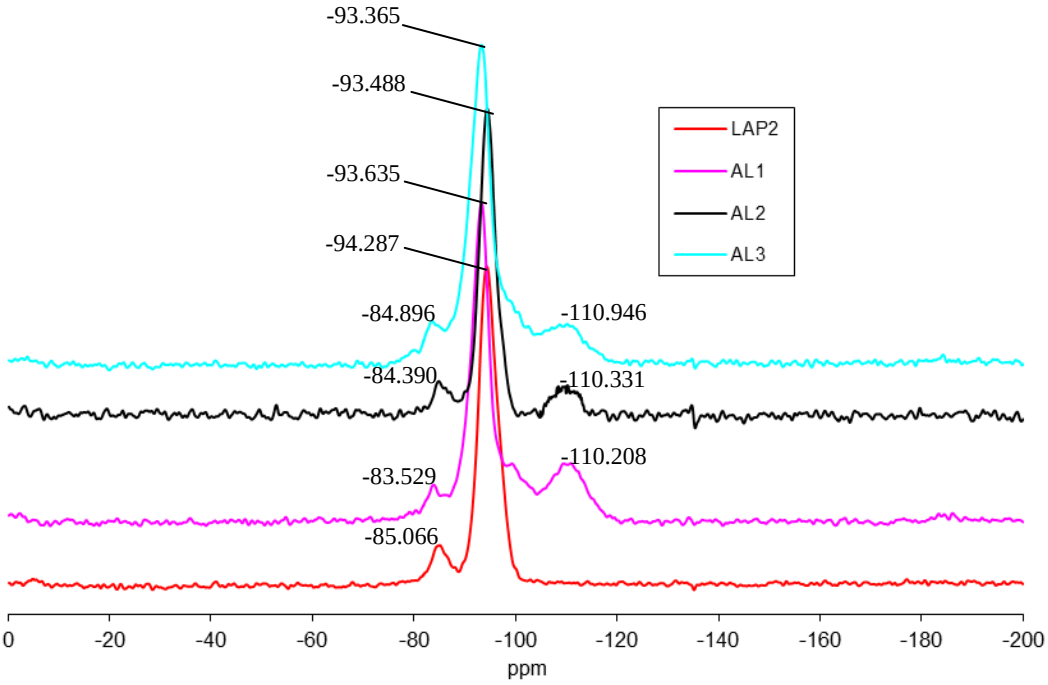

Fig. 3.22: ^{29}Si MAS NMR of Laponite® RD without silver, LAP2 and Laponite® RD incorporated with silver, AL1, AL2 and AL3.

For example, in framework silicates such as zeolite, the chemical shift increases with increasing amount of neighbouring Al^{3+} bringing about the deshielding effect (Bekkam *et al.*, 1991).

Furthermore, the chemical shift of the trioctahedral smectites was more negative (2 - 3ppm) than those of the dioctahedrals. This is largely a result of the electronegative difference in cations situated at the octahedral layer. In Laponite® RD, the apical oxygen of the Si tetrahedral is associated with $3Mg^{2+}$ while being bonded to two Si and one vacancy in the case of dioctahedral smectites. Thus, the atom-for-atom substitutions of an element with lower electronegativity in the octahedral layer results in deshielding and hence a negative ^{29}Si chemical shifts (Bekkam *et al.,* 1991). It was observed that as Ag was substituted for

Mg^{2+} there was a ^{29}Si chemical shift from -94.287 (as was similarly observed by Bekkam *et al.,* 1991; Weiss *et al*., 1987) to -93.635 (AL1) and -93.488 (AL2) and -93.365 (AL3). The appearance of the additional peaks at -110.208, -110.331 and -110.946ppm assigned to the Q^4 sites in AL1, AL2 and AL3 respectively showed the reorganisation of the silica sheet, $Si(OS)_4$ according to Palkova *et al*. (2010) and Arantes *et al.* (2012) and it was due to the presence of silver replacing magnesium in the octahedral sheet.

Table 3.3: Gel formation time of Laponite® RD and silver-Laponite® RD

Ion exchange		Isomorphous substitution	
Samples	Gel time	Samples	Gel time
AGLAP1	1-2 minutes	AL1	≥ 96 hours
AGLAP2	1-2 minutes	AL2	≥ 96 hours
AGLAP3	1-5 minutes	AL3	≥ 96 hours
AGLAP4	1-5 minutes		
AGLAP5	48-60 hours		
AGLAP6	48-60 hours		

3.4 Discussion

Laponite® RD is synthetic sodium magnesium silicate clay with the chemical composition; $Na^+_{0.7}$ $[(Si_8\ Mg_{5.5}\ Li_{0.3})\ O_{20}\ \ (OH)_4]^{-0.7}$ from which the interlayer Na^+ ions are readily accessible to ion exchange. The Laponite® RD crystal has a uniform dimension whose thickness is 0.92nm and diameter 25nm (Phuoc *et al.,* 2009) which on combination with high degree of surface charging yields complete dissolution of clay particles in water forming a clear transparent solutions (Lezhnina *et al* ., 2011). The suspension of 1wt. % Laponite® RD remained free flowing after several weeks of aging though there was mild viscosity, but was

too low to be detected on viscometer. However, the suspension of 3 – 10wt. % of Laponite® RD suspension formed gel immediately or after 5- 10 minutes while, the 2wt. % assumes a longer gel formation profile (Phuoc *et al*., 2009). The gel could easily be reverted to low viscosity liquid by simple shaking. The gel structure quickly reformed when the suspension is allowed to stand. The gelation test was carried out using the physical method of pebble and jar test (Section 2.3.10). While the AGLAP1-4 gelled immediately, AGLAP5-6 remained free flowing for several hours and then a highly viscous liquid appeared after two days. The isomorphous substituted species followed a similar trend, with formation of a viscous suspension for all the samples after four days. When Laponite RD is dispersed in water the Na^+ ions are released into solution forming a double layer (Zebrowski *et al*., 2003)

These gelation results were based on visual observation which may be different if measured with a viscometer. However, the gel property have variety of applications especially in the medical field, particularly in the wound care for the adsorption of wound/ or burns exudates.

The similarities between the commercial and synthesized sample of Laponite® RD have been confirmed as shown in Fig. 3.1, 3.2 and 3.3. However, comparative crystallographic data of Laponite® RD with hectorite have shown that the former has approximately 15,000 unit cells per nanodisk (Breu *et al.*, 2003) while the latter is much less. Laponite® RD is characterised by a moderate negative surface charge known as the cation exchange capacity, CEC, expressed in meq/100g (Alexandre and Dubois, 2000). The charge of the layer is not locally constant as it varies from one layer to the other. Therefore, the charge is considered as an average over the whole crystal rather than on individual crystals. A small charge of the balancing cation is located on the external crystallite surface. Conversely, the majority of the exchangeable cations are present in the galleries which mostly result in larger interlayer

spacing when the hydrated cations are involved in ion-exchange (Alexandre and Dubois, 2000). In addition, to the tuneable properties of Laponite® RD over hectorite, Laponite® RD possesses a high edge-to-face ratio of approximately 5%. The protrusion of the –MgOH and –SiOH from the rims is much more polar and chemically active than the coordinate saturated –Si–O–Si– groups present on the face surfaces, as asserted by Lezhnina and colleagues (2011), the siloxane (–Si–O–Si–) network been formed from the methoxysilane hydrolysis-condensation reaction (Subramani *et al*., 2007).

Furthermore, as the interlayer packing density or the chain length decrease at high temperature, the intercalated chains adopt a more disordered, liquid-like structure due to increase in the *gauche* (stereochemically, IUPAC define groups which exhibits gauche as synclinal alignment attached to adjacent atoms (Craig *et al*., 1997)) */trans* conformer ratio (Alexandre and Dubois, 2000). Therefore, as the chain length increases, the interlayer structure appears to evolve in a regular manner from a disordered to a more ordered monolayer then suddenly 'jump' to a more disordered pseudo-bilayer (Hackett *et al*., 1998; Alexandre and Dubois, 2000). However, greater interaction with physisorbed water was experienced in the silver-exchanged Laponite® RD (Fig. 3.10) than the silver incorporated Laponite® RD (Fig. 3.18) also deformation temperature was higher in the latter than the former.

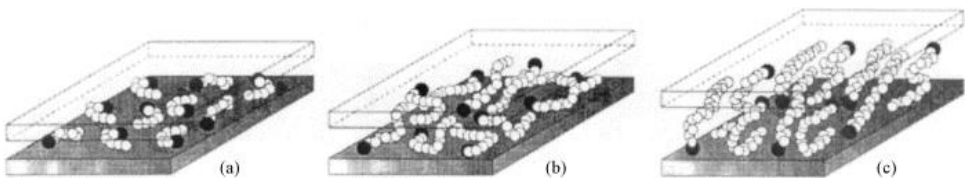

Fig. 3.23: A model of layered silicate molecular dynamic simulation proposed by Hackett *et al*. (1998). (a) Isolated molecules, lateral monolayer, (b) intermediate chain lengths: in-plane disorder and interdigitation to form quasi bilayers and (c) longer chain length: increased interlayer order, liquid crystalline-type environment. Adapted from Hackett *et al*. (1998) and supported by Alexandre and Dubois, (2000).

Although, the CEC of Laponite® RD or the modified forms were not determined in this study, research has shown that Laponite® RD CEC thus depends on the pH as well as other physicochemical factors. For example, Laponite® RD possesses a CEC of 50 - 60 meq/100g which account for 55 – 65% of the existing Na^+ ions. Notwithstanding, from literature the CEC of Laponite® RD (without silver) was as high as 62 meq/100g at pH 7 and 92 meq/100g at pH 9 (Mackenzie, 1952; Bergaya and Vayer 1997; Thompson and Butteworth 1992). But this observation is not consistent as the CEC tend to depend on other factors. As an example, the case of the adsorption with cetyltrimethylammonium cations showed Laponite® RD CEC to be of the order 85% of the Na^+ and 98% Na^+ exchangeable on adsorption of Tb^{3+} ions (but with the possibility of adsorption on the rims of the platelets forming $Tb(OH)^{2+}$) surprisingly, both occurring at pH = 7 (Lezhnina *et al.*, 2011). Such environmental and physicochemical factors may explain the variability of the CEC.

The method of production had significant effect on the surface structure as well as the particle size. The silver-exchanged Laponite® RD (Fig. 3.6) exhibited a plate-like morphology whereas, the silver incorporated Laponite® RD (Fig. 3.19) appeared lumpy with aggregates. Upon the production of the silver-exchanged Laponite® RD, they were milled and sieved with 100 micro mesh, the size and distribution were similar to the pure Laponite® RD as indicated by the flat bars in Fig 3.7. with a modal size distribution of 5µm. The composite particle size of silver incorporated Laponite® RD was not determined rather only the silver particle size was evaluated from TEM image analysis software Pro Plus version 4.5.0.19. The difference in production methods is also noted from the size distribution, with silver-exchanged Laponite® RD the modal size 13±1nm (Fig. 3.13). But data from image analysis for silver incorporated Laponite® RD modal size distribution was found to be 10nm. The

difference in the silver size range may be attributed to the aggregation which was prominent in the ion exchange species but less prominent in the isomorphous substitution species, and impacted on their thermal properties.

Chapter 4

Result and Discussion

Synthesis and characterisation of copper modified Laponite® RD

In this chapter the results based on the synthesis, ion exchange, and the characterisation of copper modified Laponite® RD before and after ion exchange, are presented. The production of copper incorporated Laponite® RD via isomorphous substitution and its characterisation is also included.

4.1 Synthesis, ion exchange and characterisation of copper-exchanged Laponite® RD

4.1.1 Synthesis and characterisation of Laponite® RD

Following the protocol described in Section 2.1 Laponite® RD was synthesised with 2.16 SiO2/MgO input ratio. Upon completion of the synthesis samples were characterised as shown in Section 3.1.2.

4.1.2 Synthesis of copper-exchanged Laponite® RD (CULAP1-6) by ion exchange

Copper-exchanged Laponite® RD was prepared as described in Section 2.2.1.2. Upon completion of the ion exchange samples were characterised with FTIR, XRD, EDX, SEM, ^{29}Si MAS NMR, TGA and TEM.

4.1.3 Characterisation

In order to examine the crystallographic structure of copper-exchanged Laponite® RD, XRD analysis was performed and the patterns of Laponite® RD, with and without copper, was acquired as shown in Figure 4.1. The copper seems not to have had a visual impact on the Laponite® RD layers as was also observed by Phuoc *et al.* (2009). However, close examination of the d_{100} spacing of each copper-exchanged Laponite® RD show marked differences.

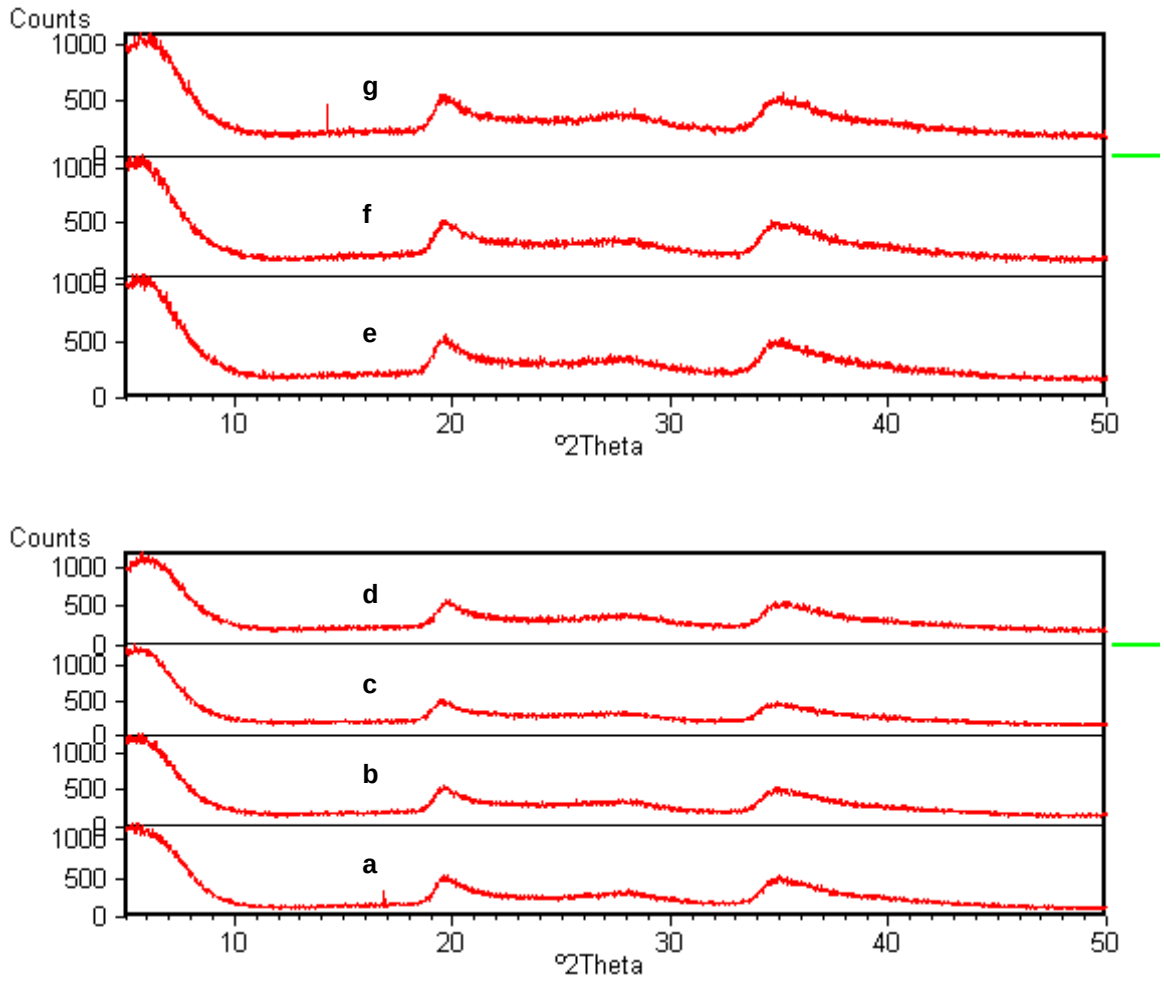

Fig. 4.1: XRD pattern of Laponite® RD without copper, LAP2 (a) and Laponite® RD with copper; CULAP1 – 6 (b -g).

Laponite® RD (without copper) basal spacing was determined to be 1.28 nm, while 1.59 nm, 1.45 nm, 1.57 nm, 1.34 nm , 1.57 nm and 1.30 nm spacing were obtained for CULAP1, CULAP2, CULAP3, CULAP4, CULAP5 and CULAP6 respectively.

Figure 4.2 shows the FTIR spectroscopy of each Laponite® RD. FTIR is a common tool to characterise metal modified Laponite® RD and provide evidence of displacement of sodium on the Laponite® RD surface through ion exchange. Laponite® RD (without copper) showed peaks approximately at 3684 cm^{-1}, corresponding to Mg – OH stretching vibration with a

shoulder near 3626cm^{-1}, corresponding to Si – OH stretching vibration as reported by Pereira *et al*. (2007) and Herrera *et al*. (2005) but absent in the spectra shown. As expected the presence of residual Mg – OH groups after the ion exchange indicate that the Mg – OH locations in the Laponite® RD structure were not accessible via ion exchange (Herrera *et al*., 2005),

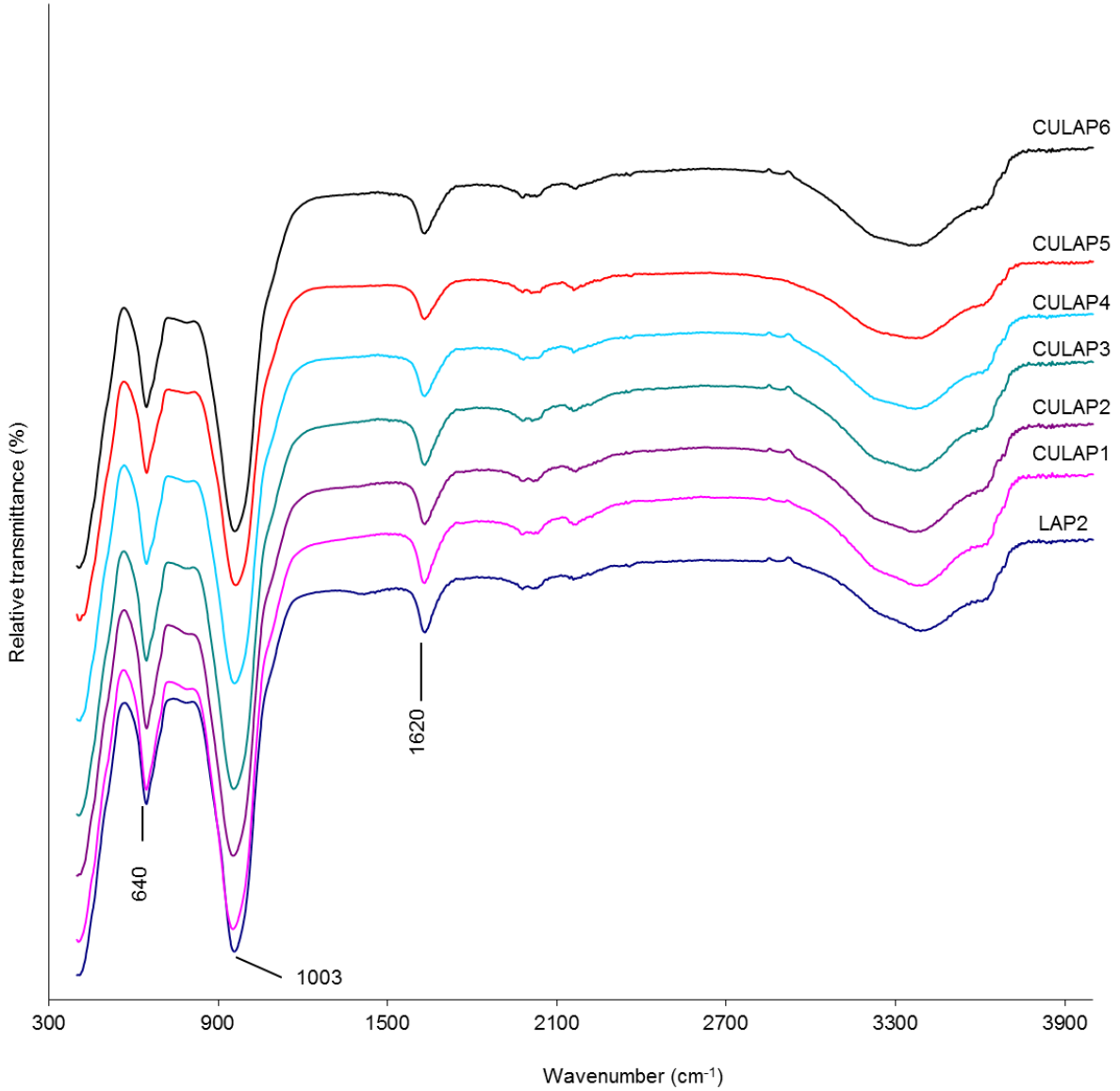

Fig. 4.2: Fourier transformed infrared spectroscopy of Laponite® RD without copper (LAP2) and Laponite® RD with copper (CULAP1 - 6).

The EDX spectrum detected copper ions in the Laponite® RD interlayer after the ion exchange (Fig. 4.3). The EDX also quantified the amount of copper ions that were trapped within the Laponite® RD layer, either at the interlayers or edges, as well as the elemental composition of Laponite® RD with and without copper (Table 4.1). The evidence of copper exchange with Laponite® RD was further supported by EDX mapping of the copper-Laponite® RD surfaces. The micro-images for the elements; Na, Si, Mg and Cu are as shown in Fig. 4.4.

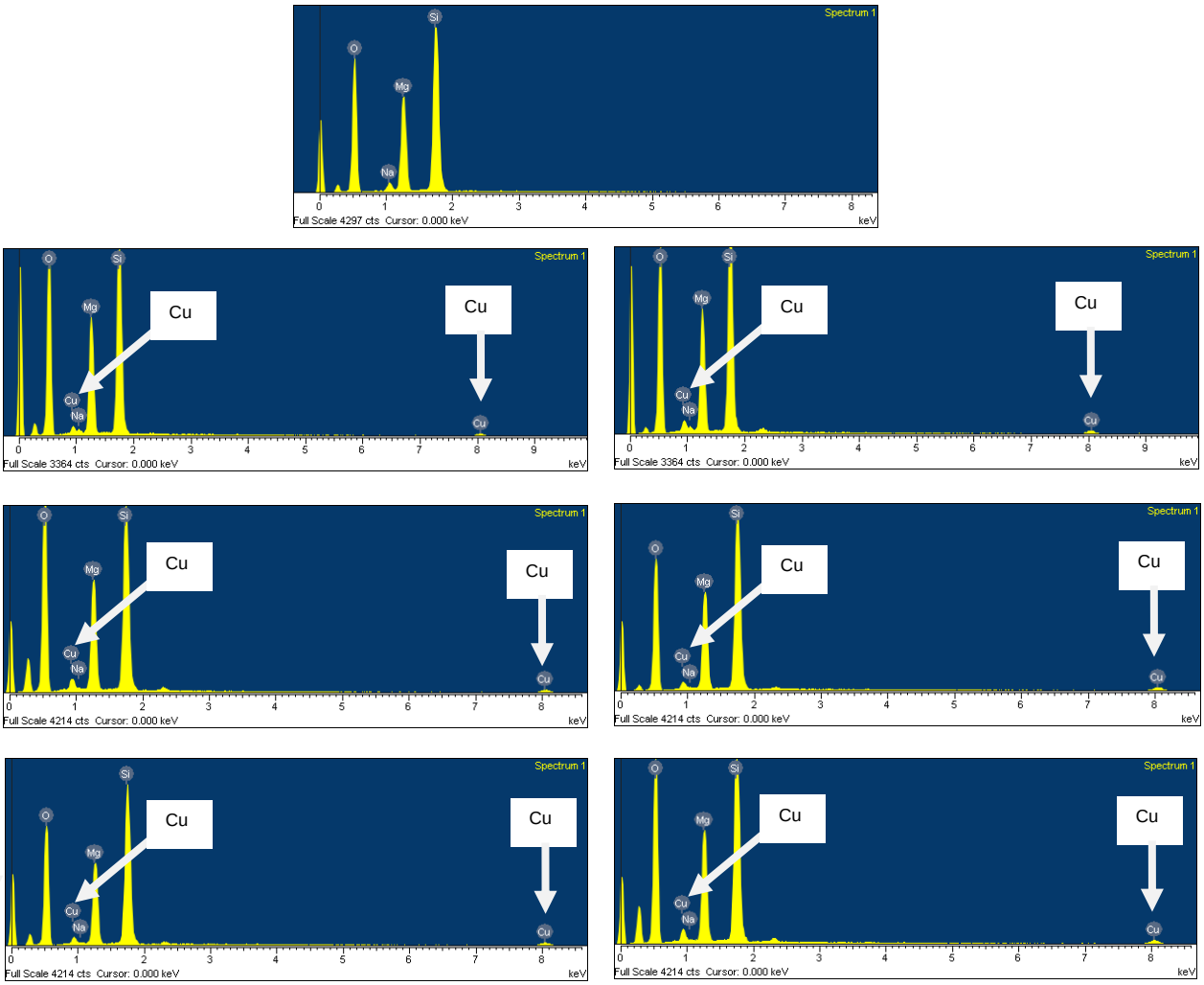

Fig. 4.3: EDX spectra of Laponite® RD without copper (a) and Laponite® RD with copper; CULAP1 (b), CULAP2 (c), CULAP3 (d), CULAP4 (e), CULAP5 (f) and CULAP6 (g).

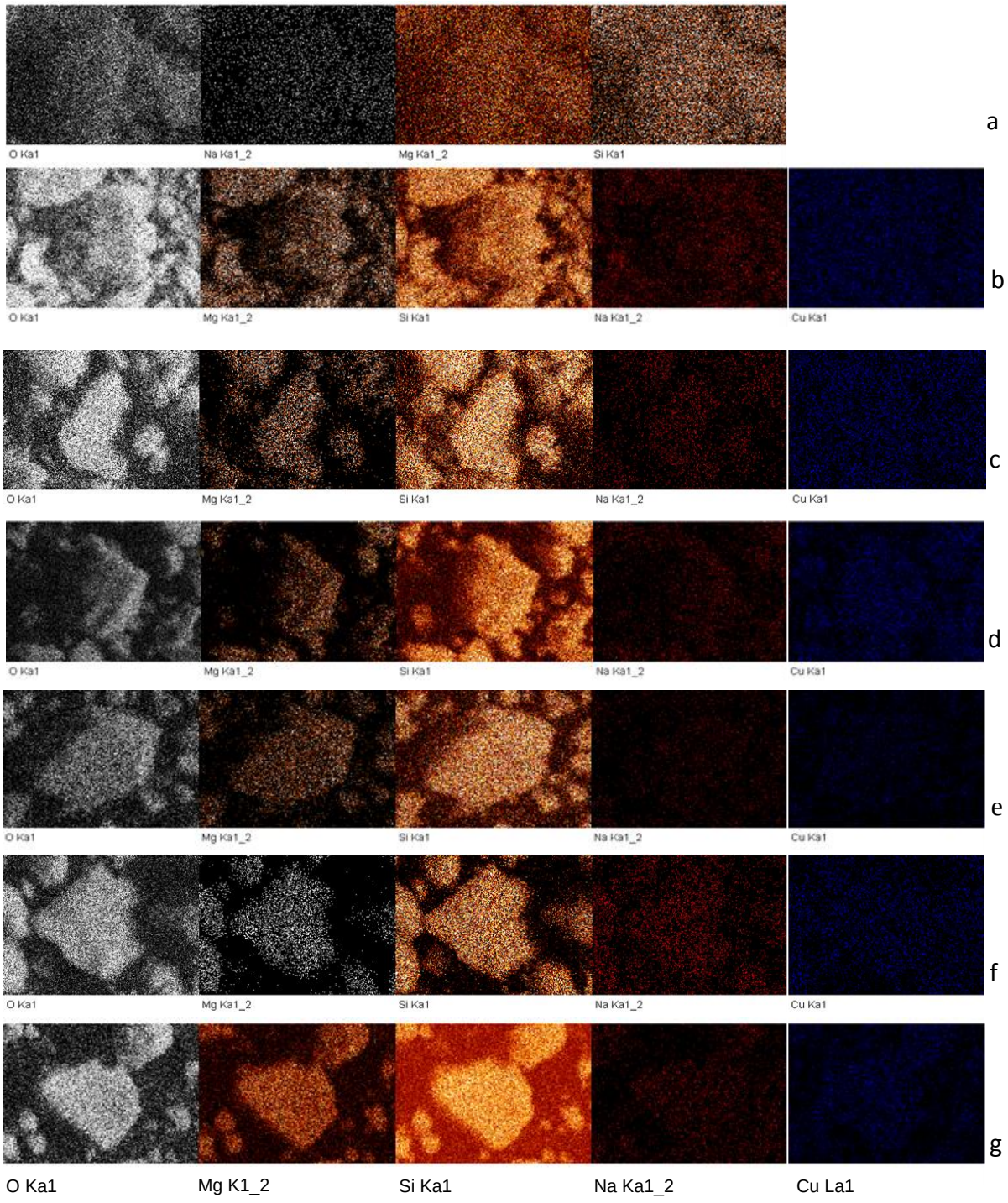

Fig. 4.4: Micro-images of elements in Laponite® RD without copper (a) and Laponite® RD with copper; CULAP1 (b), CULAP2 (c), CULAP3 (d), CULAP4 (e), CULAP5 (f) and CULAP6 (g).

Table 4.1: EDX elemental analysis of Laponite® RD without copper and copper-exchanged Laponite® RD.

	Concentration of copper-exchanged Laponite® RD (wt. %)						
Elements	LAP	CULAP1	CULAP2	CULAP3	CULAP4	CULAP5	CULAP6
Na	1.59±0.06	0.58±0.00	0.42±0.06	0.23±0.00	0.20±0.09	0.09±0.03	0.10±0.01
Mg	13.97±0.12	14.04±0.15	13.94±0.22	14.01±0.12	13.83±0.18	13.49±0.16	13.83±0.16
Si	22.23±0.16	22.24±0.04	22.10±0.01	22.14±0.10	22.20±1.09	21.90±0.10	22.01±0.08
Cu	0.00±0.00	0.69±0.07	0.94±0.07	1.23±0.04	1.37±0.17	1.82±0.23	1.85±0.10
O	59.48±0.22	59.62±0.04	59.64±0.13	59.72±0.17	59.73±1.65	60.12±0.38	59.64±0.12
Li	0.03±0.00	0.02±0.00	0.03±0.00	0.03±0.00	0.03±0.00	0.02±0.00	0.03±0.00
OH	2.66±0.03	2.69±0.08	2.53±0.24	2.53±0.24	2.59±0.18	2.50±0.27	2.50±0.27

From Table 4.1 the unit cell formula for each of the copper-exchnaged Laponite® RD was calculated thus; the wt. % was first converted to gram to determine the number of moles. Then, the number of moles was divided by the lowest factor to get the ratio of the unit cell in each case.

LAP2 $Na_{16.1}(Si_{58.0}\ Mg_{133.6.5}\ Li)\ O_{864.5}\ (OH)_{36.4}$

CULAP1 $Na_{8.9}\ Cu_{3.7}(Si_{273.0}\ Mg_{199.2}\ Li)\ O_{1281.9}\ (OH)_{54.5}$

CULAP2 $Na_{4.3}\ Cu_{3.4}(Si_{183.0}\ Mg_{133.4}\ Li)\ O_{866.9}\ (OH)_{34.6}$

CULAP3 $Na_{4.6}\ Cu_{3.8}(Si_{186.3}\ Mg_{133.1}\ Li)\ O_{868.0}\ (OH)_{34.6}$

CULAP4 $Na_{2.0}\ Cu_{5.0}(Si_{183.8}\ Mg_{132.3}\ Li)\ O_{868.2}\ (OH)_{35.0}$

CULAP5 $Na_{1.3}\ Cu_{9.9}(Si_{268.8}\ Mg_{191.1}\ Li)\ O_{1295.7}\ (OH)_{50.7}$

CULAP6 $Na\ Cu_{6.8}(Si_{183.0}\ Mg_{132.3}\ Li)\ O_{866.9}\ (OH)_{34.2}$

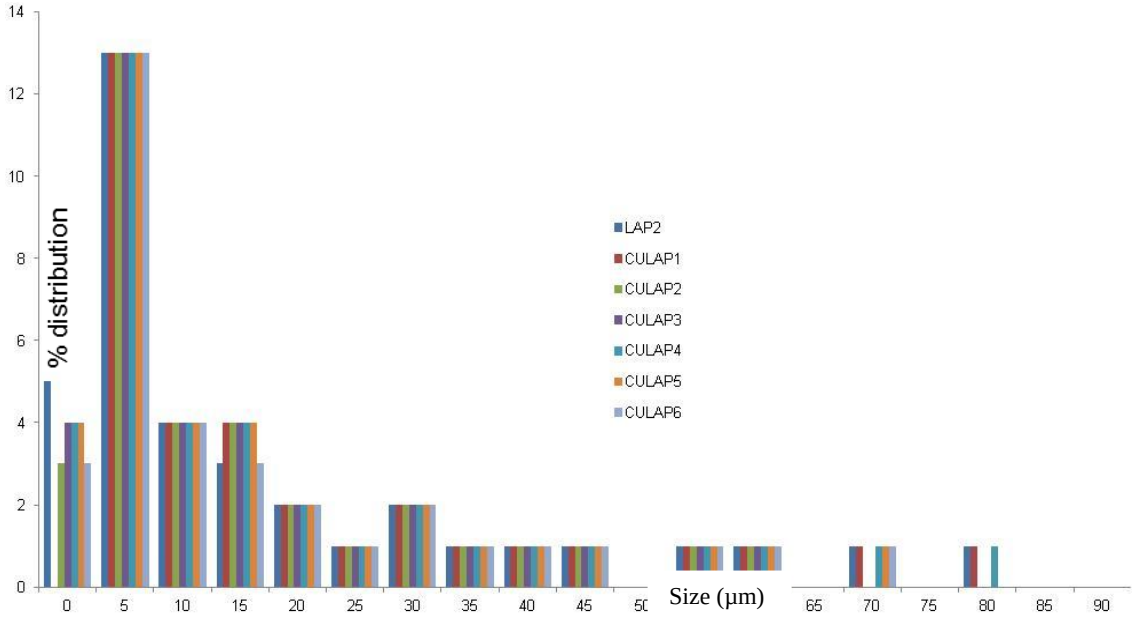

Fig. 4.5: Particle size distribution of Laponite® RD without copper and Laponite® RD with copper

The particle size distribution of Laponite® RD with and without copper was similar with a modal distribution of 5µm (Fig. 4.5). The thermal data analysis of Laponite® RD without copper and the Laponite® RD exchanged with copper is shown on the thermogram in Figure 4.6. Laponite® RD was as already described in Section 3.2.1. The physisorbed water at 125^{o}C accompanied with 15% mass loss with no apparent chemisorbed water designated 4% weight loss. The dehydroxylation temperature was at 800^{o}C with a further mass loss of 2% for the CULAP1 (Fig. 4.6b). Physisorbed water at 125^{o}C mass loss of 15%, no apparent chemisorbed water but designated mass loss 4%. Dehydroxylation occurred at 795^{o}C with further mass loss of 2% for the CULAP2. (Fig. 4.6c). Similar trend was observed for the CULAP3-6, with 128, 118, 126, 127^{o}C corresponding to 16, 14, 15, 13% mass losses respectively. Also there was no apparent chemisorbed water but 4% designated mass loss each. The dehydroxylation was complete at 790, 800, 790, and 795^{o}C for CULAP3,

CULAP4, CULAP5 and CULAP6 respectively. This indicate that the copper-exchanged Laponite® RD material is thermally more stable than the parent clay with dehydroxylation at 752°C. Therefore enhances thermal stability of Laponite® RD result from the interlayer exchange of copper and ultimately the formation of a copper-Laponite® RD hybrid.

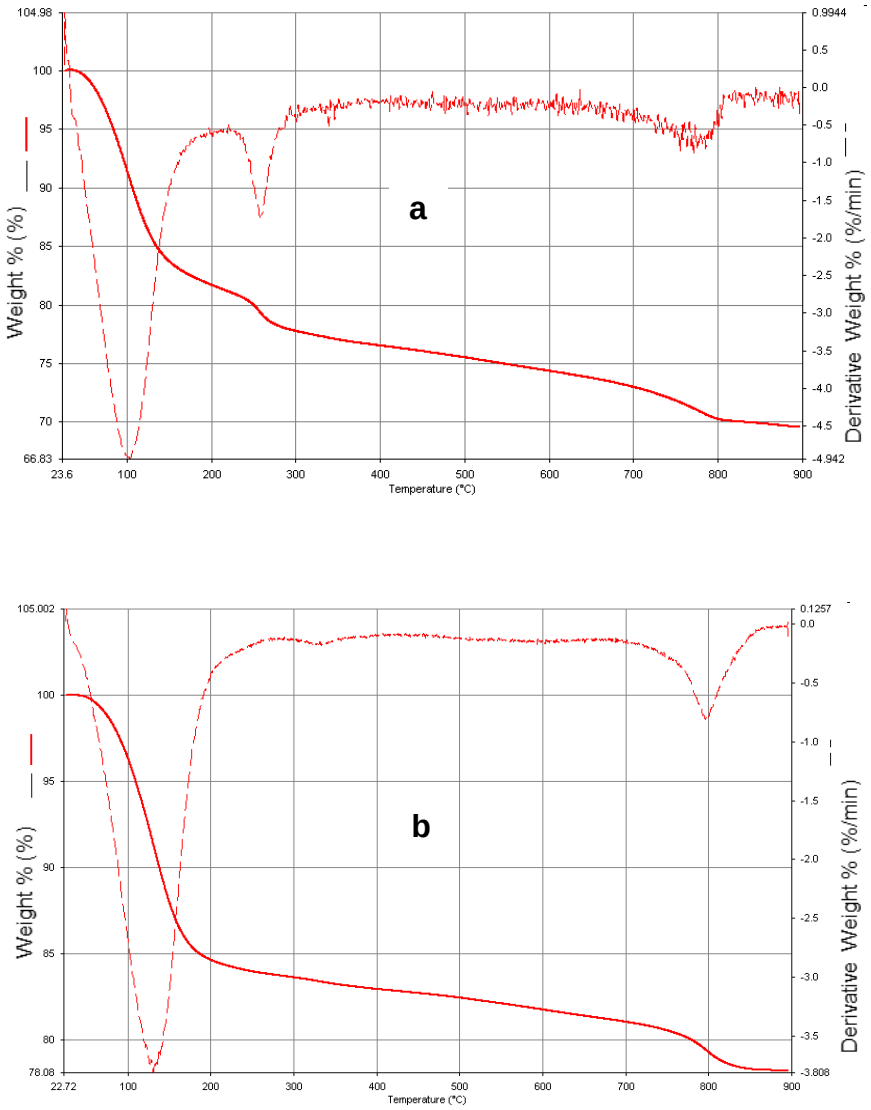

Fig. 4.6: Thermographs of Laponite® RD without copper, LAP2 (a) Laponite® RD with copper; CULAP1 (b), CULAP2 (c), CULAP3 (d), CULAP4 (e), CULAP5 (f) and CULAP6 (g). Thermographs of sample (——), sample thermographs first derivatives (-----).

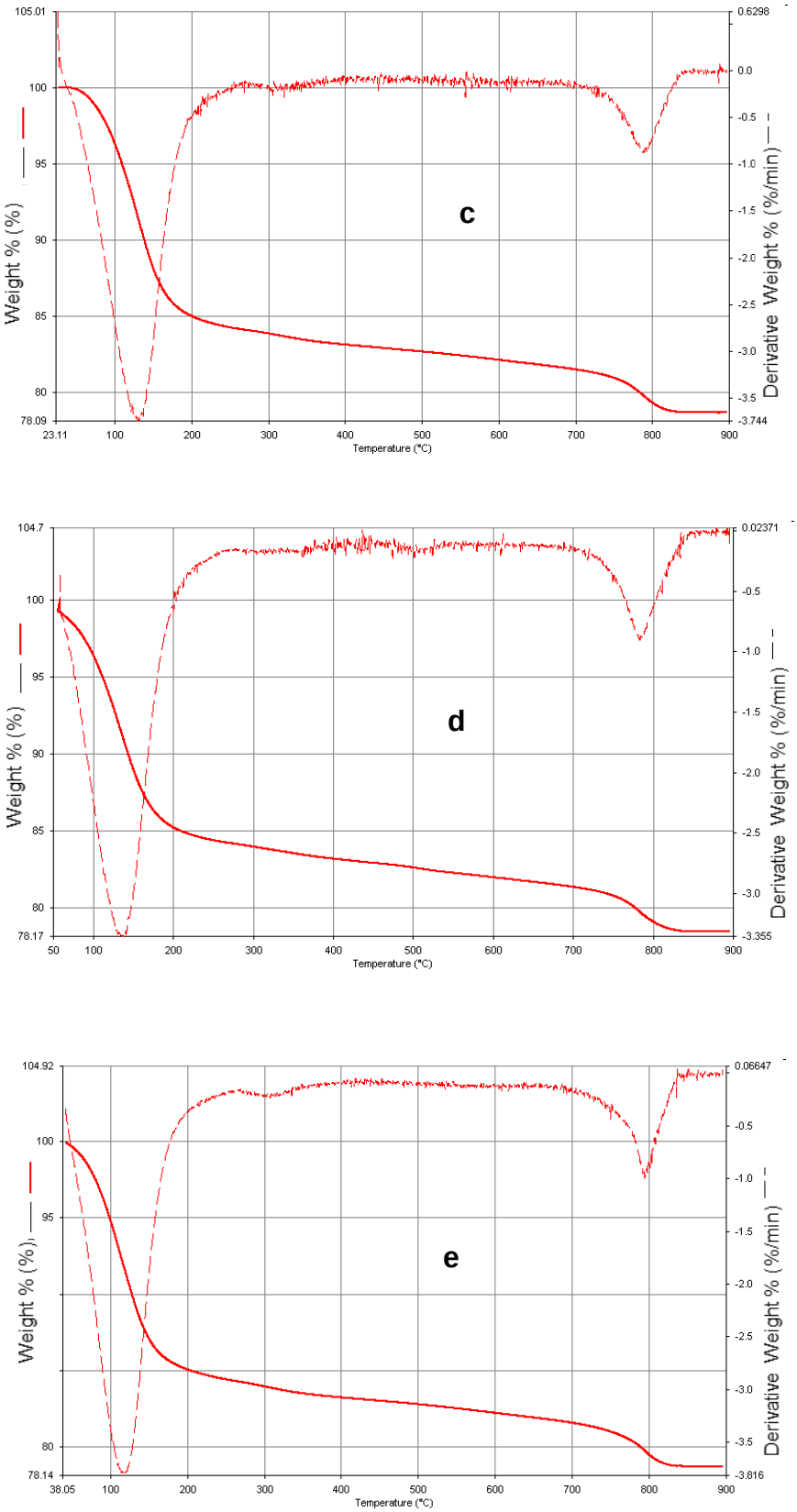

Fig. 4.6: (continued)

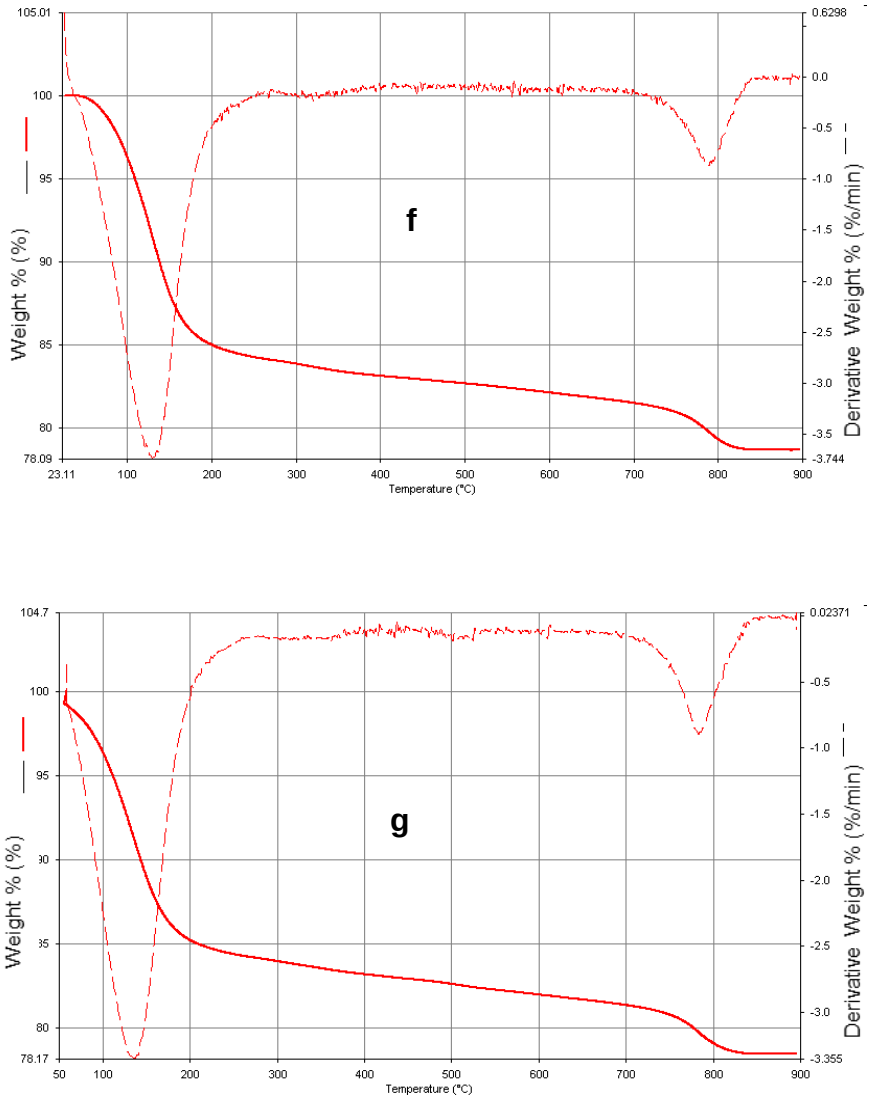

Fig. 4.6: (continued)

Figure 4.7. Shows the ^{29}Si MAS NMR of Laponite® RD without copper and the end members of the Laponite® RD modified with copper. The different species are named according to the conventional Q, T and M notation where Q^n, T^n and M^n designate tetra-, tri- and mono-functional units respectively, while *n* is the number of bridging O atoms surrounding the silicon atom. The ^{29}Si NMR spectrum of Laponite® RD without copper is characterised by two resonances at -94.287 and -85.066 ppm which correspond respectively to Q^3 trioxo coordinated framework silicon and Q^2 sites attributed to isolated silanol groups present at the silicate sheets edges (Herrera *et al.*, 2005).

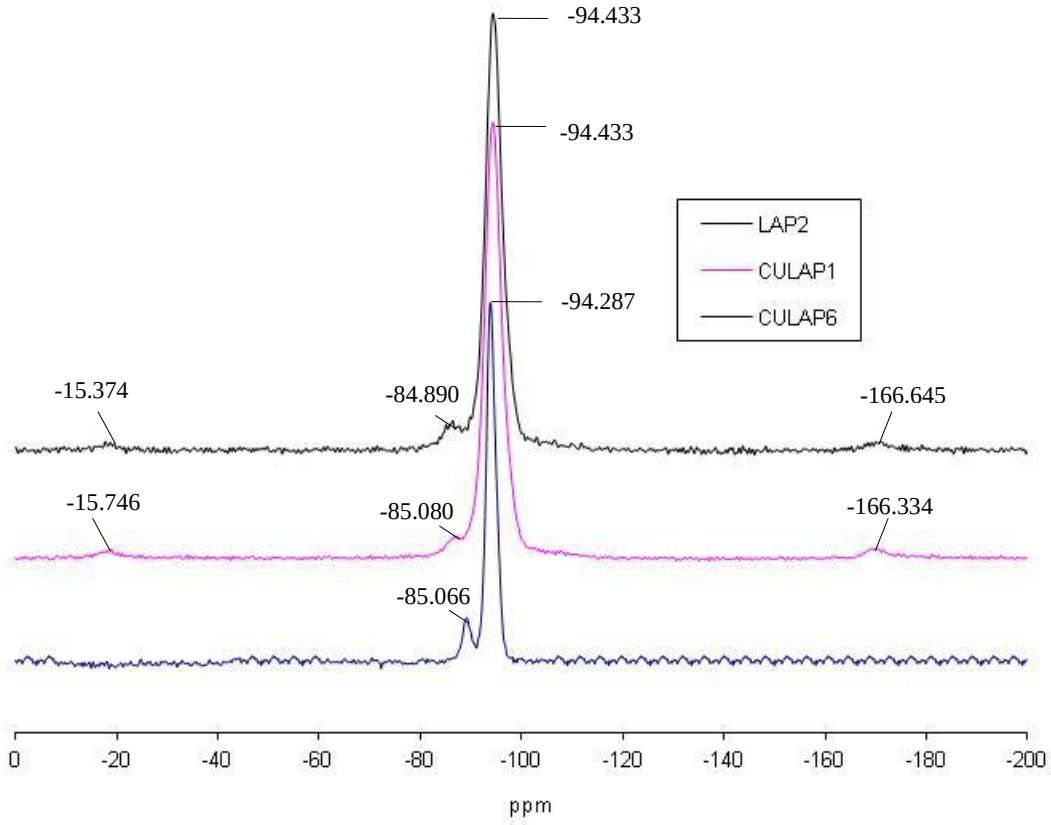

Fig 4.7: ^{29}Si MAS NMR of Laponite® RD without copper and Laponite® RD with copper.

The appearance in the ^{29}Si NMR spectra of the signals at -15.746 ppm (CULAP1), -15.334 ppm (CULAP6) assigned to M^1 (Herrera *et al*., 2005) and other signals at -166.334ppm (CULAP1), -166.645ppm (CULAP6) gave clear evidence of the presence of chemically modified Laponite® RD with copper at the interlayer surface.

The SEM micrographs shown in Fig. 4.8 confirmed the phase purity of the crystal morphology, and also show that the particles were closely similar in surface morphology, suggesting that the exchange with copper ions at the interlayer space seems to have a subtle effect on the surface structure.

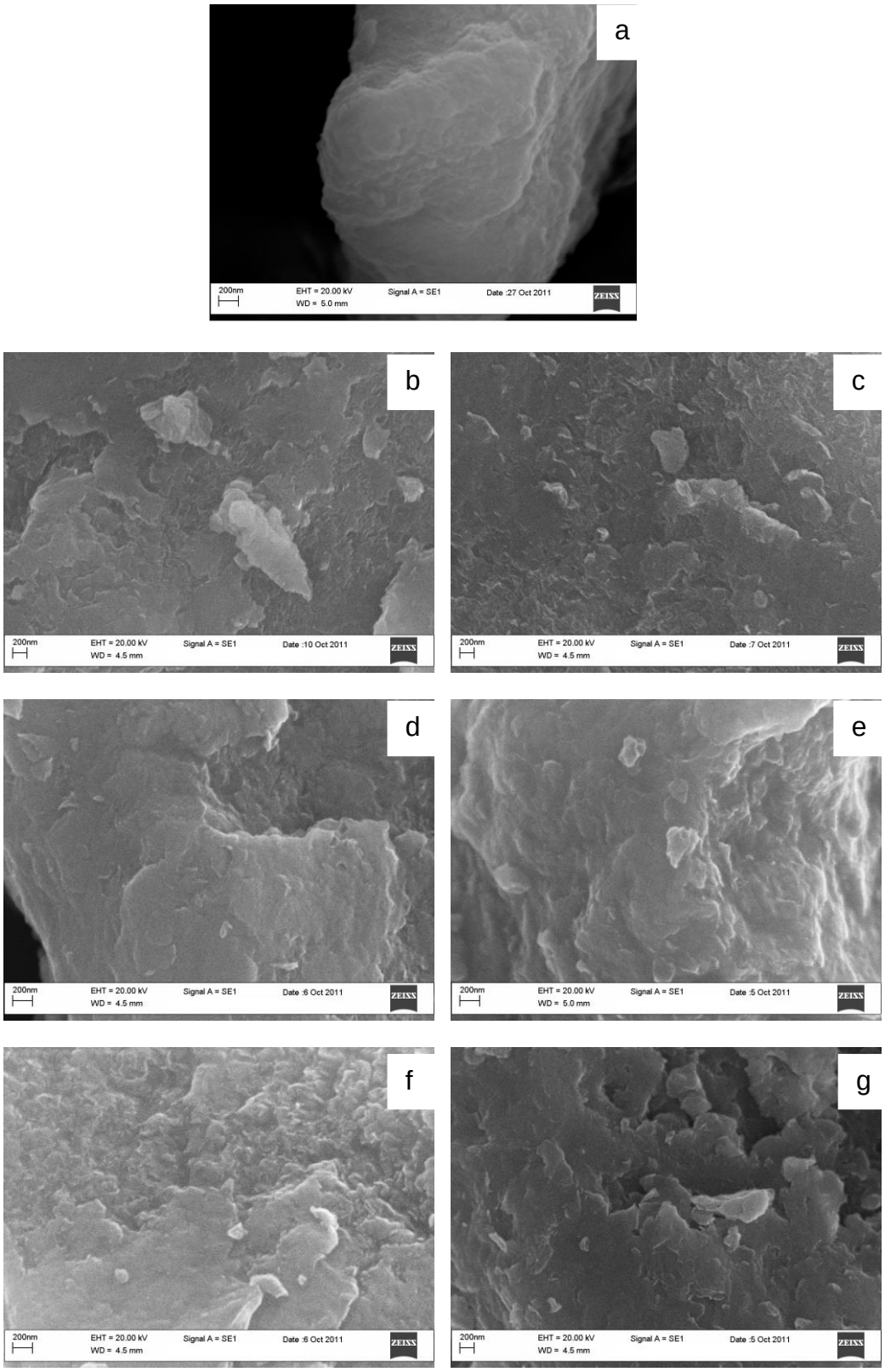

Fig. 4.8: SEM micrograph of Laponite® RD without copper, LAP2 (a) and Laponite® RD with copper; CULAP1 (b), CULAP2 (c), CULAP3 (d), CULAP4 (e), CULAP5 (f) and CULAP6 (g).

Figure 4.9 shows the TEM micrographs of Laponite® RD without and Laponite® RD with copper and confirm that the metal particles were in the nanometer range, 4 to 20nm (Fig. 4.10), and that they were approximately spherical in shape as was also observed by Ruparelia *et al*., 2008.

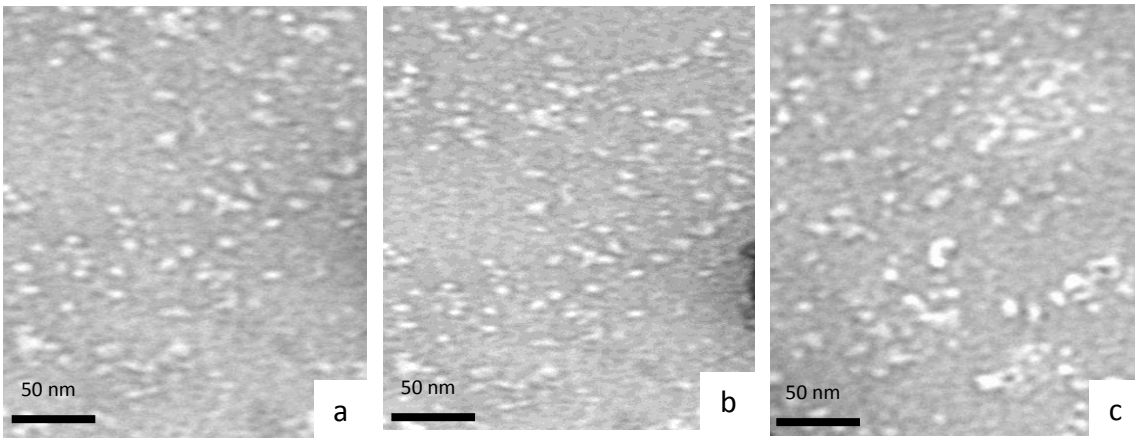

Fig. 4.9: TEM micrograph of copper modified Laponite® RD; CULAP1 (a), CULAP2 (b), CULAP3 (c).

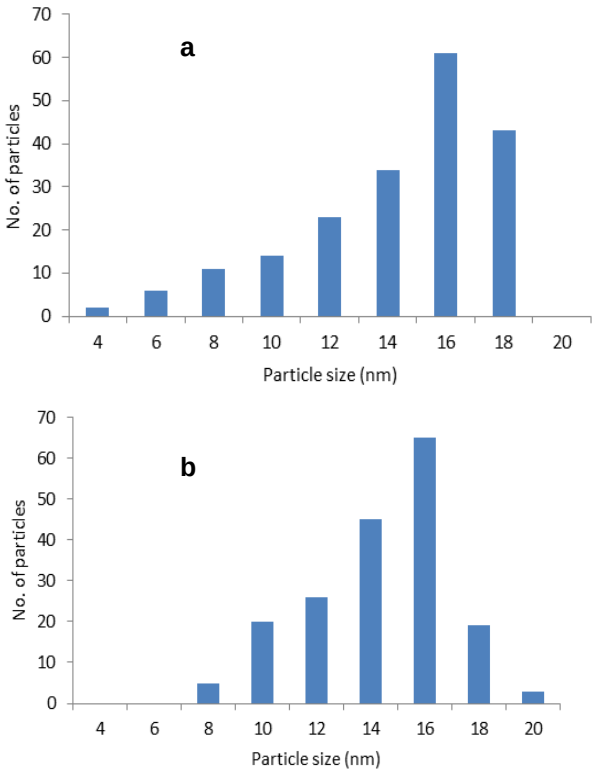

Fig. 4.10: Particle size distribution obtained by TEM image analysis for CULAP1 (a) and CULAP2 (b).

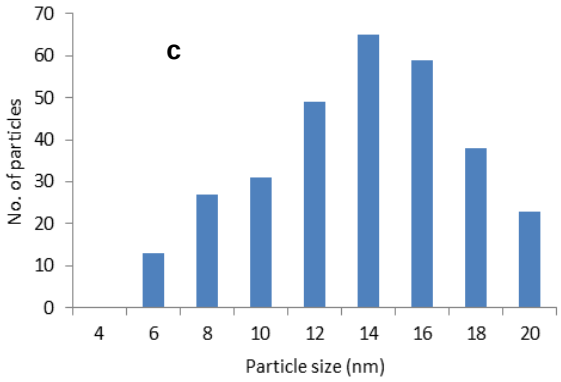

Fig. 4.10: (continued).

4.2 Synthesis, isomorphous substitution and characterisation of copper incorporated Laponite® RD

4.2.1 Synthesis of copper incorporated Laponite® RD (CL1) by isomorphous substitution

Isomorphous substitution was carried out as described in the synthesis protocol (Section 2.2.2.2). Upon completion of the substitution process, the samples were re-characterized by XRD, FTIR, EDX, SEM, ^{29}Si MAS NMR, TGA and TEM.

4.2.2 Characterisation

Figure 4.11 shows the XRD pattern of Laponite® RD without copper and Laponite® RD incorporated with copper (CL1) by isomorphous substitution. The d-spacing of Laponite® RD

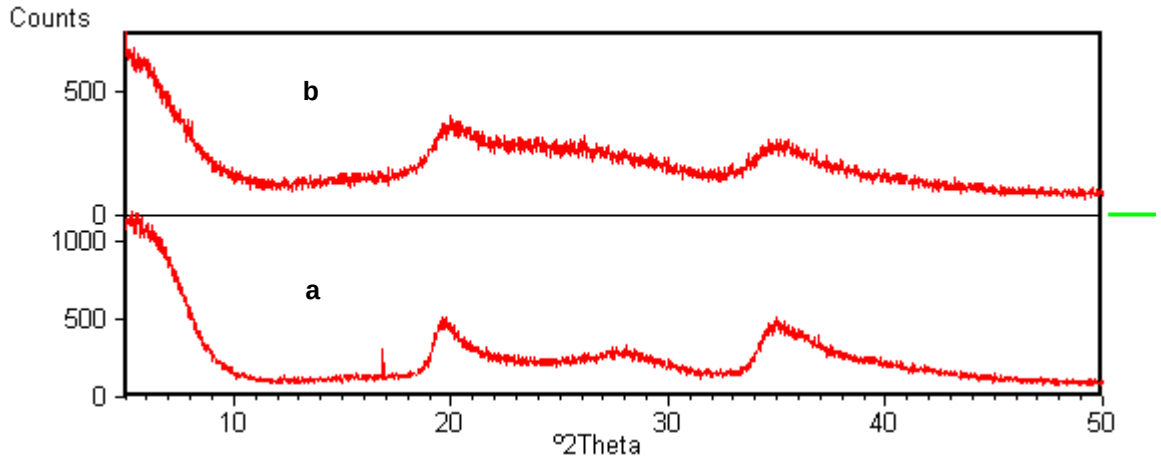

Fig 4.11: XRD pattern of Laponite® RD without copper (a) and Laponite® RD with copper, CL1 (b).

without copper was 1.28 nm and became 1.47nm in the CL1, confirming incorporation of copper at the Laponite® RD sheet. The FTIR spectra corresponding to LAP2 and CL1 are presented in Fig. 4.12. The Si-O-Si stretching vibrations are affected by Cu exchange; the band at 1003cm^{-1} (LAP2) shifted towards higher wave numbers at 1018cm^{-1} (Mosser *et al*., 1997). The appearance and shift of the band to higher wave number at 3658 cm^{-1} corresponds to Cu-Mg-OH or Cu-Mg-Li-OH vibrations and revealed the presence of Cu atoms in the octahedral layer (Mosser *et al*., 1997).

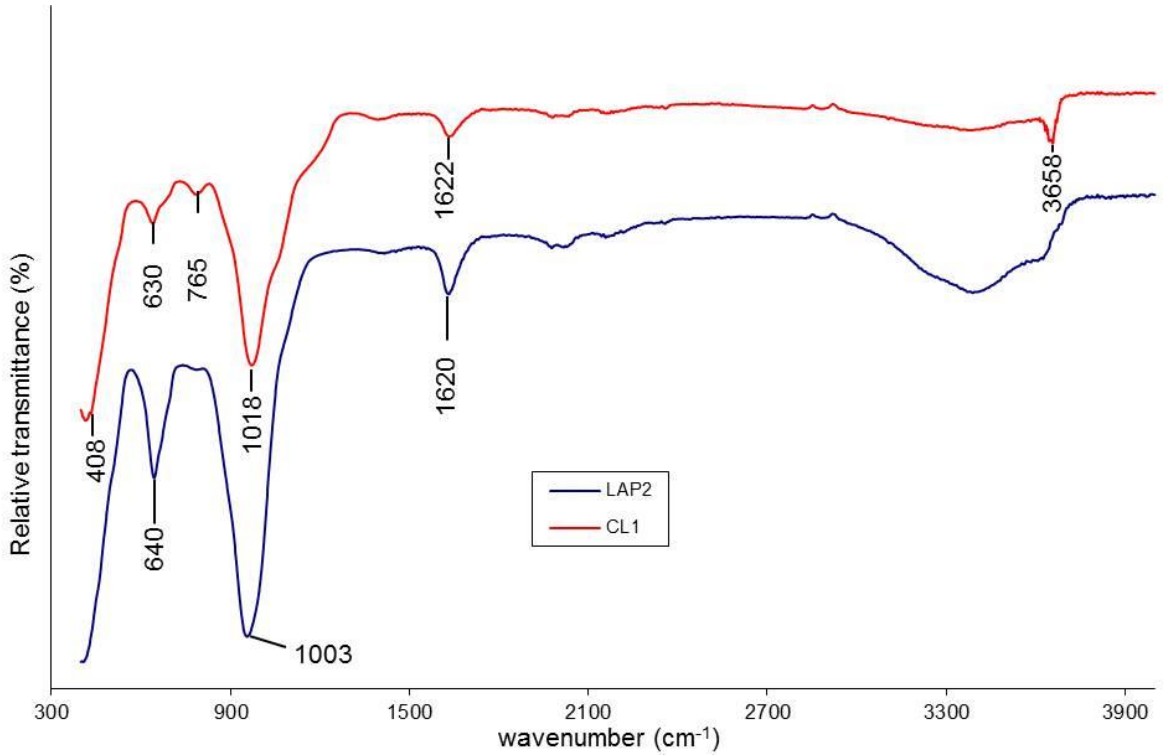

Fig. 4.12: Fourier transformed infrared spectroscopy of Laponite® RD without copper (LAP2) and Laponite® RD with copper (CL1).

Table 4.2: EDX elemental analysis of Laponite® RD without copper and copper incorporated Laponite® RD.

		Concentration of copper incorporated Laponite® RD (wt. %)
Elements	Lap	CL1
Na	1.59±0.06	1.65±0.15
Mg	13.97±0.12	12.40±1.04
Si	22.23±0.16	23.56±0.86
Li	0.03±0.00	0.04±0.00
Cu	0.00±0.00	0.53±0.33
O	59.48±0.22	60.76±0.36
OH	2.66±0.03	2.50±0.27

Spot analysis of the copper incorporated Laponite® RD was performed at different surface positions selected randomly (Table 4.2). The analysis was further supported by EDX spectra of the Laponite® RD and the copper incorporated Laponite® RD surface (Fig. 4.13). The EDX microimages for the elements; Na, Si, Mg and Cu are as shown in Figure 4.14.

From Table 4.2 the unit cell formula for copper incorporated Laponite® RD was calculated thus; the wt. % was first converted to gram to determine the number of moles. Then, the number of moles was divided by the lowest factor to get the ratio of the unit cell.

CL1 $Na_{12.4}\ Cu_{1.4}\ (Si_{144.6}\ Mg_{87.9}\ Li)\ O_{654.7}\ \ (OH)_{25.3}$

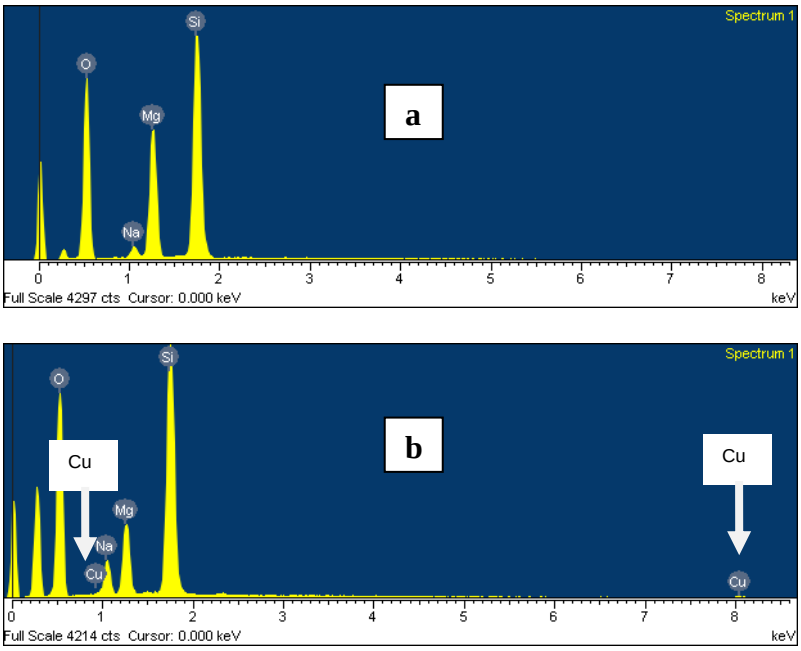

Fig.4.13: EDX spectra of Laponite® RD without copper (a) and Laponite® RD with copper; CL1 (b).

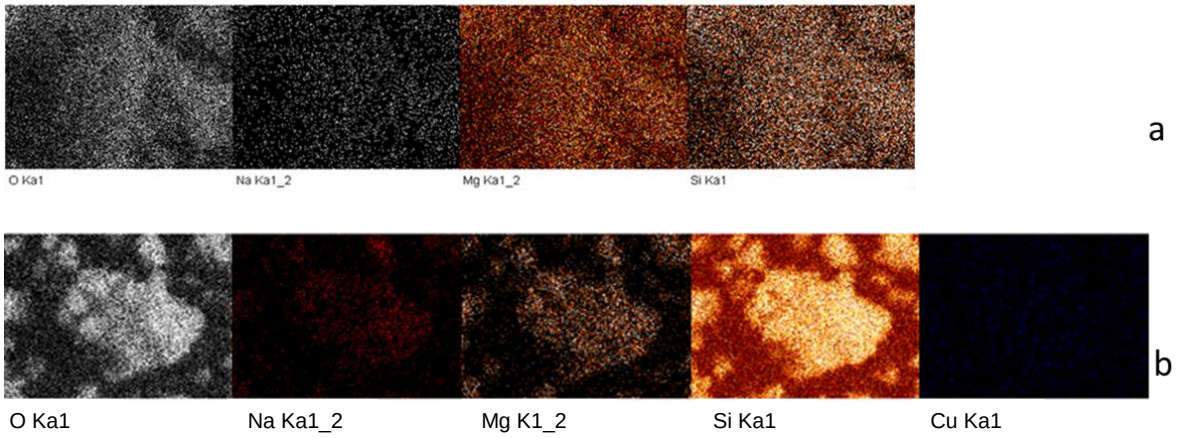

Fig. 4.14: EDX micro-images of Laponite® RD without copper (a) and Laponite® RD with copper; CL1 (b).

The thermogram of the copper incorporated Laponite® RD is shown in Fig. 4.15. The physisorbed and chemisorbed water occurred at 125 and 530°C accompanied with corresponding mass losses of 17 and 6% The dehydration of interlayer cation ha shifted towards higher temperature (530°C), revealed the stronger interaction between Cu and the water molecules (Mosser *et al*., 1997). The dehydroxylation temperature of the copper incorporated Laponite® RD shifted towards a higher temperature at 800°C and 1% mass loss with respect to pure Laponite® RD. This modification in the high temperature range revealed changes in the composition of the octahedral sheet (Mosser *et al*., 1997).

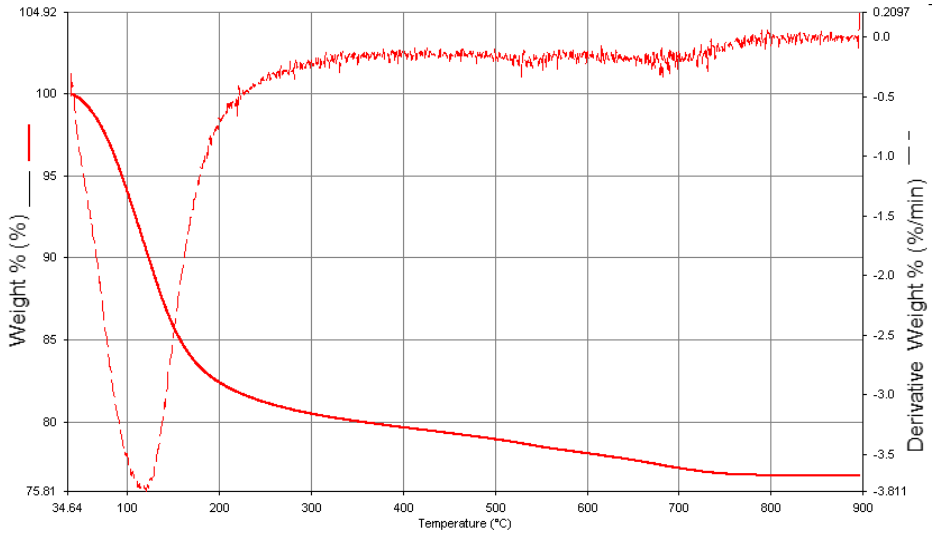

Fig. 4.15: TGA of Laponite® RD with copper, CL1. Thermographs of sample (——), sample thermographs first derivatives (-----).

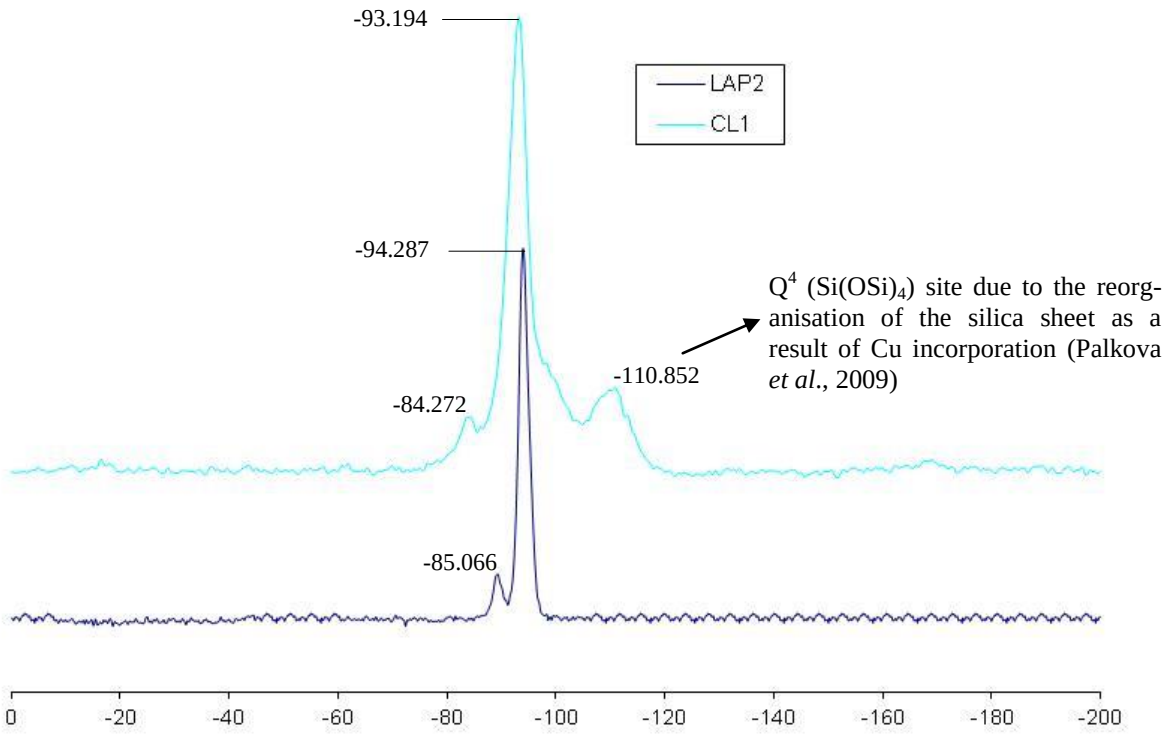

Fig. 4.16: ^{29}Si MAS NMR of Laponite® RD without copper and copper incorporated Laponite® RD.

Figure 4.16 shows the ^{29}Si MAS NMR of Laponite® RD without copper and copper incorporated Laponite® RD. The appearance of the peak at -110.852ppm and the observed shift in the resonance peak of LAP2 (-94.287ppm) to CL1 (-93.194ppm) was attributed to changes in the composition of the octahedral sheet (Sanz and Serratosa, 1984; Serratosa and Bradely, 1958) consequent on the OH bond axes being perpendicular to the layers and hence point to the hexagonal cavities, in effect, the nature of octahedral cation influenced the shift in the resonance peak of ^{29}Si MAS NMR (Chatterjee., *et al*., 2004). Furthermore, copper being more electronegative than magnesium also resulted to a less negative shift from -94. 287ppm of the parent Laponite® RD to -93.194ppm in the copper incorporated Laponite® RD.

Figure 4.17 show the surface morphology of the copper incorporated Laponite® RD as revealed by SEM micrograph.

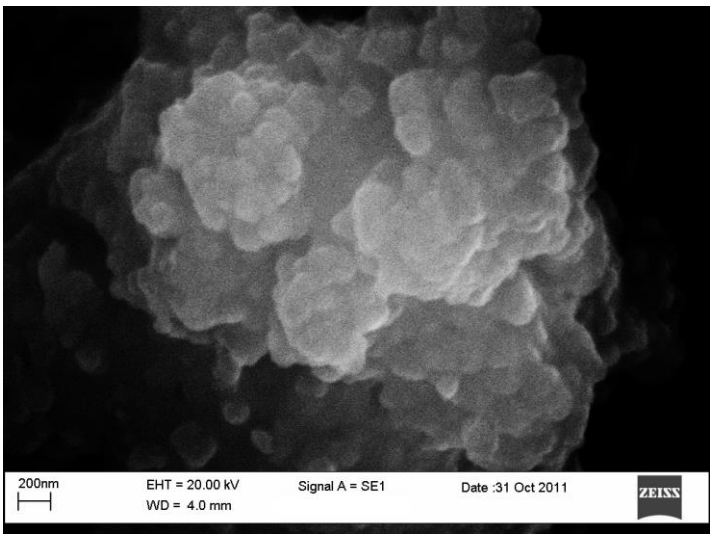

Fig. 4.17: SEM micrographs of copper incorporated Laponite® RD.

Figure 4.18 shows the TEM micrograph of copper incorporated Laponite® RD which confirms that the metal particles are in the nanometre range and approximately spherical in shape by visual observation. Subsequent image analyses revealed that the copper nanoparticles size ranged from 8 to 20nm (Fig. 4.19) and were relatively larger than the silver nanoparticles (when compared with Fig. 3.20).

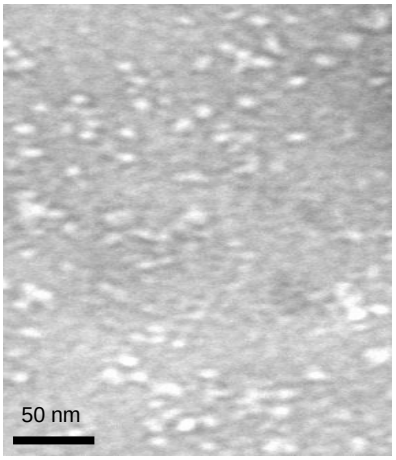

Fig.4.18: TEM micrographs of copper incorporated Laponite® RD.

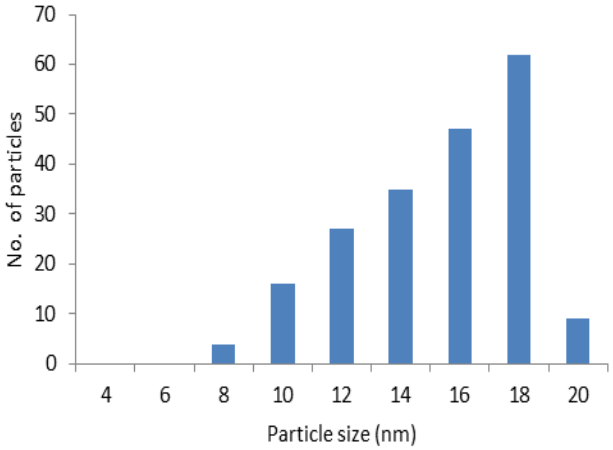

Fig. 4.19: Particle size distribution obtained by TEM image analysis for copper incorporated Laponite® RD.

Table 4.3: Gel formation time of Laponite® RD and copper-Laponite® RD

Ion exchange		Isomorphous substitution	
Samples	Gel time	Samples	Gel time
CULAP1	72-96 hours	CL1	no gel
CULAP2	72-96 hours		
CULAP3	72-96 hours		
CULAP4	≥ 96 hours		
CULAP5	≥ 96 hours		
CULAP6	no gel		

4.3 Discussion

After the synthesis of Laponite® RD and confirmation of its purity using XRD (Fig. 3.1 and 4.1), cationic exchange was performed for the replacement of the interlayer sodium by the divalent copper ions. On dispersion of Laponite® RD powder in water, the sodium ions were released from the interlayer, resulting in an increase in the interlayer separation between Laponite® RD disks. The Laponite® RD disk faces also becomes negatively charged while the edges depending on the acid-base behaviour of the Si-OH and Mg-OH amphoteric hydroxyl groups possess a positive charge which is approximately 10% of the surface charge (Phuoc and Chen, 2011; Cummins, 2007). The negatively charged site on the basal surface of the Laponite® RD crystals are the predominant adsorption site for metal ions. When cationic metals are exchanged in water containing dispersed Laponite® RD crystals, the metal ions can be absorbed on to the basal plane surface of the Laponite® RD platelets by exchanging with

the dissolved sodium ions either by intercalation of the metal ion into the interlayer separation of the Laponite® RD platelets or by adsorption of the metal ions on the negatively charge sites of the surface of the basal plane (Phuoc and Chen, 2011). The former occurs either by heating in which case the interlamellar separation between the Laponite® RD layer is increased or without heating whereby the sodium ions is replaced both in an ion exchange reaction. The latter, which is also an ion exchange reaction, occurs when the concentration of metal ion is high or concentration of Laponite® RD is less. Laponite® RD consequently becomes less effective in limiting the metallic nonoparticle size thus, leading to the formation of larger, unstable particles on Laponite® RD faces. In the case of the sodium replacement, the particle size is confined within a limited range; 2-5nm, due to restriction exacted by the interlamellar space that reduces particle growth (Phuoc and Chen, 2011). However, the particle growth restriction is limited at higher concentrations of the metal ions. This was clearly evident in the particle growth progression as shown in Fig. 4.10a-c with variations in the size distribution. During the ion exchange reaction negative charges on the Laponite® RD faces are partially balanced, giving rise to a weak electrostatic repulsive forces between the dispersed Laponite® RD disks when this occurs, the nanoparticles aggregates by the formation of electrostatic bonds between the positively charged rims and the negatively charged faces. The aggregates then grow until a space-filling structure or otherwise called gel is formed (Phuoc *et al*., 2009; Mongondry, *et al*., 2004; Baird and Walz, 2006) due to both van der Waals and electrostatic bonds between the positively charged rims and the negively chargesd surfaces (Phuoc *et al*., 2009).

The evidence of such cationic exchange can be seen from the EDX spectra and micro-images (Fig. 4.3 and 4.4), thermograph (Fig. 4.6), ^{29}Si MAS NMR (Fig. 4.7), SEM (4.8), TEM (Fig.4.9) and Table 4.1. The XRD pattern of copper-exchanged Laponite® RD (Fig. 4.1) and copper incorporated Laponite® RD (Fig. 4.11) were not different from the pure Laponite® RD

except in the basal spacing. Also, the FTIR remained unchanged as in the pure Laponite® RD for the copper-exchanged Laponite® RD (Fig. 4.2) except in the copper incorporated Laponite® RD where the octahedral presence of copper was indicated by the stretching vibration of the Cu-Mg-Li-OH band at higher wave number, 3658cm^{-1}. The degree of exchange and quantification was obtained by EDX. EDX only measures clay materials to a depth of 10µm therefore, eight different spots on the Laponite® RD surface and the modified species were selected randomly and analysed to ensure reliability and reproducibility. There was a corresponding decrease in the magnesium as the copper levels increased (Table 4.2) while, the replacement was denoted by the increase in copper with a corresponding decrease in the sodium ions (Table 4.1). EDX is a semi- quantitative technique which only detect element in excess of 5wt% (Song *et al.,* 2009 and Pichonat *et al.,* 2010). Hence, Li and OH were quantified by ICP-AES (Section 2.3.8) and TGA (Section 2.3.9) respectively due to their low atomic weight percentage in Laponite® RD. The surface structures as revealed by the SEM have suggested that the copper-exchanged Laponite® RD (Fig. 4.8) were characteristically different from the copper incorporated Laponite® RD. The former possess undulating surface structure while the latter appeared lumpy (Fig. 4.17).

The use of copper, as a compound, or additives as antibacterial agents has been an attractive idea for a long time, the reasons being to broaden the antimicrobial spectrum, minimise physical and chemical incompatibilities, and curtail toxicity via reduction of biocide dose and to produce biochemical synergy (Sondossi *et al*., 1990; Rossmoore and Sondossi 1988). The successful synthesis of copper-Laponite RD via ion-exchange and isomorphous substitution offer attractive features as potential candidate in antibacterial material. Therefore, in future the efficacy of the antibacterial activity will be assessed.

Chapter 5

Result and Discussion

Antimicrobial activity of silver modified Laponite® RD

The antimicrobial activity of silver modified Laponite® RD was assessed by disk diffusion test and viable plate counts. These results, as well as the concentration dependence of silver modified Laponite® RD produced by both ion exchange and isomorphous substitution, are presented in this chapter.

5.1 Antibacterial activity of silver-exchanged Laponite® RD (AGLAP1, 4 and 6)

5.1.1 Inhibition zone

Antibacterial activities of Ag-exchanged Laponite® RD with different exchange levels were determined by the disk diffusion method already described in Section 2.5.2. The zones of inhibition of bacterial growth which was measured as the distance between the edge of antibacterial disk and the end of clearance zone visible when the plate were viewed against a black background for *E. coli* K12W-T, *S. aureus* NCIM B6571 and *P. aeruginosa* NCIMB8295 are shown in Fig 5.1.

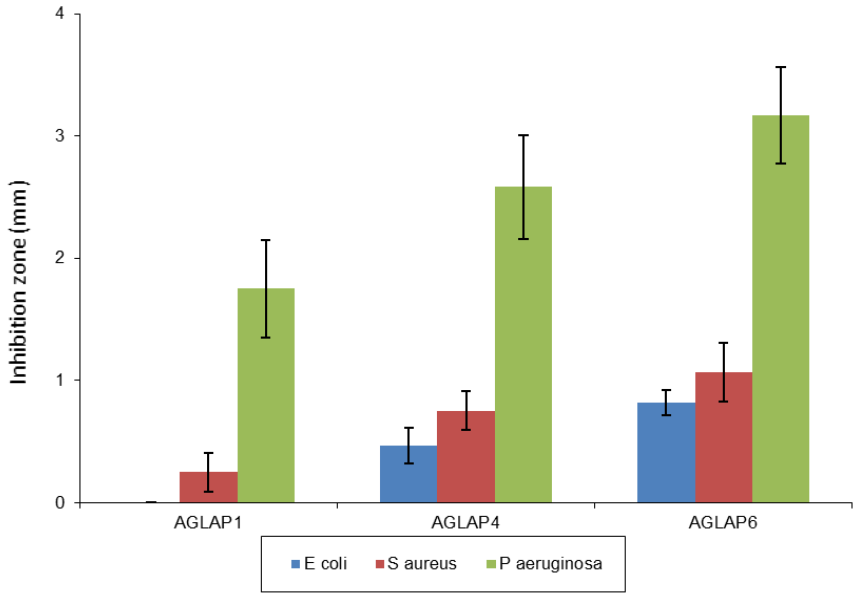

Fig. 5.1: Inhibition zones of the samples as a function of the concentration of silver-exchanged Laponite® RD against *E. coli*, *S. aureus* and *P. aeruginosa* grown on TSA at 37 °C, (n=3). Error bars represent standard error.

No antibacterial action was observed for the pure Laponite® RD. The highest inhibition zones of 3.2mm, 2.6mm, 1.8mm were observed for *P. aeruginosa* with AGLAP6, AGLAP4 and AGLAP1 respectively, followed by *S. aureus* with 1.1mm, 0.8mm, 0.3mm with AGLAP6, AGLAP4 and AGLAP1 respectively. The lowest inhibition zones were obtained for *E. coli;* 0.8mm, 0.5mm for AGLAP6, AGLAP4 respectively, but no zone of inhibition was observed for AGLAP1 (Fig. 5.1). The Ag^+ ions in agar as a fraction of the distance from the disk were not determined in this investigation.

5.1.2 Influence of concentration of silver-exchanged Laponite® RD (AGLAP1, 4 and 6) on bacteria

Antibacterial tests were performed against Gram-negative *E. coli* K12W-T and *P. aeruginosa* NCIMB8295 and Gram-positive *S. aureus* NCIM B6571 using TSB as the growth medium (Section 2.5.3). Fig. 5.2 shows the results obtained when the viable plate count method was used for the antibacterial efficacy determination using 2g l^{-1} each of the antibacterial agent. Laponite® RD (without silver) did not show any growth inhibition on all the bacteria examined (Fig. 5.2a, b, c). All concentrations of silver-exchanged Laponite® RD used showed at least some inhibitory effect on all the bacteria species when compared to media containing only the bacteria (without silver-Laponite® RD). The lag phase of *E. coli* in the medium supplemented with AGLAP1 was extended by 4 hours when compared to the control and after 72 hours there was 2.8 log cells reduction. Total inhibitory effect of $AgNO_3$, AGLAP6 and AGLAP4 were obtained at 2, 8 and 24 hours respectively (Fig. 5.2a). There was a prolonged lag phase of about 22 hours in *S. aureus* medium supplemented with AGLAP1 and 3.5 log cells reduction after 72 hours. Bactericidal action was achieved after 24 hours in the media supplemented with AGLAP4 and AGLAP6, while $AgNO_3$ was 2 hours (Fig. 5.2b).

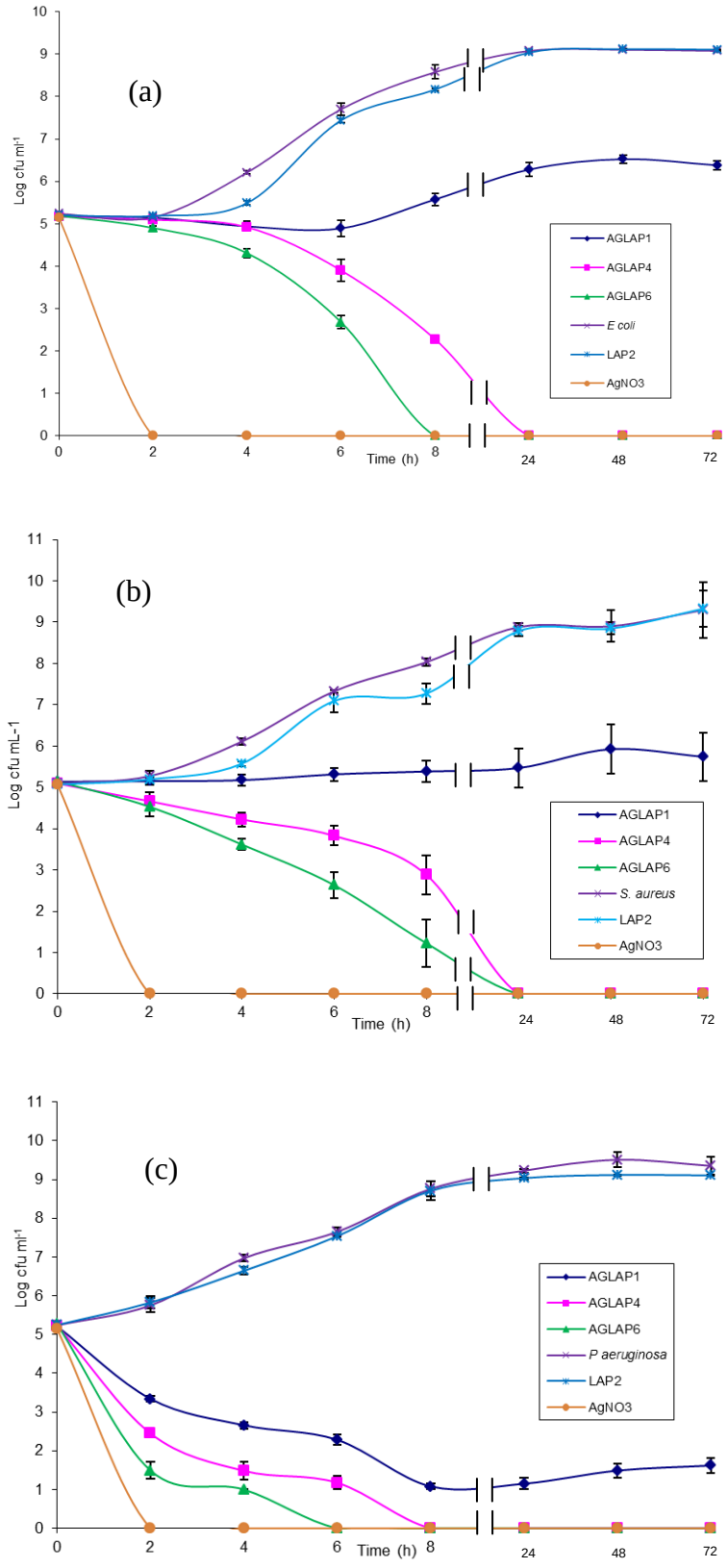

Fig 5.2: Determination of antibacterial activity of silver-exchanged Laponite® RD and $AgNO_3$ by viable plate count against *E. coli* (a), *S. aureus* (b) and *P. aeruginosa* (c) cells were treated with 2g l^{-1} each of AGLAP1, AGLAP4 and AGLAP6 at 37°C in TSB. The pH remained fairly constant within the range of 6.7 – 7.6.

With a 7.7 log cell reduction using AGLAP1, bactericidal action of AGLAP4 at 8 hours, AGLAP6 at 6 hours and $AgNO_3$ at 2 hours, *P. aeruginosa* showed the highest susceptibility to the silver-Laponite® RD throughout the duration of the experimental period (Fig. 5.2c).

5.1.3 ICP-AES analysis of silver ions eluted from silver-exchanged Laponite® RD (AGLAP1, 4 and 6)

The quantity of silver ions eluted from the silver-exchanged Laponite® RD nanocomposite in TSB containing *E. coli* K12W-T, *S. aureus* NCIM B6571 or *P. aeruginosa* NCIMB8295 was monitored and recorded (Fig.5.3). There was a steady release of silver ions with time when bacteria was present in TSB. In the presence of *E. coli*, *S. aureus* or *P. aeruginosa* the release rate of silver ions increased with time. In the presence of *E. coli* there was a burst silver ions release of 0.2, 1.4 and 2.2ppm from AGLAP1, AGLAP4 and AGLAP6 respectively at time zero, then a steady increase in the release to 2 hours and was fairly constant until the 8th hour and a further increase in the release after 24, 48 till 72 hours resulting in a total silver ions release of 4.3, 10.9 and 12.1ppm silver ions from AGLAP1, AGLAP4 and AGLAP6 (Fig. 5.3(i)). At time zero 804.2ppm was released from $AgNO_3$, and increased to 889.9ppm after 72 hours (Fig. 5.3(ii)). Comparable releases were observed for *S. aureus* (Fig. 5.3 (iii), (iv)), and *P. aeruginosa* (Fig. 5.3 (v), (vi)).

Fig. 5.3: Silver ions released from silver-exchanged Laponite® RD and $AgNO_3$ into TSB with *E. coli* (i), (ii); *S. aureus* (iii), (iv) and *P. aeruginosa* (v), (vi) with time at concentrations of 2g l^{-1} each of AGLAP1, AGLAP4 and AGLAP6 at 37°C. See attached Fig. doc.

Figure 5.4 was the release profile obtained when only silver-exchanged Laponite® RD was placed in TSB (without bacteria). The profiles show a progressive and consistent release similar to those with bacteria. Over the 72 hour period 3.5, 10.9, 12.7 and 874.5ppm of silver ions were released respectively from AGLAP1, AGLAP4, AGLAP6 and $AgNO_3$ respectively (Fig. 5.4(i) and (ii)). There was statistically no significant difference between the release profiles of silver ions in medium containing bacteria and medium without bacteria ($P > 0.05$ Appendix 1A).

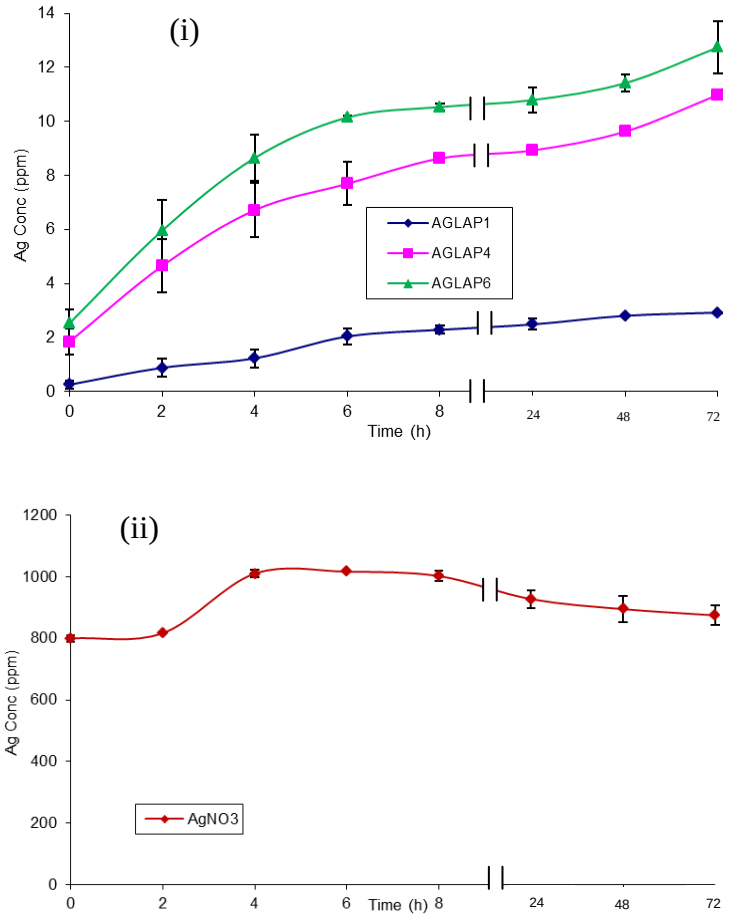

Fig. 5.4: Silver ions released from silver-exchanged Laponite® RD and $AgNO_3$ into TSB at 37 ^{o}C without bacteria with time at concentrations of 2g l^{-1} each of AGLAP1, AGLAP4 and AGLAP6, (i) and $AgNO_3$ (ii).

5.2 Antibacterial activity of silver incorporated Laponite® RD (AL1-3) by isomorphous substitution

5.2.1 Inhibition zone

The sensitivity was performed as already described in Section 2.5.2. The results obtained are as shown in (Fig. 5.5). No antibacterial action was observed for the pure Laponite® RD. The width of the inhibition zone (distance between edge of disk and end of clearance zone) of the antibacterial silver modified Laponite® RD as a function of the loading level measured in the case of three different bacterial strains, *E. coli* K12W-T, *S. aureus* NCIM B6571 and *P. aeruginosa* NCIMB8295 are shown in Fig 5.5. The largest inhibition zone were observed with *P. aeruginosa*, 1.8mm, 1.4mm, and 0.5mm for AL3, AL2 and AL1 respectively; for *S. aureus*, 1.5mm, 1.1mm, 0.4mm, and for *E. coli;* 1.3mm, 1.0mm and 0.4mm were obtained for AL3, AL2 and AL1 respectively (Fig.5.5).

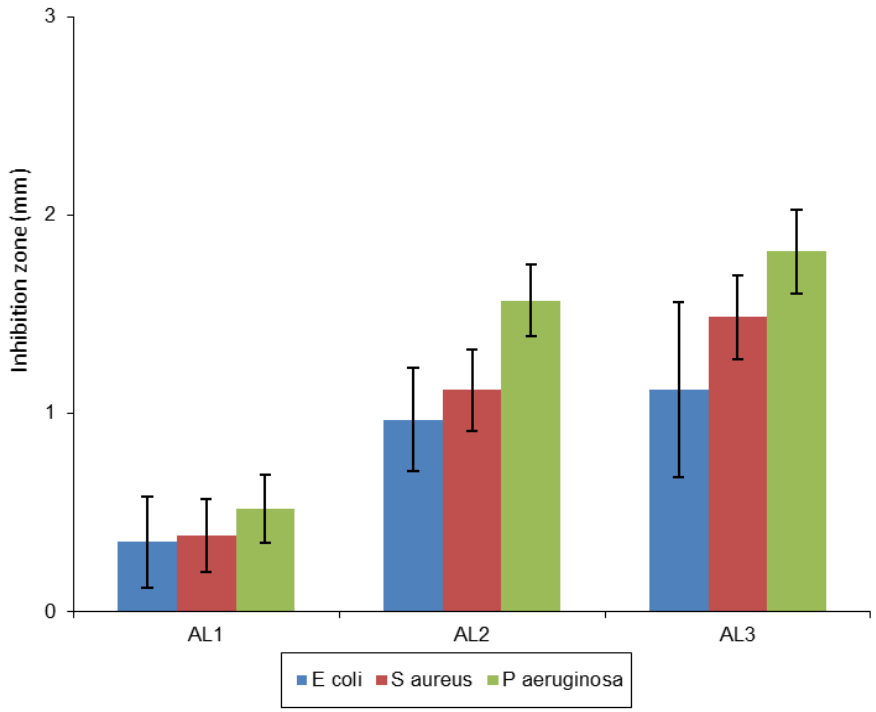

Fig. 5.5: Inhibition zones of the samples as a function of the silver incorporated Laponite® RD level against *E. coli*, *S. aureus* and *P. aeruginosa* grown on TSA at 37 °C. (n=3). Error bars represent standard error.

5.2.2 Influence of concentration of silver incorporated Laponite® RD by isomorphous substitution.

As described in Section 2.6 the inhibitory effect of silver incorporated Laponite® RD was

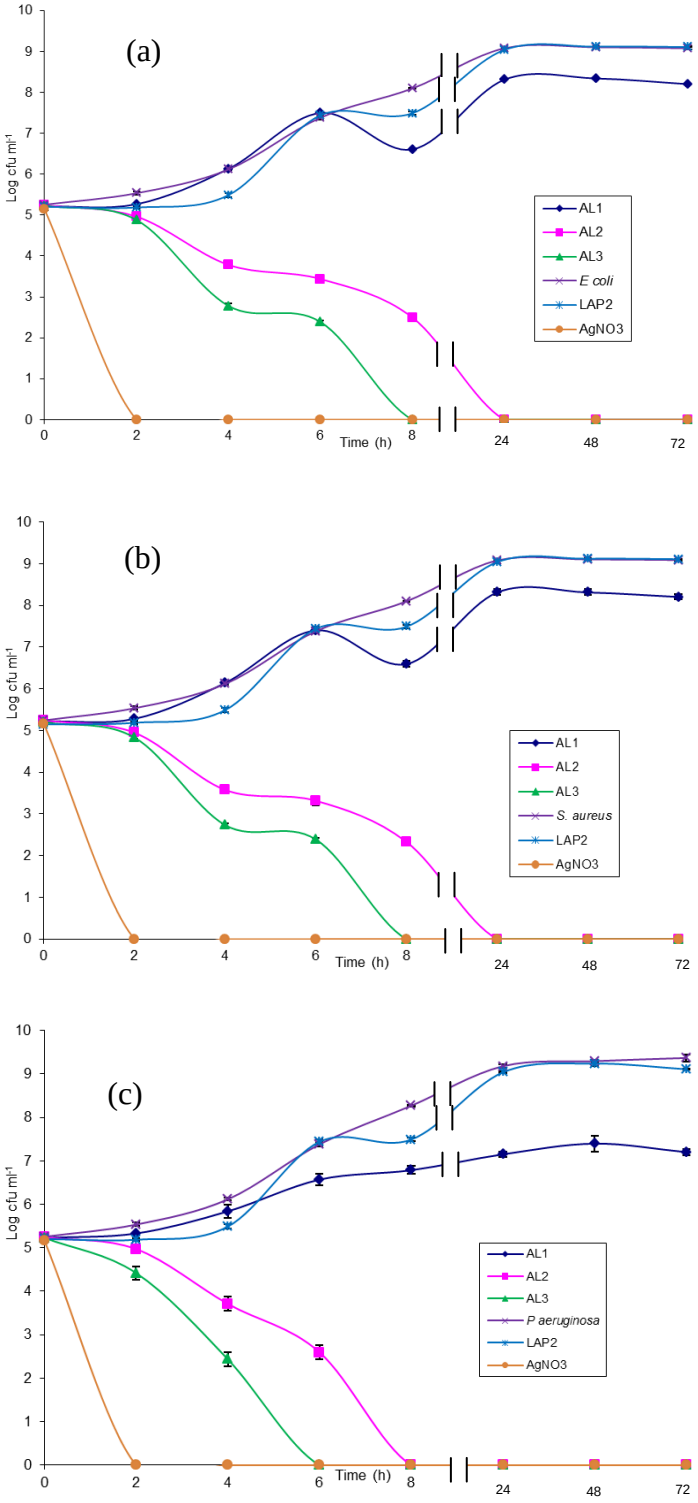

Fig. 5.6: Antibacterial activity of silver incorporated Laponite® RD and $AgNO_3$ by viable plate count at 37°C for *E. coli* (a), *S. aureus* (b) and *P. aeruginosa* (c). The bacteria were treated with 2g l^{-1} each of AL1, AL2 and AL3 in TSB. pH = 6.7-7.6.

investigated. Fig. 5.6 represents the antibacterial efficacy of 2g l^{-1} of silver incorporated Laponite® RD and $AgNO_3$ on the selected bacteria determined by the viable plate count method. The viability of *E. coli* was reduced by 3.9 and 5 log cells with AL2 and AL3 respectively, while no cell reduction effect was observed for AL1 after 6 hours, with a starting 5.2 log cells (Fig. 6.5a). After 24 hours there was 0.7 log cells reduction of *E. coli* with AL1, while a total cell reduction of 9.1 log was obtained for both AL2 and AL3 after 24 hours. After 72 hours 0.9 log cell reduction of *E. coli* was obtained for AL1. Total inhibition was obtained after 2, 8 and 24 hours in *E. coli* medium supplemented with $AgNO_3$, AL2 and AL3 respectively. Comparable antibacterial effect was obtained for *S. aureus* (Fig. 5.6b) and *P. aeruginosa* (Fig. 5.6c).

5.2.3 ICP-AES analysis of silver ions eluted from silver incorporated Laponite® RD

Fig. 5.7: Silver ion released from silver incorporated Laponite® RD and $AgNO_3$ into TSB with *E. coli* (i), (ii); *S. aureus* (iii), (iv) and *P. aeruginosa* (v), (vi) with time. The bacteria were treated with 2g l^{-1} each of AL1, AL2, AL3 and $AgNO_3$ at 37°C between the pH ranges 6.2 – 7.1. See attached Fig. doc.

The amount of silver ions eluted from silver incorporated Laponite® RD in TSB containing *E. coli, S. aureus or P. aeruginosa* are shown in Figure 5.7. There was a steady release of silver

ions with time in the presence of the bacteria. At the starting time no silver ions were released and after 2 hours 2.3, 3.5 and 4.2ppm were released from AL1, AL2 and AL3 respectively. These gradually increased to 9.3, 11.0, and 13.0ppm after 72 hours in the medium inoculated with *E. coli* (Fig. 5.7(i)). In a separate *E. coli* medium containing $AgNO_3$, there was an initial 801.5ppm burst silver ions release at time zero, at the end of 72 hours 799.7ppm were present in the bacterial medium (Fig. 5.7(ii)). Comparable silver ion releases were obtained for *S. aureus* (Fig. 5.7(iii) and (iv)) and *P. aeruginosa* (Fig. 5.7(v)). Figure 5.8 represent the release profile obtained when silver incorporated Laponite® RD place in TSB was performed without bacteria.

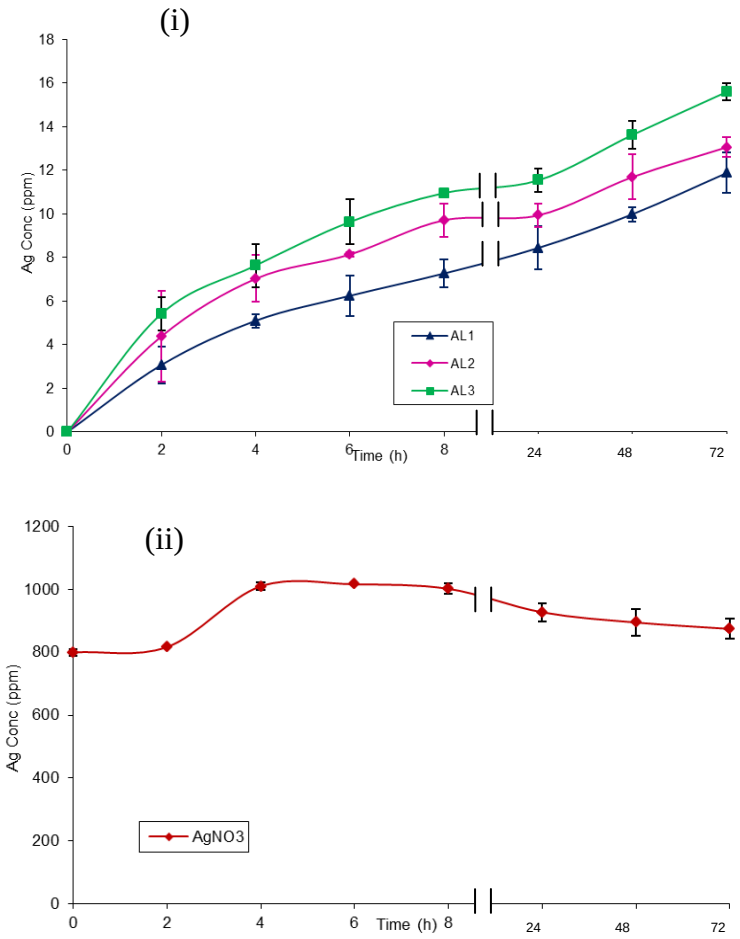

Fig. 5.8: Silver ions released from silver incorporated exchanged Laponite® RD and $AgNO_3$ into TSB at 37 ^oC without bacteria with time at concentrations of 2g l^{-1} each of AL1, AL2 and AL3, (i) and $AgNO_3$ (ii).

The profiles show a progressive and consistent release similar to those with bacteria, which indicate that the presence of bacteria in the medium did not elicit an increase in the amount of silver ions released. Previous studies by Matsumura *et al*., (2003) suggested that silver ions would only be released in aqueous media containing bacterial cells while Kwakye-Awuah *et al*. (2008) found that the amount of silver released in medium containing bacteria was significantly lower (P = 0.003) than those without the bacteria. However, the present study revealed that there was no significant difference ($P > 0.05$) between the silver ions released in medium with or without the bacterial cells (Appendix 1B).

Table 5.1: The release of silver ions in bacterial medium after 72 hours at 37^{o}C.

	Ag^{+} released in bacteria medium ±SE (ppm)		
Samples	*E. coli*	*S. aureus*	*P. aeruginosa*
Ion exchange			
AGLAP1	3.42±1.45	4.25±0.98	4.78±1.04
AGLAP4	10.89±1.56	10.93±1.51	11.29±0.17
AGLAP6	12.06±0.31	12.84±1.20	12.52±0.90
Isomorphous substitution			
AL1	9.27±1.34	7.87±0.34	8.87±2.01
AL2	10.95±1.78	10.85±1.09	12.54±1.51
AL3	12.68±1.43	13.14±1.56	13.99±1.03
$AgNO_3$	799.65±24.64	796.09±35.22	788.15±33.41

This suggests that the silver size in which the greater percentage of 65 - 89% was in the range 10 - 20nm may have been too large to diffuse into the cell, as only smaller particles mainly in the range 1 – 10nm could enter the cell, based on indirect microscopic evidence (Morones

et al., 2005 and Kloepfer *et al.,* 2005). This assertion was also supported by Choi and Hu, (2008) who found that the nanoparticle size range 8 – 14nm were impenetrable to *E. coli* cells. In the ion exchanged species approximately 17, 28 and 26% of silver ions were released from AGLAP1, AGLAP4 and AGLAP6 respectively (Table 3.1 and 5.1). While 77 and 55% of the silver ions were released from the isomorphous substituted species; AL2 and AL3 respectively (Table 3.2 and 5.1), whereas the silver ion release from $AgNO_3$ was 80% after 72 hours (Table 5.1 and Appendix 2C).

5.3 Discussion

5.3.1 The antibacterial activity of silver modified Laponite® RD

Bacteria resistance to antibacterial agents has been a challenge for a long time (Atiyeh *et al*., 2007; Rai *et al.*, 2008). The key attribute of antibacterial agents is to be present in a sufficient quantity to ensure an efficacious release level over a period of time, and a support material that would promote a consistent release. The use of silver modified Laponite® RD by both methods has demonstrated these properties.

The silver being bound to the interlayer space in the silver exchanged Laponite ® RD facilitated an immediate (AGLAP6 releasing upto 2ppm at time zero), as well as slow, release lasting for the 72 hours duration of the investigation (Fig. 5.3 and 5.4). Although, there was no Ag^+ ions release from silver incorporated Laponite ® RD i.e. AL3 at time zero (Fig. 5.7 and 5.8). The isomorphous substituted silver-Laponite® RD demonstrated similar releasing trend, surprisingly the release were quite more up to 94% (AL2) and 57% (AL3) compared to the ion exchange species which were 24% (AGLAP1), 31% (AGLAP4) and 26% (AGLAP6).

The Laponite® RD (without silver) showed no antibacterial properties. Therefore, the silver ions released from the silver modified Laponite® RD were responsible for the antibacterial action against all three bacteria examined.

The starting bacterial concentration of $10^5 – 10^6$ CFU ml^{-1} was used for the disk diffusion test to show the sensitivity of the bacteria. The batch studies revealed differences in sensitivity to silver exhibited by bacterial strains. The size of the zone of inhibition was a measure of the susceptibility of bacteria to silver-Laponite® RD. The strains susceptible to silver-Laponite® RD exhibit larger inhibition zone whereas resistant strains exhibit smaller or no inhibition zone. The silver-exchanged Laponite® RD disks were surrounded with larger inhibition zones (Fig. 5.1) compared to the silver incorporated Laponite® RD (Fig. 5.5). Perhaps due to diffusion barrier posed by the media since Ag^+ ions can only be release via an ion exchanged process, fundametally with the chloride ions component of the TSB (Ruparelia *et al*., 2008). In addition, the Ag^+ ions from the Laponite octahedral sheet would be more difficult to diffuse rather than from the interlayer surface as in the case of the silver-exchange Laponite® RD. This restricted the diffusion of the agent into the agar around the area of application preventing a greater zone of clearance around the disk. Thus reduced the diffusion rate of the silver ions from the Laponite® RD matrix. Hence, the gel nature and subsequent entrapment of silver ions within the matrix limited the diffusion rate therefore; less number of the bacterial population was killed resulting in low inhibition zones.

However, all the strains were totally inhibited after 24 hours by the viable plate count with silver-exchanged Laponite® RD. *P. aeruginosa* (Fig. 5.2c) was relatively the most susceptible of the bacterial strains examined followed by *S. aureus* (Fig. 5.2b) and then *E. coli* (Fig. 5.2a). Also, the silver incorporated Laponite® RD followed a similar trend as shown in Fig.

5.6. Since the zones of inhibition of the bacteria were measured on agar plates using a meter ruler with a 1mm resolution, the possibility of measurement errors exists. However, the method illustrates the potential bactericidal effect of silver to different bacterial strains.

5.3.2 The silver ions released from silver modified Laponite® RD

Work by Kwakye-Awuah *et al*. (2008) did not take into account the components of TSB taking part in the bactericidal action. TSB contains NaCl which participates in significant ion exchange in the bacterial media, enhancing the release of the silver via an ion exchange process (Ruparelia *et al*., 2008). The equation of the reaction that occurred in the culture media is as shown:

$$c\text{Ag-Laponite}^{®}\ \text{RD}_{(s)} + \text{TBS}_{(aq)} + \text{Na}^{+} + \text{Bacteria} \longrightarrow x\text{Ag}^{+}_{(aq)} + (c\text{-}x)\text{Ag}\ (x)\text{Na-Laponite}^{®}\ \text{RD}_{(s)} + \text{TSB}_{(ag)} + \text{Bacteria} \quad (3)$$

where *c* is the initial concentration of silver ions in the Ag-Laponite® RD

x is the concentration of silver ion released from the Ag-Laponite® RD

s is the solid state of Ag-Laponite® RD and Na-Laponite® RD

aq is aqueous state of TSB and Ag^{+} during the reaction

The result showed that NaCl participated in the efficacy of the bactericidal action of Ag-Laponite® RD. The fact that the release of silver ions was immediate in the media is an indication of the possibility of occlusion of silver ions on the silver-Laponite® RD produced by ion exchange despite sufficient washing with methanol (Section 2.2.1.1). According to Kwakye-Awuah *et al*. (2008) this type of silver ions release are instantaneous since they do not diffuse from the framework. Although, the isomorphous substituted silver incorporated

Laponite® RD demonstrated similar release characteristics, the release was not immediate (at least there was no occlusion of the silver ions as there were no Ag^+ ions releaed into the medium at sampling time zero) quite slow and may be for longer duration. Octahedrally bound silver is more difficult and slower to release than those bound to the surface, interlayer or edges. The Laponite® RD without silver showed no antibacterial properties. Therefore, the silver ions released from the Laponite® RD layers of the silver modified Laponite® RD were responsible for the antibacterial action against all three bacteria.

The TEM images (Fig. 3.14 and 3.18) confirmed the silver species were in the nanoparticle range. Silver nanoparticles interact with microbial cells through a variety of mechanisms. The silver nanoparticles have been reported to act directly with the microbial cells by causing cell pitting (Choi and Hu, 2008), interrupting transmembrane electron transfer, disrupting and penetrating the cell envelope, oxidizing cell components or producing secondary products such as reactive oxygen species or dissolved silver ions resulting in damage to the cell (Li *et al*., 2008a). The high surface area of silver nanoparticles increases the potential that silver ions are released from them (Mudunkotuwa and Grassian, 2011; Bian *et al.,* 2011). But it is not yet clear to which degree the toxicity of silver nanoparticle emanates from released silver ions and how much toxicity is attributed to the silver nanoparticle itself (Beer *et al*., 2012). Kim *et al*., (2009) suggest that the toxicity of AgNPs is principally due to oxidative stress (because in his experiment using human hepatoma cells to demonstrate the role oxidative stress plays in the cytotoxicity of AgNPs, he found that metal-responsive metallothionein 1b mRNA expression was not induced in AgNP-treated cells, while it was induced in Ag^+ ions-treated cells. So he concluded that AgNP-treated cells have limited exposure to Ag^+ ions, despite the potential release of Ag^+ ions from AgNPs in cell culture, and that the AgNPs agglomerated in the cytoplasm and nuclei of treated cells and induced intracellular oxidative

stress) and independent of the toxicity of Ag^+ ions. While, Kawata *et al.,* (2009) and Navarro *et al.,* (2008) inferred that the measured Ag^+ ions content of the AgNPs suspension could not fully explain the observed toxicity of the AgNPs suspension and that both Ag^+ ions and AgNPs contributed to the toxicity. Although, some degree of conflicts exists in these reports, the evidence presented suggests that silver ions at least account for some part of the toxicity of silver nanoparticles (Beer *et al.,* 2012).

However, the processes that may be possibly involved in the antibacterial action of silver-Laponite® RD; bacterial cells that come into contact with the silver modified Laponite® RD take up the silver ions. These ions inhibit several of the cells functions and thus cause cell damage (Matsumura *et al.,* 2003). Also, the silver ions interact with thiol-containing amino acids and bind to functional groups of protein causing denaturation (Liau *et al.,* 1997). In addition, silver ions have been demonstrated to inhibit respiratory enzymes and produce reactive oxygen species which attack the microbial cell. These by-products (such as super oxide anions, hydrogen peroxide, hydroxyl radicals and singlet oxygen) of dissolved oxygen occur in aerobic environments (Inoue *et al.,* 2002 and Galeano *et al*., 2003).

However, silver ions have been shown to inhibit the growth of pathogenic oral bacteria such as *Porphyromonas gingivalis, Prevotella intermedia* and *Streptococcus mutans* under anaerobic conditions (Kawahara *et al.,* 2000). These suggest that silver modified Laponite® RD may be useful in controlling many types of pathogenic microorganisms in both aerobic and anaerobic environments. This experiment was performed in day light, so there was possibly reduction of some of the silver ions to the metallic form that may have occurred during the addition of silver-Laponite® RD to the bacteria culture. The metallic silver was likely to become a mass of minute electrodes, making the silver modified Laponite® RD

conductive and causing it to release the silver ions (Schierholz *et al*., 2000). The observed bactericidal effect is dependent upon the concentration of silver ions as well as the initial bacterial concentration (Pal *et al*., 2007). Although, the clinical application of silver-Laponite® RD has not been established, it can potentially be exploited in medicine for treatment of burns, dental materials, coating stainless steel materials, textile fabrics, sunscreen lotions and water treatment (Rai *et al* ., 2009).

Notice:

Silver in electrochemical series (for complete table see http://www.chemguide.co.uk/physical/redoxeqia/ecs.html)

$$Ag^{+}_{(aq)} + e^{-} \overset{\text{equilibrium}}{\rightleftharpoons} Ag_{(s)} \qquad E^{o} = +0.80 \text{ volts}$$

Chapter 6

Result and Discussion

Antibacterial activity of copper modified Laponite® RD

In this chapter the antibacterial activity of copper-modified Laponite® RD was assessed preliminarily by sensitivity test and directly by viable plate counts. These results as well as the copper released from the copper-Laponite® RD composites were examined in both the ion exchange and the isomorphous substituted samples.

6.1 Antibacterial activity of copper-exchanged Laponite® RD by ion exchange

6.1.1 Inhibition zone

Antibacterial activities of copper-exchanged Laponite® RD (CULAP) with different exchange levels were determined by the disk diffusion method already described in Section 2.5.2. The width of the inhibition zones (distance between edge of disk and end of inhibition zone) of the antibacterial copper-exchanged Laponite® RD as a function of the exchange level measured in the cases of three different bacteria strains, *E. coli* K12W-T, *S. aureus* NCIM B6571 and *P. aeruginosa* NCIMB8295 are shown in Fig 6.1.

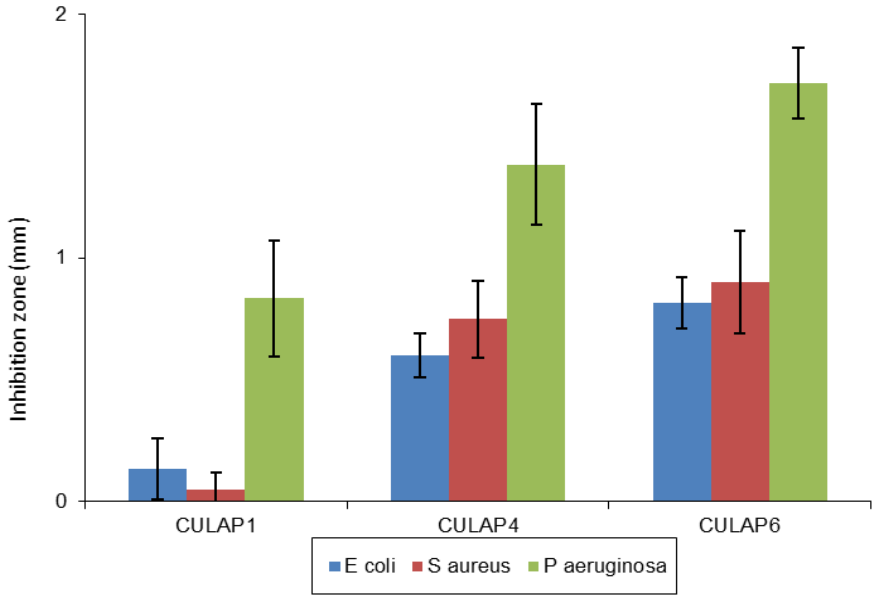

Fig. 6.1: Inhibition zones of the samples as a function of the concentration of copper-exchanged Laponite® RD against *E. coli*, *S. aureus* and *P. aeruginosa* grown on TSA at 37 °C. (n=3). Error bars represent standard error.

No antibacterial action was observed for the pure Laponite® RD. The highest inhibition zones of 1.7mm, 1.4mm, 0.9mm were observed for *P. aeruginosa* with CULAP6, CULAP4 and CULAP1 respectively, followed by *S. aureus* with 0.6 mm, 0.8mm, 0.1mm with CULAP6, CULAP4 and CULAP1 respectively. While lowest inhibition zone were obtained for *E. coli* 0.8mm, 0.6 mm and 0.6mm for CULAP6, CULAP4 and CULAP1 respectively (Fig. 5.1).

6.1.2 Influence of concentration of copper-exchanged Laponite® RD on bacteria

Antibacterial tests were performed against Gram-negative *E. coli* K12W-T and *P. aeruginosa* NCIMB8295 and Gram-positive *S. aureus* NCIM B6571 using TSB as the growth medium (Section 2.4.1). The results obtained for the viable plate count show the presence of copper-exchanged Laponite® RD at concentrations of $2gl^{-1}$ each of CULAP1, CULAP4 and CULAP6 resulting in minimal inhibition on the growth of the bacteria throughout the 72 hours dur` ation (Fig. 6.2).

Laponite® RD (without copper) did not show any growth inhibition on all the bacteria examined (Fig. 6.2). With the initial 5.23 log CFU ml^{-1}, the growth of *E. coli* was reduced by 0.19, 0.72 and 1.15 log CFU ml^{-1} at the concentration of 2g l^{-1} each of CULAP1, CULAP4 and CULAP6 respectively after 72 hours (Fig. 6.2a). At the same period 1.00, 1.42 and 1.76 log CFU ml^{-1} reduction was obtained for *S. aureus* by CULAP1, CULAP4 and CULAP6 respectively (Fig. 6.2b). The viability of *P. aeruginosa* was most affected with 1.00 log CFU ml^{-1} (CULAP1), I.60 log CFU ml^{-1} (CULAP4) and 3.10 log CFU ml^{-1} (CULAP6) reduction in growth (Fig. 6.2c). All bacteria tested were inhibited after 2 hours contact time with 2g l^{-1} of $CuSO_4$ (Fig. 6.2a,b,c).

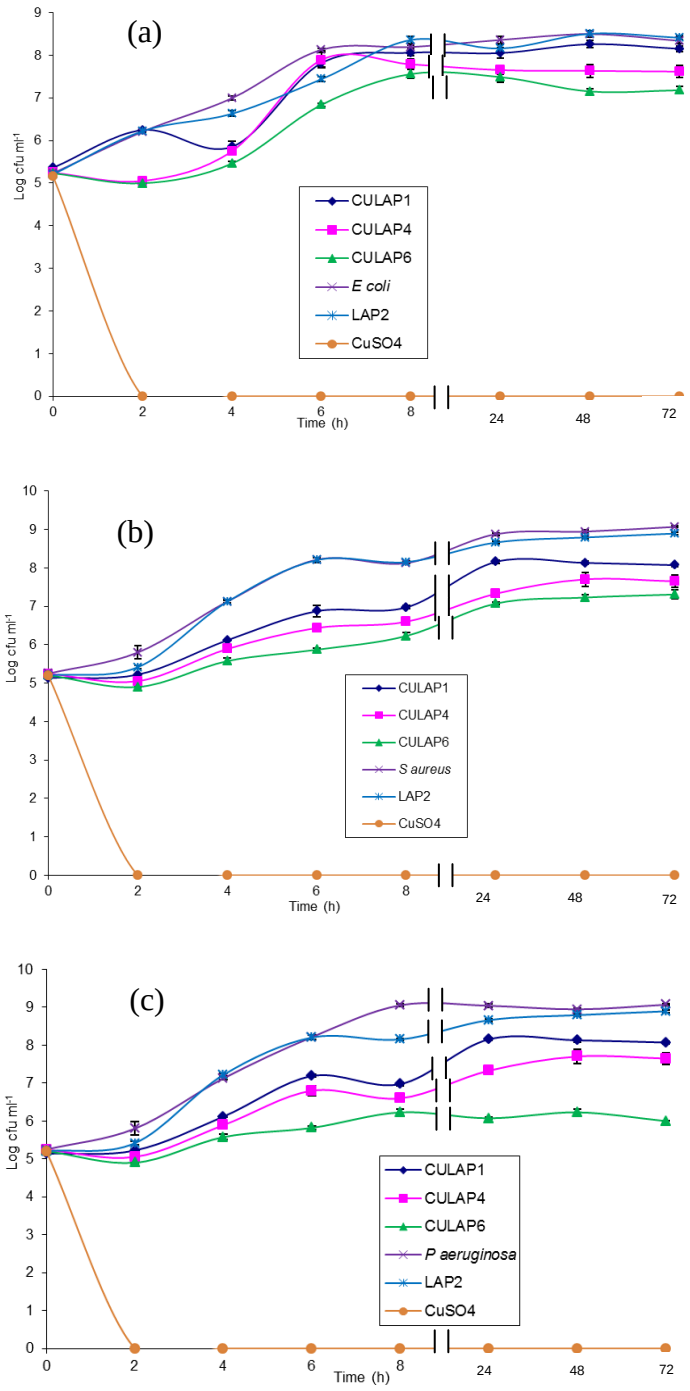

Fig 6.2: Determination of antibacterial activity of copper-exchanged Laponite® RD and $CuSO_4$ by viable plate count against *E. coli* (a), *S. aureus* (b) and *P. aeruginosa* (c). The bacteria were treated with 2g l^{-1} each of CULAP1, CULAP4 and CULAP6 at 37°C in TSB.

6.1.3 ICP-AES analysis of copper ions eluted from copper-exchanged Laponite® RD

Fig. 6.3: Copper ion released from copper-exchanged Laponite® RD and $CuSO_4$ into TSB with *E. coli* (i), (ii); *S. aureus* (iii), (iv) and *P. aeruginosa* (v), (vi) with time at concentrations of 2g l^{-1} each of CULAP1, CULAP4 and CULAP6 at 37°C. See attached Fig. doc.

Typically, intercalated species in the interlayer space of smectites is released by ion-exchange reaction with other cations. The Cu^{2+} ion was released from Cu-exchanged Laponite® RD by ion exchange with other cations present in the TSB such as Na^{+}. The Cu^{2+} ions were continuously released over the 72 hrs period and a burst release was observed for the initial 2hrs. The initial burst release may be attributed to some Cu^{2+} ions existing at or near the surface of the Laponite® RD.

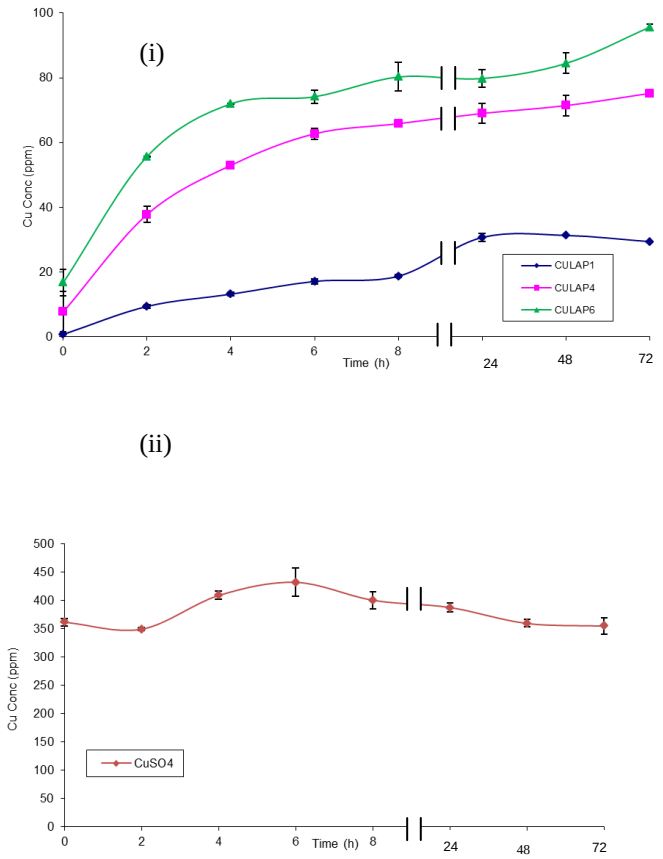

Fig. 6.4: Copper ions released from copper-exchanged Laponite® RD and $CuSO_4$ into TSB without bacteria with time at concentrations of 2g l^{-1} each of CULAP1, CULAP4 and CULAP6, (i) and $CuSO_4$ (ii) at 37°C.

The Cu^{2+} ion release profile of $CuSO_4$ was spontaneous and abrupt with 300.37ppm of Cu^{2+} ions released at time zero and 348.55ppm after 72 hours in medium inoculated with *E. coli* (Table 6.1). Equivalent Cu^{2+} ions release levels were obtained for *S. aureus* and *P.*

aeruginosa (Table 6.1). The equilibrium percentage release of Cu^{2+} ions were not up to 100%. This was expected as typical of an ion-exchange reaction, which is an equilibrium process whereby the interlayer cations cannot be completely exchanged (Meng *et al*., 2009). There was no significant difference ($P > 0.05$) between the Cu^{2+} ions release profile from all concentrations of copper-exchanged Laponite® RD in the media with or without *E. coli* (Appendix 1C), *S. aureus* and *P. aeruginosa*; except for *S. aureus* in media supplemented with CULAP1 after 6 – 72 hours; CULAP4 after 6 – 8 hours, CULAP6 after 2- 8 hours (Appendix 1C); and excerpt for *P. aeruginosa* in media supplemented with CULAP1 after 4 – 72 hours; CULAP4 after 4 – 72 hours, CULAP6 after 0 - 8hours and again after 72 hours (Appendix 1C).

6.2 Antibacterial activity of copper incorporated Laponite® RD by isomorphous substitution

6.2.1 Influence of concentration of copper incorporated Laponite® RD on bacteria

The disk diffusion test was performed as already described in Section 2.5.2. There was no inhibition zone observed for either the pure Laponite® RD nor the copper incorporated Laponite® RD in all the three bacterial strains examined therefore, the results were not included. The antibacterial efficacy of copper incorporated Laponite® RD by the viable plate count is shown in Fig. 6.5. There was a 0.39 log cell reduction of *E. coli*, 0.36 log cell reduction of *S. aureus* and 0.99 log cells reduction for *P. aeruginosa* obtained with 2g l^{-1} CL1 after 72 hours within the pH 6.7 – 7.2.

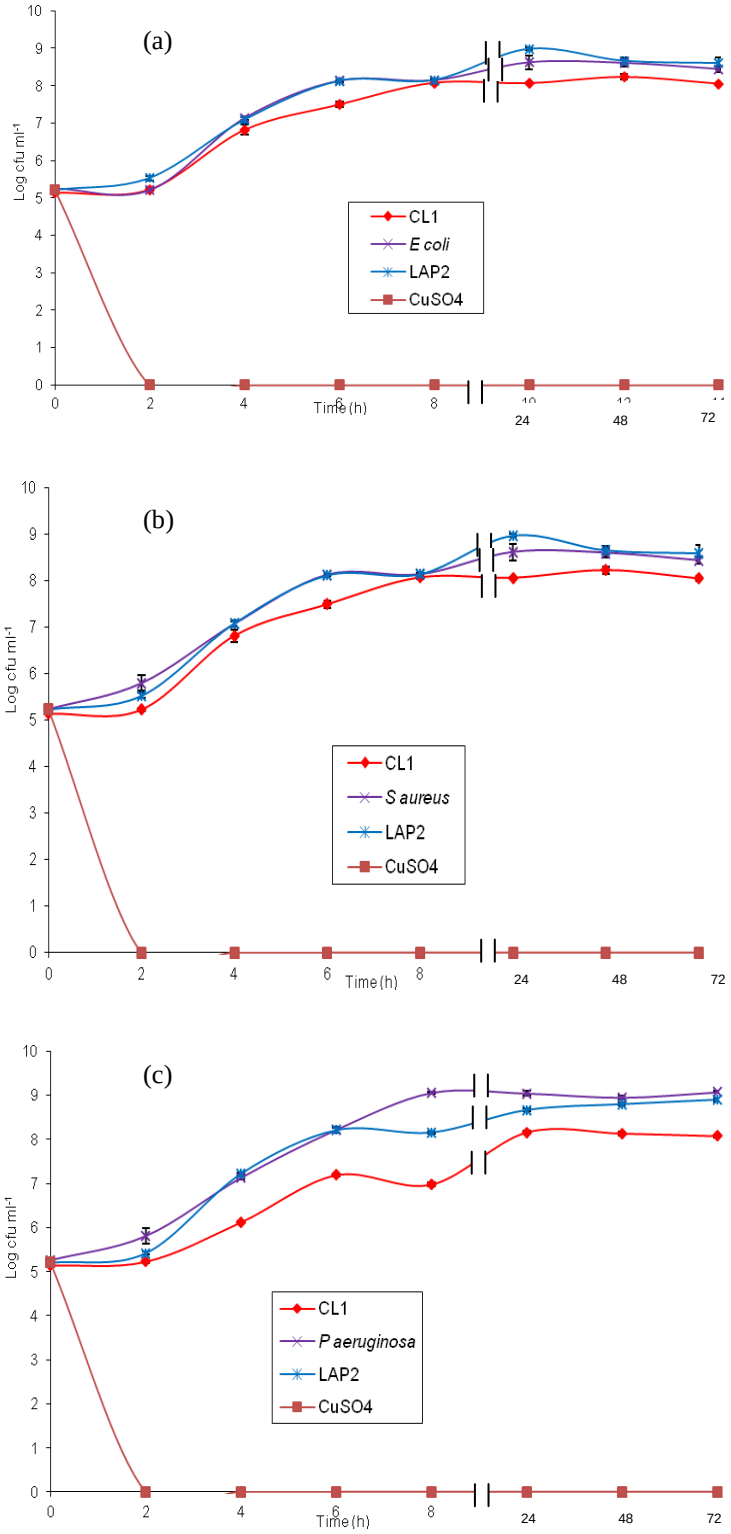

Fig. 6.5: Determination of antibacterial activity of copper incorporated Laponite® RD and $CuSO_4$ by viable plate count against *E. coli* (a), *S. aureus* (b) and *P. aeruginosa* (c). The bacteria were treated with 2g l^{-1} of CL1at 37°C in TSB.

6.2.1 ICP-AES analysis of copper ions eluted from copper incorporated Laponite® RD (CL1)

The amount of copper ions eluted from copper incorporated Laponite® RD in TSB containing *E. coli, S. aureus or P. aeruginosa* are shown in Figure 6.6. There was a steady release of copper ions with time in the presence of the bacteria.

Fig. 6.6: Copper ion released from copper incorporated Laponite® RD and $CuSO_4$ into TSB with *E. coli* (i), (ii); *S. aureus* (iii), (iv) and *P. aeruginosa* (v), (vi) with time at concentrations of 2g l^{-1} of CL1 at 37^{o}C. See attached Fig. doc.

No copper was released at time zero and after 2 hours 2.2ppm was released from CL1 which gradually increased to 6.9ppm after 8 hours, and a further release of 7.7ppm and 8.9ppm after 24 and 72 hours respectively in medium containing *E. coli* (Fig. 6.6(i)). In a different *E. coli* medium supplemented with $CuSO_4$ there was an initial 317.9ppm release of copper at starting time zero, which increased to 398.1ppm after 8 hours and 321.4ppm after 72 hours (Fig. 6.6(ii)). Comparable copper release was obtained for *S. aureus* (Fig. 6.6(iii), (iv)), and *P. aeruginosa* (Fig. 6.6(v), (vi)).

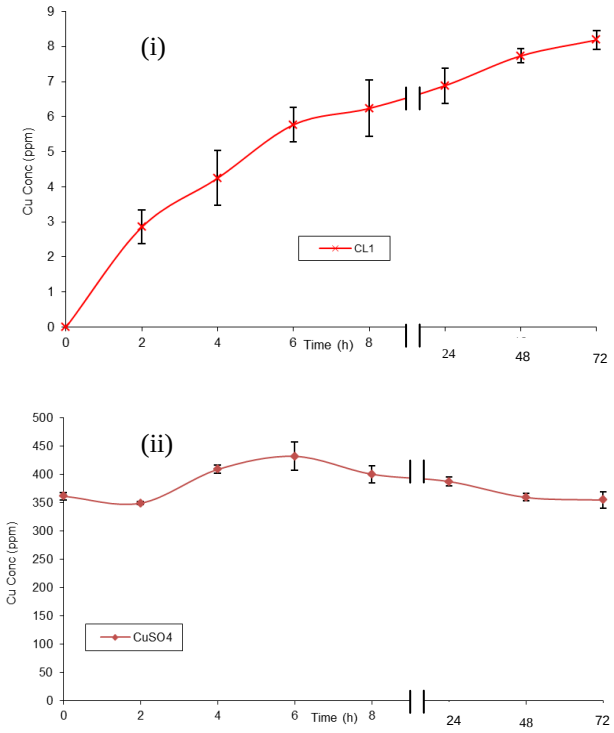

Fig. 6.7: Copper ions released from copper incorporated Laponite® RD and $CuSO_4$ into TSB without bacteria with time at concentrations of CL1 (i) and $CuSO_4$ (ii) at 37°C.

Figure 6.7 represents the release profile obtained when copper incorporated Laponite® RD place in TSB was performed without bacteria. The profiles show a progressive and consistent release similar to those with bacteria (Fig. 6.6), which indicate that the presence of bacteria in

the medium did not elicit an increase in the amount of copper released, as there was no significant difference between the two profiles for all the bacteria ($P > 0.05$, Appendix 1D).

Table 6.1: The release of copper ions in bacterial medium after 72 hours at 37°C.

	Cu^{2+} released in bacteria medium ±SE (ppm)		
Samples	*E. coli*	*S. aureus*	*P. aeruginosa*
Ion exchange			
CULAP1	18.96±0.18	19.27±0.38	17.93±0.93
CULAP4	75.22±0.73	68.34±1.65	66.27±1.31
CULAP6	95.66±0.84	89.50±1.18	88.05±0.80
Isomorphous substitution			
CL1	8.77±0.87	9.94±1.10	9.87±0.34
$CuSO_4$	348.55±39.77	359.32±57.34	347.33±48.74

6.3 Discussion

6.3.1 The antibacterial activity of copper modified Laponite® RD

In this investigation a minimal antibacterial action was observed in the copper incorporated Laponite® RD (Fig. 6.5) whereas a greater antibacterial activity was apparent in the copper-exchnaged Laponite® RD (Fig. 6.2). This was understandable, as the concentration of copper is the most important factor in bactericidal effect (Deever *et al.*, 1993). Ibrahim *et al.*, (2008) found that the presence of 50ppm of Cu^{2+} ions influenced the growth of *E. coli* O157:H7 and

thirty eight strains of *Salmonella* spp. reducing the population from 1.5 x 10^7 cfu ml^{-1} to 1.4 x 10^7 after 6 hours and from 2.7 x 10^7 to 2.0 x 10^7 cfu ml^{-1} after 12 hours with 1.0 x 10^3 bacterial population. The concentration of 50ppm Cu^{2+} was not lethal enough to inhibit the growth of *E. coli* and *Salmonella* spp. But, obtained significant bactericidal action with 100 and 200ppm within 6 hours of contact time, all at 37^{o}C (Ibrahim *et al*., 2008). In the present study, the 6ppm (Fig. 6.6(i)) and 17ppm (Fig. 6.3(i)) copper concentrations were below the lethal dose, only resulting in reduction in *E. coli* population from 1.35 x 10^8 cfu ml^{-1} to 3.33 x 10^5 cfu ml^{-1} (equivalent to (≈) 0.6 log cell reduction Fig. 6.5a) and 7.67 x 10^7 cfu ml^{-1} (≈0.3 log cell reduction Fig. 6.2a) after 6 hours contact time with 1.7 x 10^5 cfu ml^{-1} initial bacterial population.

However, the copper concentrations, 62ppm (CULAP4) and 75ppm (CULAP6) resulted in *E. coli* K12W-T (Fig. 6.3(i)) population decrease from 1.35 x 10^8 cfu ml^{-1} to 1.10 x 10^8 cfu ml^{-1} (≈0.4 log cell reduction, Fig. 6.2a) and 7.0 x 10^6 cfu ml^{-1} (≈1.29 log cell reduction, Fig. 6.2a) respectively in 6 hours contact time, with a starting population of 1.7 x 10^5 cfu ml^{-1} at 37^{o}C. Similarly, the 1.7 x 10^8 cfu ml^{-1} *S. aureus* population dercreased to 2.8 x 10^6 cfu ml^{-1} (≈1.78 log cell reduction Fig. 6.2b) and 7.6 x 10^5 cfu ml^{-1} (≈2.35 log cell reduction Fig. 6.2b) with 51ppm (CULAP4) and 65ppm (CULAP6) respectively (Fig. 6.3(ii)) with a starting population of 1.7 x 10^5 cfu ml^{-1}. Also, the *P. aeruginosa* population, 1.7 x 10^8 cfu ml^{-1} was reduced to 7.8 x 10^6 cfu ml^{-1} (≈1.4 log cell reduction Fig. 6.2c) and 6.8 x 10^5 cfu ml^{-1} (≈2.4 log cells reduction, Fig. 6.2c) respectively with 47ppm (CULAP4), and 64ppm (CULAP6), Fig. 6.3(v).

The starting bacterial population and strain may have played a role in the different inhibitory effects obtained. However, the result of this investigation showed that even the maximum 95ppm copper released was sub lethal after 72 hours (Table 6.1). But those of the literatures

cited suggest that ≥100ppm threshold Cu^{2+} concentration may exhibit significant inhibitory or bactericidal effect (Ibrahim *et al*., 2008; Nies, 1999). Due to variation in the *E. coli* strain employed, size of the nanoparticles and initial bacterial concentration, direct comparison between the studies is not feasible. Although, bactericidal activity was obtained in bacterial medium supplemented with $CuSO_4$ (Fig. 6.3(ii), (iv), (vi) and Fig. 6.6(ii), (iv), (vi)) but the release was abrupt hence, unsuitable for use in slow and sustained releasing systems. Overall these results show that copper modified Laponite® RD by ion exchange and isomorphous substitution exhibited antibacterial efficacy, an indication that it may be suitable for slow and sustained release systems. Copper modified Laponite® RD possesses attractive features and may be potentially applied in medical field for incorporation into medical devices.

6.3.2 The copper ions released from copper modified Laponite® RD

He *et al*., (2005) found three different possibilities of Cu^{2+} ion location in Cu^{2+} - adsorbed montmorillonite: Cu^{2+} ions replaced the original metal ions in the interlayer, Cu^{2+} ions moved into the hexagonal cavities of Si-O sheet, or a small quantity penetrated and was found at the octahedral vacancies. These assertions have been supported by the earlier experiments of Heller-Kallai and Mosser (1995). The heating of copper-montmorillonite caused the migration of Cu^{2+} ions into the hexagonal sites and during dehydroxylation the Cu^{2+} ions penetrated into the octahedral vacancies. These octahedral located Cu^{2+} ions may be more difficult to release than the interlayer Cu^{2+} ions. This acertion would need more research to confirm if octahedrally located Cu^{2+} ions are more difficult to release than interlayerly located Cu^{2+} ions.

Copper is an essential nutrient in many microorganisms, including bacteria, and enzyme-associated copper is a requirement for aerobic metabolism. But excess amounts of free copper

or its alloy often lead to cell toxicity; the 75ppm (CULAP4) and 95ppm (CULAP6) copper concentrations (Fig. 6.3(i)) showed toxicity by significantly reducing the cells population. This toxicity is induced when copper undergoes redox reactions alternating between Cu^{+1} and Cu^{2+} in the Fenton and Haber-Weiss reaction, leading to the generation of hydroxyl radicals and reactive oxygen intermediates (Quaranta *et al*., 2011). These hydroxyl radicals readily attack and damage cellular biomolecules (Santo *et al*., 2011), and the highly reactive oxygen intermediates cause lipid peroxidation and oxidation of protein leading to nucleic acid damage (Halliwell *et al*., 1990).

Copper also causes protein inactivation via disruption of Fe-S clusters in proteins such as cytoplasmic hydratases (Macomber and Imlay, 2009; Salhany *et al*., 1978; Christie and Costa, 1984; Sondossi *et al*., 1990, Nies, 1999). It has been well documented that heavy metals bind to thiols and other groups or protein molecules and in addition may replace naturally occurring metals in enzyme prosthetic groups (Sterritt and Lester, 1980). Damage to DNA has been reported although this has not been well proven (Tkeshelashvili *et al*., 1991). However, recent findings have shown that copper does have a significant toxicity effect on the DNA of bacteria by inappropriately binding to the purine and pyrimidine base pair leading to loss of function (Huh and Kwon, 2011).

Despite these studies and interesting results on the antimicrobial efficacy of copper and related copper compounds the mechanism by which these organisms are killed is still obscure (Quaranta *et al*., 2011). Some microorganisms, such as *E. coli*, have exhibited a variety of ways to prevent or resist copper toxicity, by developing extracellular supplementation with protective substances against the oxidative stress in the form of catalase, superoxide dismutase or by hydroxyl radical quencher (Santo *et al*., 2008). Since the copper persisted in

its antibacterial properties in the present study, against all the bacteria tested during the 72 hours duration, resistance to the copper modified Laponite® RD is unlikely.

Chapter 7

Overall Discussion and Conclusion

7.1 Overall discussion

7.1.1 Laponite® RD modification with silver and copper

Silver and copper are traditionally renowned antibacterial materials, having been known and used for centuries (Yoon *et al*., 2007). These metals have been incorporated into silicate materials for healthcare, food and the textile industry, and consumer products (Yoon *et al*., 2007).

An equivalent amount (at least approximately, unlike Michels *et al*. (2009) who compared 2.5% silver containing material with 99.9% copper alloy) of silver and copper were exchanged or incorporated with Laponite® RD using two methods to compare the antibacterial efficacy of both metals. The results suggested that while the silver was active the corresponding copper equivalent was relatively inactive, ie, silver exhibited greater antibacterial properties at lower concentrations than copper under the same conditions specified in this study. Image analysis showed that the silver nanoparticles (Fig. 3.13 and 3.21) were relatively smaller than the copper nanoparticles (Fig. 4.10 and 4.19), which further may have impacted on their antibacterial activity since, antibacterial activity was largely dependent on nanoparticles size as have also been found by Ruparelia *et al*. (2008); the smaller the nanoparticles the greater the antibacterial activity (Ruparelia *et al*., 2008).

7.1.2 Bactericidal effect of silver modified Laponite® RD and copper modified Laponite® RD

The comparison of inhibition zones showed that silver-exchanged Laponite® RD was more effective than the copper-exchanged Laponite® RD as demonstrated by the results in Fig 5.1 and 6.1. Similarly, silver incorporated Laponite® RD was more effective than copper

incorporated Laponite® RD (Fig. 5.5 and Section 6.2.1). The viable plate count method also illustrated the inhibitory effect of silver-Laponite® RD (Fig. 5.2 and 5.6) over copper-Laponite® RD (Fig. 6.2 and 6.5).

The fact that the synthesised particles were in nano sizes is significant for medical applications, as this feature offers an increased contact surface for the bacteria contact, and therefore enhanced suitability and application for medical devices as surface coating agents (Kim *et al*., 2007). Silver in nanoparticle form is of particular interest since it is more effective against bacteria than fungi and would be prescribed more for antibacterial rather than anti-fungal devices (Kim *et al*., 2007). Gram-positive bacteria were more susceptible to silver nanoparticles than gram-negative, due to differences in their cellular structures, principally the peptidoglycan (a polymer made up of amino acids and sugars that constitute the cell wall of bacteria) layer (Kim *et al*., 2007). However, the Sondi and Salopek-Sondi, 2004 result exhibited no strain specificity and was also supported by Panacek *et al*. (2006). In the present study, the strain specificity could not be established since the bacteria used exhibited differences in growth or increase in cell number with time in culture supplemented with silver-exchanged Laponite® RD when comapared with culture supplemented with copper-exchanged Laponite® RD ($P < 0.05$, Appendix 2A). Also, there was a significant difference in the increase in cell numbers between the culture supplemented with silver incoporated Laponite® RD and copper incorporated Laponite® RD ($P < 0.05$, Appendix 2B) which again eliminated ground for comparison.

Ruparelia *et al*. (2008) speculated that the nutrient media may have assisted the bactericidal action of Cu^{2+} by reacting with its constituent, and suggested that the greater significant

release of Cu^{2+} ions over Ag^{+} ions were probably due to presence of a copper oxide layer on the nanoparticulate copper, coupled with its reaction with chloride ions in the nutrient media. The attachment of silver ions, or nanoparticles has been reported by Lok *et al*. (2006), supported by Ruparelia *et al*. (2008), to cause cell wall rupture and accumulation of envelope protein precursors, resulting in dissipation of proton motive forces, destabilisation of the outer membrane, and rupture of the plasma membrane causing depletion of cellular ATP. Ruparelia *et al*. (2008) suggested a similar mode of bactericidal action of silver and copper nanoparticles and emphasise that molecules such as carbonyl groups on bacterial cell surfaces e.g. *B. subtilis,* possess an affinity for copper and are hence attracted to them. The copper ions subsequently released bind with DNA molecules leading to disorder of the helical structures via cross-linking within and between the nucleic acid strands. Once copper ions have gained entrance into the bacterial cell disruption of biochemical processes becomes apparent (Kim *et al*., 2000) even though the exact mechanism of action of the copper ions, or those of its nanoparticles, remain unknown (Stoh and Bagchi 1995, and Ruparelia *et al*., 2008), a similar mechanism of action was speculated for copper nanoparticles as for silver nanoparticles (Ruparelia *et al*., 2008).

7.1.3 Evaluation of efficacy of silver or copper ion-containing materials

The literature is replete with different ideas for the use of antimicrobial metal agents, with silver known to be most effective. Reports suggests that copper, within 2 hours was effective against bacteria (Michels *et al*., 2009), but lower silver concentrations presented total antimicrobial efficacies in minutes (Kwaye-awuah *et al*., 2008). Michels *et al.* (2009) tested silver antimicrobial activity using a Japanese standard which were unrepresentative: the Japanese standard employs a 24 hour test at 37^{o}C and 90% relative humidity; a plastic film is pressed over the samples to retain humidity which does not depict the atmospheric condition

found in the typical healthcare environment. Michels *et al.* (2009) accessed the antibacterial efficacy of silver- and copper-containing alloys; Ag-A containing 2.5% Ag (only the silver content of this proprietary was provided) and Ag-B containing 2.5% Ag, 8% Ni, 18% Cr, 74% Fe, five different copper alloys designated; C11000 with 99.9 weight % of Cu, C51000 (95% Cu, 5% Sn), C70600 (90% Cu, 10% Ni), C26000 (70% Cu, 30% Zn) and C75200 (65% Cu, 17% Zn, 18% Ni) .

The silver ion-containing materials exhibited >5 log reduction in MRSA viability after 24 hours under high humidity and high temperature conditions of >90% relative humidity (RH) and at 35^{o}C and 20 ^{o}C, but only a <0.3 log reduction at ~22% RH and 20 ^{o}C and no antibacterial efficacy was observed at ~22% RH and 35^{o}C under the JIS Z 2801 test conditions (Japanese standards association, 2000). The copper alloys however, demonstrated >5 log MRSA reductions under all the test conditions. This sort of comparison is non-classical (because it's a comparison of unequvalent quantities of silver and copper ions) as it would have been more of scientific interest if a 99.9% silver ion-containing alloy was involved (Michal *et al.,* 2009) and also the evaluation was restricted to only an indoor environment. Michels *et al.* (2009) attributed the silver antimicrobial performance to presence of excess moisture.

However, in the present investigation, closely similar quantities of silver-exchanged Laponite® RD (0.70, 1.25, 1.61, 1.76, 1.85, 2.35 wt.%) was compared with copper-exchanged Laponite® RD (0.69, 0.94, 1.23, 1.37, 1.82, 1.85 wt.%) and silver incorporated Laponite® RD (0.09, 0.58, 1.10 wt.%) compared with copper incorporated Laponite® RD (0.53 wt.%). These investigations were performed under conditions of ambient temperature, atmospheric relative humidity and near neutral pH. Under these conditions silver was discovered to be more active

antibacterially in comparison to copper. These findings, and those of others, have attested to the fact that silver even if present only in low quantity is capable of exhibiting bactericidal action against a broad spectrum of microorganisms (Silver, 2003; Inoue, *et al.,* 2002 and Kwakye-Awuah, *et al.,* 2008). The major discovery by Michels *et al.,* (2009) was that in a real life situation, typically an indoor environment (such as those found in controlled environment like hospital), copper presented the most desirable antimicrobial property and possesses the advantage of high activity at ambient temperature and relative humidity. TGA was performed to determine the stability of the silver- and copper-Laponite® RD over a wide range of temperatures and the associated water loss. Under the condition that this investigation was based, there was neither decomposition nor water loss of the silver- or copper-Laponite® RD at the ambient temperature range (approximately between 20 – 25^{o}C) which indicated that silver- or copper-Laponite® RD were stable at this temperature typical of indoor environment, and that with the same amount of water availability silver containing Laponite® RD was more antibacterially active than copper containing Laponite® RD.

Silver nanoparticles, due to their antimicrobial properties, are the most widely used in commercial products (Beer *et al*., 2012). In a report of materials specifically referenced in nanotechnology consumer products between 2005 and 2011 (Beer *et al*., 2012), the most common material mentioned in the product descriptions was silver: a total of 55.4%, followed by carbon 16.1%, titanium/titanium dioxide 10.4%, silica 7.6%, zinc/zinc oxide 5.5% and gold 5.0% (Rejeski, *et al*., 2012).

Ruparelia *et al.* (2008) compared the bactericidal effect of silver and copper nanoparticles of sizes 3 and 9 nm respectively based on the diameter of inhibition zones and the determination of minimum inhibitory concentration (MIC) and minimum bactericidal concestration (MBC)

in nutrient agar. Bacterial sensitivity to nanoparticles was found to vary depending on the microbial species. Silver nanoparticles displayed greater effectiveness for *E. coli* and *S. aureus* than the copper nanoparticles. While the MIC of silver nanoparticles for different *E. coli* strains; MTCC 443, MTCC 739, MTCC 1302 was 40, 180 and 120µg ml^{-1}, those for copper nanoparticles were 140, 220 and 200µg ml^{-1} respectively. The different strains of *S. aureus*; NCIM 2079, NCIM 5021, NCIM 5022, were 120 µg ml^{-1} and for copper nanoparticles were 140µg ml^{-1}. The MBC followed a similar trend. This further strenghten the finding of this piece of work that silver wether in the free or in composite form are more active antibacterially than copper in similar forms.

But in the case of *Bacillus subtilis* the reverse was the case, expressing an MIC of 20µg ml^{-1} and MBC of 40µg ml^{-1} for copper nanoparticles and 40µg ml^{-1} and 60µg ml^{-1} MIC and MBC respectively for silver nanoparticles. This observed difference was due to the affinity of copper towards amines and carboxyl groups present on the cell of *B. subtilis* (Ruparelia *et al.*, 2008; Moon and Peacock, 2011; Beveridge and Murray, 1980) and suggest that the bactericidal action of silver nanoparticles and those of copper nanoparticles may be strain specific. Therefore, the combination of silver and copper antibacterial nanocomposite may give rise to a more complete bactericidal effect against mixed bacterial population.

The possible source of discrepancy in the measurements (EDX and ICP-AES) is that, while the EDX data obtained for silver-exchanged Laponite RD (AGLAP1, AGLAP4 and AGLAP6) showed agreement with the values obtained form ICP-AES, the silver incorporated Laponite RD showed discrepancy. Greater amount of Ag was released than expected as seen from the EDX data Table 3.1- this may have been due to bulk Ag located on the surface of Laponite RD which may have remain bound after washing. It may also have been due to

nonhomogeneous nature of the samples since the triplicate experiments were performed on different days. In addition, EDX is a semi-quantitative method which can only measure samples to a depth of 10µm, wheras the lower detection limit for the ICP AES was 1 ppb. These reasons may also suffice for the discrepancy in the release of Cu^{2+} ions i.e. in Table 6.1 when compared to Table 4.1.

However, the differences in data that arise as a result of using these two separate analytical techniques that gave different measurement on similar Ag/Cu modified Laponite RD will form a good foundation to differentiate and identify differences between these techniques for Laponite RD analysis and may form bases for future work. Only limited publications have substituted Ag with Laponite RD and even fewer with Cu substitution. Therefore, further studies into the differences in the use of these analytical techniques will help to elucidate this area of research.

Although, the release of Cu^{2+} ions (obtained from ICP AES, Table 6.1) were higher than those obtained from EDX measurement in Table 4.1 however, the result of antimicrobial activity of Cu^{2+} ions showed agreement with findings of other authors in the literature cited. For instance, the 75ppm and 95ppm Cu^{2+} ions released significantly reduced the bacterial population without total inhibition as was also suggested by Ibrahim *et al*., 2008; Nies, 1999.

7.2 Toxicity of silver or copper.

Copper in pure or combined forms (brass or bronze) on surfaces are safe and long lasting. A voluntary risk assessment was conducted by the Italian Government's Istituto Superior di Sanita, Italy, while serving as the review country on behalf of the European Commission and EU Member States. The main conclusion of the assessment was that "the use of copper

products is, in general, safe for Europe's environment and the health of its citizens". Moreover, copper is one of the essential micronutrient needed by humans. It has been confirmed that an average adult needs 1 mg of copper every day to maintain good health to prevent a copper deficiency called osteoporosis and other chronic conditions involving bone, connective tissue, heart and blood vessels disorder (http://www.copperinfo.com/health/deficiencies.html).

The toxicity of silver has not been reported, and the only known side effect is argyra, a permanent discolouration of the skin (exhibiting a blue or grayish pigmentation) eyes and mucous membranes as a result of exposure to high levels of silver (Lide, 2001). Although these have been shown for the toxicity of silver, they are far higher than the levels or concentration used in this study which suggest that the product from this work can be used effectively without side effect such as toxicity, and in my opinion may be considered fit for safe use.

There has been a disagreement concerning the efficacy of metal antibacterial agents in the literature, some citing Ag and others Cu as the most potent metal agent. Factors and underlying conditions of reactivity, as well as dissolution potentials in the various media are critical factors for consideration before any meaningful judgement can be made as to whether these metals are used as elements or in a combined form, as macro or nanocomposite, with polymer or plastics, as metallic or ionic forms. These subtle questions need to be answered before accurate judgement on antimicrobial efficacy of these metals antibacterial agents can be ascertained.

7.3 Mode of action of antibacterial silver-Laponite® RD and copper-Laponite® RD

Although, antibacterial agents have been use to combat pathogens and antibiotic resistant bacteria, the literature is still unclear on their mechanism of action (Kwaye-awuah *et al*., 2008). The report of the literature concerning copper being used in single or free form on contact surfaces such as door handles, beds, screens and up to 99% application coating (Salgado *et al*, 2010; Santo, *et al.,* 2011) showed efficacy when applied alone as a metal in coating but the behaviour might be totally different if used in the combined or incorporated forms.

This investigation was quite different in that copper was incorporated with Laponite® RD and was then focussed on the slow release as well as the effective released amount that ultimately resulted in bactericidal activity. This makes comparison of our investigation with those of the literatures cited difficult. Those studies were primarily concerned with the use of metal antibacterial agents to combat microorganisms without attention to quantity and controlled availability. Furthermore, to overcome the potential challenge of the spread of antimicrobial resistance to metallic silver or copper, similar to what was observed immediately after the introduction of antibiotics (Santo *et al*., 2010). Therefore, this investigation examined controlled release capability, and monitored the release of silver/copper over a 72 hour period. Details on mechanism of action have been presented in Section 7.1.2.

7.4 Bacterial resistance to silver and copper.

The literature highlights instances of bacterial resistance genes. Chen *et al.,* (2009) reviewed the molecular mechanism of bacterial resistance, although the resistance to silver-Laponite® RD or copper-Laponite® RD were not determined in the present study. However, since the metal-Laponite® RD persisted in their antibacterial activity throughout the duration of the

study, resistance from the strains used were unlikely - more research will be needed to clearify this ascertion.

7.5 Overall conclusion

The syntheses of silver modified Laponite® RD and copper modified Laponite® RD have been confirmed. The silver- or copper-exchanged Laponite® RD produced by ion-exchange and the silver or copper incorporated Laponite® RD produced via isomorphous substitution were all characteristically different by the various analytical techniques; XRD, FTIR, EDX, TGA, ^{29}Si MAS MNR, SEM and TEM before use in the antibacterial investigation.

All the concentrations of the silver and copper modified Laponite® RD including $AgNO_3$ and $CuSO_4$ used, significantly reduced the growth of all the bacteria strains examined. While the release profiles of $AgNO_3$ and $CuSO_4$ were instantaneous. However, the silver and copper modified Laponite® RD nanocomposite exhibited a slow and consistent release of silver and copper ions in the TSB medium over the whole investigation period and released $\geq$ 1.9% and $\geq$ 17.7% of the total Ag^+ and Cu^{2+} ions content respectively, under the conditions specified in this study. This suggests perhaps that there was probably a slow and sustained release of the metal ions from the Laponite® RD sheet that consequently exerted effective antibacterial activity on all three bacteria strains used in this study. It is suggested that the adsorption of bacteria onto the silver- or copper-Laponite® RD from the TSB, followed by immobilisation on the Laponite® RD surface, resulted in a bactericidal or bacteriostatic effect (further work will be needed to clearify this ascertion). Furthermore, there was also the ionization of silver or copper nanoparticles producing the free ions in solution, causing a direct antibacterial effect. Hence, the attachment, penetration and impairment of cellular metabolic activities ultimately led to the cell death. Thus, silver or copper modified Laponite® RD demonstrated

features of slow release and can be potentially exploited in medicine for burns treatment and wound dressing.

7.6 Relevance of this study and potential application

Healthcare-associated infections (HCIs) continue to cause significant morbidity and mortality globally. With more than 1.4 million patients afflicted with HCI worldwide at any time (Pittet *et al.*, 2008; Pittet and Donaldson 2005); over 4 million people affected, resulting in approximately 37000 death in the Europe Union each year (Health Protection Agency (HPA), 2012a and HPA, 2012b); and over one-quarter of a million cases of HCIs occurring in England resulting in approximately 5000 deaths, costing the National Health Service (NHS) a billion pound per annum (Casey *et al*., 2010). It is estimated that 15 – 30% of all such infections could be prevented by better infection prevention and control practices (HPA, 2012a; HPA, 2012b; Casey *et al*., 2010; Pittet *et al.*, 2008; Pittet and Donaldson 2005). According to a recent report published by HPA, the prevalence of antimicrobial use was 34.7% in England last year (HPA, 2012a). These reports suggest that the use of antimicrobial agent is crucial in healthcare environments. The findings of this investigation clearly demonstrate that silver and copper modified Laponite® RD offer the potential to significantly reduce the number of microorganisms / bio burden in healthcare institutions. However, the use of these antimicrobial surface agents should be seen as a supplement to, not a substitute for, standard infection control practices. The fact that Laponite® RD can form a gel shows that silver/copper antimicrobials make for a good combination for example, in wound care for control of wound exudates. Metal nanoparticles offer unique opportunities in both hospital and transport to prevent the spread of infections, particularly since with the increase in air travel and greater desire for mobility in people, airborne, vector-borne, and zoonotic spread of infectious agents have become a major public health concern (Ren *et al.,* 2009).

7.7 Limitations of this study and future work

This investigation showed silver-Laponite® RD and copper-Laponite® RD challenged with *E. coli*, *S. aureus* and *P. aeruginosa* under similar conditions. The result may be different for different microorganisms under dissimilar conditions. The determination of the metal content of the Laponite® RD using EDX and ICP AES could not be reconciled as there was disparity in the measurement and the source could not be traced. However, this investigation can be a model for future investigation for other microorganisms. This study has provided the basis for investigating further the antibacterial efficacy of silver or copper modified Laponite® RD.

The correlation of incorporated metal particles on Laponite® RD with duration of activity would be better characteriased with TEM image analysis to gain greater understanding and insight into their similarities or differences. Activity of leachate will determine activity of cations versus nanoparticles therefore; strigent synthesis procedure is necessary to avoid excess or loosely bound Ag^+ ions in the isomorphously produced silver- Laponite® RD by sufficient washing with NaCl solution before the antibacterial activity testing. Also, necessary is the reworking to get same amount of $AgNO_3$ and silver incorporated Laponite® RD to accurately compare and distinquish them in their antibacterial efficacy. The characterisation of the silver- or copper-Laponite® RD after the antibacterial testing will help to determine the amount of silver or copper remaining in the Laponite® RD matrix after the antibacterial testing and it is important to use only one analytical technique for the characterisation such as ICP AES throughtout the characterisation period both before and after the antibacterial experiments. Studies on the antibacterial mechanism should be explored to find out if antimicrobial activity with Laponite® RD is novel or similar to what the literature have already suggested.

It is suggested that the understanding of the metal-Laponite® RD antibacterial agent will provide solution to combat antibacterial resistance. The location of the silver or copper ions in the bacterial cell can be identified with TEM. Given the growing attention being paid to natural antibacterial agents, which may be more readily accepted by consumers (Ibrahim *et al*., 2008), it would be beneficial to explore the possibility of combining metal antibacterial agents synergistically to obtain a better and more cost efficient reduction of pathogenic bacteria.

References

Abolino, O., Aceto, M., Malandrino, M., Sarzanini, C and Mentasti, E (2003) Adsorption of heavy metals on Na-montmorillonite. Effect of pH and organic substances. *Water Research*, **37**, pp.619–1627.

Abou El-Nour, K.M.M., Eftaiha, A.a., Al-Warthan, A. and Ammar, R.A.A. (2010) Synthesis and applications of silver nanoparticles. *Arabian Journal of Chemistry*, **3**(3), pp.135-140.

Aceman, S., Lahav, N. and Yariv, S. (1997) XRD study of the dehydration and rehydration behaviour of Al-pillared smectites differing in source of charge. *Journal of Thermal Analysis and Calorimetry*, **50**(1), pp.241-256.

Aceman, S., Lahav, N. and Yariv, S. (2000) A thermo-XRD study of Al-pillared smectites differing in source of charge, obtained in dialyzed, non-dialyzed and washed systems. *Applied Clay Science*, **17**(3-4), pp.99-126.

Adak, A., Bandyopadhyay, M. and Pal, A. (2005) Removal of crystal violet dye from wastewater by surfactant-modified alumina. *Separation and Purification Technology*, **44**(2), pp.139-144.

Adak, A., Bandyopadhyay, M. and Pal, A. (2006) Fixed bed column study for the removal of crystal violet (C. I. Basic Violet 3) dye from aquatic environment by surfactant-modified alumina. *Dyes and Pigments*, **69**(3), pp.245-251.

Adamis, Z., Fodor, J and Williams R. B (2005) World Health Organization Publication. *Bentonite, kaolin, and selected clay minerals, Environmental health criteria ; 231*, [online]. [Accessed on 9 November 2011]. Available at [http://www.inchem.org/documents/ehc/ehc/ehc231.htm#ref].

Adams, J.M., McCabe, R.W., Faïza Bergaya, B.K.G.T. and Gerhard, L. (2006) Chapter 10.2 Clay Minerals as Catalysts. *in Developments in Clay Science.* Elsevier, pp.541-581.

Aguzzi, C., Viseras, C., Garcés, A., Cruz, J., Cerezo, P., Ferrari, P and Caramella, C (2003) Development of new controlled release systems based on mineral supports: I. Sorption behaviour of tetrcyclines onto a pharmaceutical grade silicate. *Proc. 1st EUFEPS Conference on Optimising drug delivery and formulation: new challenges in drug delivery. Versailles (F), September 29-October 1*, pp. 132 - 133.

Aguzzi, C., Cerezo, P., Viseras, C. and Caramella, C. (2007) Use of clays as drug delivery systems: Possibilities and limitations. *Applied Clay Science*, **36**(1-3), pp.22-36.

Aihara, N., Torigoe, K. and Esumi, K. (1998) Preparation and Characterization of Gold and Silver Nanoparticles in Layered Laponite Suspensions. *Langmuir*, **14**(17), pp.4945-4949.

Al-Degs, Y., Khraisheh, M.A.M., Allen, S.J. and Ahmad, M.N. (2000) Effect of carbon surface chemistry on the removal of reactive dyes from textile effluent. *Water Research*, **34**(3), pp.927-935.

Al-Degs, Y., Khraisheh, M.A.M., Allen, S.J. and Ahmad, M.N.A. (2001) Sorption behavior of cationic and anionic dyes from aqueous solution on different types of activated carbons. *Separation Science and Technology*, **36**(1), pp.91 - 102.

Alexandre, M. and Dubois, P. (2000) Polymer-layered silicate nanocomposites: preparation, properties and uses of a new class of materials. *Materials Science and Engineering: Reports*, **28**(1-2), pp.1-63.

Al-Gohary, O., Lyall, J and Murray, J.B (1987) Adsorption of antihypertensives by suspensoids. Part 1. Adsorption of propranolol hydrochloride by attapulgite, charcoal, kaolin and magnesium trisilicate. *Pharm. Acta Helv*, **62**(3), pp. 66-72.

Al-Gohary, O., Lyall, J and Murray, J.B (1988) Adsorption of antihypertensives by suspensoids. Part 2. The adsorption of acebutolol, metoprolol, nadolol, oxprenolol and timolol by attapulgite, charcoal, kaolin and magnesium trisilicate. *Pharm. Acta Helv.*, **63**(1), pp. 13-18

Almeida, C. E, Galhardo, R. S, Felício, D. L, Cabral-Neto, J. B, Leitão, A. C. (2000) Copper ions mediate the lethality induced by hydrogen peroxide in low iron conditions in Escherichia coli. *Mutat Res.* **460**(1), pp.61-67.

Alpat, S.K., Özbayrak, Ö., Alpat, S. and Akçay, H. (2008) The adsorption kinetics and removal of cationic dye, Toluidine Blue O, from aqueous solution with Turkish zeolite. *Journal of Hazardous Materials*, **151**(1), pp.213-220.

Alt, J.C. (1988) Hydrothermal oxide and nontronite deposits on seamounts in the eastern Pacific. *Marine Geology*, **81**(1-4), pp.227-239.

Andersen, C. (2003) Channel-tunnels: outer membrane components of type I secretion systems and multidrug efflux pumps of Gram-negative bacteria. *Rev. Physiol. Biochem. Pharmacol.* **147**, pp.122-65.

Andreoli, C.Y., Robert, M. and Pons, C.H. (1989) First steps of smectite-illite transformation with humectation and desiccation cycles. *Applied Clay Science*, **4**(5-6), pp.423-435.

Anonymous (2006) *Comparing antimicrobial efficacy of copper and silver for interior touch surface applications* [online]. [Accessed on 9 November 2011]. Available at <http://www.antimicrobialcopper.com/media/70878/pub-200-comparing-antimicrobial-efficacy-copper-silver.pdf >

Appendini, P. and Hotchkiss, J. H. (2002) Review of antimicrobial food packaging. *Innovative Food Science & Emerging Technologies*, **3**(2), pp.113-126.

Arantes, T. M., Pinto, A. H., Leite, E. R., Longo, E. and Camargo, E. R. (2012) Synthesis and optimization of colloidal silica nanoparticles and their functionalization with methacrylic acid. *Colloids and Surfaces A: Physicochemical and Engineering Aspects*, **415**, pp.209-217.

Aray, Y., Marquez, M., Rodriguez, J., Coll, S., Simon-Manso, Y., Gonzalez, C. and Weitz, D.A. (2003) Electrostatics for exploring the nature of water adsorption on the Laponite sheets' surface. *The Journal of Physical Chemistry B*, **107**(34), pp.8946-8952.

Armstrong, N. C and Clarke, D (1973) Influence of solution electrolyte content and dielectric constant on drug adsorption by kaolin,. *J. Pharm. Sci. ,* **62,** pp. 379 - 382.

Atiyeh, B. S. Costagliola, M. Hayek, S. N and Dibo, S.A (2007) Effect of silver on burn wound infection control and healing: review of the literature. *Burn*, **33**, pp. 139–148

Avery, R.G. and Ramsay, J.D.F. (1986) Colloidal properties of synthetic hectorite clay dispersions : II. Light and small angle neutron scattering. *Journal of Colloid and Interface Science*, **109**(2), pp.448-454.

Avery, S. V., Howlett, N. G and Radice, S. (1996) Copper toxicity towards *Saccharomyces cerevisiae*: dependence on plasma membrane fatty acid composition. *Appl Environ Microbiol.* **62**(11), pp. 3960–3966.

Avery, S. V., Lloyd, D., Harwood, J. L (1995) Temperature-dependent changes in plasma-membrane lipid order and the phagocytotic activity of the amoeba *Acanthamoeba castellanii* are closely correlated. *Biochem J*. **312**(3), pp.811–816.

Axon, S. A., Huddersman, K and Klinowski, J (1990) Gallium EXAFS and solid-state NMR studies of Ga-substituted MFI-type zeolites. *Chemical Physics Letters*, **172**, pp. 398-404.

Bador, K (1965) Organ deposition of silver following silver nitrate therapy for burns. *PRS*, **37**, p. 550

Baek, S., Kim, J., Ihm, S., E. van Steen, M.C. and Callanan, L.H. (2004) Design of metal loaded zeolites as dual functional adsorbent/catalyst system for VOC control. *Studies in Surface Science and Catalysis*, **154**(3), pp.2458-2466.

Baek, S.-W., Kim, J.-R. and Ihm, S.-K. (2004) Design of dual functional adsorbent/catalyst system for the control of VOC's by using metal-loaded hydrophobic Y-zeolites. *Catalysis Today*, **93-95**, pp.575-581.

Bailey, S.W. (1980) Summary of recommendations of AIPEA nomenclature committee on clay minerals *American Mineralogist*, **65**, pp.1-7.

Baird, J. C, Walz, J. Y (2006) The effects of added nanoparticles on aqueous kaolinite suspensions I. Structural effects. *Journal of Colloid and Interface Science*, **297**, pp.161–169.

Beer, C., Foldbjerg, R., Hayashi, Y., Sutherland, D. S. and Autrup, H. (2012) Toxicity of silver nanoparticles: Nanoparticle or silver ion? *Toxicology Letters*, **208**(3), pp.286-292.

Bekkum, H. V (2001) Chapter 7 Clays: from two to three dimensions. *Introduction to Zeolite Science and Practice*, Elsevier pp. 320.

Bergaya, F., Hassoun, N., Gatineau, L., Barrault, J., G. Poncelet, P.A and Delmon, B. (1991) Mixed Al-Fe Pillared Laponites: Preparation, Characterization and Catalytic Properties in Syngas Conversion. *Studies in Surface Science and Catalysis.* Elsevier, pp.329-336.

Bergaya, F. and Lagaly, G. (2001) Surface modification of clay minerals. *Applied Clay Science*, **19**(1-6), pp.1-3.

Bergaya, F., Lagaly, G., Faïza Bergaya, B.K.G.T. and Gerhard, L. (2006) Chapter 1 General Introduction: Clays, Clay Minerals, and Clay Science. *in Developments in Clay Science.* Elsevier, pp.1-18.

Bergaya, F. and Vayer, M. (1997) CEC of clays: Measurement by adsorption of a copper ethylenediamine complex. *Applied Clay Science*, **12**(3), pp.275-280.

Bergaya, F., Hassoun, N., Barrault, J and Gatineau, L (1993) Pillaring of synthestic hectorite by mixed [Al_{13-x} Fe_x] pillars. *Clay minerals,* **28** pp. 109-122.

Beveridge, T.J. Murray, R.G.E. (1980) Sites of metal deposition in the cell wall of Bacillus subtilis. *J Bacteriol*, **141**, pp. 876–887

Bhatia, S., Abdullah, A.Z. and Wong, C.T. (2009) Adsorption of butyl acetate in air over silver-loaded Y and ZSM-5 zeolites: Experimental and modelling studies. *Journal of Hazardous Materials*, **163**(1), pp.73-81.

Bian, S.W., Mudunkotuwa, I.A., Rupasinghe, T., Grassian, V.H (2011) Aggregation and dissolution of 4 nm ZnO nanoparticles in aqueous environments: influence of pH, ionic strength, size, and adsorption of humic acid. *Langmuir* **27**, pp.6059–6068.

Biesta-Peters, E.G., Mols, M., Reij, M.W. and Abee, T. (2011) Physiological parameters of Bacillus cereus marking the end of acid-induced lag phases. *International Journal of Food Microbiology*, **148**(1), pp.42-47.

Bobu, M., Yediler, A., Siminiceanu, I. and Schulte-Hostede, S. (2008) Degradation studies of ciprofloxacin on a pillared iron catalyst. *Applied Catalysis B: Environmental*, **83**(1-2), pp.15-23.

Borkow, G and Gabbay, J. (2005) Copper as a biocidal tool. *Curr Med Chem*. **12**(18), pp.2163-2175.

Boyle-Vavra, S and Daum, R.S (2007) Community-acquired methicillin-resistant Staphylococcus aureus: the role of Panton-Valentine leukocidin. *Lab Invest*, **87**, pp. 3–9

Bragg, P. D., Rainnie, D. J. (1974) The effect of silver ion on the respiratory chain of *Escherichia coli*. *Can J Microbiol*, **20**, pp. 883–889.

Breu, J., Seidl, W. and Stoll, A. (2003) Fehlordnung bei Smectiten in Abhängigkeit vom Zwischenschichtkation. *Zeitschrift für anorganische und allgemeine Chemie*, **629**(3), pp.503-515.

Brian E. Viani, C.B.R., and Philip F. Low (1985) Direct Measurement of the Relation Between Swelling Pressure and Interlayer Distance in Li-Vermiculite 1. *Clays and Clay Minerals*, **33**(3), pp.244-250.

Brigatti, M.F., Colonna, S., Malferrari, D. and Medici, L. (2004) Characterization of Cu-complexes in smectite with different layer charge location: chemical, thermal and EXAFS studies. *Geochimica et Cosmochimica Acta*, **68**(4), pp.781-788.

Browne, J.E., Feldkamp, J. R. White, J. L. Hem, S. L (1980) Characterization and adsorptive properties of pharmaceutical grade clays. *Journal of Pharmaceutical Sciences*, **69**(7), pp.816-823.

Brühwiler, D. and Calzaferri, G. (2004) Molecular sieves as host materials for supramolecular organization. *Microporous and Mesoporous Materials*, **72**(1-3), pp.1-23.

Bujdak, J., Hackett, E. and Giannelis, E.P. (2000) Effect of Layer Charge on the Intercalation of Poly(ethylene oxide) in Layered Silicates: Implications on Nanocomposite Polymer Electrolytes. *Chemistry of Materials*, **12**(8), pp.2168-2174.

Buonocore, G., Perrone, S. and Tataranno, M. L (2010) Oxygen toxicity: chemistry and biology of reactive oxygen species. *Seminars in Fetal and Neonatal Medicine*, **15**, pp.186-190.

Burch, R. (1988) Introduction. *Catalysis Today*, **2**, pp.185 - 186.

Burch, R. and Warburton, C.I. (1987) Pillared clays as demetallisation catalysts. *Applied Catalysis*, **33**(2), pp.395-404.

Callaghan, I.C., and Ottewill, R. H., (1974) Interparticle forces in montmorillonite gels. *Faraday Discuss. Chem. Soc.*, **57**, pp.110 - 118.

Calzaferri, G., Bossart, O., Brühwiler, D., Huber, S., Leiggener, C., Van Veen, M.K. and Ruiz, A.Z. (2006) Light-harvesting host-guest antenna materials for quantum solar energy conversion devices. *Comptes Rendus Chimie*, **9**(2), pp.214-225.

Cao, X., Cheng, C., Ma, Y. and Zhao, C. (2010) Preparation of silver nanoparticles with antimicrobial activities and the researches of their biocompatibilities. *Journal of Materials Science: Materials in Medicine*, **21**(10), pp.2861-2868.

Carrado, K.A. (2000) Synthetic organo- and polymer-clays: preparation, characterization, and materials applications. *Applied Clay Science*, **17**(1-2), pp.1-23.

Carrado, K.A., Kostapapas, A., Suib, S.L. and Coughlin, R.W. (1986) Physical and chemical stabilities of pillared clays containing transition metal ions. *Solid State Ionics*, **22**(1), pp.117-125.

Carretero, M. and Lagaly, G. (2007) Clays and health: An introduction. *Applied Clay Science*, **36**(1-3), pp.1-3.

Carrott, P.J.M., Carrott, M.M.L.R.i.b.e.i.r.o., Mour, atilde, o, P.A.M. and Lima, R.P. (2003) Preparation of Activated Carbons from Cork by Physical Activation in Carbon Dioxide. *Adsorption Science and Technology*, **21**, pp.669-681.

Casey, A.L., Adams, D., Karpanen, T.J., Lambert, P.A., Cookson, B.D., Nightingale, P., Miruszenko, L., Shillam, R., Christian, P. and Elliott, T.S.J. (2010) Role of copper in reducing hospital environment contamination. *Journal of Hospital Infection*, **74**(1), pp.72-77.

Catlow, C. R. A., George, A. R and Freeman C. M (1996) Ab initio and molecular-mechanics studies of aluminosilicate fragments, and the origin of lowenstein's rule. *Chemical communications*. **11**, pp. 1311-1312.

Celis, R., HermosIn, M.C. and Cornejo, J. (2000) Heavy Metal Adsorption by Functionalized Clays. *Environmental Science & Technology*, **34**(21), pp.4593-4599.

Cervantes, C., Gutierrez-Corona, F. (1994) Copper resistance mechanisms in bacteria and fungi. *FEMS Microbiol. Rev*. **14**(2), pp.121-37

Chambers, H. F and Deleo, F. R (2009) Waves of resistance: *Staphylococcus aureus* in the antibiotic era. *Nat Rev Microbiol*, **7**, pp. 629–641

Chatterjee, M., Iwasaki, T., Onodera, Y., Hayashi, H., Ikushima, Y., Nagase, T., Ebina, T (2004) Hydrothermal synthesis and characterization of copper containing crystalline silicate mesoporous materials from gel mixture. *Applied Clay Science.* **25**(3–4), pp.195–205.

Chazeau, L, Cavaille, J. Y and Terech, P (1999) Mechanical behaviour above Tg of a plastcised PVC reinforced with cellolose whiskers; a SANS structural study. *Polymer.* **40**, pp. 5333-5344.

Chen, L.F., Chopra, T. and Kaye, K.S. (2009) Pathogens Resistant to Antibacterial Agents. *Infectious Disease Clinics of North America*, **23**(4), pp.817-845.

Chien, Y. W and Lin, A. S (2002) Drug delivery-controlled release. In: J. Swarbrick and J.C. Boylan, Editors (Second Edition), *Encyclopedia of Pharmaceutical Technology vol. 1*. Marcel Dekker Inc.

Choi, O and Hu, Z (2008) Size Dependent and reactive oxygen species related nanosilver toxicity to nitrifying bacteria. *Environmental Science & Technology*, **42**, pp. 4583-4588.

Choy, J. H., Jung, J. S., Oh, J. M., Park, M., Jeong, J., Kang, Y. K. and Han, O. J (2004) Layered double hydroxide as an efficient drug reservoir for folate derivatives. *Biomaterials*, **25**(15), pp.3059-3064.

Choy, J.-H., Kwak, S.-Y., Park, J.-S., Jeong, Y.-J. and Portier, J. (1999) Intercalative Nanohybrids of Nucleoside Monophosphates and DNA in Layered Metal Hydroxide. *Journal of the American Chemical Society*, **121**(6), pp.1399-1400.

Choy, J. H., Kwak, S. Y., Jeong Y. J and Park, J. S (2000) Inorganic layered double hydroxides as nonviral vectors. *Angew. Chem. Int Ed.* **39**(22), pp.4041-4045.

Chua, K. Laurent, F. Coombs, G. Grayson M.L., Howden B.P (2011) Antimicrobial resistance: not community-associated methicillin-resistant *Staphylococcus aureus* (CA-MRSA) A clinician's guide to community MRSA – its evolving antimicrobial resistance and implications for therapy. *Clin Infect Dis*, **52**, pp. 99–114

Churchman, G.J., Gates, W.P., Theng, B.K.G., Yuan, G., Faïza Bergaya, B.K.G.T. and Gerhard, L. (2006) Chapter 11.1 Clays and Clay Minerals for Pollution Control. *in Developments in Clay Science.* Elsevier, pp.625-675.

Clausen, P., Watzke, B., Hughes, E., Plummer, C.J.G. and Månson, J.A.E. (2011) Evaporation kinetics of volatile liquids and release kinetics of water from a smectite clay: Comparison between experiments and finite element calculations. *International Journal of Engineering Science*, **49**(10), pp.1125-1140.

Coche-Guérente, L., Cosnier, S., Desprez, V., Labbé, P. and Petridis, D. (1996) Organosilasesquioxane-laponite clay sols: a versatile approach for electrode surface modification. *Journal of Electroanalytical Chemistry*, **401**(1-2), pp.253-256.

Concordia Analytical Instrument Laboratory (2012) Simultaneous determination of manganese and nickel in steel by inductively coupled plasma atomic emission spectrometry. *Analytical chemistry manual.* Concordia college, Moorhead, Minnesota. [Accessed 14 March 2012]. Available at <http://www.cord.edu/dept/chemistry/analyticallabmanual/experiments/icpaes/ intro.html>.

Cook, N. (1998) Methicillin-resistant *Staphylococcus aureus* versus the burn patient. *Burns*, **24**(2), pp.91-98.

Cool, P. and Vansant, E.F. (1996) Preparation and characterization of zirconium pillared laponite and hectorite. *Microporous Materials*, **6**(1), pp.27-36.

Corker, J.M., Evans, J. and Rummey, J.M. (1991) EXAFS studies of pillared clay catalysts. *Materials Chemistry and Physics*, **29**(1-4), pp.201-209.

Cormia, R. (2011) NANO53 Nanocharactarisation. *Transmission electron microscopy* [online]. [Accessed on 12 November 2011]. Available at <http://fgamedia.org/faculty/rdcormia/NANO53/TEM.htm>

Cornelis, A. and Laszlo, P. (1985) Clay-supported copper(ii) and iron(iii) nitrates: novel multi-purpose reagents for organic synthesis. *Synthesis*, **1985**(10), pp.909-918.

Craig, N.C., Chen, A., Suh, K.H., Klee, S., Mellau, G.C., Winnewisser, B.P. and Winnewisser, M. (1997) Contribution to the study of the Gauche effect. The complete structure of the anti rotamer of 1,2-difluoroethane. *Journal of the American Chemical Society*, **119**(20), pp.4789-4790.

Çulfaz, M. and YagIz, M. (2004) Ion exchange properties of natural clinoptilolite: lead-sodium and cadmium-sodium equilibria. *Separation and Purification Technology*, **37**(2), pp.93-105.

Cummins, H.Z. (2007) Liquid, glass, gel: The phases of colloidal Laponite. *Journal of Non-Crystalline Solids*, **353**(41-43), pp.3891-3905.

Cuny, C., Friedrich, A., Kozytska, S., Layer, F., Nübel, U., Ohlsen, K., Strommenger, B., Walther, B., Wieler, L. and Witte, W. (2010) Emergence of methicillin-resistant *Staphylococcus aureus* (MRSA) in different animal species. *International Journal of Medical Microbiology*, **300**(2-3), pp.109-117.

Dag, O., Samarskaya, O., Coombs, N and Geoffrey A. O (2003) The synthesis of mesostructured silica films and monoliths functionalised by noble metal nanoparticles. *J. Mater. Chem*, **13**, pp.328 - 334.

Dallas, P., Sharma, V.K. and Zboril, R. (2011) Silver polymeric nanocomposites as advanced antimicrobial agents: Classification, synthetic paths, applications, and perspectives. *Advances in Colloid and Interface Science*, **166**(1-2), pp.119-135.

Daniel, L.M., Frost, R.L. and Zhu, H.Y. (2007) Synthesis and characterisation of clay-supported titania photocatalysts. *Journal of Colloid and Interface Science*, **316**(1), pp.72-79.

Daniel, L.M., Frost, R.L. and Zhu, H.Y. (2008) Edge-modification of laponite with dimethyl-octylmethoxysilane. *Journal of Colloid and Interface Science*, **321**(2), pp.302-309.

D'Arezzo, S., Lanini, S., Puro, V., Ippolito, G and Visca P (2012) High-level tolerance to triclosan may play a role in *Pseudomonas aeruginosa* antibiotic resistance in immunocompromised hosts: evidence from outbreak investigation. *BMC Research Notes*, **5**, p. 43

David, A.E., Zhongbao, L. and Richard, G.L. (1994) Surfactant Solubilization of Organic Compounds in Soil/Aqueous Systems. *Journal of Environmental Engineering*, **120**(1), pp.5-22.

David, M.Z and Daum, R.S (2010) Community-associated methicillin-resistant *Staphylococcus aureus*: epidemiology and clinical consequences of an emerging epidemic. *Clin Microbiol Rev*, **23**, pp. 616–687

de la Rosa-Gómez, I., Olguín, M.T. and Alcántara, D. (2008) Antibacterial behavior of silver-modified clinoptilolite-heulandite rich tuff on coliform microorganisms from wastewater in a column system. *Journal of Environmental Management*, **88**(4), pp.853-863.

de Mello, F. G. A., Ciminelli, V.S.T. and Vasconcelos, W.L. (2009) Smectite organofunctionalized with thiol groups for adsorption of heavy metal ions. *Applied Clay Science*, **42**(3-4), pp.410-414.

de Paiva, L.B., Morales, A.R. and Valenzuela Díaz, F.R. (2008) Organoclays: Properties, preparation and applications. *Applied Clay Science*, **42**(1-2), pp.8-24.

Dekov, V.M., Kamenov, G.D., Stummeyer, J., Thiry, M., Savelli, C., Shanks, W.C., Fortin, D., Kuzmann, E. and Vértes, A. (2007) Hydrothermal nontronite formation at Eolo Seamount (Aeolian volcanic arc, Tyrrhenian Sea). *Chemical Geology*, **245**(1-2), pp.103-119.

Deveer, I., Wilde, K and Ruden, H (1993) Bacericide qualities of materials containing and not containing copper. *Zentralblatt für Hygiene und Umweltmedizin*, **195**, pp. 66–87

DiGiano, F.A and Natter, A.S (1977) Disperse dye carrier interactions on activated carbon. *Journal of the Water Pollution Control Federation*, **49**(2), pp.235-244.

Ding, Z. and Frost, R.L. (2002) Controlled rate thermal analysis of nontronite. *Thermochimica Acta*, **389**(1-2), pp.185-193.

Dowjat, W. K., Kharatishvili, M., Costa, M. (1996) DNA and RNA strand scission by copper, zinc and manganese superoxide dismutases. *Biometals* **9**(4), pp.327-35.

Dunn S and Jones P (2004) The measurement of ferroelectric thin films using piezo force microscopy. *Nsti Nanotechnology Conference and Trade Show - Nsti Nanotech.* **3**, pp.362-365.

Duval, F.P., Porion, P., Faugère, A.M. and Van Damme, H. (2001) An NMR investigation of water self-diffusion and relaxation rates in controlled ionic strength laponite sols and gels. *Journal of Colloid and Interface Science*, **242**(2), pp.319-326.

Edwards, D.A., Liu, Z. and Luthy, R.G. (1994) Surfactant solubilization of organic compounds in soil/aqueous systems. *Journal of Environmental Engineering*, **120**(1), pp.5-22.

Egger, S., Lehmann, R.P., Height, M.J., Loessner, M.J. and Schuppler, M. (2009) Antimicrobial properties of a novel silver-silica nanocomposite material. *Appl. Environ. Microbiol.*, **75**(9) pp. 2973-2976

Espirito Santo, C., N. Taudte, D. H. Nies, and G. Grass. 2008. Contribution of copper ion resistance to survival of *Escherichia coli* on metallic copper surfaces. *Appl. Environ. Microbiol*. **74,** pp.977–986.

Esumi, K., Yoshida, K., Torigoe, K. and Koide, Y. (1999) Sorption of 2-naphthol and copper ions by cationic surfactant-adsorbed laponite. *Colloids and Surfaces A: Physicochemical and Engineering Aspects*, **160**(3), pp.247-250.

Everett, T. (2011) Mr Everett's web page. *Copper* [online]. [Accessed 20 August 2011]. Available at: <http://www.mrteverett.com/Chemistry/pdictable/q_elements.asp?Symbol=Cu>

Faucheu, J., Gauthier, C., Chazeau, L., Cavaillé, J.-Y., Mellon, V. and Lami, E.B. (2010) Miniemulsion polymerization for synthesis of structured clay/polymer nanocomposites: Short review and recent advances. *Polymer*, **51**(1), pp.6-17.

Faundez, G., Troncoso, M., Navarrete, P., Figueroa, G. (2004) Antimicrobial activity of copper surfaces against suspensions of *Salmonella enterica* and *Campylobacter jejuni. BMC Microbiol.* **4**, pp.19.

Favier B, LeMaoult J, Rouas-Freiss N, Moreau P, Menier C, Carosella E. D. Research on HLA-G: an update. *Tissue Antigens.* **69**(3),pp.207-211.

Fayaz, A.M., Balaji, K., Girilal, M., Yadav, R., Kalaichelvan, P.T. and Venketesan, R. (2010) Biogenic synthesis of silver nanoparticles and their synergistic effect with antibiotics: a study against gram-positive and gram-negative bacteria. *Nanomedicine: Nanotechnology, Biology and Medicine*, **6**(1), pp.103-109.

Feng, Q.L., Wu, J., Chen, G.Q., Cui, F.Z., Kim, T.N. and Kim, J.O. (2000) A mechanistic study of the antibacterial effect of silver ions on *Escherichia coli* and *Staphylococcus aureus*. *Journal of Biomedical Materials Research*, **52**(4), pp.662-668.

Fernandez-Perez, M., Villafranca-Sanchez, M., Gonzalez-Pradas, E. and Flores-Cespedes, F. (1999) Controlled release of diuron from an alginate; bentonite formulation: water release kinetics and soil mobility study. *Journal of Agricultural and Food Chemistry*, **47**(2), pp.791-798.

Fernandez-Perez, M., Villafranca-Sanchez, M., Gonzalez-Pradas, E., Martinez-Lopez, F. and Flores-Cespedes, F. (2000) Controlled Release of Carbofuran from an alginate; Bentonite Formulation: Water Release Kinetics and Soil Mobility. *Journal of Agricultural and Food Chemistry*, **48**(3), pp.938-943.

Figueroa, R.A., Leonard, A. and MacKay, A.A. (2004) Modeling Tetracycline Antibiotic Sorption to Clays. *Environmental Science & Technology*, **38**(2), pp.476-483.

Fonseca, M.G. and Airoldi, C. (2000) Mercaptopropyl magnesium phyllosilicate thermodynamic data on the interaction with divalent cations in aqueous solution. *Thermochimica Acta*, **359**(1), pp.1-9.

Fox, C.L and Modak, S.M. (1974) Mechanism of silver sulfadiazine action on burn wound infections. *Antimicrob Agents Chemother*, **5** (6), pp. 582–588

Francois, K., Devlieghere, F., Standaert, A.R., Geeraerd, A.H., Van Impe, J.F. and Debevere, J. (2006) Effect of environmental parameters (temperature, pH and aw) on the individual cell lag phase and generation time of *Listeria monocytogenes*. *International Journal of Food Microbiology*, **108**(3), pp.326-335.

Franke, S., Grass, G., Rensing, C., Nies, D. H. (2003) Molecular analysis of the copper-transporting efflux system CusCFBA of *Escherichia coli. J Bacteriol*. **185**(13), pp.3804-12.

Frost, R.L. and Kloprogge, J.T. (2000) Vibrational spectroscopy of ferruginous smectite and nontronite. *Spectrochimica Acta Part A: Molecular and Biomolecular Spectroscopy*, **56**(11), pp.2177-2189.

Furukawa, Y. and O'Reilly, S.E. (2007) Rapid precipitation of amorphous silica in experimental systems with nontronite (NAu-1) and Shewanella oneidensis MR-1. *Geochimica et Cosmochimica Acta*, **71**(2), pp.363-377.

Gardener, J and Jaye, E (2011) Bioscreen C. *Automated microbiology growth curve analysis system* [online]. [accessed on 13 November 2011]. Available at < http://www.growthcurvesusa.com/description.html >

Geierstanger BH, Kagawa TF, Chen SL, Quigley GJ, Ho PS. (1991) Base-specific binding of copper(II) to Z-DNA. The 1.3-A single crystal structure of d(m5CGUAm5CG) in the presence of CuCl2. *J. Biol Chem*. **266**(30) pp.20185-91.

Gieseking, J.E. (1939) The mechanism of cation exchange in the montmorillonite-beidellite-nontronite type of clay minerals. *Soil Science*, **47**(1), pp.1-14.

Gil, A., GandÃ-a, L.M. and Vicente, M.A. (2000) Recent advances in the synthesis and catalytic applications of pillared clays. *Catalysis Reviews*, **42**(1), pp.145 - 212.

Gong, P. Li, H. He, X. Wang, J. Hu, W., Tan, K (2007) Preparation and antibacterial activity of Fe_3O_4 Ag nanoparticles. *Nanotechnology*, **18**, pp. 604–611

González-Pradas, E., Villafranca-Sánchez, M., Del Rey-Bueno, F., Ureña-Amate, M.D., Socías-Viciana, M. and Fernández-Pérez, M. (1999) Removal of diquat and deisopropylatrazine from water by montmorillonite-(Ce or Zr) phosphate crosslinked compounds. *Chemosphere*, **39**(3), pp.455-466.

Gottschaldt, M., Pfeifer, A., Koth, D., Görls, H., Dahse, H.-M., Möllmann, U., Obata, M. and Yano, S. (2006) Silver(I) complexes based on novel tripodal thioglycosides: synthesis, structure and antimicrobial activity. *Tetrahedron*, **62**(48), pp.11073-11080.

Grandjean, J. and Laszlo, P. (1991) Microdynamics of exchangeable lithium and sodium ions in laponite gels. *Journal of Magnetic Resonance (1969)*, **92**(2), pp.404-408.

Greaves, R. C., Bond, S. P and McWhinnie, W. R (1995) Conductivity studies on modified laponites. *Polyhedron*, **14** (23–24), pp. 3635-3639

Gu, H. Ho, P.L. Tong, E. Wang, L. Xu, B (2003) Presenting vancomycin on nanoparticles to enhance antimicrobial activities. *Nano Lett*, **3**(9), pp. 1261–1263

Gupta, V.K., Mohan, D. and Saini, V.K. (2006) Studies on the interaction of some azo dyes (naphthol red-J and direct orange) with nontronite mineral. *Journal of Colloid and Interface Science*, **298**(1), pp.79-86.

Gupta, V.K. and Suhas (2009) Application of low-cost adsorbents for dye removal; A review. *Journal of Environmental Management*, **90**(8), pp.2313-2342.

Hackett, E. Manias, E and Giannelis, E. P (1998) Molecular dynamics simulations of organically modified layered silicates. *Journal of Chemical Physics.* **108**(17) pp. 7410–7415

Halliwell, B and Gutteridge, J. M. **(**1990) Role of free radicals and catalytic metal ions in human disease: An overview. *Methods Enzymol*. **186**, pp.1–85.

Hammond, S.A., Morgan, J.R. and Russell, A.D. (1987) Comparative susceptibility of hospital isolates of Gram-negative bacteria to antiseptics and disinfectants. *Journal of Hospital Infection*, **9**(3), pp.255-264.

Han, Z., Yang, Q., Shi, J., Lu, G.Q. and Lewis, S.W. (2008) Well-dispersed cadmium sulfide prepared in the presence of laponite by microwave irradiation. *Solid State Sciences*, **10**(5), pp.563-568.

Hári, J. and Pukánszky, B. (2011) Nanocomposites: Preparation, Structure, and Properties. *in Applied Plastics Engineering Handbook.* Oxford: William Andrew Publishing, pp.109-142.

Hazel, J. R., Williams, E. E. (1990) The role of alterations in membrane lipid composition in enabling physiological adaptation of organisms to their physical environment. *Prog. Lipid Res.* **29**(3), pp.167-227.

Health Protection Agency (2012a) English National Point Prevalence Survey on Healthcare-associated Infections and Antimicrobial Use, 2011, Preliminary Data. Published May 2012 [online] [Accessed 2 June 2012]. Available at <http://www.hpa.org.uk/webc/HPAwebFile/HPAweb_C/1317134304594>

Health Protection Agency (2012b) English National Point Prevalence Survey on Healthcare-associated Infections and Antimicrobial Use, 2011, Appendices. Published May 2012 [online] [Accessed 2 June 2012]. Available at <http://www.hpa.org.uk/webc/HPAwebFile/HPAweb_C/1317134305239>

He, H., Duchet, J., Galy, J. and Gerard, J. F. (2005) Grafting of swelling clay materials with 3-aminopropyltriethoxysilane. *Journal of Colloid and Interface Science*, **288**(1), pp.171-176.

Hedges, A.J. (2002) Estimating the precision of serial dilutions and viable bacterial counts. *International Journal of Food Microbiology*, **76(**3), pp.207-214.

Heidbrink, J.L., Li, J., Pan, W.-P., Gooding, J.L., Aubuchon, S., Foreman, J. and Lundgren, C.J. (1996) Distinction of nontronite from palagonite by thermal analysis and evolved-gas analysis: Application to Mars surface exploration. *Thermochimica Acta*, **284**(1), pp.241-251.

Herrera, N.N., Letoffe, J.-M., Reymond, J.-P. and Bourgeat-Lami, E. (2005) Silylation of laponite clay particles with monofunctional and trifunctional vinyl alkoxysilanes. *Journal of Materials Chemistry*, **15**(8), pp.863-871.

Herrera, N.N., Putaux, J.L and Lami, E.B (2006) Synthesis of polymer/laponite nanocomposite latex particles via emulsion polymerization using silylated and cation-exchanged laponite clay platelets. *Progress in Solid State Chemistry*, **34**, pp. 121–137.

Herron, N and Thorn, D. L (1998) Nanoparticles: Uses and Relationships to Molecular Cluster Compounds. *Advanced Materials*. **10**(15), pp.1173-1184

Hostynek, J. J and Maibach, H. I (2003) Copper hypersensitivity: dermatologic aspects--an overview. *Rev. Environ. Health*, **18**(3) pp. 153-83

Hou, S, Dan L, Shawn L, Christine N, Kelsi S, Andrea H, Neenu G, Elizabeth M, Ellen, N. Liliana F, Webb M, Tamberlyn S, Michael N, Robert W and Richard K. W (2001) Complete genome sequence of Salmonella enterica serovar Typhimurium LT2. *Letters to Nature*. **413**. pp. 852-856

Hou, Z. J, Narindrasorasak, S, Bhushan, B, Sarkar, B, Mitra, B (2001) Functional analysis of chimeric proteins of the Wilson Cu(I)-ATPase (ATP7B) and ZntA, a Pb(II)/Zn(II)/Cd(II)-ATPase from *Escherichia coli. J Biol Chem* **276**, pp.40858-63.

Hoyle, B. D and Beveridge, T. J (1984) Metal binding by the peptidoglycan sacculus of *Escherichia coli* K-12. *Can J Microbiol*. **30**(2), pp.204–211.

Hoyle, B and Beveridge, T. J (1983) Binding of metallic ions to the outer membrane of *Escherichia coli*. *Appl Environ Microbiol*. **46**(3), pp.749–752.

Hu, C.H., Xu, Z.R. and Xia, M.S. (2005) Antibacterial effect of Cu^{2+}-exchanged montmorillonite on *Aeromonas hydrophila* and discussion on its mechanism. *Veterinary Microbiology*, **109**(1-2), pp.83-88.

Hu, C.-H. and Xia, M.-S. (2006) Adsorption and antibacterial effect of copper-exchanged montmorillonite on *Escherichia coli* K88. *Applied Clay Science*, **31**(3-4), pp.180-184.

Huang, Y.-H., Hsueh, C.-L., Huang, C.-P., Su, L.-C. and Chen, C.-Y. (2007) Adsorption thermodynamic and kinetic studies of Pb(II) removal from water onto a versatile Al_2O_3-supported iron oxide. *Separation and Purification Technology*, **55**(1), pp.23-29.

Huang, H. and Yang, Y. (2008) Preparation of silver nanoparticles in inorganic clay suspensions. *Composites Science and Technology*, **68**(14), pp.2948-2953.

Huh, A.J. and Kwon, Y.J (2011) "Nanoantibiotics": A new paradigm for treating infectious diseases using nanomaterials in the antibiotics resistant era. *Journal of Controlled Release*, **156**(2), pp.128-145.

Ibrahim, S. A., Yang, H. and Seo, C. W (2008) Antimicrobial activity of lactic acid and copper on growth of Salmonella and Escherichia coli O157:H7 in laboratory medium and carrot juice. *Food Chemistry*, **109**(1), pp.137-143.

Imlay, J. A., Chin, S. M., Linn, S. (1988) Toxic DNA damage by hydrogen peroxide through the Fenton reaction in vivo and in vitro. *Science*. **240**(4852), pp.640-642.

Imlay, J. A., Linn, S. (1988) DNA damage and oxygen radical toxicity. *Science* **240**(4857), pp.1302-1309.

Inoue, Y., Hoshino, M., Takahashi, H., Noguchi, T., Murata, T., Kanzaki, Y., Hamashima, H. and Sasatsu, M. (2002) Bactericidal activity of Ag-zeolite mediated by reactive oxygen species under aerated conditions. *Journal of Inorganic Biochemistry*, **92**(1), pp.37-42.

Inoue, Y. and Kanzaki, Y. (1997) The mechanism of antibacterial activity of silver-loaded zeolite. *Journal of Inorganic Biochemistry*, **67**(1-4), pp.377-377.

IWG-SCC (International Working Group on the Classification of Staphylococcal Cassette Chromosome Elements) (2009) Classification of staphylococcal cassette chromosome *mec* (SCC*mec*): guidelines for reporting novel SCC*mec* elements. *Antimicrob Agents Chemother*, **53**, pp. 4961–4967

Jaber, M. and Lambert, J.-F.o. (2009) A New Nanocomposite: L-DOPA/Laponite. *The Journal of Physical Chemistry Letters*, **1**(1), pp.85-88.

Jaisi, D.P., Dong, H. and Liu, C. (2007) Influence of biogenic Fe(II) on the extent of microbial reduction of Fe(III) in clay minerals nontronite, illite, and chlorite. *Geochimica et Cosmochimica Acta*, **71**(5), pp.1145-1158.

Jaisi, D.P., Kukkadapu, R.K., Eberl, D.D. and Dong, H. (2005) Control of Fe(III) site occupancy on the rate and extent of microbial reduction of Fe(III) in nontronite. *Geochimica et Cosmochimica Acta*, **69**(23), pp.5429-5440.

Jaisi, D.P., Liu, C., Dong, H., Blake, R.E. and Fein, J.B. (2008) Fe^{2+} sorption onto nontronite (NAu-2). *Geochimica et Cosmochimica Acta*, **72**(22), pp.5361-5371.

Japanese Standards Association. (2000) Antimicrobial products-Test for antimicrobial activity and efficacy, *Japanese Industrial Standard JIS Z 2801*, Reference number: JIS Z 2801: 2000 (E), First English edition published in 2001.

Johnson, J.A., McDonald, R.G., Muir, D.M. and Tranne, J.P. (2005) Pressure acid leaching of arid-region nickel laterite ore: Part IV: Effect of acid loading and additives with nontronite ores. *Hydrometallurgy*, **78**(3-4), pp.264-270.

Johnston, M.D. (1998) A simple and rapid test for quality control of liquid media, using the bioscreen microbiological growth analyser. *Journal of Microbiological Methods*, **32**(1), pp.37-43.

Jung, H., Kim, H.-M., Choy, Y.B., Hwang, S.-J. and Choy, J.-H. (2008a) Laponite-based nanohybrid for enhanced solubility and controlled release of Itraconazole. *International Journal of Pharmaceutics*, **349**(1-2), pp.283-290.

Jordan, F. T and Nassar, T. J (1971) The influence of copper on the survival of infectious bronchitis vaccine virus in water. *Vet. Rec*, **89**, pp.609-610.

Jung, H., Kim, H.-M., Choy, Y.B., Hwang, S.-J. and Choy, J.-H. (2008b) Itraconazole-Laponite: Kinetics and mechanism of drug release. *Applied Clay Science*, **40**(1-4), pp.99-107.

Jung, W.K., Koo, H.C., Kim, K.W., Shin, S., Kim, S.H. and Park, Y.H. (2008c) Antibacterial activity and mechanism of action of the silver ion in *Staphylococcus aureus* and *Escherichia coli*. *Appl. Environ. Microbiol.*, **74**(7), pp.2171-2178.

Kaviratna, P.D., Pinnavaia, T.J. and Schroeder, P.A. (1996) Dielectric properties of smectite clays. *Journal of Physics and Chemistry of Solids*, **57**(12), pp.1897-1906.

Kawahara, K., Tsuruda, K., Morishita, M. and Uchida, M. (2000) Antibacterial effect of silver-zeolite on oral bacteria under anaerobic conditions. *Dental Materials*, **16**(6), pp.452-455.

Kawata, K., Osawa, M., Okabe, S (2009) *In vitro* toxicity of silver nanoparticles at noncytotoxic doses to HepG2 human hepatoma cells. *Environ. Sci. Technol*. **43**, pp.6046–6051.

Kearns, K. L., Swallen, S. F. Ediger, T. Wu, M. D. and Yu, L (2007) (2007). Influence of substrate temperature on the stability of glasses prepared by vapor deposition. *Journal of Chemical Physics.* **127**, pp. 154702

Kegel, W. K. and Lekkerkerker, H. N. W. (2011) Colloidal gels: Clay goes patchy. *Nature materials*, **10**, pp. 5-6.

Kim, J.-H., Cho, H., Ryu, S.-E. and Choi, M.-U. (2000) Effects of metal ions on the activity of protein tyrosine phosphatase VHR: Highly potent and reversible oxidative inactivation by cu^{2+} ion. *Archives of Biochemistry and Biophysics*, **382**(1), pp.72-80.

Kim, J.S., Kuk, E., Yu, K.N., Kim, J.-H., Park, S.J., Lee, H.J., Kim, S.H., Park, Y.K., Park, Y.H., Hwang, C.-Y., Kim, Y.-K., Lee, Y.-S., Jeong, D.H., Cho, M.-H. (2007) Antimicrobial effects of silver nanoparticles. *Nanomedicine,* **3**(1), pp. 95**–**101

Kim, S., Choi, J.E., Choi, J., Chung, K.H., Park, K., Yi, J., Ryu, D.Y (2009) Oxidative stressdependent toxicity of silver nanoparticles in human hepatoma cells. *Toxicol. In Vitro* **23**, pp.1076–1084.

Klasen, H.J (2000) A historical review of the use of silver in the treatment of burns. Part I early uses. *Burns*, **30**, pp. 1–9

Kloepfer, J.A. Mielke, R.E and Nadeau, J.L (2005) Uptake of CdSe and CdSe/ZnS quantum dots into bacteria via purine-dependent mechanisms. *Appl. Environ. Microbiol*., **71**, pp. 2548–2557

Kollár, T., Kónya, Z., Pálinkó, I. and Kiricsi, I. (2001) Intercalation of various oxide species in-between Laponite layers studied by spectroscopic methods. *Journal of Molecular Structure*, **563-564**, pp.417-420.

Komadel, P., Madejová, J., Faïza Bergaya, B.K.G.T. and Gerhard, L. (2006) Chapter 7.1 Acid activation of clay minerals. *in Developments in Clay Science.* Elsevier, pp.263-287.

Korichi, S., Elias, A. and Mefti, A. (2009) Characterization of smectite after acid activation with microwave irradiation. *Applied Clay Science*, **42**(3-4), pp.432-438.

Kroon, M., Vos, W.L. and Wegdam, G.H. (1998) Structure and formation of a gel of colloidal disks. *Physical Review E*, **57**(2), p.1962.

Kumar, N.V.N., Muralidhar, K. and Joshi, Y.M. (2008) On the refractive index of ageing dispersions of Laponite. *Applied Clay Science*, **42**(1-2), pp.326-330.

Kuzniarska-Biernacka, I., Silva, A.R., Carvalho, A.P., Pires, J. and Freire, C. (2005) Organo-Laponites as novel mesoporous supports for manganese(iii) salen catalysts. *Langmuir*, **21**(23), pp.10825-10834.

Kwakye-Awuah, B., Williams, C., Kenward, M. and Radecka, I. (2008) Antimicrobial action and efficiency of silver-loaded zeolite X. *Journal of Applied Microbiology*, **104**(5), pp.1516-1524.

Labanda, J. and Llorens, J. (2008) Effect of aging time on the rheology of Laponite dispersions. *Colloids and Surfaces A: Physicochemical and Engineering Aspects*, **329**(1-2), pp.1-6.

Labbé, P., Brahimi, B., Reverdy, G., Mousty, C., Blankespoor, R., Gautier, A. and Degrand, C. (1994) Possible analytical application of laponite clay modified electrodes. *Journal of Electroanalytical Chemistry*, **379**(1-2), pp.103-110.

Lagaly, G. (2001) Pesticide-clay interactions and formulations. *Applied Clay Science*, **18**(5-6), pp.205-209.

Lambert, R.J.W. and Van Der Ouderaa, M.L.H. (1999) An Investigation into the differences between the Bioscreen and the traditional plate count disinfectant test methods. *Journal of Applied Microbiology*, **86**(4), pp.689-694.

Langella, A., Pansini, M., Cappelletti, P., de Gennaro, B., de' Gennaro, M. and Colella, C. (2000) NH^{+4}, Cu^{2+}, Zn^{2+}, Cd^{2+} and Pb^{2+} exchange for Na^{+} in a sedimentary clinoptilolite, North Sardinia, Italy. *Microporous and Mesoporous Materials*, **37**(3), pp.337-343.

Laszlo, P. (1986) Catalysis of organic reactions by inorganic solids. *Accounts of Chemical Research*, **19**(4), pp.121-127.

Lee, W., and Fu, Y., (2003) Effect of montmorillonite on the swelling behavior and drug-release behavior of nanocomposite hydrogels. *Journal of Applied Polymer Science*, **89**(13), pp.3652-3660.

Leon-Morales, C.F., Leis, A.P., Strathmann, M. and Flemming, H.-C. (2004) Interactions between laponite and microbial biofilms in porous media: implications for colloid transport and biofilm stability. *Water Research*, **38**(16), pp.3614-3626.

Levitz, P., Lecolier, E., Mourchid, A., Delville, A and Lyonnard, S (2000) Liquid-solid transition of Laponite suspensions at very low ionic strength: Long-range electrostatic stabilisation of anisotropic colloids. *Europhysics Letters*, **49**, pp.672 - 677.

Lewis, R.M. and Kuroda, H. (1989) Delaminated layered materials. *Solid State Ionics*, **32-33**(Part 1), pp.373-377.

Lezhnina, M.M., Bentlage, M. and Kynast, U.H. (2011) Nanoclays: Two-dimensional shuttles for rare earth complexes in aqueous solution. *Optical Materials*, **33**(10), pp.1471-1475.

Li, J.J., Mu, Z., Xu, X.Y., Tian, H., Duan, M.H., Li, L.D., Hao, Z.P., Qiao, S.Z. and Lu, G.Q. (2008a) A new and generic preparation method of mesoporous clay composites containing dispersed metal oxide nanoparticles. *Microporous and Mesoporous Materials*, **114**(1-3), pp.214-221.

Li, Q., Mahendra, S., Lyon, D.Y., Brunet, L., Liga, M.V., Li, D. and Alvarez, P.J.J. (2008b) Antimicrobial nanomaterials for water disinfection and microbial control: Potential applications and implications. *Water Research*, **42**(18), pp.4591-4602.

Li, P., Kim, N.H., Hui, D., Rhee, K.Y. and Lee, J.H. (2009a) Improved mechanical and swelling behavior of the composite hydrogels prepared by ionic monomer and acid-activated Laponite. *Applied Clay Science*, **46**(4), pp.414-417.

Li, P., Kim, N.H., Siddaramaiah and Lee, J.H (2009b) Swelling behavior of polyacrylamide/laponite clay nanocomposite hydrogels: pH-sensitive property. *Composites Part B: Engineering*, **40**(4), pp.275-283.

Lianou, A. and Koutsoumanis, K.P. (2011) Effect of the growth environment on the strain variability of Salmonella enterica kinetic behavior. *Food Microbiology*, **28**(4), pp.828-837.

Lillo-Ródenas, M.A., Marco-Lozar, J.P., Cazorla-Amorós, D. and Linares-Solano, A. (2007) Activated carbons prepared by pyrolysis of mixtures of carbon precursor/alkaline hydroxide. *Journal of Analytical and Applied Pyrolysis*, **80**(1), pp.166-174.

Lin, F.H., Lee, Y.H., Jian, C.H., Wong, J.-M., Shieh, M.-J. and Wang, C.-Y. (2002) A study of purified montmorillonite intercalated with 5-fluorouracil as drug carrier. *Biomaterials*, **23**(9), pp.1981-1987.

Lin, X.Z., Teng, X. and Yang, H. (2003) Direct Synthesis of Narrowly Dispersed Silver Nanoparticles Using a Single-Source Precursor. *Langmuir*, **19**(24), pp.10081-10085.

Liu, Q., Zhang, S., Sun, D. and Xu, J. (2009) Aqueous foams stabilized by hexylamine-modified Laponite particles. *Colloids and Surfaces A: Physicochemical and Engineering Aspects*, **338**(1-3), pp.40-46.

Liu, X. and Thomas, J.K. (1989) Effect of interlayer spacing on intercalation of CdS in clays. *Journal of Colloid and Interface Science*, **129**(2), pp.476-482.

Loeffler, A.B., A.K. Sung, J. Lindsay, J.A.Guardabassi, L. Dalsgaard, A. Smith, H.Stevens K.B. and Lloyd D.H. (2005) Prevalence of methicillin-resistant *Staphylococcus aureus* among staff and pets in a small animal referral hospital in the UK. *Journal of Antimicrobial Chemotherapy*, **56**, pp.692-697.

Lok, C.-N., Ho, C.-M., Chen, R., He, Q.-Y., Yu, W.-Y., Sun, H., Tam, P.K.-H., Chiu, J.-F. and Che, C.-M. (2006) Proteomic analysis of the mode of antibacterial action of silver nanoparticles. *Journal of Proteome Research*, **5**(4), pp.916-924.

Mackenzie, K.J.D., Fry, B.M., Brown, I.W.M. and Bowden, M.E. (1993) The effect of magnetic fields on the thermal reactions of nontronite. *Thermochimica Acta*, **60**(1), pp.93-103.

Mackenzie, R.C., (1952). A micromethod for determination of cation exchange capacity of clay. *Clay Minerals Bull*, (**1**), pp.203-204.

Macomber, L., and Imlay. J. A (2009). The iron-sulfur clusters of dehydratases are primary intracellular targets of copper toxicity. *Proc. Natl. Acad.Sci. U. S. A.* **106,** pp.8344–8349.

Madejová, J. (2003) FTIR techniques in clay mineral studies. *Vibrational Spectroscopy*, **31**(1), pp.1-10.

Maes, N., Heylen, I., Cool, P. and Vansant, E.F. (1997) The relation between the synthesis of pillared clays and their resulting porosity. *Applied Clay Science*, **12**(1-2), pp.43-60.

Magaña, S.M., Quintana, P., Aguilar, D.H., Toledo, J.A., Ángeles-Chávez, C., Cortés, M.A., León, L., Freile-Pelegrín, Y., López, T. and Sánchez, R.M.T. (2008) Antibacterial activity of montmorillonites modified with silver. *Journal of Molecular Catalysis A: Chemical*, **281**(1-2), pp.192-199.

Mark, J.E. (1996) Ceramic-reinforced polymers and polymer-modified ceramics. *Polymer Engineering & Science*, **36**(24), pp.2905-2920.

Marnett, L.J (2000) Oxyradicals and DNA damage. *Carcinogenesis*, **21**(3), pp. 361–370

Martínez-Castañón, G., Niño-Martínez, N., Martínez-Gutierrez, F., Martínez-Mendoza, J. and Ruiz, F. (2008) Synthesis and antibacterial activity of silver nanoparticles with different sizes. *Journal of Nanoparticle Research*, **10**(8), pp.1343-1348.

Martinez, M. V. (2011) A basic understanding of scanning electron microscopy (sem) and energy dispersive x-ray detection (EDX) [online] [Accessed 12 November 2011]. Available at <http://www.forensicevidence.net/iama/sem-edxtheory.html>

Matsuda, T., Nagashima, H. and Kikuchi, E. (1988) Physical and catalytic properties of smectite clays pillared by alumina in disproportionation of1,2,4-trimethylbenzene. *Applied Catalysis*, **45**(2), pp.171-182.

Matsuda, T., Yogo, K., Pantawong, C. and Kikuchi, E. (1995) Catalytic properties of copper-exchanged clays for the dehydrogenation of methanol to methyl formate. *Applied Catalysis A: General*, **126**(1), pp.177-186.

Matsumura, Y., Yoshikata, K., Kunisaki, S.-i. and Tsuchido, T. (2003) Mode of bactericidal action of silver zeolite and its comparison with that of silver nitrate. *Appl. Environ. Microbiol.*, **69**(7), pp.4278-4281.

Mcdonnell, G and Russell, A. D (1999) Antiseptics and disinfectants: Activity, action, and resistance. *Clinical Microbiology Reviews*, **12**(1), pp. 147-179.

Mcginity, J.W., Hill, J. A (1975) Influence of monovalent and divalent electrolytes on sorption of neomycin sulfate to attapulgite and montmorillonite clays. *Journal of Pharmaceutical Sciences*, **64**(9), pp.1566-1568.

McKay, G., Porter, J.F. and Prasad, G.R. (1999) The Removal of Dye Colours from Aqueous Solutions by Adsorption on Low-cost Materials. *Water, Air, & Soil Pollution*, **114**(3), pp.423-438.

McWhinnie, L.W., Christopher J. J,. McCleverty, J. A., Collison, D and Mabbs, F. E (1992) Synthesis and characterization of 17-electron species of nitrosyl[tris-3,5-dimethylpyrazolylborato]molybdenum. *Polyhedron.***11**(20), pp. 2639-2643

Mehtar S., Shisana O., Mosala T., Dunbar R. (2007) Infection control practices in public dental care services: findings from one South African Province. *J. Hosp. Infect*. **66**, pp.65-70.

Meng, N., Zhou, N.-L., Zhang, S.-Q. and Shen, J. (2009) Controlled release and antibacterial activity chlorhexidine acetate (CA) intercalated in montmorillonite. *International Journal of Pharmaceutics*, **382**(1-2), pp.45-49.

Mercier, L. and Pinnavaia, T.J. (1998) A functionalized porous clay heterostructure for heavy metal ion (Hg^{2+}) trapping. *Microporous and Mesoporous Materials*, **20**(1-3), pp.101-106.

Mewis, J. and Wagner, N.J. (2009) Thixotropy. *Advances in Colloid and Interface Science*, **147-148**, pp.214-227.

Michels, H.T., Michels, H. T, and Keevil, C. W. (2009) Effects of temperature and humidity on the efficacy of methicillin-resistant *Staphylococcus aureus* challenged antimicrobial materials containing silver and copper. *Letters in Applied Microbiology*, **49**, pp.191 - 195.

Miyoshi, H., Ohno, H., Sakai, K., Okamura, N. and Kourai, H. (2010) Characterization and photochemical and antibacterial properties of highly stable silver nanoparticles prepared on montmorillonite clay in n-hexanol. *Journal of Colloid and Interface Science*, **345**(2), pp.433-441.

Modric, J. (2011) *Staphylococcus aureus*, *Health Hype* [online] cited 1 November 2012, available via < http://www.healthhype.com/*staphylococcus-aureus*.html>

Mohamed Abdelhaye, Y.O., Chaouche, M. and Van Damme, H. (2008) The tackiness of smectite muds. 1. The dilute regime. *Applied Clay Science*, **42**(1-2), pp.163-167.

Molteni, C., Abicht, H. K. and Solioz., M. (2010) Killing of bacteria by copper surfaces involves dissolved copper. *Appl. Environ. Microbiol*. **76**, pp.4099–4101.

Mondal, M., Chattopadhyay, P.K., Chattopadhyay, S. and Setua, D.K. (2010) Thermal and morphological analysis of thermoplastic polyurethane-clay nanocomposites: Comparison of efficacy of dual modified laponite vs. commercial montmorillonites. *Thermochimica Acta*, **510**(1-2), pp.185-194.

Mongondry, P., Nicolai, T., Tassin, J., F (2004) Influence of pyrophosphate or polyethylene oxide on the aggregation and gelation of aqueous laponite dispersions. *Journal of Colloid and Interface Science*, **275**, pp.191–196.

Mongondry, P., Tassin, J.F. and Nicolai, T. (2005) Revised state diagram of Laponite dispersions. *Journal of Colloid and Interface Science*, **283**(2), pp.397-405.

Moon, E. M. and Peacock, C. L (2011) Adsorption of Cu(II) to *Bacillus subtilis*: A pH-dependent EXAFS and thermodynamic modelling study. *Geochimica et Cosmochimica Acta*, **75**, pp. 6705-6719.

Moon, J.S., Lee, A.R., Kang, H.M., Lee, E.S., Kim, M.N., Paik, Y.H., Park, Y.H., Joo, Y.S. and Koo, H.C. (2007) Phenotypic and Genetic Antibiogram of Methicillin-Resistant Staphylococci Isolated from Bovine Mastitis in Korea. *Journal of Dairy Science*, **90**(3), pp.1176-1185.

Moraes, E. C., Keyse, S. M., Pidoux, M., Tyrrell, R. M (1989) The spectrum of mutations generated by passage of a hydrogen peroxide damaged shuttle vector plasmid through a mammalian host. *Nucleic Acids Res.* **17**(20), 8301-12.

Morones, J.L. Elechiguerra, A. Camacho, J.T. Ramirez, J.R.(2005) The bactericidal effect of silver nanoparticles. *Nanotechnology*, **16**, pp. 2346–2353

Morris, P., and Hay, R. W. (2001) In Metal ions in biological sciences; Sigel, Health. Education. Marcel Dekker: New York, **5**, pp. 173-243.

Morton, J.R. and Preston, K.F. (1987) Superhyperfine interactions of Ag^{6+} clusters in silver loaded 4A zeolite. *Zeolites*, **7**(1), pp.2-4.

Mousty, C. (2004) Sensors and biosensors based on clay-modified electrodes--new trends. *Applied Clay Science*, **27**(3-4), pp.159-177.

Motulsky, H. J. (1999) Analyzing Data with GraphPad Prism GraphPad Software Inc., San Diego CA, pp. 12.

Moyer, C.A. Brentano, D.L. Gravens, H.W. Margraf, W.W. Monafo, L. (1965) Treatment of large human burns with 0.5% silver nitrate solution. *Arch Surg,* **90**, pp. 812–867

Murnane, R. and Clague, D.A. (1983) Nontronite from a low-temperature hydrothermal system on the Juan de Fuca Ridge. *Earth and Planetary Science Letters,* **65**(2), pp.343-352.

Mudunkotuwa, I.A., Grassian, V.H., (2011) The devil is in the details (or the surface): impact of surface structure and surface energetics on understanding the behavior of nanomaterials in the environment. *J. Environ. Monit*. **13**, pp.1135–1144.

Murata N. (1989) Low-temperature effects on cyanobacterial membranes. *J Bioenerg Biomembr.* **21**(1), pp.61–75.

Murray, H.H. and Haydn, H.M. (2006) Chapter 1 Introduction. *in Developments in Clay Science.* Elsevier, pp.1-6.

Nanda, A. and Saravanan, M. (2009) Biosynthesis of silver nanoparticles from *Staphylococcus aureus* and its antimicrobial activity against MRSA and MRSE. *Nanomedicine: Nanotechnology, Biology and Medicine*, **5**(4), pp.452-456.

Nascimento, A. M., Chartone-Souza, E. (2003) Operon mer: bacterial resistance to mercury and potential for bioremediation of contaminated environments. *Genet. Mol. Res*. **2**(1), pp.92-101

Navarro, E., Piccapietra, F., Wagner, B., Marconi, F., Kaegi, R., Odzak, N., Sigg, L., Behra, R (2008) Toxicity of silver nanoparticles to *Chlamydomonas reinhardtii*. *Environ. Sci. Technol*. **42**, pp.8959–8964.

Negrete-Herrera, N., Putaux, J.-L., David, L., Haas, F.D. and Bourgeat-Lami, E. (2007) Polymer/Laponite Composite Latexes: Particle Morphology, Film Microstructure, and Properties. *Macromolecular Rapid Communications*, **28**(15), pp.1567-1573.

Nies, D. H. (2003) Efflux-mediated heavy metal resistance in prokaryotes. *FEMS Microbiol. Rev*. **27**(2-3), pp.313-39.

Nies, H (1999) Microbial heavy-metal resistance. *Applied Microbiology and Biotechnology,* **51**, pp. 730–750

Noyce, J.O., Michels, H. and Keevil, C.W. (2006) Potential use of copper surfaces to reduce survival of epidemic meticillin-resistant *Staphylococcus aureus* in the healthcare environment. *Journal of Hospital Infection*, **63**(3), pp.289-297.

Occelli, M.L. (1988) Surface properties and cracking activity of delaminated clay catalysts. *Catalysis Today*, **2**(2-3), pp.339-355.

Occelli, M.L. and Finseth, D.H. (1986) Preparation and characterization of pillared hectorite catalysts. *Journal of Catalysis*, **99**(2), pp.316-326.

Occelli, M.L., Hsu, J.T. and Galya, L.G. (1985) Propylene oligomerization with pillared clays. *Journal of Molecular Catalysis*, **33**(3), pp.371-389.

Occelli, M.L., Iyer, P.S., Sanders, J.V., Jacobs, P.A. and Santen, R.A.v. (1989) The Pillaring of A Synthetic Hectorite With Organic Cations. *in Studies in Surface Science and Catalysis.* Elsevier, pp.469-480.

Occelli, M.L., Landau, S.D. and Pinnavaia, T.J. (1984) Cracking selectivity of a delaminated clay catalyst. *Journal of Catalysis*, **90**(2), pp.256-260.

Occelli, M.L., Landau, S.D. and Pinnavaia, T.J. (1987) Physicochemical properties of a delaminated clay cracking catalyst. *Journal of Catalysis*, **104**(2), pp.331-338.

Ohsumi Y, Kitamoto K, Anraku Y. (1988) Changes induced in the permeability barrier of the yeast plasma membrane by cupric ion. *J Bacteriol*. **170**(6), pp.2676–2682.

Okutomo, S., Kuroda, K. and Ogawa, M. (1999) Preparation and characterization of silylated-magadiites. *Applied Clay Science*, **15**(1-2), pp.253-264.

Olphen, H. (1977) *An Introduction to Clay Colloid Chemistry.* New York: Wiley. pp. 19-25

Onodera, Y., Iwasaki, T., Chatterjee, A., Ebina, T., Satoh, T., Suzuki, T. and Mimura, H. (2001) Bactericidal allophanic materials prepared from allophane soil: I. Preparation and characterization of silver/phosphorus-silver loaded allophanic specimens. *Applied Clay Science*, **18**(3-4), pp.123-134.

Onodera, Y., Sunayama, S., Chatterjee, A., Iwasaki, T., Satoh, T., Suzuki, T. and Mimura, H. (2001) Bactericidal allophanic materials prepared from allophane soil: II. Bactericidal activities of silver/phosphorus-silver-loaded allophanic specimens. *Applied Clay Science*, **18**(3-4), pp.135-144.

O'Reilly, S.E., Furukawa, Y. and Newell, S. (2006) Dissolution and microbial Fe(III) reduction of nontronite (NAu-1). *Chemical Geology*, **235**(1-2), pp.1-11.

Ovcharenko, F.D. (1982) *Dev. Sedimentol.*, **35**, p.239.

Pal, S., Tak, Y.K. and Song, J.M. (2007) Does the Antibacterial Activity of Silver Nanoparticles Depend on the Shape of the Nanoparticle? A Study of the Gram-Negative Bacterium Escherichia coli. *Appl. Environ. Microbiol.*, **73**(6), pp.1712-1720.

Pálková, H., Madejová, J., Zimowska, M., Bielańska, E., Olejniczak, Z., Lityńska-Dobrzyńska, L. and Serwicka, E.M (2010) Laponite-derived porous clay heterostructures: I. Synthesis and physicochemical characterization. Microporous and Mesoporous Materials, **127**(3), pp. 228-236.

Panáček, A., Kvítek, L., Prucek, R., Kolář, M., Večeřová, R., Pizúrová, N., Sharma, V.K., Nevěčná, T.j. and Zbořil, R. (2006) Silver Colloid Nanoparticles: Synthesis, Characterization, and Their Antibacterial Activity. *The Journal of Physical Chemistry B*, **110**(33), pp.16248-16253.

Park, J.K., Choy, Y.B., Oh, J.-M., Kim, J.Y., Hwang, S.-J. and Choy, J.-H. (2008) Controlled release of donepezil intercalated in smectite clays. *International Journal of Pharmaceutics*, **359**(1-2), pp.198-204.

Park, K.-W.b., Kwon, O.-Y (2004) Interlamellar silylation of montmorillonite with 3-aminopropyltriethoxysilane. *Bulletin of the Korean Chemical Society* **25**(7), pp.965-968

Park, M., Shim, I.-K., Jung, E.-Y. and Choy, J.-H. (2004) Modification of external surface of laponite by silane grafting. *Journal of Physics and Chemistry of Solids*, **65**(2-3), pp.499-501.

Patakfalvi, R. and Dékány, I. (2004) Synthesis and intercalation of silver nanoparticles in kaolinite/DMSO complexes. *Applied Clay Science*, **25**(3-4), pp.149-159.

Patakfalvi, R., Oszkó, A. and Dékány, I. (2003) Synthesis and characterization of silver nanoparticle/kaolinite composites. *Colloids and Surfaces A: Physicochemical and Engineering Aspects*, **220**(1-3), pp.45-54.

Pavlidou, S. and Papaspyrides, C.D. (2008) A review on polymer-layered silicate nanocomposites. *Progress in Polymer Science*, **33**(12), pp.1119-1198.

Pawar, N. and Bohidar, H.B. (2009) Hydrophobic hydration mediated universal self-association of colloidal nanoclay particles. *Colloids and Surfaces A: Physicochemical and Engineering Aspects*, **333**(1-3), pp.120-125.

Pelekani, C. and Snoeyink, V.L. (2000) Competitive adsorption between atrazine and methylene blue on activated carbon: the importance of pore size distribution. *Carbon*, **38**(10), pp.1423-1436.

Perkins, R., Brace, R. and Matijevic, E. (1974) Colloid and surface properties of clay suspensions. I. Laponite CP. *Journal of Colloid and Interface Science*, **48**(3), pp.417-426.

Persoons D, V.H.S., Hermans K, Butaye P, de Kruif A, Haesebrouck F and Dewulf, J (2009) Methicillin-Resistant *Staphylococcus aureus* in Poultry. *Emerging Infectious Disease*, **15**(3), pp.285-296.

Phuoc, T.X. and Chen, R.-H. (2011) Synthesis of cation-exchanged laponite suspensions by laser ablation of microsized-metal particles in liquid. *Optics and Lasers in Engineering*, **49**(3), pp.396-402.

Phuoc, T.X., Howard, B.H. and Chyu, M.K. (2009) Synthesis and rheological properties of cation-exchanged Laponite suspensions. *Colloids and Surfaces A: Physicochemical and Engineering Aspects*, **351**(1-3), pp.71-77.

Pichonat, T., Lethien, C., Tiercelin, N., Godey, S., Pichonat, E., Roussel, P., Colmont, M. and Rolland, P.A. Further studies on the lithium phosphorus oxynitride solid electrolyte. *Materials Chemistry and Physics*, **123**(1), pp.231-235.

Pinnavaia, T.J., Tzou, M.-S., Landau, S.D. and Raythatha, R.H. (1984) On the pillaring and delamination of smectite clay catalysts by polyoxo cations of aluminum. *Journal of Molecular Catalysis*, **27**(1-2), pp.195-212.

Pittet, D., Allegranzi, B., Storr, J., Nejad, S. B., Dziekan, G., Leotsakos, A. and Donaldson, L. (2008) Infection control as a major World Health Organization priority for developing countries. Journal of Hospital Infection, 68, 285-292.

Pittet, D. and Donaldson, L. (2005) Clean Care is Safer Care: a worldwide priority. The Lancet, 366, 1246-1247.

Plee, D., Fripiat, J.J., Schutz, A., Poncelet, G., B. Imelik, C.N and Vedrine, J.C. (1985) Acid Properties Of A Bidimensional Zeolite. *in Studies in Surface Science and Catalysis.* Elsevier, pp.343-350.

Plumb, J. A. (1991) Major diseases of striped bass and redfish. Vet. Hum. *Toxicol.* , **33**(1), pp. 34

Pozzo, D.C. and Walker, L.M. (2004) Reversible shear gelation of polymer-clay dispersions. *Colloids and Surfaces A: Physicochemical and Engineering Aspects*, **240**(1-3), pp.187-198.

Prado, L.A.S.d.A., Karthikeyan, C.S., Schulte, K., Nunes, S.P. and de Torriani, I.L. (2005) Organic modification of layered silicates: structural and thermal characterizations. *Journal of Non-Crystalline Solids*, **351**(12-13), pp.970-975.

Pruissen, D.J., Capkova, P., Driessen, R.A.J. and Schenk, H. (2000) Structure analysis of intercalated smectites using molecular simulations. *Applied Catalysis A: General*, **193**(1-2), pp.103-112.

Quaranta, D ., Krans, T., Santo, E C., Christian G. E, Dylan D, Christopher J. Chang, J and Grass, G (2011) Mechanisms of yeast contact-killing on dry metallic copper surfaces, *Applied and Environmental Microbiology*. **77**, pp. 416–426.

Rai M, Yadav A, Gade A (2009) Silver nanoparticles as a new generation of antimicrobials. *Biotechnol Adv.* **27**(1), pp.76-83.

Ravi Kumar, N.V.N., Muralidhar, K. and Joshi, Y.M. (2008) On the refractive index of ageing dispersions of Laponite. *Applied Clay Science*, **42**(1-2), pp.326-330.

Raythatha, R. and Pinnavaia, T.J. (1983) Clay intercalation catalysts interlayered with rhodium phosphine complexes. Surface effects on the hydrogenation and isomerization of 1-hexene. *Journal of Catalysis*, **80**(1), pp.47-55.

Rejeski, D., Kuiken, T., Patrick, P. and Eleonore, P. (2012) The project on emerging nanotechnologies. Analysis, first publicly available on-line inventory of nanotechnology-based consumer products [online]. [accessed 16 March 2012] Available via <http://www.nanotechproject.org/inventories/consumer/analysis_draft/>

Ren, X., Keith, K., Megan, A. H., Manju, R., Sara, M., John, S., George, E. C., Alexander, L. E and Todd, D. K (2009) Non-blinking semiconductor nanocrystals. *Nature* **459**, pp.686-689

Rensing, C and Grass, G. (2003) *Escherichia coli* mechanisms of copper homeostasis in a changing environment. *FEMS Microbiol Rev*. **27**(2-3), 197-213.

Retchkiman-Schabes, P.S., Canizal, G. Becerra-Herrera, C., Zorrilla, H.B., Liu, J.A. Ascencio M. (2006) Biosynthesis and characterization of Ti/Ni bimetallic nanoparticles. *Opt. Mater.*, **29**, pp. 95–99

Reynaud, E. Kloppfer, M.H. Vigier, G and Varlet, J (2001) Clay–reinforced polyamide: preferential orientation of the montmorillonite sheets and the polyamide crystalline lamellae. *Journal of Polymer Science Part B: Polymer Physics.* **39**(12), pp.1360–1370

Rich, M.R., L. and Kearns, A.M. (2005) Methicillin-resistant *Staphylococcus aureus* isolates from companion animals. *Veterinary Microbiology*, **105**(3-4), pp.313-314.

Rieder, M., Cavazzini, G., D'yakonov, Y. Sm, Frank-Kamenetskii, V. A., Gottardi, G., , Guggenheim, S., Koval, P. V., Müller, G., Neiva, A. M. R., Radoslovich, E. W., Robert, and J. L., S., F. P., Takeda, H., Weiss, Z and Wones, D. R (1998) Nomenclature of micas. *Clays and Clay Minerals*, **46**, pp.586 - 595.

Rivera-Garza, M., Olguín, M.T., García-Sosa, I., Alcántara, D. and Rodríguez-Fuentes, G. (2000) Silver supported on natural Mexican zeolite as an antibacterial material. *Microporous and Mesoporous Materials*, **39**(3), pp.431-444.

Roberts F., Roberts C.W., Johnson J., Kyle D.E., Krell T., Coggins J.R., Coombs G.H., Milhous W.K., Tzipori S., Ferguson D.J.P., Chakrabarti D., McLeod R., (1998) Evidence for the shikimate pathway in apicomplexan parasites. *Nature*. **393**(6687) pp.801-805

Rosen, B.P. (2002) Transport and detoxification systems for transition metals, heavy metals and metalloids in eukaryotic and prokaryotic microbes. *Comp Biochem Physiol A Mol Integr Physiol* **133**, pp.689-693

Rosenkranz, H. S. and Carr, H. S. (1972) Silver sulfadazine: effect on growth and metabolism of bacteria. *Antimicrob Agents Chemother*, **5**, pp. 199–201.

Rosta, L., von Gunten, H.R. and Giovanoli, R. (1991) Packed bed filtration of laponite sols. *Colloids and Surfaces*, **55**, pp.205-221.

Ruggerone, R., Plummer, C.J.G., Negrete Herrera, N., Bourgeat-Lami, E. and Månson, J.A.E. (2009) Fracture mechanisms in polystyrene/laponite nanocomposites prepared by emulsion polymerization. *Engineering Fracture Mechanics*, **76**(18), pp.2846-2855.

Ruparelia, J.P., Chatterjee, A.K., Duttagupta, S.P. and Mukherji, S. (2008) Strain specificity in antimicrobial activity of silver and copper nanoparticles. *Acta Biomaterialia*, **4**(3), pp.707-716.

Russell, A.D. (1999) Bacterial resistance to disinfectants: present knowledge and future problems. *Journal of Hospital Infection*, **43**(Supplement 1), pp.S57-S68.

Russell, A.D. (2003) Biocide use and antibiotic resistance: the relevance of laboratory findings to clinical and environmental situations. *The Lancet Infectious Diseases*, **3**(12), pp.794-803.

Russell, A.D. (2004) Bacterial adaptation and resistance to antiseptics, disinfectants and preservatives is not a new phenomenon. *Journal of Hospital Infection*, **57**(2), pp.97-104.

Russell, A.D. and Furr, J.R. (1986) The effects of antiseptics, disinfectants and preservatives on smooth, rough and deep rough strains of *Salmonella typhimurium*. *International Journal of Pharmaceutics*, **34**(1-2), pp.115-123.

Russell, A.D. and Furr, J.R. (1986) Susceptibility of porin- and lipopolysaccharide-deficient strains of Escherichia coli to some antiseptics and disinfectants. *Journal of Hospital Infection*, **8**(1), pp.47-56.

Russell, A.D., Hammond, S.A. and Morgan, J.R. (1986) Bacterial resistance to antiseptics and disinfectants. *Journal of Hospital Infection*, **7**(3), pp.213-225.

Ruzicka,P., Marek C, Martins, A. Teixeira, B., Jose. A (2011) Meniscus dynamics in bubble formation: A parametric study. *Chemical Engineering Science*, **66**(14), pp. 3258 - 3267

Sagripanti, J. L (1991) Metal-based formulations with high microbicidal activity. *Appl Environ Microbiol*. **58**(9) pp.3157–3162.

Sagripanti, J. L. (1992) Metal based formulations with high microbial activity. *Appl. Environ. Microbiol.* **58**, pp.3157-3162.

Sagripanti, J. L., Goering, P. L., Lamanna, A. (1991) Interaction of copper with DNA and antagonism by other metals. *Toxicol Appl Pharmacol*. **110**(3), pp.477–485.

Sagripanti, J. L and Lightfoote, M. M. (1996) Cupric and ferric ions inactivate HIV. *AIDS Res. Hum. Retroviruses*, **12**(4), pp.333-337.

Sagripanti, J. L, Routson, L. B and Lytle, C. D (1993) Virus inactivation by copper or iron ions alone and in the presence of peroxide. *Appl Environ Microbiol*. **59**(12), pp.4374–4376.

Sagripanti, J. L and Kraemer, K. H (1989) Site-specific oxidative DNA damage at polyguanosines produced by copper plus hydrogen peroxide. *J Biol Chem*. **264**(3), pp.1729–1734

Salgado., C. D., Morgan, A and Sepkowitz, K. A (2010) A Pilot Study to Determine the Effectiveness of Copper in Reducing the Microbial Burden (MB) of Objects in Rooms of Intensive Care Unit (ICU) Patients, Poster 183, 5th Decennial International Conference on Healthcare-Associated Infections, Atlanta.

Sánchez-Camazano, M., Sánchez Martin, M.J., Vicente, M, T and Dominguez-Gil, A (1980) Adsorption of chlorpheniramine maleate by montmorillonite, . *Int. J. Pharm.*, **6**, pp.243 - 251.

Sandoval, M.V., Henao, J.A., Ríos, C.A., Williams, C.D. and Apperley, D.C. (2009) Synthesis and characterization of zeotype ANA framework by hydrothermal reaction of natural clinker. *Fuel*, **88**(2), pp.272-281.

Sanjay, G. and Sugunan, S. (2005) Glucoamylase immobilized on montmorillonite: Synthesis, characterization and starch hydrolysis activity in a fixed bed reactor. *Catalysis Communications*, **6**(8), pp.525-530.

Santo, C.E., Lam, E.W., Elowsky, C.G., Quaranta, D., Domaille, D.W., Chang, C.J. and Grass, G. (2011) bacterial killing by dry metallic copper surfaces. *Appl. Environ. Microbiol.*, **77**(3), pp.794-802.

Sanz, J and Serratosa, J.M (1984) Silicon-29 and aluminum-27 high-resolution MAS-NMR spectra of phyllosilicates. *J. Am. Chem. Soc.*, **106**, pp. 4790–4793

Sastry, M., Ahmad, A., Khan, M and Kumar, R (2003) Biosynthesis of metal nanoparticles using fungi and actinomycete. *Current Science*, **85**(2), pp.162-170.

SayIlkan, H., Erdemoglu, S., Sener, S., SayIlkan, F., Akarsu, M. and Erdemoglu, M. (2004) Surface modification of pyrophyllite with amino silane coupling agent for the removal of 4-nitrophenol from aqueous solutions. *Journal of Colloid and Interface Science*, **275**(2), pp.530-538.

Sazama, P., Jirglová, H. and Dedecek, J. (2008) Ag-ZSM-5 zeolite as high-temperature water-vapor sensor material. *Materials Letters*, **62**(27), pp.4239-4241.

Scott, J. A and Palmer, S. J (1990) Sites of cadmiun uptake in bacteria used for biosorption *Appl. Microbiol. Biotechnol*. **33**(2), pp. 221-25.

Serratosa, , J.M Bradely, W.F (1958) Determination of the orientation of OH bond axes in layer silicates by infrared absorption *J. Phys. Chem.*, **62**, pp. 1164–1167

Schoonheydt, R.A., H. van Bekkum, E.M.F. and Jansen, J.C. (1991) Chapter 6 Clays: From Two to Three Dimensions. *in Studies in Surface Science and Catalysis.* Elsevier, pp.201-239.

Sergio, D.M.B., Koh, T.H., Hsu, L.-Y., Ogden, B.E., Goh, A.L.H. and Chow, P.K.H. (2007) Investigation of meticillin-resistant *Staphylococcus aureus* in pigs used for research. *J Med Microbiol*, **56**(8), pp.1107-1109.

Shan, D., Zhang, J., Xue, H.-G., Ding, S.-N. and Cosnier, S. Colloidal laponite nanoparticles: Extended application in direct electrochemistry of glucose oxidase and reagentless glucose biosensing. *Biosensors and Bioelectronics*, **25**(6), pp.1427-1433.

Sharma, V.K. Yngard, R.A and Lin. Y. (2009) Silver nanoparticles: green synthesis and their antimicrobial activities. *Adv Coll Interf Sci*, **145**(1-2), p. 83-96

Silver, S. (2003) Bacterial silver resistance: molecular biology and uses and misuses of silver compounds. *FEMS Microbiology Reviews*, **27**(2-3), pp.341-353.

Singh, N.D., Arndt, P.F., Petrov, D.A. (2006). Minor shift in background substitutional patterns in the Drosophila saltans and willistoni lineages is insufficient to explain GC content of coding sequences. *BMC Biol*. **4**, pp. 37.

Smith, A.R., Pryer, K.M., Schuettpelz, E., Korall, P., Schneider, H. & Wolf, P.G. (2006) A classification for extant ferns. *Taxon* **55**(3) pp. 705-731.

Sondi, I. and Salopek-Sondi, B. (2004) Silver nanoparticles as antimicrobial agent: a case study on *E. coli* as a model for Gram-negative bacteria. *Journal of Colloid and Interface Science*, **275**(1), pp.177-182.

Sondi, I. Salopek-Sondi. B (2007) Silver nanoparticles as antimicrobial agent: a case study on *E. coli* as a model for gram-negative bacteria. *J Colloid Interface*, **275**, pp. 177–182

Sondossi, M., Riha, V.F. and Rossmoore, H.W. (1990) The potentiation of industrial biocide activity with Cu^{2+} I. Synergistic effect of Cu^{2+} with formaldehyde. *International Biodeterioration*, **26**(1), pp.51-61.

Song, Y., Shan, D., Chen, R. and Han, E.-H. (2009) Corrosion characterization of Mg-8Li alloy in NaCl solution. *Corrosion Science*, **51**(5), pp.1087-1094.

Sprynskyy, M., Buszewski, B., Terzyk, A.P. and Namiesnik, J. (2006) Study of the selection mechanism of heavy metal (Pb^{2+}, Cu^{2+}, Ni^{2+}, and Cd^{2+}) adsorption on clinoptilolite. *Journal of Colloid and Interface Science*, **304**(1), pp.21-28.

Stacey, M.H. (1988) Alumina-pillared clays and their adsorptive properties. *Catalysis Today*, **2**(5), pp.621-631.

Stefanescu, E.A., Stefanescu, C., Daly, W.H., Schmidt, G. and Negulescu, I.I. (2008) Hybrid polymer-clay nanocomposites: A mechanical study on gels and multilayered films. *Polymer*, **49**(17), pp.3785-3794.

Stohs, S.J. and Bagchi, D. (1995) Oxidative mechanisms in the toxicity of metal ions. *Free Radical Biology and Medicine*, **18**(2), pp.321-336.

Stul, M.S., Van Leemput, L (1982) Particle-size distribution, cation exchange capacity and charge density of deferrated montmorillonites. *Clay Minerals* **17**(2), pp.209 - 215.

Subramani, S., Lee, J.-Y., Choi, S.-W. and Kim, J.H. (2007) Waterborne trifunctionalsilane-terminated polyurethane nanocomposite with silane-modified clay. *Journal of Polymer Science Part B: Polymer Physics*, **45**(19), pp.2747-2761.

Su, H. L., Chou, C. C., Hung, D. J., Lin, S. H., Pao, I. C., Lin, J. H., Huang, F. L., Dong, R. X and Lin, J. J (2009) The disruption of bacterial membrane integrity through ROS generation induced by nanohybrids of silver and clay. *Biomaterials*, **30**, pp. 5979-5987.

Sum, O.S.N., Feng, J., Hub, X. and Yue, P.L. (2005) Photo-assisted fenton mineralization of an azo-dye acid black 1 using a modified laponite clay-based Fe nanocomposite as a heterogeneous catalyst. *Topics in Catalysis*, **33**(1), pp.233-242.

Sung, J.M.L., Lloyd, D.H. and Lindsay, J.A. (2008) *Staphylococcus aureus* host specificity: comparative genomics of human versus animal isolates by multi-strain microarray. *Microbiology*, **154**(7), pp.1949-1959.

Szlyk, E., Piszczek, P., Grodzicki. A., Chaberski, M., Golinski, A., Szatkowski, J. and Blaszczyk, T. (2001) CVD of Ag^{1} Complexes with Tertiary Phosphines and Perfluorinated Carboxylates - A New Class of Silver Precursors. *Chemical Vapor Deposition*, **7**(3), pp.111-116.

Sze Nga Sum, O., Feng, J., Hu, X. and Lock Yue, P. (2004) Pillared laponite clay-based Fe nanocomposites as heterogeneous catalysts for photo-Fenton degradation of acid black 1. *Chemical Engineering Science*, **59**(22-23), pp.5269-5275.

Taleb, A., Petit, C. and Pileni, M.P. (1997) Synthesis of highly monodisperse silver nanoparticles from AOT reverse micelles: A way to 2D and 3D self-organization. *Chemistry of Materials*, **9**(4), pp.950-959.

Tanaka, H. Meunier, J.and Bonn, D. (2004) Nonergodic states of charged colloidal suspensions: Repulsive and attractive glasses and gels. *Phys. Rev. E.* **69**, pp.031404

Tang, J.A. and Valix, M. (2006) Leaching of low grade limonite and nontronite ores by fungi metabolic acids. *Minerals Engineering*, **19**(12), pp.1274-1279.

Tenover, F.C and Goering R.V. (2009) Methicillin-resistant *Staphylococcus aureus* strain USA300: origin and epidemiology. *J Antimicrob Chemother*, **64**, pp. 441–446

Temuujin, J., Jadambaa, T., Burmaa, G., Erdenechimeg, S., Amarsanaa, J. and MacKenzie, K.J.D. (2004) Characterisation of acid activated montmorillonite clay from Tuulant (Mongolia). *Ceramics International*, **30**(2), pp.251-255.

Thomas, V., Yallapu, M.M., Sreedhar, B. and Bajpai, S.K. (2007) A versatile strategy to fabricate hydrogel-silver nanocomposites and investigation of their antimicrobial activity. *Journal of Colloid and Interface Science*, **315**(1), pp.389-395.

Thompson, D.W. and Butterworth, J.T. (1992) The nature of laponite and its aqueous dispersions. *Journal of Colloid and Interface Science*, **151**(1), pp.236-243.

Thompson, D.W. and Tahir, N.M. (1991) The influence of a smectite clay on the hydrolysis of iron(III). *Colloids and Surfaces*, **60**, pp.369-398.

Tkeshelashvili, L. K., McBride, T., Spence, K and Loeb. L. A (1991) Mutation spectrum of copper-induced DNA damage. *J. Biol. Chem*. **266**, pp.6401–6406.

Todar, K (2012) Pathogenesis of *S. aureus* infections. *Todar's Online Textbook of Bacteriology*. Cited 1 Novenber 2012, available via <http://textbookofbacteriology.net/staph_2.html>

Tolls, J. (2001) Sorption of Veterinary Pharmaceuticals in Soils: A Review. *Environmental Science & Technology*, **35**(17), pp.3397-3406.

Tong, G., Yulong, M., Peng, G. and Zirong, X. (2005) Antibacterial effects of the Cu(II)-exchanged montmorillonite on *Escherichia coli* K88 and *Salmonella choleraesuis*. *Veterinary Microbiology*, **105**(2), pp.113-122.

Tonle, A.K., Ngameni, E and Walcarius, A (2006) From clay to organoclays film modified electrodes: tunning charge selectivity in ion exchange voltammetry. *Electrochimica Acta* **49**, pp. 3435–3443.

Tonle, I.K. Ngameni, E and Walcarius, A. (2004) From clay- to organoclay-film modified electrodes: tuning charge selectivity in ion exchange voltammetry. *Electrochimica Acta*, **49**, pp. 3435-3443

Top, A. and Ülkü, S. (2004) Silver, zinc, and copper exchange in a Na-clinoptilolite and resulting effect on antibacterial activity. *Applied Clay Science*, **27**(1-2), pp.13-19.

Totsuka, A and Otaki, K (1974) The effects of amino acids and metals on the infectivity of poliovirus ribonucleic acid. *Jpn. J. Microbiol*.**18**(2), pp. 107-712.

Tronto, J., Ribeiro, S.J.L., Valim, J.B. and Gonçalves, R.R. (2009) Visible and near-infrared luminescent Eu3+ or Er3+ doped laponite-derived xerogels and thick films: Structural and spectroscopic properties. *Materials Chemistry and Physics*, **113**(1), pp.71-77.

Tsoufis, T., Jankovic, L., Gournis, D., Trikalitis, P.N. and Bakas, T. (2008) Evaluation of first-row transition metal oxides supported on clay minerals for catalytic growth of carbon nanostructures. *Materials Science and Engineering: B*, **152**(1-3), pp.44-49.

Ug, A and Ceylan, O. (2003) Occurrence of resistance to antibiotics, metals, and plasmids in clinical strains of *Staphylococcus* spp. *Arch. Med. Res.* **34**(2), pp.130-6.

Vaccari, A. (1995) Introduction. *Applied Clay Science*, **10**(1-2), pp.1-3.

Vaccari, A. (1998) Preparation and catalytic properties of cationic and anionic clays. *Catalysis Today*, **41**(1-3), pp.53-71.

Vaccari, A. (1999) Clays and catalysis: a promising future. *Applied Clay Science*, **14**(4), pp.161-198.

Van Bekkum, H., Jean-Roger Desmurs, B.G. and Melvin, J.G. (1995) Bromides in zeolite synthesis / zeolites in bromide synthesis and conversion. *in Industrial Chemistry Library*. Elsevier, pp.202-216.

Vansant, E.F.a.P., G. (1978) The exchange of alkylammonium ion on Na-Laponite. *Clays and clay Minerals*, **26**(4), pp.279-284.

Vansant, E.F and Peeters., G. (1978) The exchange of alkylammonium ions on Na-laponite. *Clays and Clay Minerals*, **26**(4), pp.279-284.

Vicente-Rodríguez, M.A., Suarez, M., Bañares-Muñoz, M.A. and de Dios Lopez-Gonzalez, J. (1996) Comparative FT-IR study of the removal of octahedral cations and structural modifications during acid treatment of several silicates. *Spectrochimica Acta Part A: Molecular and Biomolecular Spectroscopy*, **52**(13), pp.1685-1694.

Vikas, A., Raghupathi., K and Sanjay, G (2001) Ion-exchange resins: carrying drug delivery forward,. *ddt*, **6**(17), pp.905 - 914.

Viseras, M.T., Cerezo, P., Aguzzi, C., Garcés, A., López-Galindo, A and Viseras, C (2004) Retención del ácido 5 amino salicílico por halloisitas,. *Proc. Jornadas Cientificas de la Sea. Madrid (E), November 15*, P-**15**, pp.15.

Viseras, M. T., Aguzzi, C., Cerezo, P., Viseras, C., López-Galindo, A., Valenzuela, C and Caramella, C (2005) Study of adsorption kinetics of 5-aminosalicilyc acid in phyllosilicates for controlled drug delivery in the treatment of inflammatory bowel disease. *Proc. 1st PharmSciFair, Pharmaceutical Sciences Fair and Exhibition. Nice (F), June 12–17*, PO-**253**.

Walcarius, A., Etienne, M. and Delacote, C. (2004) Uptake of inorganic HgII by organically modified silicates: influence of pH and chloride concentration on the binding pathways and electrochemical monitoring of the processes. *Analytica Chimica Acta*, **508**(1), pp.87-98.

Walker, G.M. and Weatherley, L.R. (1999) Kinetics of acid dye adsorption on GAC. *Water Research*, **33**(8), pp.1895-1899.

Wang, J., Liu, G., Wang, L., Li, C., Xu, J. and Sun, D. Synergistic stabilization of emulsions by poly(oxypropylene)diamine and Laponite particles. *Colloids and Surfaces A: Physicochemical and Engineering Aspects*, **353**(2-3), pp.117-124.

Wang, M.C. and Huang, P. M. (1989) Catalytic power of nontronite, kaolinite and quartz and their reaction sites in the formation of hydroquinone-derived polymers. *Applied Clay Science*, **4**(1), pp.43-57.

Wang, S. and Ariyanto, E. (2007) Competitive adsorption of malachite green and Pb ions on natural zeolite. *Journal of Colloid and Interface Science*, **314**(1), pp.25-31.

Wayne, PA (2011) Performance standards for antimicrobial susceptibility testing: twenty-first informational supplement. Document M100-S21. *Clinical and Laboratory Standards Institute.* CLSI.

Wayne, PA (2012) Performance standards for antimicrobial susceptibility testing: twenty-second informational supplement. Document M100-S22. *Clinical and Laboratory Standards Institute.* CLSI,

Weenk, G.H., Janet E.L. Corry, G.D.W.C. and Rosamund, M.B. (2003) Chapter 1 Microbiological assessment of culture media: Comparison and statistical evaluation of methods. *in Progress in Industrial Microbiology.* Elsevier, pp.1-23.

Wei, T.-Y., Pan, Y.-F., Lu, G.-Q., Tong, Z.-F. and Xiao, H.-N. (2010) Activated Clay Prepared by Waste Acid Recycling: Technology and Mechanism. *Environmental Engineering Science*, **27**(6), pp.531-535.

Weir, E., Lawlor, A., Whelan, A. and Regan, F. (2008) The use of nanoparticles in anti-microbial materials and their characterization. *Analyst*, **133**(7), pp.835-845.

Willenbacher, N. (1996) Unusual Thixotropic Properties of Aqueous Dispersions of Laponite RD. *Journal of Colloid and Interface Science*, **182**(2), pp.501-510.

Williams, D., Ehrman, S. and Pulliam Holoman, T. (2006) Evaluation of the microbial growth response to inorganic nanoparticles. *Journal of Nanobiotechnology*, **4**(1), p.3.

Wittberger, D., Berens, C., Hammann, C., Westhof, E., Schroeder, R (2000) Evaluation of uranyl photocleavage as a probe to monitor ion binding and flexibility in RNAs. *J. Mol. Biol.* **300**(2), pp.339-52.

Wong, C.T., Abdullah, A.Z. and Bhatia, S. (2008) Catalytic oxidation of butyl acetate over silver-loaded zeolites. *Journal of Hazardous Materials*, **157**(2-3), pp.480-489.

Wright, H.J.L. and Kitchener, J.A. (1976) The problem of dewatering clay slurries: Factors controlling filtrability. *Journal of Colloid and Interface Science*, **56**(1), pp.57-63.

Xiao, M., Wang, Y., Yang, Q.-W., Fan, X., Brown, M., Kong, F. & Xu, Y.-C (2012) Antimicrobial susceptibility of *Pseudomonas aeruginosa* in China: a review of two multicentre surveillance programmes, and application of revised CLSI susceptibility breakpoints. *International Journal of Antimicrobial Agents*, **40**, pp445-449.

Xiao, Y. H., Giske, C. G., Wei, Z. Q., Shen, P., Heddini, A and Li, L. J (2011) Epidemiology and characteristics of antimicrobial resistance in China. *Drug Resist Updat*, **14**, pp. 236–250

Xu, G., Qiao, X., Qiu, X. and Chen, J. (2011) Preparation and Characterization of Nano-silver Loaded Montmorillonite with Strong Antibacterial Activity and Slow Release Property. *Journal of Materials Science & Technology*, **27**(8), pp.685-690.

Yamanaka, M., Hara, K. and Kudo, J. (2005) Bactericidal actions of a silver ion solution on escherichia coli, studied by energy-filtering transmission electron microscopy and proteomic analysis. *Appl. Environ. Microbiol.*, **71**(11), pp.7589-7593.

Yamamoto, K., Kawanishi, S. J. (1989) Hydroxyl free radical is not the main active species in site-specific DNA damage induced by copper (II) ion and hydrogen peroxide. *Biol. Chem.* **264**, pp.15435-15440.

Yan, L. and Stucki, J.W. (2000) Structural perturbations in the solid-water interface of redox transformed nontronite. *Journal of Colloid and Interface Science*, **225**(2), pp.429-439.

Yi, J.-Z. and Zhang, L.-M. (2008) Removal of methylene blue dye from aqueous solution by adsorption onto sodium humate/polyacrylamide/clay hybrid hydrogels. *Bioresource Technology*, **99**(7), pp.2182-2186.

Yoon, K.-Y., Hoon Byeon, J., Park, J.-H. and Hwang, J. (2007) Susceptibility constants of *Escherichia coli* and *Bacillus subtilis* to silver and copper nanoparticles. *Science of The Total Environment*, **373**(2-3), pp.572-575.

Yu, C.H., Norman, M.A., Newton, S.Q., Miller, D.M., Teppen, B.J. and Schäfer, L. (2000) Molecular dynamics simulations of the adsorption of proteins on clay mineral surfaces. *Journal of Molecular Structure*, **556**(1-3), pp.95-103.

Yu, F., Li, T., Huang, X., Xie, J., Xu, Y., Tu, J., Qin, Z., Parsons, C., Wang, J., Hu, L., Wang L. (2012) Virulence gene profiling and molecular characterization of hospital-acquired *Staphylococcus aureus* isolates associated with bloodstream infection. *Diagnostic Microbiology and Infectious Disease,* Article in press. Available online 26 September 2012.

Yuan, G. and Cranston, R. (2008) Recent Advances in Antimicrobial Treatments of Textiles. *Textile Research Journal*, **78**(1), pp.60-72.

Yuan, P., Annabi-Bergaya, F., Tao, Q., Fan, M., Liu, Z., Zhu, J., He, H. and Chen, T. (2008) A combined study by XRD, FTIR, TG and HRTEM on the structure of delaminated Fe-intercalated/pillared clay. *Journal of Colloid and Interface Science*, **324**(1-2), pp.142-149.

Yuan, X., Zhuo, S.-P., Xing, W., Cui, H.-Y., Dai, X.-D., Liu, X.-M. and Yan, Z.-F. (2007) Aqueous dye adsorption on ordered mesoporous carbons. *Journal of Colloid and Interface Science*, **310**(1), pp.83-89.

Zebrowski, J., Prasad, V., Zhang, W., Walker, L.M. and Weitz, D.A. (2003) Shake-gels: shear-induced gelation of laponite-PEO mixtures. *Colloids and Surfaces A: Physicochemical and Engineering Aspects*, **213**(2-3), pp.189-197.

Zen, J.-M., Jeng, S.-H. and Chen, H.-J. (1996) Catalysis of the electroreduction of hydrogen peroxide by nontronite clay coatings on glassy carbon electrodes. *Journal of Electroanalytical Chemistry*, **408**(1-2), pp.157-163.

Zhao, Z. H., Sakagami, Y., Osaka, T. Can. (1998) Toxicity of hydrogen peroxide produced by electroplated coatings to pathogenic bacteria. *J. Microbiol*. **44**(5), pp. 441-147.

Appendices

Appendix 1

1 Descriptive statistics of silver and copper ions eluted from silver and copper modified Laponite® RD

Table A: Silver ions eluted from silver-exchanged Laponite® RD in medium containing bacteria and bacteria free medium

(i) Bacterial medium supplemented with AGLAP1

Bacteria free AGLAP1 vs *E. coli* AGLAP1				
Time (h)	Difference	t	P value	Summary
0	-0.06	0.1772	P > 0.05	ns
2	0.259	0.765	P > 0.05	ns
4	0.7023	2.074	P > 0.05	ns
6	0.3913	1.156	P > 0.05	ns
8	0.2427	0.7168	P > 0.05	ns
24	0.6187	1.827	P > 0.05	ns
48	0.685	2.023	P > 0.05	ns
72	1.397	4.127	P < 0.01	**
Bacteria free AGLAP1 vs *S. aureus* AGLAP1				
Time (h)	Difference	t	P value	Summary
0	-0.086	0.254	P > 0.05	ns
2	-0.2117	0.6252	P > 0.05	ns
4	-0.3703	1.094	P > 0.05	ns
6	-0.2837	0.838	P > 0.05	ns
8	0.2003	0.5917	P > 0.05	ns
24	0.2167	0.64	P > 0.05	ns
48	-0.1413	0.4174	P > 0.05	ns
72	0.3563	1.052	P > 0.05	ns
Bacteria free AGLAP1 vs *P. aeruginosa* AGLAP1				
Time (h)	Difference	t	P value	Summary
0	-0.086	0.254	P > 0.05	ns
2	-0.2117	0.6252	P > 0.05	ns
4	-0.3703	1.094	P > 0.05	ns
6	-0.4837	1.429	P > 0.05	ns
8	0.2003	0.5917	P > 0.05	ns
24	0.2167	0.64	P > 0.05	ns
48	-0.1413	0.4174	P > 0.05	ns
72	0.3563	1.052	P > 0.05	ns

(ii) Bacterial medium supplemented with AGLAP4

Bacteria free AGLAP4 vs *E. coli* AGLAP4				
Time (h)	Difference	t	P value	Summary
0	-0.414	0.4109	P > 0.05	ns
2	0.897	0.8903	P > 0.05	ns
4	1.592	1.58	P > 0.05	ns
6	0.926	0.9191	P > 0.05	ns
8	0.13	0.129	P > 0.05	ns
24	1.293	1.283	P > 0.05	ns
48	0.343	0.3404	P > 0.05	ns
72	-0.091	0.09032	P > 0.05	ns
Bacteria free AGLAP4 vs *S. aureus* AGLAP4				
Time (h)	Difference	t	P value	Summary
0	-0.787	0.7811	P > 0.05	ns
2	-1.64	1.627	P > 0.05	ns
4	0.238	0.2362	P > 0.05	ns
6	-0.42	0.4169	P > 0.05	ns
8	-0.11	0.1092	P > 0.05	ns
24	0.115	0.1141	P > 0.05	ns
48	-0.123	0.1221	P > 0.05	ns
72	-0.558	0.5538	P > 0.05	ns
Bacteria free AGLAP4 vs *P. aeruginosa* AGLAP4				
Time (h)	Difference	t	P value	Summary
0	-0.787	0.7811	P > 0.05	ns
2	-1.64	1.627	P > 0.05	ns
4	-0.762	0.7563	P > 0.05	ns
6	-0.42	0.4169	P > 0.05	ns
8	-0.11	0.1092	P > 0.05	ns
24	0.115	0.1141	P > 0.05	ns
48	-0.123	0.1221	P > 0.05	ns
72	-0.558	0.5538	P > 0.05	ns

(iii) Bacterial medium supplemented with AGLAP6

Bacteria free AGLAP6 vs *E. coli* AGLAP6				
Time (h)	Difference	t	P value	Summary
0	-0.28	0.3774	P > 0.05	ns
2	0.636	0.8573	P > 0.05	ns
4	1.235	1.665	P > 0.05	ns
6	0.204	0.275	P > 0.05	ns
8	0.067	0.09031	P > 0.05	ns
24	0.361	0.4866	P > 0.05	ns
48	-0.214	0.2885	P > 0.05	ns
72	-0.675	0.9099	P > 0.05	ns
Bacteria free AGLAP6 vs *S. aureus* AGLAP6				
Time (h)	Difference	t	P value	Summary
0	-0.741	0.9988	P > 0.05	ns
2	-0.552	0.7441	P > 0.05	ns
4	-0.253	0.341	P > 0.05	ns
6	-1.042	1.405	P > 0.05	ns
8	-0.336	0.4529	P > 0.05	ns
24	0.451	0.6079	P > 0.05	ns
48	0.483	0.6511	P > 0.05	ns
72	-0.164	0.2211	P > 0.05	ns
Bacteria free AGLAP6 vs *P. aeruginosa* AGLAP6				
Time (h)	Difference	t	P value	Summary
0	-0.741	0.9988	P > 0.05	ns
2	-1.452	1.958	P > 0.05	ns
4	-0.253	0.341	P > 0.05	ns
6	-1.042	1.405	P > 0.05	ns
8	-0.336	0.4529	P > 0.05	ns
24	0.451	0.6079	P > 0.05	ns
48	0.483	0.6511	P > 0.05	ns
72	-0.164	0.2211	P > 0.05	ns

Table B: Silver ions eluted from silver incorporated Laponite® RD in medium containing bacteria and bacteria free medium

(i) Bacterial medium supplemented with AL1

Bacteria Free AL1 vs *E. coli* AL1				
Time (h)	Difference	t	P value	Summary
0	0	0	P > 0.05	ns
2	-0.9	0.7301	P > 0.05	ns
4	-1	0.8112	P > 0.05	ns
6	-0.7	0.5679	P > 0.05	ns
8	-1.2	0.9735	P > 0.05	ns
24	-2	1.622	P > 0.05	ns
48	-1.9	1.541	P > 0.05	ns
72	-2.6	2.109	P > 0.05	ns
Bacteria Free AL1 vs *S. aureus* AL1				
Time (h)	Difference	t	P value	Summary
0	0	0	P > 0.05	ns
2	-0.9	0.7301	P > 0.05	ns
4	-1	0.8112	P > 0.05	ns
6	-1	0.8112	P > 0.05	ns
8	-1.698	1.377	P > 0.05	ns
24	-2	1.622	P > 0.05	ns
48	-2.909	2.36	P > 0.05	ns
72	-4	3.245	P > 0.05	ns
Bacteria Free AL1 vs *P. aeruginosa* AL1				
Time (h)	Difference	t	P value	Summary
0	0	0	P > 0.05	ns
2	-1.319	1.07	P > 0.05	ns
4	-1.7	1.379	P > 0.05	ns
6	-1	0.8112	P > 0.05	ns
8	-1	0.8112	P > 0.05	ns
24	-2	1.622	P > 0.05	ns
48	-1.909	1.549	P > 0.05	ns
72	-3	2.434	P > 0.05	ns

(ii) Bacterial medium supplemented with AL2

Bacteria Free AL2 vs *E. coli* AL2				
Time (h)	Difference	t	P value	Summary
0	0	0	P > 0.05	ns
2	0.282	0.1937	P > 0.05	ns
4	-0.318	0.2184	P > 0.05	ns
6	-0.207	0.1422	P > 0.05	ns
8	-1.176	0.8078	P > 0.05	ns
24	-0.525	0.3606	P > 0.05	ns
48	-1.249	0.858	P > 0.05	ns
72	-2.104	1.445	P > 0.05	ns
Bacteria Free AL2 vs *S. aureus* AL2				
Time (h)	Difference	t	P value	Summary
0	0	0	P > 0.05	ns
2	-0.567	0.3895	P > 0.05	ns
4	-0.919	0.6313	P > 0.05	ns
6	-0.959	0.6588	P > 0.05	ns
8	-1.07	0.735	P > 0.05	ns
24	-0.824	0.566	P > 0.05	ns
48	-1.711	1.175	P > 0.05	ns
72	-2.103	1.445	P > 0.05	ns
Bacteria Free AL2 vs *P. aeruginosa* AL2				
Time (h)	Difference	t	P value	Summary
0	0	0	P > 0.05	ns
2	-1.9	1.305	P > 0.05	ns
4	-1.1	0.7556	P > 0.05	ns
6	-0.1	0.06869	P > 0.05	ns
8	-1.1	0.7556	P > 0.05	ns
24	-0.5	0.3435	P > 0.05	ns
48	-1	0.6869	P > 0.05	ns
72	-0.514	0.3531	P > 0.05	ns

(iii) Bacterial medium supplemented with AL3

Bacteria Free AL3 vs *E. coli* AL3				
Time (h)	Difference	t	P value	Summary
0	0	0	P > 0.05	ns
2	0.398	0.3314	P > 0.05	ns
4	0.639	0.5321	P > 0.05	ns
6	-0.407	0.3389	P > 0.05	ns
8	-0.527	0.4388	P > 0.05	ns
24	-0.044	0.03664	P > 0.05	ns
48	-1.817	1.513	P > 0.05	ns
72	-2.913	2.425	P > 0.05	ns
Bacteria Free AL3 vs *S. aureus* AL3				
Time (h)	Difference	t	P value	Summary
0	0	0	P > 0.05	ns
2	-0.923	0.7685	P > 0.05	ns
4	-0.632	0.5262	P > 0.05	ns
6	-0.498	0.4147	P > 0.05	ns
8	0.049	0.0408	P > 0.05	ns
24	-0.177	0.1474	P > 0.05	ns
48	-1.532	1.276	P > 0.05	ns
72	-2.454	2.043	P > 0.05	ns
Bacteria Free AL3 vs *P. aeruginosa* AL3				
Time (h)	Difference	t	P value	Summary
0	0	0	P > 0.05	ns
2	-2	1.665	P > 0.05	ns
4	0	0	P > 0.05	ns
6	0	0	P > 0.05	ns
8	0	0	P > 0.05	ns
24	0.053	0.04413	P > 0.05	ns
48	-0.5	0.4163	P > 0.05	ns
72	-1.6	1.332	P > 0.05	ns

Table C: Copper ions eluted from copper-exchanged Laponite® RD in medium containing bacteria and bacteria free medium

(i) Bacterial medium supplemented with CULAP1

Bacteria free CULAP1 vs *E. coli* CULAP1				
Time (h)	Difference	t	P value	Summary
0	0	0	P > 0.05	ns
2	0	0	P > 0.05	ns
4	0	0	P > 0.05	ns
6	0	0	P > 0.05	ns
8	0	0	P > 0.05	ns
24	0	0	P > 0.05	ns
48	0	0	P > 0.05	ns
72	0	0	P > 0.05	ns
Bacteria free CULAP1 vs *S. aureus* CULAP1				
Time (h)	Difference	t	P value	Summary
0	-0.0877	0.1656	P > 0.05	ns
2	-0.582	1.099	P > 0.05	ns
4	-1.615	3.049	P > 0.05	ns
6	-3.283	6.198	P < 0.0001	****
8	-2.796	5.279	P < 0.0001	****
24	-13.46	25.41	P < 0.0001	****
48	-13.13	24.78	P < 0.0001	****
72	-10.03	18.94	P < 0.0001	****
Bacteria free CULAP1 vs *P. aeruginosa* CULAP1				
Time (h)	Difference	t	P value	Summary
0	0.698	1.318	P > 0.05	ns
2	-1.261	2.381	P > 0.05	ns
4	-1.937	3.657	P < 0.05	*
6	-3.54	6.684	P < 0.0001	****
8	-2.475	4.673	P < 0.001	***
24	-13.97	26.37	P < 0.0001	****
48	-12.34	23.29	P < 0.0001	****
72	-10.29	19.43	P < 0.0001	****

(i) Bacterial medium supplemented with CULAP4

Bacteria free CULAP4 vs *E. coli* CULAP4				
Time (h)	Difference	t	P value	Summary
0	0	0	P > 0.05	ns
2	0	0	P > 0.05	ns
4	0	0	P > 0.05	ns
6	0	0	P > 0.05	ns
8	0	0	P > 0.05	ns
24	0	0	P > 0.05	ns
48	0	0	P > 0.05	ns
72	0	0	P > 0.05	ns
Bacteria free CULAP4 vs *S. aureus* CULAP4				
Time (h)	Difference	t	P value	Summary
0	1.395	0.5507	P > 0.05	ns
2	-4.408	1.74	P > 0.05	ns
4	-7.14	2.819	P > 0.05	ns
6	-11.12	4.39	P < 0.01	**
8	-8.341	3.293	P < 0.05	*
24	-7.923	3.128	P > 0.05	ns
48	-5.356	2.114	P > 0.05	ns
72	-7.117	2.809	P > 0.05	ns
Bacteria free CULAP4 vs *P. aeruginosa* CULAP4				
Time (h)	Difference	t	P value	Summary
0	1.547	0.6106	P > 0.05	ns
2	-4.609	1.82	P > 0.05	ns
4	-5.231	2.065	P > 0.05	ns
6	-14.71	5.808	P < 0.0001	****
8	-17.66	6.97	P < 0.0001	****
24	-13.72	5.415	P < 0.0001	****
48	-8.44	3.332	P < 0.05	*
72	-8.75	3.454	P < 0.05	*

(i) Bacterial medium supplemented with CULAP6

Bacteria free CULAP6 vs *E. coli* CULAP6				
Time (h)	Difference	t	P value	Summary
0	0	0	P > 0.05	ns
2	0	0	P > 0.05	ns
4	0	0	P > 0.05	ns
6	0	0	P > 0.05	ns
8	0	0	P > 0.05	ns
24	0	0	P > 0.05	ns
48	0	0	P > 0.05	ns
72	0	0	P > 0.05	ns
Bacteria free CULAP6 vs *S. aureus* CULAP6				
Time (h)	Difference	t	P value	Summary
0	-6.47	3.058	P > 0.05	ns
2	-13.73	6.489	P < 0.0001	****
4	-8.053	3.806	P < 0.01	**
6	-9.827	4.645	P < 0.001	***
8	-8.778	4.149	P < 0.01	**
24	-1.177	0.5565	P > 0.05	ns
48	2.009	0.9494	P > 0.05	ns
72	-6.44	3.044	P > 0.05	ns
Bacteria free CULAP6 vs *P. aeruginosa* CULAP6				
Time (h)	Difference	t	P value	Summary
0	-8.417	3.978	P < 0.01	**
2	-16.32	7.711	P < 0.0001	****
4	-10.8	5.103	P < 0.0001	****
6	-11.24	5.311	P < 0.0001	****
8	-12.11	5.722	P < 0.0001	****
24	-3.319	1.569	P > 0.05	ns
48	-1.417	0.6699	P > 0.05	ns
72	-8.157	3.855	P < 0.01	**

Table D: Copper ions eluted from copper incorporated Laponite® RD in medium containing bacteria and bacteria free medium

Bacteria Free CL1 vs *E. coli* CL1				
Time (h)	Difference	t	P value	Summary
0	0	0	P > 0.05	ns
2	-0.367	0.5922	P > 0.05	ns
4	-0.969	1.564	P > 0.05	ns
6	0.812	1.31	P > 0.05	ns
8	0.5	0.8069	P > 0.05	ns
24	1	1.614	P > 0.05	ns
48	0.4	0.6455	P > 0.05	ns
72	0.836	1.349	P > 0.05	ns
Bacteria Free CL1 vs *S. aureus* CL1				
Time (h)	Difference	t	P value	Summary
0	0	0	P > 0.05	ns
2	-0.7	1.13	P > 0.05	ns
4	-1.314	2.12	P > 0.05	ns
6	-0.144	0.2324	P > 0.05	ns
8	-0.553	0.8924	P > 0.05	ns
24	-0.016	0.02582	P > 0.05	ns
48	0.399	0.6439	P > 0.05	ns
72	0.78	1.259	P > 0.05	ns
Bacteria Free CL1 vs *P. aeruginosa* CL1				
Time (h)	Difference	t	P value	Summary
0	0	0	P > 0.05	ns
2	0.679	1.096	P > 0.05	ns
4	0.515	0.8311	P > 0.05	ns
6	1.207	1.948	P > 0.05	ns
8	1.235	1.993	P > 0.05	ns
24	1.848	2.982	P > 0.05	ns
48	1.154	1.862	P > 0.05	ns
72	1.461	2.358	P > 0.05	ns

Table E: Silver ions eluted from AgNO3 in medium containing bacteria and bacteria free medium

Bacteria Free $AgNO_3$ vs *E. coli* $AgNO_3$				
Time (h)	Difference	t	P value	Summary
0	0	0	P > 0.05	ns
2	0	0	P > 0.05	ns
4	0	0	P > 0.05	ns
6	0	0	P > 0.05	ns
8	0	0	P > 0.05	ns
24	-10.35	0.7571	P > 0.05	ns
48	-5.4	0.395	P > 0.05	ns
72	31.5	2.304	P > 0.05	ns

Bacteria Free $AgNO_3$ vs *S. aureus*$AgNO_3$				
Time (h)	Difference	t	P value	Summary
0	0	0	P > 0.05	ns
2	0	0	P > 0.05	ns
4	0	0	P > 0.05	ns
6	0	0	P > 0.05	ns
8	0	0	P > 0.05	ns
24	79.65	5.826	P < 0.0001	****
48	84.6	6.188	P < 0.0001	****
72	31.5	2.304	P > 0.05	ns

Bacteria Free $AgNO_3$ vs *P. aeruginosa* $AgNO_3$				
Time (h)	Difference	t	P value	Summary
0	0	0	P > 0.05	ns
2	0	0	P > 0.05	ns
4	0	0	P > 0.05	ns
6	0	0	P > 0.05	ns
8	0	0	P > 0.05	ns
24	52.65	3.851	P < 0.01	**
48	30.6	2.238	P > 0.05	ns
72	31.5	2.304	P > 0.05	ns

Table F: Copper ions eluted from $CuSO_4$ in medium containing bacteria and bacteria free medium

Bacteria Free $CuSO_4$ vs $CuSO_4$ *E. coli*				
Time (h)	Difference	t	P value	Summary
0	-50.86	6.906	P < 0.0001	****
2	-57.01	7.74	P < 0.0001	****
4	-68.89	9.354	P < 0.0001	****
6	-69.08	9.38	P < 0.0001	****
8	-53.66	7.286	P < 0.0001	****
24	-2.608	0.3541	P > 0.05	ns
48	-10.33	1.403	P > 0.05	ns
72	-10.24	1.391	P > 0.05	ns

Bacteria Free $CuSO_4$ vs $CuSO_4$ *S. aureus*				
Time (h)	Difference	t	P value	Summary
0	-61.57	8.36	P < 0.0001	****
2	25.54	3.468	P < 0.05	*
4	-65.05	8.833	P < 0.0001	****
6	-70.94	9.632	P < 0.0001	****
8	-49.93	6.779	P < 0.0001	****
24	-2.308	0.3134	P > 0.05	ns
48	0.9258	0.1257	P > 0.05	ns
72	-9.508	1.291	P > 0.05	ns

Bacteria Free $CuSO_4$ vs $CuSO_4$ *P. aeruginosa*				
Time (h)	Difference	t	P value	Summary
0	-60.49	8.214	P < 0.0001	****
2	-71.48	9.705	P < 0.0001	****
4	-77.71	10.55	P < 0.0001	****
6	-76.54	10.39	P < 0.0001	****
8	-64.84	8.805	P < 0.0001	****
24	-34.2	4.644	P < 0.001	***
48	-17.26	2.344	P > 0.05	ns
72	-18.97	2.576	P > 0.05	ns

Appendix 2

2 Descriptive statistics of silver and copper modified Laponite® RD antibacterial activity after 72 hours.

Table A: Silver-exchanged Laponite® RD antibacterial activity after 72 hours. Comparison of growth of bacteria in silver incorporated Laponite RD (control) and copper incorporated Laponite RD (control)

AGLAP *E. coli* vs CULAP *E. coli*				
Time (h)	Difference	t	P value	Summary
0	-0.0098	0.06237	P > 0.05	ns
2	1.052	6.696	P < 0.0001	****
4	0.7842	4.991	P < 0.001	***
6	0.4265	2.715	P > 0.05	ns
8	-0.3831	2.439	P > 0.05	ns
24	-0.7175	4.567	P < 0.001	***
48	-0.6049	3.85	P < 0.05	*
72	-0.7366	4.689	P < 0.001	***
AGLAP *S. aureus* vs CULAP *S. aureus*				
Time (h)	Difference	t	P value	Summary
0	0.1605+	1.021	P > 0.05	ns
2	0.5246	3.339	P > 0.05	ns
4	1.015	6.458	P < 0.0001	****
6	0.8868	5.645	P < 0.0001	****
8	0.09507	0.6051	P > 0.05	ns
24	-0.00263	0.01676	P > 0.05	ns
48	0.04512	0.2872	P > 0.05	ns
72	-0.2257	1.436	P > 0.05	ns
AGLAP *P. aeruginosa* vs CULAP *P. aeruginosa*				
Time (h)	Difference	t	P value	Summary
0	0.01095	0.06968	P > 0.05	ns
2	0.04807	0.306	P > 0.05	ns
4	0.1559	0.9921	P > 0.05	ns
6	0.5645	3.593	P < 0.05	*
8	0.2955	1.881	P > 0.05	ns
24	-0.1874	1.193	P > 0.05	ns
48	-0.5628	3.582	P < 0.05	*
72	-0.2826	1.799	P > 0.05	ns

Table B: Silver incorporated and copper incorporated Laponite® RD antibacterial activity after 72 hours. Comparison of growth of bacteria in silver incorporated Laponite RD, AL (control) and copper incorporated Laponite RD, CL (control).

AL *E. coli* vs CL *E. coli*				
Time (h)	Difference	t	P value	Summary
0	0.004138	0.04467	P > 0.05	ns
2	-0.3241	3.499	P > 0.05	ns
4	0.9929	10.72	P < 0.0001	****
6	0.7322	7.905	P < 0.0001	****
8	0.02117	0.2286	P > 0.05	ns
24	-0.373	4.027	P < 0.01	**
48	-0.4605	4.972	P < 0.001	***
72	-0.5861	6.328	P < 0.0001	****
AL *S. aureus* vs CL *S. aureus*				
Time (h)	Difference	t	P value	Summary
0	-0.00096	0.01034	P > 0.05	ns
2	0.2657	2.869	P > 0.05	ns
4	0.9576	10.34	P < 0.0001	****
6	0.7472	8.067	P < 0.0001	****
8	0.04199	0.4534	P > 0.05	ns
24	-0.4602	4.968	P < 0.001	***
48	-0.501	5.409	P < 0.0001	****
72	-0.6474	6.99	P < 0.0001	****
AL *P. aeruginosa* vs CL *P. aeruginosa*				
Time (h)	Difference	t	P value	Summary
0	-0.00391	0.04224	P > 0.05	ns
2	0.2657	2.869	P > 0.05	ns
4	1.01	10.9	P < 0.0001	****
6	0.835	9.015	P < 0.0001	****
8	0.7883	8.51	P < 0.0001	****
24	-0.1355	1.463	P > 0.05	ns
48	-0.3461	3.736	P < 0.05	*
72	-0.2985	3.223	P > 0.05	ns

Table C: EDX elemental analysis of $AgNO_3$

Elements	Concentration of $AgNO_3$ (wt %)
Ag	49.84±1.38
N	37.95±2.03
O	12.21±0.77

Table D: EDX elemental analysis of $CuSO_4$

Elements	Concentration of $CuSO_4$ (wt %)
Cu	65.06±2.44
S	17.15±0.62
O	17.79±1.85

Appendix 3

Determination of unit cell (emperical) formula from EDX table 3.1

From Table 3.1 the chemical formula then becomes; The wt. % was converted to gram to calculate the number of moles. Number of moles was then divided by the lowest factor to get the ratio of the unit cell in each case.

LAP2

Na 1.59/22.99 = 0.0692 / 0.0043 = 16.08

Mg 13.97/24.31 = 0.5747 / 0.0043 =133.64

Si 22.23/28.09 = 0.2494/0.0043 = 58.03

O 59.48/16.0 = 3.7175/0.0043 = 864.53

Li 0.03/6.94 = 0.0043/0.0043 = 1.00

OH 2.66/17.01 = 0.1564/0.0043 = 36.37

$Na_{16.1}\,(Si_{58.0}\,Mg_{133.6.5}\,Li)\,O_{864.5}\;\;(OH)_{36.4}$

AGLAP1

Na 1.27/22.99 = 0.0552/0.0029 = 19.05

Mg 13.41/24.31 = 0.5588/0.0029 = 190.22

Si 22.92/28.09 = 0.8186/0.0029 = 281.36

Ag 0.70/107.87 = 0.0065/0.0029 = 2.24

O 59.35/16.00 = 3.7094/0.0029 = 1279.09

Li 0.02/6.94 = 0.0029/0.0029 = 1.00

OH 2.69/17.01 = 0.1582/0.0029 = 54.53

$Na_{19.1}\;\;Ag_{2.2}\,(Si_{281.4}\,Mg_{190.2}\,Li)\,O_{1279.1}\;\;(OH)_{54.5}$

AGLAP2

Na 0.74/22.99 = 0.0322/0.0043 = 7.49

Mg 13.98/24.31 = 0.5751/0.0043 = 133.74

Si 22.11/28.09 = 0.7871/0.0043 = 183.05

Ag 1.25/107.87 = 0.0116/0.0043 = 2.70

O 59.51/16.00 = 3.7194/0.0043 = 864.98

Li 0.03/6.94 = 0.0043/0.0043 = 1.00

OH 2.53/17.01 = 0.1487 = 34.58

$Na_{7.5}(Si_{183.1}\ Mg_{133.7}\ Li)\ O_{865.0}\ (OH)_{34.6}$

AGLAP3

Na 0.66/22.99 = 0.0287/0.00430 = 6.67

Mg 13.62/24.31 = 0.5603/0.00430 = 130.30

Si 22.18/28.09 = 0.7896/0.00430 = 183.63

Ag 1.61/107.87 = 0.0149/0.00430 = 0.35

O 59.30 = 16.00 = 3.7063/0.00430 = 861.93

Li 0.03/6.94 = 0.0043/0.00430 = 1.00

OH 2.53/17.01 = 0.1487/0.00430 = 34.58

$Na_{6.7}\ Ag_{0.4}(Si_{183.5}\ Mg_{130.3}\ Li)\ O_{862.0}\ (OH)_{34.6}$

AGLAP4

Na 0.45/22.99 = 0.0196/0.0043 = 4.55

Mg 13.91/24.31 = 0.5722/0.0043 = 133.07

Si 22.50/28.09 = 0.0801/0.0043 = 186.28

Ag 1.76/107.87 = 0.0163/0.0043 = 3.79

O 59.17/16.00 = 3.6981/0.0043 = 860.03

Li 0.03/6.94 = 0.0043/0.0043 = 1.00

OH 2.59/17 = 0.1523/0.0043 = 35.41

$Na_{4.6}\ Ag_{3.8}(Si_{186.3}\ Mg_{133.1}\ Li)\ O_{860.0}\ (OH)_{35.4}$

AGLAP5

Na	0.16/22.99 = 0.0070/0.0043 = 1.62
Mg	13.83/24.31 = 0.5689/0.0043 = 132.30
Si	22.01/28.09 = 0.7836/0.0043 = 182.22
Ag	1.85/107.87 = 0.0172/0.0043 = 3.99
O	59.64/16.00 = 3.7275/0.0043 = 866.86
Li	0.03/6.94 = 0.0043/0.0043 = 1.00
OH	2.50/17.01 = 0.1470/0.0043 = 34.18

$Na_{1.6}\ Ag_{4.0}\ (Si_{182.2}\ Mg_{132.3}\ Li)\ O_{866.9}\ (OH)_{34.2}$

AGLAP6

Na	0.11/22.99 = 4.7847/0.0029 = 1.65
Mg	13.26/24.31 = 0.5455/0.0029 = 188.09
Si	21.70/28.09 = 0.7725/0.0029 = 266.39
Ag	2.35/107.87 = 0.0218/0.0029 = 7.51
O	59.81/16.00 = 3.7381/0.0029 = 1289.01
Li	0.02/6.94 = 0.0029/0.0029 = 1.00
OH	2.50/17.01 = 0.1470/0.0029 = 50.68

$Na_{1.7}\ Ag_{7.5}\ (Si_{266.4}\ Mg_{188.1}\ Li)\ O_{1289.0}\ (OH)_{50.7}$

List of publications, posters and conferences attended

Publication /Poster Presentation

- Ituah, F. I., Radecka, I and Williams, C. D (2011) Synthesis of silver exchanged Laponite and its antibacterial efficacy, Promoting the science of nanoporous materials. *British zeolite association XXXIV annual conference proceedings*, p35.

- Ituah, F. I., Radecka, I and Williams, C. D (2010) Antimicrobial effect of silver-zeolite on *Escherichia coli*, Promoting the science of nanoporous materials. *British zeolite association XXXIII annual conference proceedings*, p26.

- Ituah, F. I., Radecka, I and Williams, C. D (2010) Synthesis of silver-Laponite for potential application in wound dressing. Presented at the UK's Medilink Northwest and the Materials Knowledge Transfer Network, 'Dressed to Heal' on Wound Healing, Regenerative Medicine and Medical Textiles.

- F. I., Radecka F. I., Radecka, I and Williams, C. D (2009) Synthesis of silver exchange Laponite®. Promoting Promoting the science of nanoporous materials. *British zeolite association XXXII annual conference proceedings*, p83

Pending Publications

- Patent in preparation.

- Ituah, F. I., Radecka, I. and Williams, C. D (2012) Antibacterial effect of silver exchanged Laponite on *Staphylococcus aureus*.

- Li, F., Ituah, F. and Williams, C. D (2012) Synergistic effect of H_2O_2/O_3 inactivation to the disinfection of *Cryptosporidium parvum.*

Oral Presentation

- Laponite® RD Properties and Uses. RIHS, University of Wolverhamptom Presentation to research peers April, 2011

- Antimicrobial efficacy of silver-Laponite® RD nanocomposite, Research Centre in Applied Sciences 2010 (RCAS) held at School of Applied Sciences, University of Wolverhampton

- The synthesis, modification and antimicrobial activity of Laponite® RD Rockwood Company Ltd, Cheshire (2010), held at School of Applied Sciences, University of Wolverhampton

- The synthesis of Laponite® RD and modification Research Centre in Applied Sciences 2009 (RCAS) held at School of Applied Sciences, University of Wolverhampton

- Laponite® RD synthesis and modification Research Centre in Applied Sciences 2009 (RCAS) held at School of Applied Sciences, University of Wolverhampton

- The use of Laponite® RD and its production Staff presentation programme (2009) held at Science Park, Wolverhampton

Conference Attended

- XXXIV annual conference of the British Zeolite Association (BZA) held at the University of Edinburgh, UK.

- Dress to heal - wound healing, regenerative medicine and medical textiles conference held at chancellors hotel and conference centre, Manchester, UK

- XXXIII annual conference of the British Zeolite Association (BZA) held at the University of Southampton, UK.

- XXXII annual conference of the British Zeolite Association (BZA) held at the University of Cumbria, Ambleside, UK.